

**SCANNING ELECTRON MICROSCOPY OF THE MAMMALIAN RENAL
GLOMERULUS IN HEALTH AND DISEASE**

VOLUME ONE - TEXT

IAN W. GIBSON BSc (Hons) MB ChB

**University Department of Pathology,
Western Infirmary, Glasgow**

**Thesis submitted for the degree of Doctor of Medicine,
in the Faculty of Medicine, University of Glasgow,
December 1994**

ProQuest Number: 11007646

All rights reserved

INFORMATION TO ALL USERS

The quality of this reproduction is dependent upon the quality of the copy submitted.

In the unlikely event that the author did not send a complete manuscript and there are missing pages, these will be noted. Also, if material had to be removed, a note will indicate the deletion.



ProQuest 11007646

Published by ProQuest LLC (2018). Copyright of the Dissertation is held by the Author.

All rights reserved.

This work is protected against unauthorized copying under Title 17, United States Code
Microform Edition © ProQuest LLC.

ProQuest LLC.
789 East Eisenhower Parkway
P.O. Box 1346
Ann Arbor, MI 48106 – 1346

Thru

10239

Copy 1

Vol 1

ACKNOWLEDGEMENTS

I would like to express my sincere gratitude to Dr GBM Lindop, for his inspiration throughout the period of this work, and for his supervision in the preparation of this thesis. His many helpful comments and suggestions have guided my research, and have been invaluable.

Dr IAR More has also been a much appreciated source of encouragement, advice and discussion.

I would also thank:

- Professor RNM MacSween for his motivation, and allowing me the opportunity to perform this study while working in his department.
- Professor WR Lee kindly permitted free access to the scanning electron microscope in the Tenant Institute of Ophthalmology, Western Infirmary.
- Dr B Clark helped in the presentation of statistical data.

I am indebted to Mr TT Downie, Mr I Downie and Miss F Macpherson for their friendly and practical help in technical matters, to Mr D McComb for his enthusiastic assistance in the presentation of diagrams, and to Mrs J Hair and Mr G Neasham in the Electron Microscopy Unit for their patient work in the production of photographic illustrations.

Finally, I acknowledge that this work would not have been possible without the unremitting and loving support of my parents throughout the whole of my studies; for this no earthly reward is worthy.

DECLARATION

The work described in this thesis was commenced while I was an undergraduate medical student, doing summer vacation research projects (funded by the Scottish Home and Health Department) in the Department of Pathology, Western Infirmary, Glasgow. I have continued the project whilst working as a trainee pathologist in the same department.

I have been responsible for the collection of all tissue used in this study, for most of the tissue preparation, for all of the scanning electron microscopy, and much of the film developing.

Mr I Downie and Miss F Macpherson helped with some of the tissue preparation and film developing; the latter was funded for one year by a grant from the Research Support Group, Greater Glasgow Health Board.

The following papers have been published, and consist of material included in this thesis:

1. Gibson IW, More IAR, Lindop GBM
A scanning electron-microscopic study of the peripolar cell of the rat renal glomerulus.
Cell Tiss. Res. 257: 201-206 1989
2. Gibson IW, Downie I, Downie TT, Han SW, More IAR, Lindop GBM
The parietal podocyte: a study of the vascular pole of the human glomerulus.
Kidney Int. 41: 211-214 1992

3. Gibson IW, Gardiner DS, Downie I, Downie TT, More IAR, Lindop GBM

A comparative study of the glomerular peripolar cell and the renin-secreting cell in twelve species of mammal.

Cell Tiss. Res. 277: 385-390 1994

4. Gibson IW, Downie TT, More IAR, Lindop GBM

Immune complex deposition in Bowman's capsule is associated with parietal podocytes.

J. Pathol. 173: 53-59 1994

Aspects of this work have also been presented at meetings of the following societies from 1988 to 1994:

- Pathological Society of Great Britain and Ireland
- Association of Clinical Pathologists,
Caledonian Branch
- Renal Association
- European Dialysis and Transplant Association /
European Renal Association

CONTENTS

	Page
VOLUME ONE - TEXT	
SUMMARY	1
CHAPTER 1: INTRODUCTION	4
A. The Mammalian Renal Corpuscle:	4
B. The Glomerular Peripolar Cell:	6
1. Species Distribution:	6
2. Peripolar Cell Structure:	6
3. Peripolar Cell Function:	8
a) Secretory activity:	8
b) Sodium homeostasis:	9
c) Granule content:	10
d) Relationship with the JGA:	12
C. Lesions of the Glomerular Vascular and Tubular Poles:	13
1. Vascular Pole:	13
a) Glomerular Tuft:	13
- Hilar sclerosis:	13
b) Bowman's Capsule:	15
- Perihilar rupture:	15
- Parahilar hyaline deposits:	15
- Capsular drops:	16

	Page
2. Tubular Pole:	16
a) Glomerular Tuft:	16
- Glomerular tip lesion:	16
- Glomerular tip changes:	17
b) Bowman's Capsule:	18
- Renal transplant rejection:	18
- Fanconi syndrome:	19
- "Infraglomerular epithelial reflux":	19
 D. Atubular Glomeruli:	 20
 E. Aims of this Study:	 22

CHAPTER 2: A TECHNIQUE FOR SCANNING ELECTRON MICROSCOPY OF THE GLOMERULAR VASCULAR AND TUBULAR POLES	23
 A. Glomerular Microdissection:	 25
a) Perfusion v immersion fixation:	26
b) Vibratome- v scalpel-cut surfaces:	27
c) Microdissection before v after CPD:	27
 B. Conclusion:	 28
 C. Discussion:	 30
1. Advantages of the Technique:	30
2. Limitations of the Technique:	31

	Page
CHAPTER 3: THE NORMAL HUMAN GLOMERULUS	33
A. Source of Tissue:	33
B. Parietal Podocytes:	35
1. Morphology:	35
2. Distribution:	36
3. Parietal Podocyte / Squamous Parietal Junction:	36
4. Prevalence:	38
5. Discussion:	38
a) Origin of parietal podocytes:	38
b) Are parietal podocytes "normal"?:	38
c) Physiological significance of parietal podocytes:	40
d) Pathological significance of parietal podocytes:	42
C. Podocyte Connections between the Capillary Tuft and Bowman's Capsule:	46
D. The Vascular Pole:	49
1. Afferent and Efferent Arterioles:	49
2. Number of Vessels:	51
3. Endothelial Morphology:	52
4. Extraglomerular Mesangium:	52
E. The Tubular Pole:	53
1. Anatomical Variations:	53

	Page
2. Discussion:	55
a) Tubularization of Bowman's capsule:	55
b) The neck segment:	58
c) The "double-opening" tubular pole:	59
3. Tubular Pole Diameters:	60
F. Squamous Parietal Cells:	62
1. Morphology:	62
2. Discussion:	62
CHAPTER 4: COMPARATIVE ANATOMY OF THE PERIPOLAR CELL 64	
A. Source of Tissue:	64
B. Peripolar Cell Morphology:	65
1. Dendritic Peripolar Cells:	65
2. Globular Peripolar Cells:	66
3. Intermediate Forms:	67
a) Dendritic / globular peripolar cells:	67
b) Peripolar cell / parietal cell:	68
c) Peripolar cell / podocyte:	68
C. Peripolar Cell Quantification:	69
D. Discussion:	71
1. Peripolar Cell Structure:	71
2. Peripolar Cell Granules:	73
3. Peripolar Cell Numbers:	75

	Page
E. The Human Peripolar Cell:	77
F. Parietal Podocytes in Mammalian Kidney:	79
CHAPTER 5: LESIONS OF THE GLOMERULAR POLES IN HUMAN RENAL ALLOGRAFTS	80
A. Source of Tissue:	80
B. The Vascular Pole:	81
1. Peripolar Cells:	81
2. Parietal Podocytes:	82
3. Tuft-to-Capsule Adhesions:	83
4. Discussion:	83
a) Peripolar cells:	83
b) Parietal podocytes:	83
c) Tuft-to-capsule adhesions:	85
C. The Tubular Pole:	86
1. Glomerular Changes:	86
a) Tuft-to-capsule adhesions:	86
b) Capillary tuft:	88
c) Parietal epithelium:	88
d) Intraglomerular inflammatory cells:	89
2. Tubular Changes:	90
a) Tubular pole narrowing:	90
b) Proximal tubule:	91

	Page
3. Discussion:	92
a) Tubular pole adhesions:	92
b) Intraglomerular inflammatory cells:	96
c) Tubular pole narrowing:	97
d) Proximal tubule:	97
 CHAPTER 6: ATUBULAR GLOMERULI AND GLOMERULAR CYSTS	99
 A. Source of Tissue:	99
 B. Anatomy of Atubular Glomeruli:	99
1. The Parietal Epithelium:	99
2. The Glomerular Capillary Tuft:	100
3. Intraglomerular Inflammatory Cells:	101
4. Glomerular Cysts:	102
 C. Numbers of Atubular Glomeruli and Glomerular Cysts:	103
 D. Discussion:	105
1. Atubular Glomeruli in Normal Kidney:	105
2. Atubular Glomeruli in Renal Transplants:	105
3. Pathogenesis of Atubular Glomeruli / Glomerular Cysts:	106
4. Parietal Podocytes in Atubular Glomeruli:	109
5. Filtration in Atubular Glomeruli:	110
6. Atubular Glomeruli in Renal Disease:	111

Page

CONCLUSIONS **113**

REFERENCES **118**

VOLUME TWO - FIGURES

S U M M A R Y

SUMMARY

The vascular and tubular poles of the renal glomerulus are structurally and functionally highly specialised areas. The vascular pole forms part of the juxtaglomerular apparatus, involved in the control of renin synthesis and secretion, and it is the site of the peripolar cell, a recently recognised glomerular cell whose function is unknown.

In both experimental and human renal disease, lesions can specifically affect the glomerular vascular pole (eg. hilar sclerosis) or tubular pole (eg. glomerular tip changes). These two sites of glomerular damage reflect different pathogenetic mechanisms. In addition, glomeruli can lose their tubular pole connection to the rest of the nephron, forming atubular glomeruli.

In this study, I have used scanning electron microscopy (SEM) to study the glomerular poles in normal and diseased kidney. To facilitate this, I have developed a new technique of glomerular microdissection, allowing detailed study of the vascular and tubular poles of large numbers of glomeruli. The advantages and limitations of this technique are discussed.

I have studied the normal vascular and tubular poles of the adult human glomerulus. I have shown that many glomeruli have parietal podocytes lining Bowman's capsule around the vascular pole. The significance of this finding for both normal nephron function and glomerular disease is discussed. I have demonstrated podocytic connections between the glomerular tuft and

Bowman's capsule, and detailed the anatomical variations at the human vascular and tubular poles.

I have performed a species survey of the mammalian glomerular peripolar cell, defining two distinct types of peripolar cell. The dendritic peripolar cell, with a cell body and processes around the arterioles of the vascular pole, predominated in rodent species; the globular peripolar cell, with abundant cytoplasmic granules, predominated in the sheep and goat. I have discussed the significance of interspecies variations in peripolar cell numbers and morphology, emphasising the distinctiveness of the peripolar cell as a specific glomerular cell type.

I have studied lesions at the vascular and tubular poles in human renal allografts. The effect of renal damage on peripolar cells and parietal podocytes was investigated. Structural differences were demonstrated between tuft-to-capsule adhesions at the two glomerular poles. Vascular pole adhesions were formed by podocytes at areas with parietal podocytes; they may develop from pre-existing normal podocyte connections. In contrast, tubular pole adhesions did not involve podocytes, and were associated with variable abnormalities in squamous parietal epithelium. The significance of glomerular adhesions, and their underlying pathogenesis, is discussed. Additional varied tubular pole abnormalities have also been detailed.

Finally, I have used SEM to investigate atubular glomeruli in human kidney. I have shown that they are lined extensively by parietal podocytes, they contain

contracted capillary tufts, and many form glomerular cysts. I have found that atubular glomeruli are associated with narrowing of the tubular pole orifice in those glomeruli which retain a tubular connection. The significance of these findings to the pathogenesis of atubular glomeruli, and for filtration within atubular glomeruli, is discussed.

C H A P T E R 1

CHAPTER 1: INTRODUCTION

A. The Mammalian Renal Corpuscle:

The **nephron** is the structural and functional unit of the kidney; in man there are approximately 600,000/kidney (Nyengaard and Bendtsen 1989). At its commencement, the nephron is indented by a capillary network to form an ovoid-shaped filtering body called the **renal corpuscle** (diagram 1.1). In each renal corpuscle, the capillary network develops within a double-walled envelope, ie. **Bowman's capsule**. The outer wall is the **parietal layer** of Bowman's capsule, which is itself often referred to as **Bowman's capsule**. The inner wall is the **visceral (or podocyte) epithelium**; the potential space between the two walls is the **urinary space**. The capillary network is covered by the **visceral podocyte epithelium** to form the **glomerular capillary tuft**.

The parietal layer is lined by an epithelium which is classically described as a uniform population of flattened polygonal **squamous parietal cells**; these rest on the thick **parietal basement membrane**. The podocyte epithelium consists of dendritic cells with branching processes which terminate in interdigitating **foot processes** or **pedicels**. Between the pedicels are **filtration slit diaphragms**, specialised cell junctions through which the **glomerular filtrate** passes. The podocyte epithelium rests on the **glomerular basement membrane**, which is shared with the **fenestrated endothelium** of the glomerular capillaries. The balance

Diagram 1.1: The normal renal corpuscle and juxtaglomerular apparatus.

MD = Macula densa of the distal tubule

EGM = Extraglomerular mesangium

AA = Afferent arteriole

EA = Efferent arteriole

VP = Vascular pole

PPC = Peripolar cell

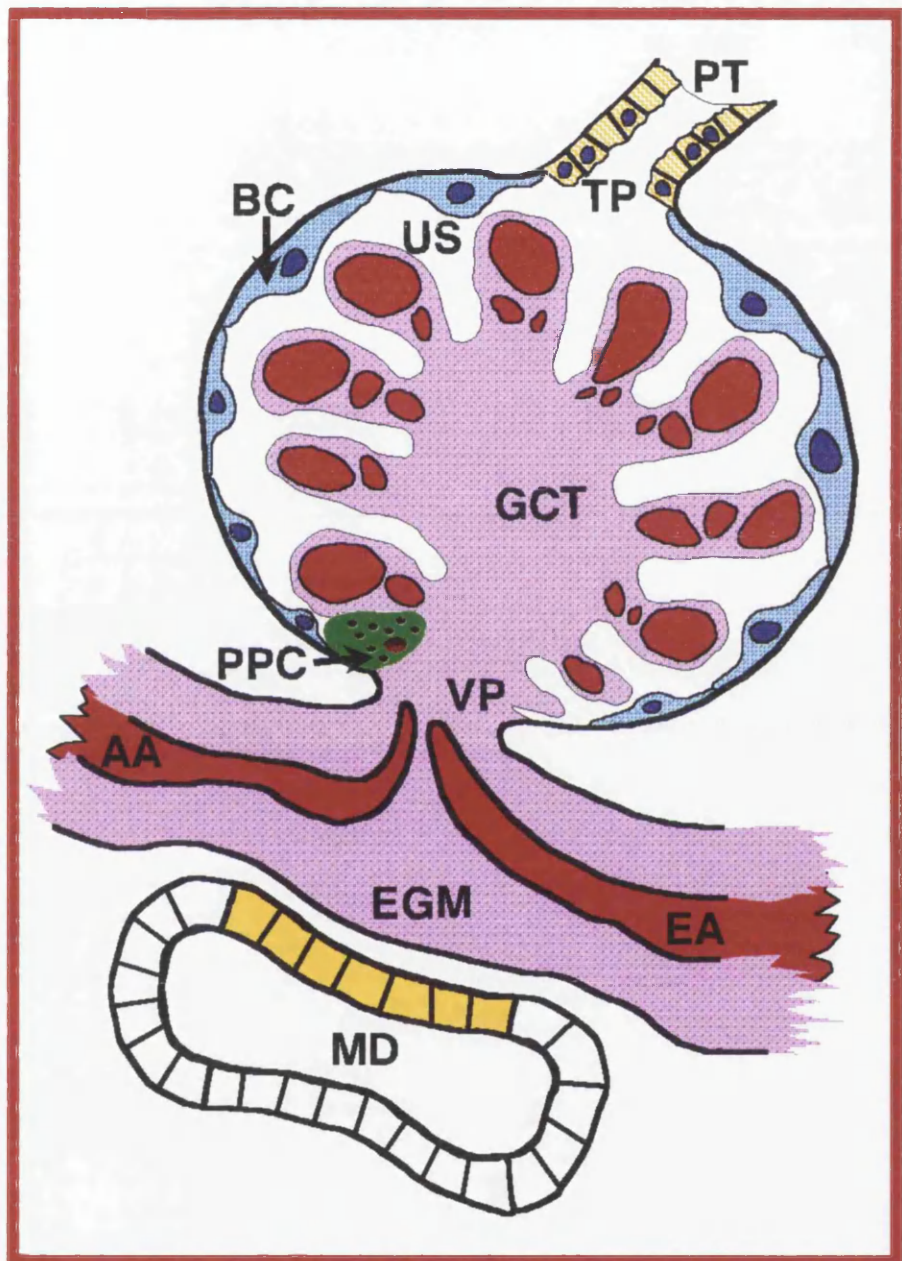
GCT = Glomerular capillary tuft

BC = Bowman's capsule

US = Urinary space

TP = Tubular pole

PT = Proximal tubule



of hydrostatic and oncotic pressures provide the forces for filtration of water and small molecules from the capillaries across the glomerular filtration barrier into the urinary space (Brenner *et al* 1971).

The **vascular pole** of the renal corpuscle is where the **afferent and efferent arterioles** deliver blood to and from the glomerulus respectively. Around the vascular pole is the reflection of the parietal epithelium to form the **visceral layer**, and this is traditionally considered as the point of transition of squamous parietal cells to podocytes (Jorgensen 1967). Located approximately opposite the vascular pole is the **tubular pole** where the parietal epithelium is continuous with the epithelium of the tubular portion of the nephron, commencing with the **proximal convoluted tubule**. The urinary space is therefore continuous with the lumen of the remaining nephron, such that the glomerular filtrate enters the proximal tubule.

At the vascular pole, the two arterioles are intimately associated with the **macula densa** (a specialised region of the distal tubule), and the intervening **extraglomerular mesangium**, forming the **juxtaglomerular apparatus** (Barajas 1979). Modified smooth muscle cells in the arteriolar walls synthesise and secrete the enzyme renin (Gomez *et al* 1989). It is therefore firmly established that the structures at the vascular pole are functionally highly specialised. This has been emphasized in the last 15 years, following the discovery of a proposed new cell type - the **glomerular peripolar cell** - at the vascular pole (Ryan *et al* 1979).

B. The Glomerular Peripolar Cell:

In 1979, Ryan et al described for the first time a heavily granulated cell in the sheep glomerulus. It was positioned around the vascular pole of the glomerulus, and was therefore called the "peripolar cell". It was suggested that this cell may be an additional secretory component of the JGA.

1. Species Distribution:

The peripolar cell occurs also in foetal (Mitchell et al 1982) and neonatal lamb (Alcorn et al 1984), and a wide range of other mammalian species, ie. mouse, rat, rabbit, guinea pig, dog, giraffe, kangaroo, koala, possum, quokka, echidna, platypus, antelope, goat, monkey and man (Ryan et al 1979, Gardiner and Lindop 1985, Gardiner et al 1986, Gall et al 1986, Mbassa 1989). It is also present in fish (Lacy and Reale 1989), amphibians eg. axolotl and toad (Hanner and Ryan 1980) and Japanese newt (Sakai and Kawahara 1983), reptiles eg. sand lizard (Koval'chuk 1987) and birds eg. chicken (Morild et al 1988).

2. Peripolar Cell Structure:

The peripolar cell is an epithelial cell at the vascular pole of the glomerular tuft. The cell has an apical surface exposed to the urinary space. It forms apical junctional complexes and desmosomes with adjacent parietal cells, podocytes and, if present, other peripolar cells. In the sheep, up to four peripolar

cells are found around any one vascular pole (Ryan et al 1979). They rest on the basement membrane of Bowman's capsule, with basal cytoplasmic microfilaments forming hemidesmosome-like attachment sites. In man, cytoplasmic extensions from adjacent parietal cells, rich in pinocytotic activity, may separate peripolar cells from the basement membrane of Bowman's capsule (Gardiner et al 1986).

Peripolar cells are recognisable by light microscopy due to their multiple closely packed cytoplasmic granules. The granules stain positively with methylene blue, PAS, brilliant crystal scarlet and Bowie's stain (Ryan et al 1979). Electron microscopy shows membrane-bound, variably electron-dense granules; less dense granules are more apically positioned (Thumwood et al 1993). Peripolar cell cytoplasm also contains rough endoplasmic reticulum, Golgi membranes, mitochondria, free ribosomes, glycogen, coated vesicles, microfilament bundles and microtubules (Ryan et al 1979, Hanner and Ryan 1980, Hill et al 1983, Gardiner et al 1986). The basal regions of human peripolar cells show prominent micropinocytosis (Gardiner et al 1986).

There may be close apposition between the peripolar cell and the renin-containing cells of the JGA, with only Bowman's capsule basement membrane between the two cell types (Ryan et al 1982, Gardiner and Lindop 1985, Gardiner et al 1986, Gall et al 1986, Lacy and Reale 1989). It has been frequently alleged that species with prominent granulated peripolar cells (eg. sheep, goat, antelope, axolotl, fish) have sparse JGA renin granules;

in contrast, species with more abundant renin granules have sparse peripolar cell granules (eg. rat, mouse, toad, human) (Ryan et al 1979, 1982, Hanner and Ryan 1980, Mbassa 1989, Lacy and Reale 1989).

3. Peripolar Cell Function:

a) Secretory activity: The peripolar cell resembles an exocrine secretory cell, consistent with a function of protein synthesis, storage and secretion (Ryan et al 1979, Alcorn et al 1984). Electron-dense material resembling granule contents is identifiable in dilated Golgi membrane sacs. In some species, granules have a paracrystalline matrix in keeping with newly-synthesised protein (Hanner and Ryan 1980, Lacy and Reale 1989). Coalescence and fusion of peripolar cell granules with apical membrane, interpreted as exocytotic secretion into the urinary space, has been described in sheep (Hill et al 1983, 1984a, 1984b, Thumwood et al 1993), newborn lamb (Alcorn et al 1984) and axolotl (Hanner and Ryan 1980). Although peripolar cells show no morphological evidence of polarity (Gardiner and Lindop 1985, Gardiner et al 1986), there has been no evidence of granule release basally, ie. in the direction of the juxtaglomerular apparatus (JGA).

Human peripolar cells contain little synthetic machinery and also lack microtubules (Gardiner et al 1986). In exocytosis, microtubules are involved in granule migration to the cell surface. However, human peripolar cells do have cell membrane invaginations extending deeply between granules (Gardiner et al 1986), similar

to those which have been described in association with renin granule exocytosis (Peter 1976).

The peripolar cell is ideally situated to release a factor into the glomerular filtrate which modulates tubular function (Ryan et al 1979). Possible triggering factors for granule release could be alterations in the electrolyte content of the glomerular filtrate bathing the cells; the presence of filterable circulating hormones; changes in the diameter of the polar region of the glomerular tuft resulting from variations in arteriolar calibre; or diffusing mediators released from the JGA (Ryan et al 1979).

b) Sodium homeostasis: Most evidence for peripolar cell stimulation has been in sodium-depleted states. Increase in protein synthetic activity, heterogeneity of granule density and exocytosis are all seen in sheep peripolar cells after rapid sodium depletion (Hill et al 1983 1984a). Mitotic activity and exocytosis have been observed in ovine toxæmia of pregnancy, a condition associated with sodium depletion (Hill et al 1984b). Peripolar cells increase in number in sodium-depleted and hypovolaemic chickens (Morild et al 1988). Exocytosis is also described in newborn lambs subjected to acute volume expansion and diuresis (Alcorn et al 1984) and in one axolotl after immersion in distilled water (Hanner and Ryan 1980).

Furthermore, peripolar cells in newborn lambs and rats are larger and more numerous in the first week of life than in foetal and adult animals, with larger granules (Alcorn et al 1984, Gall et al 1986). This is when the

postnatal kidney assumes responsibility for water and electrolyte homeostasis. Similar peripolar cell stimulation is triggered in foetal lambs with corticosteroids (Alcorn *et al* 1984). Its significance in relationship to altered renal function in the neonatal period is not clear, although the enlarged peripolar cell granules could result from inhibition of granule release. It does further suggest a role for the peripolar cell in electrolyte homeostasis, perhaps promoting tubular sodium reabsorption (Ryan *et al* 1982).

c) Granule content: The prominence of granulated peripolar cells in species with sparse renin granules prompted suggestions that the peripolar cell could secrete renin (Ryan *et al* 1979). However, several studies have confirmed that peripolar cell granules contain no immunoreactive renin (Gardiner and Lindop 1985, 1992b, Morild *et al* 1988, Trahair *et al* 1989, Taugner and Hackenthal 1989).

Peripolar cell granules do contain plasma proteins, e.g. albumin, fibrinogen, alpha-1-antitrypsin, complement components and (apart from IgM) immunoglobulins (Trahair and Ryan 1988, Trahair *et al* 1989, Nakajima *et al* 1989, Gardiner and Lindop 1992a). This is considered to be due to resorption from the urinary space (Trahair and Ryan 1988, Gardiner and Lindop 1992a). Despite the absence of demonstrable lysosomal enzymes, some consider peripolar cell granules to represent non-specific protein resorption (Morild *et al* 1988). The extent to which the peripolar cell is a specific glomerular cell type or simply a modified epithelial cell has therefore

been raised (Turner 1985, Morild et al 1988, Nakajima et al 1989).

In 1984, a preliminary report (Gall et al 1984) suggested that peripolar granules contain a kallikrein-like protease. Kallikrein interacts with the renin/angiotensin system (Watson et al 1985), and peripolar cells would be ideal candidates for its secretion. The localisation of kallikrein or its mRNA to ovine peripolar cells was not confirmed in subsequent studies by the same group (Trahair and Ryan 1989, Trahair et al 1989). However, others do describe immunoreactive kallikrein in peripolar cells (Walsh et al 1987), and kallikrein mRNA at the human (Jenkins et al 1991) and rat (Xiong et al 1989) vascular pole. Peripolar cell synthesis and secretion of kallikrein remains controversial.

Ovine peripolar cells contain transthyretin (Hollywell et al 1992), a protein which has a role in thyroxine and retinol transport. Its presence in peripolar cells could reflect a similar role in the kidney, although whether the accumulation reflects peripolar cell synthesis or resorption from the glomerular filtrate is unknown.

Immunocytochemical studies have reported peripolar cell expression of neuroendocrine markers, e.g. neurone-specific enolase (Trahair et al 1989, Trahair and Ryan 1989) and chromogranin (Alcorn et al 1992). This has been considered as evidence for a secretory function. However, others have found no such staining (Gardiner 1992), and no neurosecretory dense-core

granules have been demonstrated in peripolar cells, so this area remains controversial.

d) Relationship with the JGA: In human kidney, the numbers of peripolar cells and renin-containing JGAs correlate, and the majority of glomeruli with peripolar cells also have adjacent renin-containing cells (Gardiner and Lindop 1985), suggesting a functional relationship (Ryan *et al* 1979, Gardiner and Lindop 1985, Turner 1985). However, conditions in which the renin/angiotensin system is activated through different mechanisms, eg. malignant hypertension, renal artery stenosis and untreated Addison's disease, show no correlative alterations in peripolar cells, (Gardiner and Lindop 1992b, Gardiner *et al* 1992a), contrary to the hypothesis that peripolar cells are part of the JGA.

In conclusion, the function of the peripolar cell awaits clarification. It may synthesise and secrete factors involved in modulating renal tubular function, but a novel secretory substance has yet to be identified. Its anatomical site, and its presence in normal kidney of a wide range of species, suggest a particular physiological function. However, its acceptance as a specific cell type in the glomerulus is not universal, and one of the aims of this present study is to further investigate this controversy.

C. Lesions of the Glomerular Vascular and Tubular Poles:

The concept of specialisation of the vascular and tubular poles of the glomerulus has been further reinforced by their selective involvement in renal diseases in both experimental animals and man. Sclerosing lesions within the glomerulus may only involve a portion of the affected tuft ie. **segmental** (unlike **global** lesions that affect all the tuft), and they may affect only a proportion of glomeruli ie. **focal** (compared with **diffuse** lesions in every glomerulus). Observations in experimental animals and in man show three main types of segmental glomerular lesions which correspond to different pathogenetic mechanisms (Howie et al 1989, 1993, Newbold and Howie 1990). Lesions at the vascular pole (or **glomerular hilum**) are seen in conditions associated with glomerular overload or hyperfiltration; lesions at the tubular pole (or **glomerular tip**) occur in association with proteinuria; and lesions scattered variably throughout the tuft occur as a consequence of glomerular toxic damage. Despite their different pathogeneses, it should be noted that both vascular pole and tubular pole lesions may be present in the same glomerulus (Ito et al 1984, Poucell et al 1985, Yoshikawa et al 1986, Howie et al 1989).

1. Vascular Pole:

a) Glomerular Tuft:

Hilar sclerosis: Hilar sclerosing lesions occur in

experimental animals, either spontaneously (Elema and Arends 1975), following reduced renal mass eg. sub-total or unilateral nephrectomy, or given a high protein diet (Grond et al 1982, Olson et al 1985, Howie et al 1989, Nagata and Kriz 1992). These hilar lesions consist of glomerular sclerosis (ie. increased mesangial matrix with fibrosis), hyalinosis (ie. insudation of plasma proteins into the subendothelial space of the capillary wall and obliteration of capillaries) and tuft-to-capsule adhesion (ie. adhesion of capillary loops to the parietal layer of Bowman's capsule).

The underlying pathogenesis of hilar sclerosis is sustained renal vasodilatation, with increases in single nephron glomerular filtration rate, transcapillary pressures and plasma flow rates (Hostetter et al 1981, Brenner et al 1982). These haemodynamic factors cause injury to all glomerular cell types, allowing increased protein flux across capillaries. A low protein diet protects against hyperfiltration damage (Hostetter et al 1981); excess protein or hypercholesterolaemia exacerbates the hyperfiltration effect (Brenner et al 1982, Green et al 1992).

In human renal disease, the glomerular segmental lesions of classical focal segmental glomerulosclerosis (FSGS) are most commonly related to the vascular pole, particularly early in the disease (Niall 1965, Velosa et al 1975, Newman et al 1976, Brown et al 1978, Whitworth et al 1978, Morita et al 1990a, Howie et al 1993). Some have suggested that "hilar FSGS" has a poorer prognosis compared with cases with no hilar lesions ie.

"peripheral FSGS" (Ito et al 1984, Yoshikawa et al 1986, Howie et al 1993); other studies find less clearcut differences in outcome (Poucell et al 1985, Morita et al 1990a).

Hilar lesions are the predominant type of segmental sclerosing lesion in hypertensive patients (Harvey et al 1992), following pre-eclampsia (Heaton and Turner 1985) and in conditions of reduced renal mass, eg. reflux nephropathy (Morita et al 1990b) and unilateral nephrectomy (Zucchelli et al 1983, Newbold and Howie 1990). They are described also in some forms of glomerulonephritis, eg. membranous glomerulonephritis (Van Damme et al 1990).

b) Bowman's Capsule:

Perihilar rupture: Rupture of the parietal layer of Bowman's capsule specifically at the vascular pole of the glomerulus has been noted in two cases of crescentic glomerulonephritis (Morley 1988). This led to the displacement of the glomerular tuft away from the crescent, and its apparent "ejection" from Bowman's capsule.

Parahilar hyaline deposits: Rounded or crescent-shaped accumulations of PAS-positive material at the reflection of Bowman's capsule, are common in children with reflux nephropathy (Morita et al 1990b). Similar small deposits are observed in benign recurrent haematuria, rarely in minimal change nephropathy (Morita et al 1990b), and in rats following five-sixths renal ablation (Olson et al 1985). They also occur in association with hilar segmental glomerulosclerosis, and are probably

precursors of such lesions ie. very early hilar FSGS (Velosa et al 1975, Morita et al 1990a, 1990b).

Capsular drops: Hyaline eosinophilic and PAS-positive globules within the parietal layer of Bowman's capsule, unrelated to capillary loops of the glomerular tuft, can be found in different renal diseases and in all parts of Bowman's capsule. In membranous glomerulonephritis, it has been noted that they are often located near the vascular pole (Van Damme et al 1990).

2. Tubular Pole:

a) Glomerular Tuft:

In several rodent models of proteinuria, Howie et al (1989) mapped the position of segmental lesions within the glomerulus. Sclerosing lesions were almost totally confined to the glomerular tip (ie. opposite the hilum), with tuft-to-capsule adhesion adjacent to the tubular pole.

Glomerular tip lesion: A similar lesion, called the "glomerular tip lesion" (GTL) or "glomerular tip nephropathy", is described in human renal biopsies from patients with a steroid-responsive nephrotic syndrome (Howie and Brewer 1984, Beaman et al 1987). The early GTL has intracapillary foam cells, vacuolated podocytes, epithelial protein reabsorption droplets and fusion of capillary loop and Bowman's capsule basement membranes, producing an adhesion at the tubular pole. There may be prolapse of the lesion into the tubule, with adhesion to the tubular wall. There is associated damage for a variable length at the beginning of the proximal tubule,

with a flattened basophilic or vacuolated epithelium; clinically, tubular dysfunction may be apparent. With time, the intracapillary material becomes sclerosed and hyaline (PAS-positive), and larger areas of the tuft may become damaged (Howie and Brewer 1985). The tuft-to-capsule adhesion is permanent, and the GTL is therefore irreversible, although the tubular damage does recover. Serial section studies suggest that the GTL is, in some patients, not a focal abnormality, but is present in every glomerulus (Howie and Brewer 1984, Howie 1986a, Beaman et al 1987, Morita et al 1990a, Howie et al 1993).

By definition, the term GTL is used only when the glomeruli show minimal change nephropathy (ie. appear normal by light microscopy and show podocyte foot process fusion by electron microscopy) complicated by the glomerular tip changes (Howie 1986a, Beaman et al 1987, Howie and Brewer 1988). Prior to its recognition, the GTL was probably included in series of focal segmental glomerular sclerosis; its response to steroids and good prognosis justifies distinction from FSGS (Beaman et al 1987, Howie and Brewer 1988), although this view has been contested (Huppes et al 1988a, 1988b).

Glomerular tip changes: Similar glomerular tip changes are also seen in other renal diseases causing proteinuria eg. membranous, mesangial proliferative and mesangiocapillary glomerulonephritis, IgA nephropathy, lupus nephritis, amyloidosis and diabetic nephropathy (Howie 1986a), focal glomerulonephritis (Hurley and

Painter 1988), renal transplant rejection and glomerulopathy (Lee and Howie 1988), classical nephrotic-associated FSGS (Morita et al 1990a, Howie 1993, Howie et al 1993), pre-eclampsia (Heaton and Turner 1985) and hypertension (Harvey et al 1992). In these conditions, the additional presence of tip changes has no prognostic significance; the prognosis is determined by the underlying pathology in the glomerulus away from the tip (Howie 1986a).

The frequent finding of tip changes (13.5% of biopsies with segmental disease, Howie and Brewer 1984), at a specific part of the glomerulus, in such a variety of clinical conditions suggests a common pathogenesis. However, the aetiology of glomerular tip changes must involve more than simply proteinuria, since many cases of eg. minimal change nephropathy have no tip changes.

b) Bowman's Capsule:

Renal transplant rejection: In renal transplant rejection, collection of inflammatory cells and their infiltration into epithelium occurs particularly at, and is sometimes even confined to, the tubular pole (Lee and Howie 1988). This is associated with irregularity, splitting and even rupture of the basement membrane at the glomerulo-tubular junction. A similar feature, with narrowing of the tubular pole, is described in dog allografts (Darmady et al 1955). The tubular pole appears therefore to be a favoured site for entry of interstitial inflammatory cells into the nephron, further evidence that it has specific properties.

Fanconi syndrome: In this rare hereditary condition, a specific morphological lesion has been described at the tubular pole, consisting of a narrow elongated "swan-neck" deformity of the first part (up to 1mm) of the proximal tubule, lined by low cuboidal epithelium with no brush border (Clay et al 1953, Darmady and Stranack 1957).

"Infraglomerular epithelial reflux": The tubular pole can be the site of accumulation of pyknotic proximal tubule cells after their detachment and upward displacement (ie. so-called "infraglomerular epithelial reflux" or "glomerular tubular reflux"). This has been described in the early stage of acute renal failure in association with oliguria and hypotension (Waugh et al 1964) and in the hepatorenal syndrome (Kanel and Peters 1984). In both cases, it is probably a manifestation of acute renal ischaemia. A similar appearance, not associated with acute renal failure, has been suggested as a marker of glomerular haematuria (Valdes and Zhang 1987).

D. Atubular Glomeruli:

The atubular glomerulus is one that has lost its connection to the proximal tubule. Its detection requires a three-dimensional method, eg. nephron microdissection or serial histological sectioning.

The disparity between glomerular perfusion and filtration in pyelonephritic dogs (Damadian *et al* 1965) and in rats with experimental chronic renal failure (Kramp *et al* 1974) provided indirect evidence that some glomeruli made no contribution to urine production.

Atubular glomeruli were confirmed by microdissection in experimental chronic pyelonephritis in dog (Damadian *et al* 1965) and rabbit (Shimamura and Heptinstall 1963).

Serial sectioning has since shown atubular glomeruli in rats with chronic pyelonephritis (Heptinstall *et al* 1963, Tribe and Heptinstall 1964, Heptinstall and Hill 1967), experimental hydronephrosis (Ras and Heptinstall 1969), lithium-induced nephropathy (Marcussen *et al* 1989, 1990, 1991), cisplatin-induced tubulointerstitial nephropathy (Marcussen 1990, Marcussen and Jacobsen 1992) and at the edges of infarcts (Olson *et al* 1985).

Atubular glomeruli were first demonstrated in man by microdissection studies of chronic end-stage kidneys (Oliver 1939). Subsequent serial section studies of human kidney have shown they constitute 52% of glomeruli in renal artery stenosis (Marcussen 1991), 35% in chronic pyelonephritis (Marcussen and Olsen 1990) and upto 15% in diabetic nephropathy with renal failure (Marcussen 1992), compared with 3% of glomeruli in

control kidneys. Occasional atubular glomeruli have also been incidentally noted in serial sections of biopsies from children with focal segmental glomerulosclerosis (Morita et al 1990a).

The glomerular capillary tufts of atubular glomeruli are small, but appear to remain structurally intact, with open capillary loops perfused by blood (Olson et al 1985, Marcussen 1992). Ultrastructural examination of those seen in the rat after lithium therapy show only mild changes (Marcussen et al 1990), and there is no associated tuft sclerosis (Marcussen 1990, Marcussen et al 1990, Marcussen and Jacobsen 1992). However, in these experimental models, the number of atubular glomeruli correlates with the degree of renal impairment (Marcussen 1990), and it is considered that atubular glomeruli will cease to produce an ultrafiltrate once the pressure in the blind capsular space exceeds the capillary hydrostatic pressure (Marcussen 1992).

Atubular glomeruli are most prominent in primary tubulo-interstitial diseases, and it is likely that tubular atrophy and loss, particularly affecting the proximal tubule, due to ischaemic, inflammatory or toxic damage, leads to the irreversible disconnection of the glomeruli (Marcussen 1992). The poor correlation between glomerular abnormalities and functional impairment often found in human renal disease is well known (Schainuck et al 1970). The presence of atubular glomeruli provides an explanation for progressive and irreversible loss of renal function in the absence of glomerular sclerosis in chronic renal diseases.

E. Aims of this Study:

1. To develop a technique which combines glomerular microdissection and scanning electron microscopy (SEM), allowing detailed study of the interior of Bowman's capsule and the glomerular vascular and tubular poles (**chapter 2**).
2. To study the anatomy of the adult human glomerulus, and characterize the normal vascular and tubular pole structure (**chapter 3**).
3. To study the glomerular peripolar cell in a range of mammalian species, investigating its specificity as a glomerular epithelial cell (**chapter 4**).
4. To study pathological changes affecting the human glomerulus, particularly at the vascular and tubular poles (**chapter 5**).
5. To study atubular glomeruli in human kidney (**chapter 6**).

C H A P T E R 2

CHAPTER 2: A TECHNIQUE FOR SCANNING ELECTRON MICROSCOPY OF THE GLOMERULAR VASCULAR AND TUBULAR POLES

Scanning electron microscopy (SEM) enables high resolution observation of three-dimensional surface morphology. To investigate three-dimensional structure using light and transmission electron microscopy (TEM) requires complex reconstructions of serial sections, as used for example to elucidate the anatomical specialisations at the vascular pole of the glomerulus (Barajas 1970). SEM overcomes many of the technical demands of such studies, and it has been used extensively to study the kidney (reviewed by Andrews 1979). SEM was important in uncovering the complex structure of the podocyte (Buss and Kronert 1969) and its interdigitating pedicels (Fujita *et al* 1970), since previous attempts utilising TEM images (Pease 1955) proved to be inaccurate. The larger size of SEM specimens also permits greater tissue sampling than is possible with TEM.

However, there have been few SEM studies specifically examining the vascular pole of the glomerulus (Frank and Kriz 1982, Casellas 1986), because of its concealment by the capillary tuft within Bowman's capsule. In a slice of renal cortex, glomerular tufts remain attached at their vascular poles (Bulger *et al* 1974, Spinelli 1974), and whilst tubular poles are frequently found, exposure of vascular poles by a random mechanical process is rare (Frank and Kriz 1982). This problem has been overcome by breaking the glomerular tuft off the arterioles at

the vascular pole and directly removing it from Bowman's capsule (Casellas 1986).

As a preliminary study to this investigation, a technique of glomerular microdissection was developed allowing SEM examination of the entire interior of Bowman's capsule, including the vascular and tubular poles and the isolated capillary tuft of the same glomerulus.

A. Glomerular Microdissection:

Kidney tissue was obtained from normal young adult male Wistar rats. Animals were terminally anaesthetized with intraperitoneal pentobarbital sodium (50mg/kg). The kidneys were dissected out, sliced into thin horizontal sections using a razor blade and immersed in 2% glutaraldehyde in Millonig's buffer for 24 hours.

Perfusion-fixed kidney was obtained according to the method of Andrews (1979). A cannula was inserted into the aorta, proximal to its bifurcation; the inferior vena cava was cut and an isotonic saline solution containing 5000 units/ml of heparin and 0.1% lignocaine chloride was perfused at 120mmHg, until the kidneys blanched. The aorta was clamped above the renal vessels and the kidneys were perfused with 2% buffered glutaraldehyde. After perfusion, thin slices of kidney were immersed in fixative for a further 24 hours.

After fixation, 1mm tissue slices were washed in buffer, osmicated for 1 hour in 1% OsO₄, dehydrated in an ascending series of alcohols (30 minutes each in 25%, 50%, 75%, 100% and 100% ethanol) and critical point dried, using liquid carbon dioxide, in a Polaron critical point dryer. Dried specimens were mounted on metal stubs using conductive paint, gold-coated in a Polaron sputter-coater, and viewed with a Jeol scanning electron microscope (JSM 6400).

Intact glomerular capillary tufts were removed from their Bowman's capsules by microdissection using a fine-pointed ophthalmic knife and a Nikon dissecting

microscope (at magnifications upto x200). The capillary tufts were removed by levering them from Bowman's capsule, causing fracture through the arterioles at the vascular pole (fig. 2.01). The isolated tufts were retained by transferring them, using the fine-pointed knife, to SEM stubs covered with double-sided adhesive tape.

To determine the optimal technique for glomerular microdissection, it was performed on immersion- and perfusion-fixed rat tissue, before and after critical point drying (CPD), using sectioned surfaces exposed after fixation by both scalpel and vibratome.

a) Perfusion v immersion fixation: Perfusion fixation was superior for all subsequent steps in the process of exposing vascular and tubular poles; for example:-

(i) It resulted in less ragged vibratome- and scalpel-cut surfaces.

(ii) Urinary spaces were accentuated, and glomeruli were more easily manipulated out of their capsules, compared with the "snug-fitting" tufts obtained after immersion.

(iii) Lesser amounts of granular cellular/proteinaceous debris remained in Bowman's capsules, probably due to the washing effect of the pre-fixation saline perfusion. With TEM a pale protein deposit in the urinary space is not important, but in SEM it obscures the parietal cell surface, and possibly occludes the tubular pole of Bowman's capsule.

(iv) Tubules were in general more open, allowing a more satisfactory examination of the tubular pole.

b) Vibratome- v scalpel-cut surfaces: Vibratome-cut surfaces were superior. It was advantageous to microdissection for glomeruli to be intact. A scalpel sectioned through many glomeruli, leaving the tuft portions difficult to dislodge. The vibratome slowly advances a vibrating razor blade through the tissue and its blade was often deflected over (rather than through) capillary tufts, leaving more intact glomeruli available for microdissection.

c) Microdissection before v after CPD: The technique was more successful, and very much more easily performed after CPD for the following reasons:-

(i) Glomerular tufts were more clearly visible on stereomicroscopy of dry tissue (fig. 2.01), and were more easily removed from tissue slices attached to SEM stubs, compared with slices lying free in a petri dish, submerged in buffer.

(ii) The differential shrinkage of the capillary tuft and Bowman's capsule after CPD further accentuated the urinary space, leaving glomeruli looser within their capsules and therefore more easily removed.

(iii) The brittleness of tissue after CPD caused a less traumatic fracture through the glomerular arterioles. When glomeruli were removed before CPD, the parietal epithelium and basement membrane of Bowman's capsule was sometimes stripped out, either completely or partially, revealing the underlying interstitial collagen network.

(iv) Tissue debris resulting from the fracture of glomeruli at the vascular pole could be removed from the surface of dried tissue using a "dust-off" air spray.

B. Conclusion:

The removal of individual tufts using microdissection has been considered to be "tedious" and to require "technical skills to avoid tissue damage" (Casellas 1986). I have found this technique to be relatively easily performed, and reproducible in all species studied including human kidney.

In occasional randomly-sectioned Bowman's capsules, both the vascular and tubular poles were present (fig. 2.02); careful rotation and tilting of the specimen on the stage of the scanning microscope enabled examination of both. To consistently examine the vascular and tubular poles and the isolated capillary tuft of the same glomerulus, two consecutive 1mm-thick vibratome slices were prepared for SEM. After critical point drying, the slices were mounted with the complementary faces uppermost and coated with gold. Low-power scanning micrographs were used to number each glomerulus in the two opposing slices. Glomerular microdissection was then performed, and the tissue slices and isolated tufts were re-coated with gold. At low-power, the two hemispheres of each glomerulus were easily identified (fig. 2.03a and b), and examined for the glomerular poles. The isolated capillary tufts were arranged in rows (fig. 2.03c), allowing documentation of individual Bowman's capsules and their appropriate tuft.

There are approximately 100 randomly-sectioned Bowman's capsules per 1cm^2 slice of normal human cortex (fig. 2.03); in such a prepared slice, the percentage of

Bowman's capsules containing vascular poles is approximately 30-35%, the tubular pole yield is also 30-35%, the remaining capsules have neither glomerular pole. Examination of complementary faces ensures identification of the vascular and tubular poles of each glomerulus.

At the vascular pole, the clean epithelial fracture line around the glomerular arterioles is at the reflection of Bowman's capsule epithelium (fig. 2.04). The peripolar area of Bowman's capsule surrounding the vascular pole is preserved. In addition, the area between the arterioles where the extraglomerular mesangium is continuous with the mesangium of the capillary tuft (ie. the mesangial root) can be examined.

C. Discussion:

1. Advantages of the Technique:

This technique reveals large numbers of vascular and tubular poles for SEM examination, and enables study of anatomical variations, morphological specialisations and pathological changes at these important sites in the glomerulus.

It has a number of advantages over the methods employed previously to expose vascular poles. Frank and Kriz (1982) relied on accidental mechanical dissociation of glomerular tufts from their vascular poles. In my experience, this produces a very low number of exposed vascular poles. Also, the capillary tufts from Bowman's capsules with exposed vascular poles are not available for examination.

Casellas (1986) used a wooden rod coated with double-sided adhesive tape to remove tufts by rolling it across the surface of critical point dried kidney slices. This gave a vascular pole yield of approximately 30%, similar to my technique. However, it caused damage to the surface of the specimen, evident on his low-power micrograph (Casellas 1986). Furthermore, whilst capillary tufts are available for study after such removal, examination of the tuft from a specific Bowman's capsule is not possible.

My method of capillary tuft microdissection using a fine-pointed knife does not damage the cortical surface (fig. 2.03). Almost every capillary tuft can be adequately removed from its Bowman's capsule. Also most

of the tuft surface is intact and clean, and podocyte structure is readily assessed (fig. 2.05). Specimen rotation and tilting again allows SEM examination of all parts of the tuft, and the vascular pole and glomerular tip can be located.

A number of previous workers have isolated animal and human capillary tufts for SEM examination (Arakawa et al 1976 1977, Jones 1977 1978, Ng et al 1982 1983, Or et al 1983) and examined the vascular pole of the isolated rat glomerulus (Tokunaga et al 1975). In these studies, tufts dissected from wet fixed tissue were processed for SEM. The residual renal tissue, including Bowman's capsules, was not studied, and some glomeruli were lost during processing. In contrast, my technique permits study of both isolated tufts and Bowman's capsules, in addition to other parts of the kidney.

2. Limitations of the Technique:

The preference for perfusion-fixed tissue limits the range of human pathological kidney available. Biopsy samples of the many glomerular diseases consist of small pieces of tissue suitable only for immersion fixation. Perfusion fixation ideally requires a nephrectomy specimen, and the indications for nephrectomy are restricted, ie. renal tumour, trauma, transplant rejection, chronic pyelonephritis, hydronephrosis and renal artery stenosis. Glomerular microdissection is possible after immersion fixation, but the quality of the material is limited for the reasons stated above. The second major limitation to the application of this

method to human pathological material is the nature of glomerular damage. In diseases characterised by the presence of glomerular crescents, or adhesions between the capillary tuft and Bowman's capsule, glomerular microdissection and subsequent examination of the glomerular poles may be restricted.

In this present study, a glomerular microdissection problem was apparent when studying human renal transplant nephrectomies (chapter 5). The vascular damage related to chronic rejection produced areas of ischaemic parenchyma, with severe tubular atrophy and interstitial fibrosis (fig. 2.06). In these ischaemic areas, the crowded glomerular tufts were small, and after critical point drying remained tightly fitting within contracted Bowman's capsules. In contrast, in preserved areas of parenchyma, urinary spaces were accentuated, presumably due to better perfusion fixation compared with the ischaemic areas. As a result, most glomerular tufts within severely damaged areas could not be microdissected (fig. 2.06). There is therefore a bias in the technique for the examination of less damaged glomeruli, within less damaged areas of renal tissue.

C H A P T E R 3

CHAPTER 3: THE NORMAL HUMAN GLOMERULUS

A. Source of Tissue:

I obtained adult human kidney from the macroscopically and histologically normal parts of twelve kidneys surgically removed for renal or transitional cell carcinomas (see table 3.1). The kidneys were obtained fresh from the operating theatre, as soon as they were available, and were perfused at a pressure of 120mmHg, first with isotonic saline and then with 2% glutaraldehyde in Millonig's buffer. Perfused renal parenchyma from as far away from the tumour as possible was further fixed by overnight immersion in 2% glutaraldehyde. Glomerular microdissection and SEM

Table 3.1: Twelve tumour nephrectomies.

Kidney No.	Age of Patient	Tumour Type
1	49	Renal cell carcinoma
2	68	Renal cell carcinoma
3	67	Transitional cell carcinoma
4	51	Transitional cell carcinoma
5	49	Renal cell carcinoma
6	65	Transitional cell carcinoma
7	72	Renal cell carcinoma
8	80	Transitional cell carcinoma
9	61	Renal cell carcinoma
10	69	Renal cell carcinoma
11	65	Renal cell carcinoma
12	62	Renal cell carcinoma

preparation was then carried out as described in chapter 2.

In each kidney, at least 62 and upto 169 Bowman's capsules were examined. The position in the renal cortex of each glomerulus was mapped. Low power scanning electron micrographs were used to measure the distance from the surface of the kidney to the glomerulus and the distance from the capsular surface to the deepest glomerulus in the same straight line. In this way, a ratio was derived for the position of each glomerulus, with 0 representing the capsular surface of the cortex and 1 representing the corticomedullary junction. A ratio <0.5 counted as a superficial cortical glomerulus; a ratio >0.5 counted as a deep cortical glomerulus.

B. Parietal Podocytes:

An unexpected but consistent finding in all kidneys was the presence of podocytic cells lining Bowman's capsule around the vascular pole, ie. parietal podocytes (figs. 3.01 - 3.10). These were defined as the presence of podocyte cell bodies on the parietal basement membrane of Bowman's capsule. In some glomeruli, pedicels and processes of visceral podocytes extended from the capillary tuft onto Bowman's capsule, up to 10um around the vascular pole, without there being a podocyte cell body on Bowman's capsule.

1. Morphology:

Parietal podocytes had the same dendritic structure as visceral podocytes (figs. 3.02 - 3.04). The cell bodies (approximately 10um diameter) had a smooth surface and sparse microvilli. Long major processes extended out from the cell body in all directions, and further branched into secondary and tertiary processes. Their cell bodies and major processes often had bossellated surface protrusions (figs. 3.03, 3.07), probably due to small aggregates of cytoplasmic granules.

The major processes of neighbouring parietal podocytes crossed over one another, and formed enclosed circles from which secondary processes branched (figs. 3.03, 3.04). Branching from all processes were thin interdigitating terminal processes or pedicels (1-2um long), with sparse overlying microblebs (fig. 3.05) or microvilli (fig. 3.06). Each pedicel interdigitated

with two pedicels derived from an adjacent parietal podocyte, analogous to visceral podocytes.

Some glomeruli, in addition to fully differentiated parietal podocytes, had dendritic cells with interdigitating major processes, but absent or incomplete pedicel formation (fig. 3.07).

2. Distribution:

Parietal podocytes were always in continuity with visceral podocytes at the vascular pole, and were related to both afferent and/or efferent arterioles. They extended from the vascular pole for variable distances, up to a maximum of 100um (fig. 3.08). This resulted in parietal podocytes occasionally encroaching close to the tubular pole (fig. 3.09). Examination of complete Bowman's capsules showed that up to two thirds of the parietal epithelium could be formed by parietal podocytes. In some cases, the area of parietal epithelium composed of parietal podocytes was irregularly-shaped such that parietal podocytes completely encircled areas of squamous parietal epithelium (fig. 3.10).

3. Parietal Podocyte / Squamous Parietal Junction:

Parietal podocytes formed distinct junctions with squamous parietal cells. Usually, a major or secondary process extended to the junction, to form a long sweeping, sometimes scalloped border with squamous cells on the outside, and branching processes and pedicels on the vascular pole side (fig. 3.04). The bordering

squamous cells often overlapped such that parietal podocyte processes and pedicels were covered by overriding squamous cells (figs. 3.02, 3.04, 3.08b). At the outer boundary, some parietal podocytes had fully formed pedicels branching from processes on the vascular pole side, and on the opposite side formed a junction typical of that seen between squamous parietal cells (fig. 3.05).

Table 3.2: Prevalence of Parietal Podocytes.

Kidney No.	SVP	SPPI	DVP	DPPI	VP	PPI
1	14	43%	16	31%	30	37%
2	10	70%	10	80%	20	75%
3	40	80%	46	67%	86	76%
4	41	88%	45	87%	86	87%
5	52	37%	29	48%	81	41%
6	50	80%	58	72%	108	76%
7	10	70%	10	60%	20	65%
8	15	73%	15	87%	30	80%
9	14	57%	13	54%	27	56%
10	11	64%	10	60%	21	62%
11	24	79%	25	76%	49	78%
12	57	67%	67	88%	124	78%
Totals/Mean	338	67%	344	68%	682	68%

SVP = Number of superficial vascular poles examined.

SPPI = Superficial parietal podocyte index.

DVP = Number of deep vascular poles examined.

DPPI = Deep parietal podocyte index.

VP = Number of vascular poles examined.

PPI = Parietal podocyte index.

4. Prevalence:

This was expressed as a parietal podocyte index (PPI), ie. the percentage of vascular poles with parietal podocytes (see table 3.2). In 10 of the 12 kidneys, the majority of glomeruli had parietal podocytes. In total, 68% of the 682 vascular poles examined had parietal podocytes; 67% of the superficial vascular poles and 68% of the deep vascular poles.

5. Discussion:

a) Origin of parietal podocytes:

The dendritic parietal cells around some vascular poles with interdigitating processes and only partial or absent pedicel formation suggests an intermediate stage in the differentiation of parietal podocytes by a process of metaplasia of squamous parietal cells.

In the developing glomerulus, capillary endothelium is necessary for visceral podocyte differentiation, in both rat (Spinelli 1974) and dog (Hay and Evan 1979). In TEM study of these same tumour nephrectomies (Gibson *et al* 1992), only occasional periglomerular capillaries were closely related to parietal podocytes. The role of endothelium and the factors which determine the morphological phenotype of the parietal epithelium of human Bowman's capsule remain unclear.

b) Are parietal podocytes "normal"?:

Glomerular microdissection and SEM permits a comprehensive view of Bowman's capsule, and has allowed the first detailed description of parietal podocytes in

apparently normal human glomeruli. Parietal podocytes are previously described only in isolated case reports of human renal diseases: haemolytic-uraemic syndrome (Wilson 1977), renal cystic dysplasia (Pardo-Mindan et al 1978), hypertension (Jones 1978), medullary cystic kidney disease (Evan and Gardner 1976), glomerulonephritis (Wilson 1977, Marcus 1977), familial glomerulocystic kidney (Rizzoni et al 1982) and autosomal dominant polycystic kidney disease (Grantham et al 1987). Parietal podocytes are also found in experimental cystic disease in rabbits (Ojeda et al 1979, Ojeda and Garcia-Porrero 1982), and in glomerular cysts in the macaque monkey (Miyoshi et al 1984).

The present study demonstrates the close relationship of parietal podocytes to the vascular pole of the glomerulus, the extent to which they line Bowman's capsule, and their presence in the majority of glomeruli. In contrast, Wilson (1977) using SEM found them in only 16% of glomeruli, but no specific effort was made to examine the vascular poles of glomeruli. Marcus (1977) using TEM estimated the extent of parietal podocytes to be approximately one sixth of the glomerular circumference. The SEM technique I have used shows that some glomeruli have a far greater extent of parietal podocyte lining.

The inability to correlate parietal podocytes with any specific pathology led Wilson (1977) to suggest that they are a feature of normal human kidney. In contrast, Jones (1979) considered parietal podocytes to be an occasional feature of diseased glomeruli, and Gaffney

(1982) dismissed them as merely a "curiosity". The nephrectomies that I have studied were performed for renal tumours and, although histologically normal parenchyma was examined, most kidneys were from an elderly population. It is therefore possible that parietal podocytes are related to ageing, or perhaps chronic ischaemic damage. I have also found parietal podocytes in kidneys removed from younger adults for persistent haematuria, transplant rejection (see chapter 5), renal artery stenosis, hydronephrosis and chronic pyelonephritis. Entirely normal human nephrectomies are not available for study.

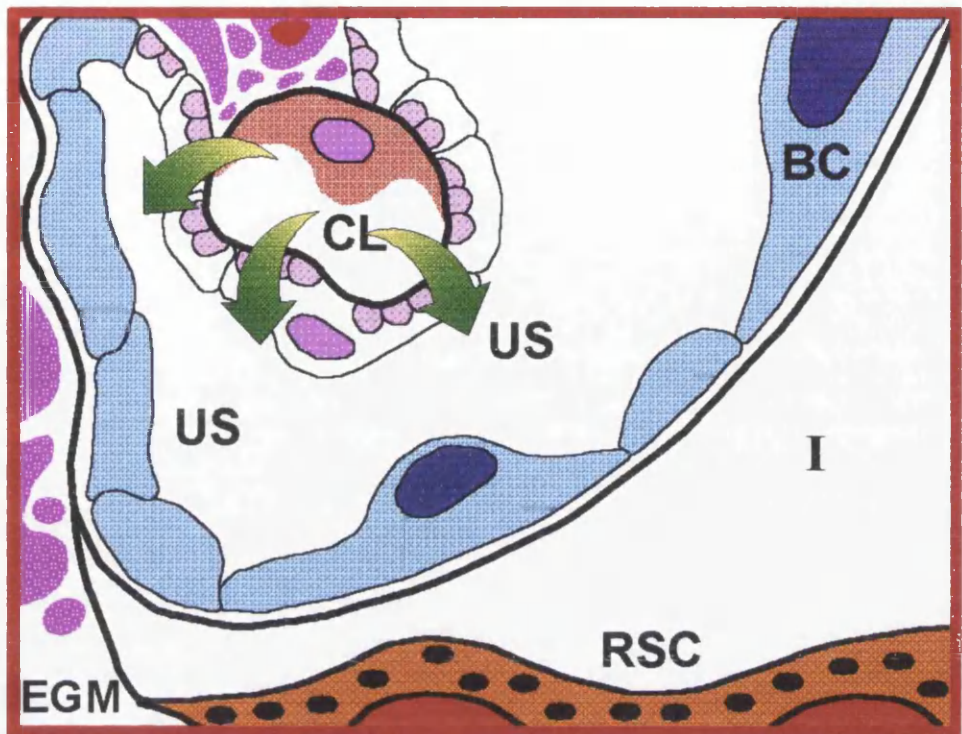
c) Physiological significance of parietal podocytes:

Parietal podocytes have interdigitating pedicels identical to those covering the capillary tuft, and TEM studies show normal slit diaphragms between parietal pedicels (Wilson 1977, Gibson et al 1992, 1994). This indicates that they are morphologically fully differentiated for filtration.

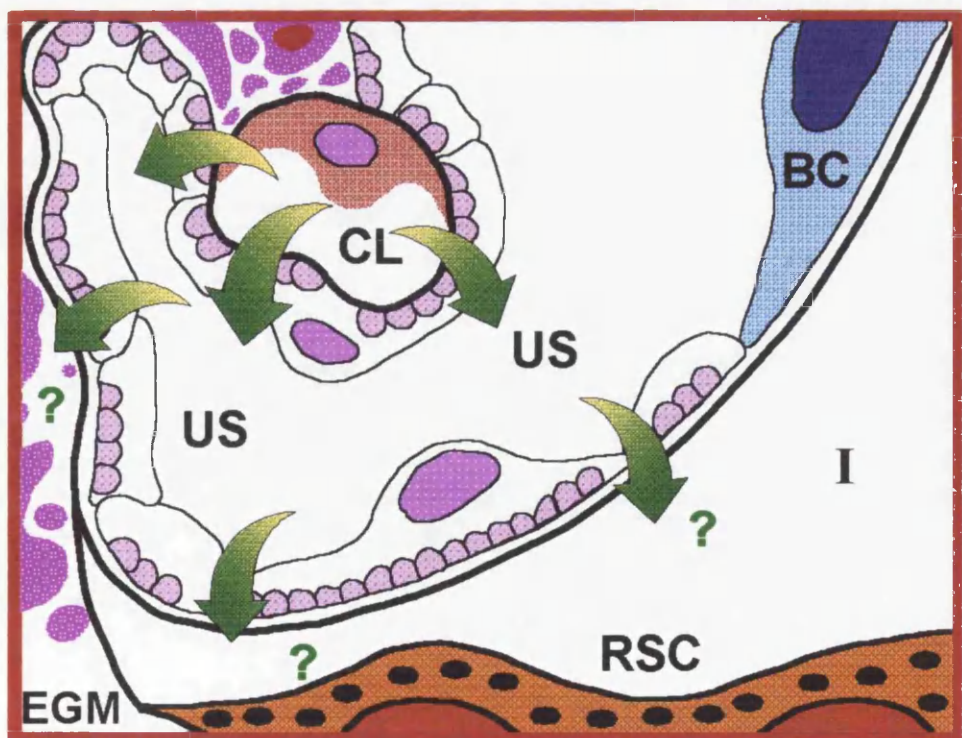
The direction of filtration across podocytes is determined by the balance of hydrostatic and oncotic pressures (Brenner et al 1971). These pressures in urinary space and the interstitium have been assessed in experimental animals. The hydrostatic pressure in urinary space is approximately 12-15mmHg (Dworkin and Brenner 1988). In the cortical interstitium, hydrostatic pressure is approximately 2mmHg, and is kept low by renal lymphatic drainage (Wilcox et al 1984). The oncotic pressure in urinary space should be close to

zero; in the interstitium, it is approximately 2-3mmHg. These pressure gradients would therefore drive filtration across parietal podocytes from the urinary space into the interstitial compartment (diagram 3.1). The permeability of the parietal layer of Bowman's capsule has been previously considered, but only in the context of squamous parietal cells (Webber and Blackbourn 1971, Taugner et al 1976). Bowman's capsule is considered as simply a passive container, to conduct the glomerular filtrate into the proximal tubule. The overlapping of squamous parietal cells, together with their typical intercellular zonulae occludentes consisting of two to five tight junction strands, will reliably separate the urinary space from the interstitium and prevent leakage of filtrate (Taugner et al 1976). However, the presence of parietal podocytes means that filtrate could move into the renal interstitium in the region of the vascular pole. The vascular pole is a vital area of the nephron, with its close anatomical relationship to the JGA (chapter 1). Pedicels cover the arterioles at the glomerular stalk and, in some rodent and primate species, extend partly onto the parietal epithelium of Bowman's capsule (Rosivall and Taugner 1986). These pedicels on Bowman's capsule are in close proximity with both extraglomerular mesangial cells and renin-secreting cells of the afferent arteriole (diagram 3.1). Tracer studies with filtered macromolecules in rodents suggest that there is fluid flow from the urinary space into the interstitium of the JGA (Rosivall and Taugner 1988). Fluid balance

Diagram 3.1: Glomerular filtration in the human glomerulus: (a) a glomerulus with no parietal podocytes on Bowman's capsule (BC); (b) a glomerulus with parietal podocytes lining Bowman's capsule around the vascular pole. The arrows indicate filtration from capillary loops (CL) into the urinary space (US), and proposed filtration across parietal podocytes from the urinary space into the extraglomerular mesangium (EGM) and the interstitial compartment (I), particularly in close association with the granulated renin-secreting cells (RSC) of the juxtaglomerular apparatus.



(a)



(b)

and the interstitial milieu in the JGA may not depend solely on the tubulo-glomerular feedback (TGF) mechanism due to macula densa reabsorption. Perihilar filtration across parietal podocytes could modulate the influence of the macula densa reabsorbate and TGF, and/or provide an additional shorter (and faster) feedback signal for controlling JGA function, including renin release (Rosivall 1990).

The extraglomerular mesangial cells of the JGA are tightly bound by basement membrane material and cell junctions (Taugner and Hackenthal 1989), which would prevent a high flow rate. The extensive parietal podocyte lining in human glomeruli implies filtration and flow from the urinary space, not only into the interstitium of the JGA, but also into the periglomerular interstitium, where there is greater potential for bulk fluid flow. This would affect not only the JGA, but also the pressures, composition and movement of fluid in the renal interstitium.

Not all glomeruli have parietal podocytes at any one point in time, and it may be that they are acquired for specific functional reasons. Both morphological and functional internephron heterogeneities are well recognised in the JGA.

d) Pathological significance of parietal podocytes:

In glomerular disease, parietal podocytes are damaged in a similar way to the visceral podocytes of the capillary tuft, showing similar fusion of pedicels in cases of glomerulonephritis and focal segmental

glomerulosclerosis (Marcus 1977, Gibson et al 1994). Filtration across parietal podocytes could influence the glomerular haemodynamic factors which are associated with glomerular hilar sclerosing lesions (see chapter 1), and thus have a role in this type of glomerular damage. Glomerular hyperfiltration may lead to excess accumulation in the glomerular root of macromolecules derived from glomerular filtrate passing through parietal podocytes covering the glomerular hilum.

The presence of parietal podocytes makes Bowman's capsule a potential site of immune complex deposition and subsequent damage in immune complex-mediated glomerulonephritis. Immunostaining has revealed a variety of immune molecules in Bowman's capsule, eg. IgG, IgA, C3 and fibrinogen in crescentic glomerulonephritis (Olsen et al 1974, Teague et al 1978, Border et al 1979, Morley 1988), IgG and albumin in advanced diabetic glomerulosclerosis (Miller and Michael 1976), C3 in type II membranoproliferative glomerulonephritis (Silva 1992) and light chains in the plasma cell dyscrasias (Hill 1992).

In a renal biopsy study using TEM (Gibson et al 1994), I have shown that immune complex deposition in Bowman's capsule occurs only in association with parietal podocytes. The deposits in Bowman's capsule were similar in size, appearance and distribution to those in the capillary tuft. In membranous glomerulonephritis for example, the immune complexes were subepithelial in both the capillary tuft and Bowman's capsule.

These capsular deposits are indirect evidence for

filtration across parietal podocytes. The identical location of deposits in both tuft and capsule does not necessarily indicate the same direction of filtration at both sites. Immune complex deposition involves more than just passive trapping within the glomerular filter. In membranous glomerulonephritis, subepithelial immune complexes form *in-situ* in relation to target antigens (eg. gp330) expressed on the basal membrane of podocytes (Kerjaschki and Farquhar 1983, Ronco *et al* 1986, Andres *et al* 1986, Verroust 1989). Parietal podocytes probably express the same antigens, which result in similar *in-situ* immune complex formation. The subepithelial position of deposits in Bowman's capsule reflects this antigen expression; it does not indicate direction of filtration, although it does imply that there is filtration of the necessary antibody.

Immune complex deposits in Bowman's capsule associated with parietal podocytes may lead to damage at the vascular pole of the glomerulus. Ruptures occur in Bowman's capsule, as well as in capillary walls, in crescentic glomerulonephritis, often at an early stage of crescent formation (Bohman *et al* 1974, Olsen 1974, Silva and Verani 1984, Boucher *et al* 1987, Lan *et al* 1992). Defects in Bowman's capsule are also described in membranous glomerulonephritis (Prescott *et al* 1993). The specific perihilar rupture of Bowman's capsule reported in two cases of anti-glomerular basement membrane antibody disease (Morley 1988) could also have been related to immune-mediated damage associated with parietal podocytes at the vascular pole.

Furthermore, in experimental glomerulonephritis, interstitial inflammation initially appeared around the hilar arterioles, and spread out from the vascular pole area into the entire cortical interstitium (Lan et al 1991 1992, Eldridge et al 1991). Damage to Bowman's capsule occurred at sites of prominent and activated interstitial inflammation (Lan et al 1992). In human renal disease, immune complex deposition in Bowman's capsule associated with parietal podocytes could be responsible for antigen-directed leucocyte attraction. Likewise, leakage of antigens, chemotactic factors and cytokines from an inflamed glomerulus into the extraglomerular compartment via parietal podocytes around the vascular pole, could be important in the migration, accumulation and activation of inflammatory cells in the perihilar interstitium. Parietal podocytes could thus contribute to glomerular and interstitial damage, and hence to the chronic renal impairment of kidney disease.

C. Podocyte Connections between the Capillary Tuft and Bowman's Capsule:

The glomerular tuft is traditionally thought to be anchored at the vascular pole by the arterioles, mesangium and the epithelium of the viscero-parietal junction, with no other connections to Bowman's capsule. In this study, I found additional "tuft-to-capsule" cell connections, mostly related to the presence of parietal podocytes, in all 12 kidneys.

Around the vascular pole, some of the larger processes of parietal podocytes had been in contact with the capillary tuft, and were broken when the tuft was microdissected from Bowman's capsule (fig. 3.04). Examination of the vascular pole area of the isolated capillary tufts revealed similar broken podocyte processes. These were therefore "bridging processes" across the urinary space, which were seen intact if glomerular microdissection was not performed (fig. 3.11). They often arose from the periphery of parietal podocytes, at their junction with squamous parietal cells (fig. 3.08b).

In this way, a parietal podocyte with processes and pedicels lining Bowman's capsule also had processes and pedicels on a glomerular capillary. Likewise, a visceral podocyte on the capillary tuft could have processes and pedicels on Bowman's capsule. In 100 glomeruli with parietal podocytes, I found a total of 120 bridging processes in 55 glomeruli; 46% (55 of 120) originated from cell bodies on Bowman's capsule and 54%

(65 of 120) arose from cells on the capillary tuft (see fig. 3.12b).

Sometimes podocyte cell bodies bridged across the urinary space (fig. 3.11); these "bridging podocytes" had processes and pedicels on both the parietal and glomerular basement membranes. This was also observed by Marcus (1977), and is analogous to the way visceral podocytes regularly "straddle" adjacent capillary loops. Wilson (1977) also describes similar broken processes projecting from parietal podocytes into the urinary space.

In just 2 of the 12 kidneys, occasional small discrete patches of podocytic cells were found within the parietal epithelium of Bowman's capsule, in <1% of glomeruli. These were separate from the parietal podocytes around the vascular pole, and were sometimes closer to the tubular pole. They were composed of dendritic cells with processes and a variable degree of pedicel differentiation (fig. 3.13). Their boundary was marked by curved, overlapping squamous parietal cells (figs. 3.13, 3.14), similar to the junction between parietal podocytes and squamous parietal cells described earlier. These were also the site of bridging podocyte connections between tuft and capsule, broken during glomerular microdissection (fig. 3.14).

Finally, a very occasional thin connecting podocytic process was seen adjacent to a tubular pole (fig. 3.15), but with no related parietal podocytes on Bowman's capsule.

Such tuft-to-capsule connections will presumably

restrict glomerular mobility within Bowman's capsule. The individual lobules of a glomerulus are considered relatively independent of one another with respect to mobility, and podocyte cell bodies and processes are not thought to bridge across capillary loops of two separate lobules. The presence of tuft connections to Bowman's capsule may restrict tuft mobility. They also raise the possibility of movement of podocytes between the tuft and Bowman's capsule, across the urinary space.

D. The Vascular Pole:

In each kidney, at least 20 and up to 124 vascular poles were examined (see table 3.2, page 37).

1. Afferent and Efferent Arterioles:

Vascular poles had at least two arterioles passing through Bowman's capsule (figs. 2.02, 3.01); in most cases there was a larger arteriole (luminal diameter 25-35 μ m) and a smaller vessel (approximately 15 μ m in diameter).

Histological and micro-angiographical studies of normal human kidney (Edwards 1956, Ljungqvist and Lagergren 1962) have shown that in most cortical glomeruli, the efferent arteriole is narrower than the corresponding afferent arteriole. Only in juxtamedullary glomeruli are efferent arterioles of larger calibre and as wide as corresponding afferent vessels. Similar observations have been made in a wide range of mammalian species, including monkey (Nopanitaya 1980), dog (Beeuwkes 1971, Barger and Herd 1971), cat (Marais 1987), rabbit (Bankir and Farman 1973) and rat (Murakami 1972, Evan and Dail 1977, Kriz and Bachmann 1985). A larger diameter afferent arteriole is therefore a consistent finding.

Previous SEM studies of the rat vascular pole (Frank and Kriz 1982) used the thicker wall of the afferent arteriole to identify it, on the basis that it has more smooth muscle in its wall. I found no major difference in vessel wall thickness between afferent and efferent arterioles (apart from cases with multiple efferent

vessels, see below). Histological studies describe human efferent vessels as "well-formed ... which resemble in all respects those found in afferent arterioles" (Smith 1956). Similarly in rodents, the media of the proximal efferent arteriole has a thickened cuff of several layers of branched and overlapping smooth muscle cells (Barajas and Latta 1963, Gattone et al 1984, Kriz and Bachmann 1985). It is likely therefore that, at the vascular pole, there will be little difference in wall thickness between the afferent and efferent arterioles. In addition, the media of both arterioles merges with extraglomerular mesangial cells in the region of the JGA (Barajas and Latta 1963, Rosivall 1990) making wall thickness difficult to assess. Differences in luminal diameters would seem to be a more reliable parameter to distinguish these vessels in such SEM studies of the vascular pole.

The differing luminal diameters of afferent and efferent arterioles may be important in determining hydrostatic pressures in the glomerular capillary tuft and in the post-glomerular peritubular capillary plexus. The wider afferent arteriole will offer less resistance, transmitting higher pressures to the glomerulus for filtration. The narrow efferent arteriole will offer increased resistance, producing a greater pressure drop, helping to lower pressure in the peritubular capillary plexus, where fluid reabsorption occurs. A wider efferent arteriole in juxta-glomerular nephrons will help maintain pressure in the long descending vasa rectae which supply the medulla.

2. Number of Vessels:

I found a minority of vascular poles (less than 5%) had three vessels, due to the presence of two efferents, with thinner walls compared to single efferent arterioles (fig. 3.12a). In a serial section study of normal human kidney, Smith (1956) described <5% of glomeruli as having multiple efferent capillaries arising directly from glomerular capillaries. Murakami et al (1985) found multiple efferents in just over 1% of 3000 vascular casts of human glomeruli; 2 tufts had 4-5 efferent vessels and 2 tufts had double afferent arterioles. I found no examples of more than one afferent arteriole. Multiple efferent vessels may be more frequent in elderly human kidney compared with foetal and young adult kidney (Hitomi et al 1987). Double efferent arterioles are also described in the rat, with a similar low frequency of 5-6% (Murakami et al 1971, Frank and Kriz 1982). The rarity of multiple efferent glomerular vessels probably excludes a major functional significance.

An alternative explanation for multiple efferent vessels would be early branching of the efferent arteriole before it penetrates Bowman's capsule. Vascular cast studies in the rat (Murakami et al 1971, Evan and Dail 1977, Weinstein and Szyjewicz 1978) show that the efferent arterioles of outer and middle cortical glomeruli can run a very short course before dividing to form the peritubular capillary plexus, close to or surrounding the parent glomerulus.

3. Endothelial Morphology:

It has been suggested in rodents that there is more prominent bulging of endothelial nuclei in the proximal efferent arteriole of inner cortical glomeruli compared with the afferent vessel (Kriz and Bachmann 1985, Gattone *et al* 1984). I found no specific features of human arteriolar endothelium that helped differentiate afferent and efferent vessels. The abrupt transition to extensively fenestrated endothelium enabled identification of the beginning of the glomerular capillary. Endothelial fenestrations were not noted in the juxtaglomerular portions of either arteriole, in contrast to their presence in the afferent arteriole in rodents (Casellas 1986, Rosivall 1990, see also fig. 4.03). I also found no evidence of an "endothelial sphincter" at the juxtaglomerular portion of the afferent arteriole, as described in monkey kidney (Nopanitaya 1980). It appears that there are inter-species variations in the detailed morphology of this vitally important site.

4. Extraglomerular Mesangium:

The arterioles were separated by a variable extraglomerular mesangium region, ranging from less than 5um up to 40um (fig. 3.01). This measurement showed no relationship to the depth of the vascular pole within the cortex, and it is unlikely that it reflects JGA function since the exact level of fracture through the extraglomerular mesangium is variable.

E. The Tubular Pole:

1. Anatomical Variations:

In the 12 kidneys studied, a total of 678 tubular poles were examined. The transition from the squamous parietal cells of Bowman's capsule to proximal tubule-type cells with a brush border of microvilli was invariably abrupt. However, the exact site of this transition was variable (see table 3.3).

Table 3.3: Tubular Pole Variations.

Kidney No.	n	BB at TP	NS	BB on BC	BB patch
1	30	23	4	3	5
2	20	16	2	2	3
3	96	78	9	9	10
4	80	68	8	4	8
5	82	68	5	9	4
6	107	84	12	11	12
7	21	17	2	2	2
8	10	8	1	1	1
9	18	14	3	1	3
10	15	11	2	2	3
11	80	65	8	7	7
12	119	95	20	4	8
Totals/ (%)	678	547(81%)	76(11%)	55(8%)	66(10%)

n = Number of tubular poles examined.

BB at TP = Brush border at anatomical tubular origin.

NS = Neck segment of squamous cells at start of tubule.

BB on BC = Tubular cells extend onto Bowman's capsule.

BB patch = Patch of tubular cells next to tubular pole.

In the majority of glomeruli (over 80%), the transition to cells with a brush border was at the anatomical tubular origin (fig. 3.16). At 8% of tubular poles, there was tubularization of Bowman's capsule, with a brush border continuous with that of the proximal tubule extending up to 30um into the parietal epithelial layer (fig. 3.17). In a further 11% of tubular poles, no brush border was visible at the tubular orifice (fig. 3.18). When the latter were seen in longitudinal section (fig. 3.19a), there was a proximal tubule neck segment. These formed straight tubes in the line of the glomerular poles, up to 60um long, and lined by squamous cells with single cilia (identical to squamous parietal cells). Occasional brush border cells were present within these neck segments (fig. 3.19b), before the start of the definitive proximal tubule brush border.

In a mean of 10% of glomeruli (table 3.3), close to the tubular pole were small groups (figs. 3.16, 3.18) or individual parietal cells (fig. 3.17) which had a fully developed brush border of long microvilli (about 2um long), as well as a single cilium. The SEM appearance of these cells was identical to the cells lining proximal tubules, and these brush border patches also constitute tubularization of Bowman's capsule. They were completely surrounded by squamous parietal cells, forming islands of tubularization, in contrast to the tubular cells which extended into Bowman's capsule in continuity with the proximal tubule. Some of the cells in these patches had only a partial brush border covering, suggesting a transitional stage of

differentiation between squamous cells and complete tubularization.

Finally, in just one of the 12 kidneys (no.6), a very occasional tubular pole (3 out of 107) appeared to have two separate orifices branching out in opposite directions, both lined by cells with a luminal brush border (fig. 3.21), ie. "double-opening" tubular poles.

2. Discussion:

a) Tubularization of Bowman's capsule:

Tubularization of the parietal epithelium of Bowman's capsule around the tubular pole has been previously described in normal human kidney (Ward 1970, Wilson 1977, Haensly 1987), and in human disease eg. hydronephrosis (Risak 1928), pyelonephritis (Risak 1928, Helmholtz 1935), diabetes (Schutz 1924, Finckh and Joske 1954, Honey *et al* 1962), glomerulonephritis (Hutt *et al* 1958), acute tubular necrosis (Solez *et al* 1979) and acute renal failure (Jones 1982, Kanel and Peters 1984). Ultrastructurally, the parietal cells with a brush border fully resemble proximal tubule cells (Wilson 1977). Haensly (1987), in an autopsy study using light microscopy, found tubularization in approximately 50% of human kidneys, and in only 4% of their glomeruli. Counting both tubular poles with a brush border extending into Bowman's capsule, and those with an adjacent brush border patch, I have found tubularization in all 12 kidneys, affecting a mean of 18% of glomeruli (see table 3.3). The technique of SEM, together with specific examination of the tubular pole, provides a far

more accurate estimation of this phenomenon.

A similar pattern of tubularization of the parietal epithelium is seen extensively in the mouse (Selye 1939, Crabtree 1940 1941, Dunn 1948, Dietert 1967, Melis et al 1974, Carpino et al 1976, Barberini et al 1984, Ahmadizadeh et al 1984, Lee et al 1993), and is also described in the rat (Foley et al 1964, Andrews 1981, Haensly et al 1982, Haley and Bulger 1983, Castelletto and Goya 1990), pig (Lee et al 1993) and a wide range of other mammals including cat, dog, mink and woodchuck (Helmholz 1935).

Tubular parietal cells have also been demonstrated using histochemical staining for brush border enzymes, eg. alkaline phosphatase, succinic dehydrogenase and gamma-glutamyl transpeptidase, in mouse and rat (Dunn 1948, Foley et al 1964, Briere et al 1983) and in developing human foetal nephrons (Briere 1986). Similar to my findings in adult kidney, Briere (1986) found alkaline phosphatase-positive parietal cells in continuity with those of the proximal tubule and also as aggregates separate from the tubular orifice.

Ward (1970) suggested that tubularization of Bowman's capsule may be a consequence of maldevelopment. Briere (1986) suggested that tubular parietal cells in the human foetal nephron may be remnants of the columnar cells which form the primitive lower portion of the S-shaped body; these cells represent the presumptive parietal epithelium and most progressively flatten to become squamous parietal cells (Gruenwald and Popper 1940). Interestingly, the latter study found that the

parietal epithelium remains columnar longest near the tubular pole, ie. where tubularization is found in the adult.

Most studies have regarded tubularization of Bowman's capsule as metaplasia, ie. transformation of the squamous parietal epithelium. My finding of intermediate cell types is consistent with this, and such intermediates were also described in rat (Andrews 1981, Haley and Bulger 1983, Lee et al 1993) and pig (Lee et al 1993). Tubular metaplasia is also suggested by its apparent response to varying hormonal stimuli (Selye 1939, Crabtree 1940 and 1941, Dunn 1948, Deitert 1967, Carpino et al 1976, Barberini et al 1984).

There is good evidence that tubular parietal cells can function in reabsorption. Deitert (1967) showed in the mouse that their absorption of horseradish peroxidase is identical to proximal tubular cells. The presence of brush border enzymes on their luminal membrane (Briere et al 1983, Briere 1986) indicates phosphate and amino acid transport.

Tubularization of the parietal epithelium could therefore have functional significance. Andrews (1981) described a dramatic increase in tubularization in the remaining kidney of rats five months after unilateral nephrectomy. Tubularization also increased in rats given diets high in protein or low in potassium (Foley et al 1964). Haensly et al (1982) reported greater tubularization in spontaneously hypertensive rats compared with a normotensive strain. There is also an increase in tubularization in aging rats (Foley et al

1964, Haensly et al 1982, Haley and Bulger 1983), proportional to the degree of glomerulosclerosis (Castelletto and Goya 1990).

Thus, by functioning in the uptake and modification of glomerular filtrate, tubularization may be an attempt to increase functional capacity in response to an increase in workload or functional deterioration of the nephron. In the present study, the prevalence of tubularization showed no correlation with patient age, and it occurred randomly in glomeruli from all depths of the cortex. It may nevertheless be relevant that these kidneys, whilst histologically normal, are mostly from an elderly population.

Finally, irrespective of functional significance, the morphological diversity of the parietal epithelium, including tubular parietal cells and parietal podocytes, reflects a pluripotency in keeping with its embryological origin. Proximal tubular, parietal and visceral epithelial cells are all derived from the same nephrogenic vesicle epithelium (Risak 1928, Zamboni and DeMartino 1968, Reeves et al 1978, Spitzer 1985).

b) The neck segment:

I have found a tubular pole neck segment in a minority of human glomeruli (11%). It is not regarded as a feature of the normal human kidney (Ward 1970), though it has been previously described to be present in "certain nephrons" (Bulger 1983).

A neck segment of the proximal tubule is a constant feature of the kidneys of lower vertebrates such as fish

and amphibia (Edwards and Schnitter 1933, Youson and McMillan 1970b, Lacy *et al* 1987, Sakai *et al* 1988). The lining cells have many cilia and microvilli, and since the hydrostatic pressure gradients are much lower in the nephrons of these species compared with mammals, this specialised ciliated segment may be important in maintaining flow into the proximal tubule of the nephron.

In mammals, only the rabbit has a neck segment in the majority of glomeruli (Schonheyder and Maunsbach 1975, Ojeda and Icardo 1991, Lee *et al* 1993). This is lined predominantly by squamous cells identical to squamous parietal cells, with each cell having a single cilium only. Most rabbit neck segments also contain tubule-like cells and intermediate cells (Ojeda and Icardo 1991), interpreted as metaplastic transformation of the squamous cells. These features are essentially identical to the neck segments I have observed in human kidney. It has been suggested that the lining cells of the rabbit neck segment may be capable of altering the luminal diameter, and so influence single nephron glomerular filtration rate (Schonheyder and Maunsbach 1975), but this is unproven. In normal human kidney, the presence of a neck segment in a small minority of nephrons may simply be an anatomical variation with no specific functional significance.

c) The "double-opening" tubular pole:

The appearance of two separate orifices at occasional tubular poles in one of the 12 kidneys is of uncertain

significance. Two tubular orifices from a single Bowman's capsule has been described in a case of so-called "adenomatoid transformation", a stratified columnar metaplasia of the parietal epithelium seen rarely in association with neoplastic disease (Knowlson and Cameron 1979). The two tubular orifices were considered a manifestation of epithelial overgrowth, producing blind-ending diverticula. It is possible that one of the "double-openings" I have observed is also a blind-ending diverticulum, arising simply due to aberrant development.

3. Tubular Pole Diameters:

For six of the kidneys, the maximum diameter of tubular pole orifices was measured (see table 3.4).

In these kidneys, a total of 486 tubular poles were measured. The mean tubular pole diameter was 32um (standard deviation = 8.19um, range 12-62um).

To determine if there was any correlation between the tubular pole diameter and the presence of parietal podocytes, mean tubular pole diameters for the glomeruli with parietal podocytes, and for the glomeruli with no parietal podocytes were also calculated. As table 3.4 shows, the tubular pole diameter was unaffected by the presence or absence of parietal podocytes.

Table 3.4: Tubular Pole Diameters in Tumour Nephrectomies.

Kidney No.	n	TPD range	TPD(PP)	TPD(NoPP)	Mean TPD
3	82	15 - 48	29	29	29
4	70	22 - 60	35	32	35
5	73	16 - 42	29	29	29
6	92	13 - 56	35	34	35
11	67	15 - 62	34	36	34
12	102	12 - 56	29	29	29
Totals/Mean	486	12 - 62	32	32	SD=8.19

n = Number of tubular poles accurately measured.

TPD range = Range of tubular pole diameters (um).

TPD(PP) = Mean tubular pole diameter (um) in glomeruli with parietal podocytes.

TPD(NoPP) = Mean tubular pole diameter (um) in glomeruli with no parietal podocytes.

Mean TPD = Mean tubular pole diameter (um) for all the glomeruli.

SD = Standard deviation.

F. Squamous Parietal Cells:

1. Morphology:

This was the commonest cell-type in the parietal layer of Bowman's capsule. The cells were polygonal, and had nuclear bulges, single (or rarely two) cilia (about 5-10um long) and variable numbers of microvilli (fig. 3.22). The microvillous covering ranged from a complete covering of short microvilli to a very scanty number of rudimentary microvilli mainly at the cell boundaries. Clusters of around 4-6 nuclear bulges were often seen near both the urinary and vascular poles (figs. 3.15, 3.24). In the rest of Bowman's capsule, nuclear bulges were more evenly distributed.

Many squamous parietal cells possessed small bulges and bossellated protrusions, ranging from 1-5um in size, which appeared like bulging intracellular granules (figs. 3.22, 3.23). The bossellated protrusions were sometimes indented resembling "pore-like" openings (fig. 3.23), and in one such opening several intracellular granules could be seen. A very occasional Bowman's capsule contained an inflammatory cell lying on the squamous parietal epithelium (fig. 3.24).

2. Discussion:

These findings are essentially in agreement with previous SEM studies of normal human kidney (Webber and Lee 1974, Andrews 1975, Arakawa and Tokunaga 1977, Wilson 1977) and other species (Andrews and Porter 1974, Bulger *et al* 1974). The variability of the surface

microvilli observed suggests they are transitory dynamic structures, perhaps responding to local conditions.

Single cilia have been shown with TEM to possess an irregular microtubule skeleton (Andrews 1975). Webber and Lee (1974) suggested a possible sensory function for these cilia. They are thought to represent primary cilia, ie. providing an alternative pathway for expression of centriole activity after a cell has been subjected to mitotic inhibition (Rash *et al* 1969).

The bossellated bulges are too large to be the surface indentations described by Webber and Lee (1974) and interpreted as micropinocytotic vesicles. Their size suggests that they are formed by intracellular granules or lysosomes, and they are similar to the bossellated protrusions described earlier on parietal podocytes. The "pore-like" openings may represent either an exo- or endocytotic process, or more likely an artefact of tissue preparation.

C H A P T E R 4

CHAPTER 4: COMPARATIVE ANATOMY OF THE PERIPOLAR CELL

A. Source of Tissue:

Five laboratory species (rat, guinea pig, hamster, mouse and rabbit) were given terminal anaesthesia (intraperitoneal sodium pentobarbital, 50mg/kg) and the kidneys fixed by perfusion through the abdominal aorta using 2% buffered glutaraldehyde. Ovine, porcine and bovine kidneys were obtained from recently-slaughtered animals at a commercial abattoir. Kidneys from dog, goat and baboon were obtained immediately after sacrifice, either by terminal anaesthesia (dog and baboon) or by captive bolt (goat). Also, the 12 human kidneys removed for renal tumours (chapter 3) were studied. In all species, perfusion fixation and SEM preparation was performed, as described in chapters 2 and 3.

The number of animals for each species is shown in table 4.2 (page 69). In each species, I examined all Bowman's capsules in at least two slices per kidney; not less than 70 Bowman's capsules were studied and the presence of vascular poles and peripolar cells were recorded. A peripolar cell index (PCI) was derived by expressing the number of vascular poles with at least one peripolar cell as a percentage of the total number of vascular poles. For vascular poles which contained peripolar cells, the mean number of peripolar cells per vascular pole (PC_m) was also determined.

B. Peripolar Cell Morphology:

In all species, peripolar cells were found throughout the depth of renal cortex, adjacent to the arterioles of the vascular pole (figs. 4.01 - 4.10), ie. at the junction between podocytes and parietal epithelial cells. Peripolar cells were distinguishable from both parietal cells and podocytes and fell into two main groups: dendritic peripolar cells were elongated with cell processes; globular peripolar cells were rounder and had no processes.

1. Dendritic Peripolar Cells:

This type (figs. 4.01 - 4.04) was universal in rodent, dog and baboon and formed the majority in porcine, bovine, canine and human kidney; they were never seen in sheep or goat (table 4.2). Dendritic peripolar cells had fusiform, ovoid or pyramidal cell bodies (3-10um in diameter). The cell bodies of some guinea pig peripolar cells (fig. 4.04) were larger than those in other species (see table 4.1). Unlike podocytes, dendritic peripolar cells had variable microvilli, longer and more numerous than those on parietal epithelial cells. Underlying the microvilli, there was an essentially smooth cell body surface (figs. 4.02 - 4.04). Single cilia, similar to those on squamous parietal cells, were found on dendritic peripolar cells in the guinea pig (fig. 4.04) and pig, but not in other species. Most cells had one or at most two tapering non-branching processes which curved around the vascular pole (figs.

4.01, 4.03). Interdigitating pedicels, characteristic of podocytes, were not a feature of dendritic peripolar cells. Some peripolar cells lay in the niche between the afferent and efferent vessels with processes extending in opposite directions towards both vessels. When there was more than one dendritic peripolar cell, the processes from different cells sometimes overlapped. Some peripolar cell processes had a short, blunted, fractured ending, apparently having been broken during glomerular microdissection (fig. 4.01). Occasionally, a distinct cell body and cell process was not apparent and the entire cell encircled most of the circumference of an arteriole (figs. 4.02, 4.04b).

2. Globular Peripolar Cells:

These were abundant and the only type found in sheep and goat kidney (figs. 4.05 - 4.07), and formed a minority in porcine, bovine and human kidney. None were found in rodents, dog or baboon (table 4.2). Several such cells often formed an incomplete cuff around the vascular pole. They were mainly spherical or ovoid (figs. 4.05, 4.06), without cell processes, and were larger than dendritic peripolar cells (10-30um in diameter). Characteristically, their surface was bossellated due to numerous large cytoplasmic granules. These were visible in cells which had been cracked open by the tissue processing (fig. 4.08). The granules were faceted, presumably secondary to their close packing. Some peripolar cells in sheep and goat kidney had a well-delineated smooth area, possibly due to

displacement of granules by the underlying nucleus (fig. 4.06). Occasional cells had scanty short microvilli, but most had no surface micropressions or cilia.

3. Intermediate Forms:

A summary of the morphological characteristics of the cell types distinguished at the vascular pole is given in table 4.1. Some cells were also identified with intermediate features.

a) Dendritic / globular peripolar cells: An occasional rat dendritic peripolar cell, with cell processes around

Table 4.1: Characteristic morphological features of glomerular epithelial cells.

	Pod	DPC	GPC	PEC
Size (um)	rodent 5-10, others 10-20	guinea pig 5-10 others 3-6	10-30	10-20
Surface	ruffled	mostly smooth, some irregular	bossellated	mostly smooth
Processes	many, branching	max. of 2, no branching	no	no
Pedicels	yes	none	no	no
MV	few, short	none, or many and long	very few, short	variable, short
SC	no	guinea pig, pig	no	yes
NB	no	no	no	yes

Pod = podocyte, DPC = dendritic peripolar cell, GPC = globular peripolar cell, PEC = squamous parietal cell, MV = microvilli, SC = single cilia, NB = nuclear bulges

the arteriole, had a bossellated cell body due to cytoplasmic granules). Also in rodents (particularly guinea pig), some peripolar cells were plumper and ovoid, with no cell processes (fig. 4.04). Their surface was similar to other dendritic peripolar cells (ie. non-bossellated with microvilli), but some contained granules identical to those found in globular peripolar cells (fig. 4.10).

In the sheep and goat, occasional peripolar cells were elongated, similar to dendritic peripolar cells, but they lacked cell processes and had a bossellated surface typical of globular peripolar cells (fig. 4.07).

b) Peripolar cell / parietal cell: In sheep and goat, there were large polygonal cells which were flat and elongated, like squamous parietal cells, but which lacked nuclear bulges and cilia and had a bossellated surface typical of globular peripolar cells (fig. 4.08). Also, otherwise typical parietal cells sometimes had a focally bossellated surface, presumably due to small numbers of granules (fig. 4.06).

In rodents, there were cells which at one end resembled a dendritic peripolar cell and at their other end resembled a squamous parietal cell (fig. 4.09).

c) Peripolar cell / podocyte: In rodents, there were occasional dendritic cells which did not form pedicels, but which had ruffled cell bodies with dimensions similar to the podocytes on the glomerular tuft. In some cases, I had difficulty distinguishing between these two cell types, especially when examining cells at the vascular pole of isolated glomerular tufts.

C. Peripolar Cell Quantification:

Table 4.2: Quantification of vascular poles and peripolar cells in mammalian kidney.

<u>Species</u>	<u>1</u>	<u>2</u>	<u>3</u>	<u>4</u>	<u>5</u>	<u>6</u>	<u>7</u>	<u>8</u>	<u>9</u>
Guinea pig	2	50	23	32	46%	100%	0%	1.4	3
Hamster	2	33	13	14	39%	100%	0%	1.1	2
Mouse	2	20	9	12	45%	100%	0%	1.3	2
Rat	10	579	278	310	48%	100%	0%	1.1	4
Rabbit	2	39	9	10	23%	100%	0%	1.1	2
Dog	1	22	3	3	14%	100%	0%	1.0	1
Baboon	1	24	11	12	46%	100%	0%	1.1	2
Human	12	322	21	21	6.5%	86%	14%	1.0	1
Cow	3	37	4	5	11%	60%	40%	1.3	2
Pig	3	55	12	14	22%	57%	43%	1.2	3
Sheep	3	52	43	67	84%	0%	100%	1.6	10
<u>Goat</u>	<u>1</u>	<u>35</u>	<u>35</u>	<u>100</u>	<u>100%</u>	<u>0%</u>	<u>100%</u>	<u>2.9</u>	<u>11</u>

Column 1: No. of animals studied.

Column 2: No. of vascular poles.

Column 3: No. of vascular poles with peripolar cells

Column 4: Total no. of peripolar cells.

Column 5: Peripolar cell index (PCI%).

Column 6: Percentage of dendritic peripolar cells.

Column 7: Percentage of globular peripolar cells.

Column 8: Mean no. of peripolar cells/vascular pole
(PC_m).

Column 9: Max. no. of peripolar cells at a vascular pole.

The results for the 12 species studied (table 4.2) show marked interspecies variation in peripolar cell numbers. Peripolar cells were most numerous in those species in which they were all of the globular type (PCIs of 84% and 100% for sheep and goat respectively). In the goat there was a mean of almost three per glomerulus (PC_m = 2.9), and a maximum of 11 at one vascular pole. Species with exclusively dendritic peripolar cells had fewer (most PCIs around 40-45%), with at most 3 (guinea pig) or 4 (rat) peripolar cells at a vascular pole. Rabbit kidney (PCI = 23%) contained notably fewer than the other rodents. Canine, bovine and human peripolar cells were sparse (PCIs = 14%, 11% and 6.5% respectively). In all species, peripolar cells were found adjacent to both the afferent and efferent arterioles. When this was quantified in the rat, the majority (about 60%) were related to afferent arterioles. Only in sheep and goat were peripolar cells sufficiently numerous to form a cuff around both arterioles.

D. Discussion:

1. Peripolar Cell Structure:

The existence of the peripolar cell as a specific cell type has recently been questioned (Morild et al 1988, Nakajima et al 1989), primarily because peripolar cell granules are similar to granules which occur in podocytes and parietal epithelial cells in glomerular disease. In this study, I have shown that peripolar cells are clearly distinguishable from podocytes and parietal epithelial cells by their surface morphology, and that they are common to a range of mammalian species. This confirms that they are a morphologically distinct glomerular epithelial cell.

For descriptive purposes, peripolar cells can be separated into two main types, dendritic and globular, on the basis of their variable size, shape and granule content. Both types have an apical membrane bulging into the urinary space, suitable for sampling of, or secretion into the glomerular filtrate. The microvillous apical surface could detect alterations in the concentration of electrolytes or hormonal factors entering the urinary space.

The dendritic peripolar cell, with its cell body and (sometimes overlapping) processes encircling around the glomerular arterioles, has a structure ideally suited to sense the pressure or to react to changes in the calibre of the glomerular root (ie. a "baroreceptor"-type function). Peripolar cell contractility is feasible, but the cells are in a mechanically disadvantageous

position to alter vessel luminal sizes. The vascular pole constitutes an opening in Bowman's capsule, and the distending forces of intracapsular pressure will tend to expand this opening. Ultrastructural studies in the rat have shown specialised organization of parietal cells and basement membrane around the vascular pole, forming "microligament structures" to provide active wall tension to counteract these distending forces (Mbassa et al 1988). These studies described peripolar cells as having prominent basal furrows containing cytoskeletal bundles of actin microfilaments, a feature described by others (Ryan et al 1982), leading to the suggestion that peripolar cells may also perform some mechanical function in glomerular dynamics (Mbassa et al 1988). Peripolar cells surround afferent arterioles at its myosin-negative and renin-positive juxtaglomerular portion (Taugner et al 1987, Rosivall 1990), i.e. where the vessel is mechanically passive, with limited capability for vasoconstriction. Such a non-contractile segment would be suitable for function as a juxtaglomerular mechanoreceptor, responding to pressure variations which could be transmitted to surrounding peripolar cells. Stretching of the peripolar cell could lead to its activation through membrane depolarisation, analogous to other cell-types.

Dendritic peripolar cells resemble podocytes rather than parietal epithelial cells. By comparison, globular peripolar cells are morphologically closer to parietal epithelial cells and there are cells intermediate between peripolar cells and both parietal cells and

podocytes. Interestingly, an SEM study of neonatal lamb kidney reported some otherwise typical peripolar cells having projections resembling pedicels, characteristic of podocytes (Thumwood et al 1989); this was not observed in the present study. In an SEM study of the elasmobranch glomerulus, cuboidal cells with a morphology intermediate between squamous parietal cells and podocytes were described around the vascular pole (Lacy et al 1987). Likewise, Youson and McMillan (1970a) described in the lamprey kidney a gradual transition from squamous parietal cells, to "spherical podocytes" with tight junctions, to "columnar podocytes" with pedicels, to typical flattened podocytes. Thus, although the peripolar cell is a distinctive glomerular cell type, it is situated at the junction between two other epithelial cell types. Like other junctions in epithelia, (eg. the transformation zone of the cervix) there may be a gradual change of differentiation from one cell type to another, with the formation of intermediates.

2. Peripolar Cell Granules:

Globular peripolar cells have a bossellated surface due to their numerous cytoplasmic granules. Using a combination of SEM and subsequent sectioning, it has been previously shown that the globular peripolar cells of sheep are all granulated (Kelly et al 1990), whereas in the rat most of the dendritic peripolar cells contain no granules (Downie et al 1992). This accounts for the marked discrepancy between rodent dendritic PCIs

obtained by SEM (40-45%) and rodent PCIs obtained by light microscopy (<5%, Gall et al 1986, Taugner and Hackenthal 1989, Downie et al 1992). Non-granulated dendritic peripolar cells are identified by SEM, but are not seen by light microscopy. Gall et al (1986) described "inconspicuous" granulation in rodents; in one mouse species, small peripolar cells were identified only with careful transmission electron microscopy. The degree of granulation of the peripolar cell appears to govern its surface appearance. The finding of peripolar cells with morphology intermediate between dendritic and globular cells suggests that acquisition of numerous granules results in a morphological change from dendritic to globular cells; the functional significance of such a change remains unclear.

The marked interspecies variation in peripolar cell granulation has been confirmed, and the nature of peripolar cell granules remains unclear. I found no convincing evidence of exocytosis, although apical cup-like invaginations interpreted as exocytosis were described in a recent SEM study of the sheep peripolar cell (Thumwood et al 1993). In rodents, their sparse granules do take up exogenous tracers consistent with lysosomes (Taugner and Hackenthal 1989). This does not, however, exclude a secretory process, since other known secretory granules have lysosomal properties, including renin granules (Taugner et al 1985, Morild et al 1988). Peripolar cell granules are morphologically identical to those in podocytes and parietal cells in states of proteinuria (Hill et al 1988, Morild et al 1988,

Gardiner and Lindop 1992b, Gardiner et al 1992a), and all show the same immunolabelling pattern with central fibrin/fibrinogen and peripheral IgM (Nakajima et al 1989).

Peripolar cells do not, however, simply reflect proteinuria, and they do not always correlate with other granulated glomerular epithelial cells. In one species of fish, peripolar cells could not be identified among numerous granulated cells (Lacy and Reale 1989). In DOC/salt hypertension in chickens, many epithelial cells become granulated, while peripolar cells are unchanged (Morild et al 1988). Finally, in human renal biopsies, peripolar cells are prominent in different disease groups to those in which other granulated cells are most numerous (Gardiner et al 1992b).

3. Peripolar Cell Numbers:

The considerable interspecies variation in peripolar cell numbers (table 4.2) is similar to that found by Gall et al (1986), who found peripolar cells in 17 mammalian species. In this present study, only in the goat did every glomerulus contain at least one peripolar cell (PCI = 100%); serial section studies suggest the same is true in neonatal lamb kidney (Alcorn et al 1984). In the rat, the majority of peripolar cells were related to afferent arterioles; a similar distribution is described in sheep (Thumwood et al 1989, Kelly et al 1990).

It was originally suggested that the peripolar cell could be part of the JGA (Ryan et al 1979), although

more recent evidence argues against this (see chapter 1). Some workers have specifically suggested an inverse relationship between numbers of peripolar cells and juxtaglomerular renin-containing cells (Gall et al 1986). In additional work, the number of peripolar cells I have counted in these 12 species has been compared with the number of renin-containing cells stained by renin antibodies and immunocytochemistry in the same kidneys (Gibson et al 1994). No statistical correlations were found, providing no support to the view that the peripolar cell is part of the JGA. Likewise, in experimental manipulation of the renin-angiotensin system using altered renal perfusion and dietary sodium manipulation in the rat (Lindop et al 1993), the numbers of both dendritic peripolar cells counted by SEM and granulated peripolar cells counted by light microscopy were unaltered, in contrast to the numbers of renin-containing cells. Peripolar cells therefore did not respond to the main stimuli to renin secretion in the rat.

E. The Human Peripolar Cell:

In human kidney, peripolar cells were a mixture of dendritic cells (fig. 4.11) and globular cells (fig. 4.12), and their number was particularly low (PCI = 6.5%). The PCI for human kidney obtained by serial light microscopy sections on a small number of cases was around 12% (Gardiner and Lindop 1985). In man, parietal podocytes surround many vascular poles (see chapter 3). It is well recognised that podocytes can be granulated as a result of protein absorption and concentration related to lysosomal action (Lawrence and Brewer 1982). It is also likely that some parietal podocytes are granulated, as suggested by their bossellated protrusions (figs. 3.03, 3.07). Such granulated parietal podocytes would obviously appear as "peripolar" cells by light microscopy. In immunocytochemical studies, some human granulated peripolar cells express the intermediate filament vimentin, typical of podocytes (Gardiner and Lindop 1992a), and possibly representing parietal podocytes. The relationship between the peripolar cell and the parietal podocyte in human kidney needs to be clarified.

In human kidney, I also found small numbers of distinct fusiform- or spindle-shaped cells at the boundary between parietal podocytes and squamous parietal cells (fig. 4.13). These elongated "junctional cells" had processes which extended around the boundary between squamous cells and parietal podocytes, but they showed no evidence of pedicel formation, ie. they were similar

in morphology to dendritic peripolar cells. They also showed no evidence of granulation. Similar linearly arranged "rod-shaped cells" were described at the transitional zone between podocytes and parietal cells in an SEM study of the lamprey kidney (Miyoshi 1978). Also, identical slender fusiform cells were seen at the junction between parietal podocytes and squamous parietal cells in glomerular cysts in the macaque monkey (Miyoshi et al 1984).

This finding in human kidney raises the possibility that the location of the peripolar cell may be modified by the presence of parietal podocytes, ie. it may be determined by the site of the junction between squamous parietal cells and podocytes, and not simply by the vascular pole. In human glomeruli with parietal podocytes, this junction is on Bowman's capsule distant from the vascular pole.

F. Parietal Podocytes in Mammalian Kidney:

In some other species in addition to man (ie. rabbit, cow and pig), parietal podocytes extended out from the glomerular tuft to line Bowman's capsule around the vascular pole (fig. 4.14). These parietal podocytes had cell bodies and major processes, but unlike peripolar cells, the processes branched extensively and terminated as interdigitating pedicels. The parietal podocytes extended out radially, up to 100um from the vascular pole.

Parietal podocytes were found in only one of the three porcine kidneys, and likewise in just one of the three bovine kidneys, in both cases in approximately 30% of glomeruli. Parietal podocytes were present in both rabbit kidneys, in a minority (<10%) of glomeruli. It is worth noting that it is in the species with low PCIs that parietal podocytes are present (see table 4.2), again raising interest in the relationship between these two glomerular cell types.

Also, in the rabbit, fusiform "junctional cells" were found, with processes extending around the boundary between squamous parietal cells and parietal podocytes, identical to those seen in human kidney (compare figs. 4.14 and 4.13).

C H A P T E R 5

CHAPTER 5: LESIONS OF THE GLOMERULAR POLES
IN HUMAN RENAL ALLOGRAFTS

A. Source of Tissue:

Pathological changes at the vascular and tubular poles of the human glomerulus were studied using glomerular microdissection and SEM of twelve transplanted kidneys removed for irreversible allograft rejection. These kidneys were chosen because this is a relatively common indication for nephrectomy, and they show a range of pathological changes of variable aetiology (eg. inflammatory, ischaemic and toxic). Rejected allografts represent a useful model for studying glomerular damage. Histological examination showed a combination of acute and chronic rejection; 5 cases showed predominantly chronic rejection (kidney nos.1,2,7,8,11), 6 showed acute-on-chronic changes (nos.4,5,6,9,10,12) and 1 kidney (no.3) showed acute rejection only. Perfusion fixation and SEM preparation of randomly sampled cortex was performed, as described in chapters 2 and 3.

B. The Vascular Pole:

1. Peripolar Cells:

Peripolar cells, predominantly dendritic in type, though not exclusively (fig. 5.01) were present in all 12 transplant kidneys in small numbers (mean PCI = 4.8%). There were no significant differences in morphology or quantity compared with normal kidney (PCI = 6.5%). Occasional junctional cells between parietal podocytes and squamous parietal cells were also present (fig. 5.02b), as in normal kidney.

Table 5.1: Prevalence of Parietal Podocytes.

Kidney No.	VP	PPI
1	26	38%
2	30	33%
3	30	73%
4	48	58%
5	69	81%
6	88	65%
7	33	30%
8	35	94%
9	29	48%
10	38	55%
11	26	38%
12	21	33%
Totals/Mean	473	54%

VP = Number of vascular poles examined.

PPI = Parietal podocyte index.

2. Parietal Podocytes:

Parietal podocytes were found in all 12 transplant nephrectomies (table 5.1).

Compared to normal kidney (see table 3.2, page 37), the parietal podocyte indices were more variable (range 30%-94%), and the mean PPI was lower (54% versus 68%). The extent of Bowman's capsule around the vascular pole lined by parietal podocytes was similar to that in normal kidney.

The observed difference between the mean PPIs of the 2 groups is 14%. Confidence interval studies for the difference between the means suggest that this is not a statistically significant difference. If, however, the overall proportions for the 2 groups are compared, a significant difference is demonstrated. In all 12 tumour nephrectomies, 480 out of the 682 vascular poles (70.4%) had parietal podocytes; in all 12 transplant nephrectomies, 278 out of the 473 vascular poles (58.8%) had parietal podocytes. The observed difference between proportions is 11.6%; the 99% confidence interval for the difference between these proportions is 4.3% to 18.9%. Since this confidence interval does not span 0, this implies a significant difference.

The parietal podocytes in transplant kidneys differed from those in normal kidney. They had more microvilli which predominated on the pedicels and larger processes. Pedicel fusion, surface blebs and bossellated protrusions were also seen (fig. 5.02). These changes in the parietal podocytes, which varied in severity within and between kidneys, also affected the visceral

podocytes covering the capillary tuft to a similar extent (see page 88, fig. 5.11).

3. Tuft-to-Capsule Adhesions:

All 12 transplant nephrectomies had connections between the capillary tuft and Bowman's capsule which were more substantial than the single cell connections observed in normal kidney (see chapter 3, page 46). These connections in the transplant kidneys amounted to **tuft-to-capsule adhesions**.

Adhesions around the vascular pole, though present in all 12 cases, were infrequent (1-2% of glomeruli). They were always associated with parietal podocytes, the adhesion being formed by several podocyte cell bodies (fig. 5.03) and their processes (fig. 5.04), shared between the tuft and Bowman's capsule.

4. Discussion:

a) **Peripolar cells:** The JGA has not been specifically investigated in this study. It should be stimulated in these renal allografts as a consequence of chronic vascular rejection, secondary ischaemia and cyclosporin therapy (Porter *et al* 1966). The absence of peripolar cell alterations compared with normal kidney is consistent with the conclusion from experimental studies (detailed in chapter 4) that the peripolar cell does not respond to JGA stimuli. This is therefore further indirect evidence that the peripolar cell is not a functional part of the JGA.

b) **Parietal podocytes:** The lower mean PPI in the 12

transplant nephrectomies (54%) compared with normal kidney (68%) indicates that the presence of parietal podocytes is not simply a non-specific feature of chronic renal damage. In these kidneys, chronic vascular rejection will have produced secondary ischaemic damage of variable severity, but the mean PPI is not greater than that of normal kidney.

On the contrary, the statistical analysis suggests a significantly lower prevalence of parietal podocytes in the transplant nephrectomies than in normal kidney. This could indicate loss of parietal podocytes with chronic damage, assuming that the donor kidneys at transplantation had a similar prevalence of parietal podocytes as the tumour nephrectomies. However, this assumption may be invalid, since donor kidneys for transplant are from a different (ie. younger) age-group than tumour nephrectomies.

There are therefore no positive conclusions as to the nature of parietal podocytes from this study of renal allografts. The study does, however, confirm the existence of parietal podocytes in a group of human kidneys which have no tumours, excluding neoplasia as a sole explanation for their presence.

The morphological changes in parietal (and visceral) podocytes of these allografts represent non-specific features of podocyte injury. Scanning EM studies of glomerular diseases show that the surface of damaged visceral podocytes is essentially limited to these alterations, regardless of the type of glomerular disease (Arakawa et al 1976 1977, Jones 1977 1978 1979,

Ng et al 1982). These surface changes indicate the extent and severity of glomerular damage, but they are of no diagnostic value.

c) Tuft-to-capsule adhesions: These were related to the presence of bridging and parietal podocytes and processes. Tuft-to-capsule adhesions are seen in human hilar sclerosing lesions associated with glomerular hyperfiltration or hyperperfusion (page 14). It is likely that similar mechanisms operate in chronically-damaged transplant kidneys, with compensatory hyperperfusion in residual non-obsolescent glomeruli. It would be of great interest to study animal models of glomerular hyperfiltration and hilar sclerosis using these SEM techniques, to investigate any role of parietal podocytes and bridging podocyte connections in the associated hilar tuft-to-capsule adhesions.

It is also a possibility that the podocytic connections between tuft and capsule in the normal kidney (pages 46-48) represent precursors of vascular pole-related glomerular adhesions. They could provide the nidus for the development of adhesions around the vascular pole in glomeruli subjected to the appropriate haemodynamic stresses.

C. The Tubular Pole:

1. Glomerular Changes:

Glomerular abnormalities were present around the tubular pole, some of which equate with "glomerular tip changes", as described in chapter 1. The changes comprised tuft-to-capsule adhesions, visceral podocyte and squamous parietal epithelial changes and intraglomerular inflammatory infiltration.

a) Tuft-to-capsule adhesions: Connections between the

Table 5.2: Numbers of tubular pole-related adhesions.

Kidney No.	TPs	% adhesions	Mean no./TP	Max. no./TP
1	18	11%	1	1
2	14	29%	1	1
3	76	13%	1.1	2
4	55	0%	0	0
5	66	0%	0	0
6	83	7%	1.2	2
7	45	20%	1.1	2
8	46	70%	2.8	5
9	25	16%	1	1
10	25	4%	1	1
11	36	8%	1	1
12	14	29%	1.2	2
Totals/ Mean	503	17%	1.03	5

TPs = Number of tubular poles examined.

% adhesions = % of tubular poles with adhesions.

Mean no./TP = Mean number of adhesions per tubular pole.

Max. no./TP = Maximum number of adhesions per tubular pole.

glomerular tuft and Bowman's capsule around the tubular pole, amounting to tuft-to-capsule adhesions, were identified in 10 of the 12 transplant nephrectomies. They were present in highly variable numbers (table 5.2), but in most cases were more common than adhesions related to the vascular pole.

The percentage of tubular poles with tuft-to-capsule adhesions in each kidney ranged from 0-70% (mean = 17%). In 9 of the 10 kidneys, most affected glomeruli had just one adhesion at the tubular pole, and an occasional glomerulus had 2 adhesions (fig. 5.04). In kidney no.8, with 70% of tubular poles affected, the mean number of adhesions at affected tubular poles was 2.8, with a maximum number of 5 (fig. 5.05).

Tubular pole adhesions varied greatly in appearance. This was partly a consequence of the random site of fracture following glomerular microdissection; in some cases the fracture passed through the adhesion at the level of Bowman's capsule (fig. 5.06), in other cases the fracture was through the capillary loops adjacent to the adhesion, which therefore remained intact (figs. 5.07 - 5.10). In the latter situation, it was apparent that some consisted of thin elongated structures bridging across the urinary space (fig. 5.07), while others had a more substantial broader-based area of contact (fig. 5.08).

Tubular pole adhesions were associated with a number of parietal epithelial cell abnormalities, and sometimes with inflammatory cells (fig. 5.10). Adjacent squamous parietal cells were sometimes bossellated due to large

numbers of cytoplasmic granules (figs. 5.08, 5.09); around other adhesions, the parietal cells possessed prominent microvilli (fig. 5.05). In addition, many tubular pole adhesions formed at sites of apparent defects in the parietal epithelium (figs. 5.05 - 5.07). In contrast to vascular pole adhesions (page 83), those around the tubular pole did not involve parietal podocytes.

b) Capillary tuft: Visceral podocyte abnormalities, ie. surface blebs, increased microvilli and loss of pedicels (figs. 5.11), affected the capillary tufts diffusely. The severity of these changes varied extensively. In occasional glomeruli, accentuation of these abnormalities occurred at the tubular pole tip of the tuft (fig. 5.12). Also, occasional podocytes around the glomerular tip had bossellated cell bodies, in keeping with the presence of intracellular granules. At tubular pole adhesions, however, there was no accentuation of these diffuse podocyte changes, (in contrast to the localisation of parietal cell changes). Adhesions which had been fractured through the attached capillary loops showed, in some cases, marked thickening of the capillary loop walls (fig. 5.09).

Another occasional finding in all kidneys was herniation of the tip of a capillary tuft into a rather dilated tubular pole orifice. In some cases, this was associated with adhesion of the glomerular tip to the proximal part of the proximal tubule (fig. 5.13).

c) Parietal epithelium: Most of the abnormalities of the squamous parietal epithelium have been described in

association with the tubular pole adhesions. In the rare cases of tubularization of Bowman's capsule, the damage to the Bowman's capsule brush border was similar to that in the proximal tubule (see page 91, fig. 5.23). An occasional small patch of parietal epithelium, unrelated to an adhesion, was granulated with a bossellated surface (fig. 5.14). Also, in two of the 12 transplant nephrectomies, an occasional ciliated parietal epithelial cell (ie. with multiple cilia instead of a single cilium) was present close to or at the tubular pole (fig. 5.15).

d) Intraglomerular inflammatory cells: In the normal kidney, inflammatory cells were very rarely seen within the urinary space of Bowman's capsule (fig. 3.24). In contrast, in the transplant kidneys inflammatory cells within the urinary space were present in the majority of glomeruli (60%, range 17-94%).

There were two main cell-types (fig. 5.16). The larger (up to 15-20um diameter) had a surface covered by small blebs and fine strands, and usually had an irregular branching shape; this most likely represents either an activated lymphoid cell (lymphoblast) or a macrophage. The smaller (5-8um diameter) was spherical, with a ruffled surface and no strands, in keeping with a small lymphocyte.

These cells were in the urinary space, either on Bowman's capsule epithelium, or on the capillary tufts (fig. 5.17). On Bowman's capsule, there was a clear predilection for the squamous epithelium in the tubular pole half of the glomerulus (fig. 5.18), and

inflammatory cells often aggregated around the tubular pole (fig. 5.19). Around the vascular pole, inflammatory cells were rarely found overlying parietal podocytes (fig. 5.18).

Occasional inflammatory cell aggregates were enmeshed by a network of fibrillar material, possibly fibrin (fig. 5.20). These aggregates had an imprint of visceral podocyte cell bodies and processes, suggesting the inflammatory meshwork formed a connection between the capillary tuft and Bowman's capsule.

Also, appearances suggestive of infiltration of inflammatory cells between Bowman's capsule epithelial cells (fig. 5.21) were seen occasionally in all kidneys. This showed no specific relationship to the glomerular poles.

2. Tubular Changes:

a) Tubular pole narrowing: The tubular pole orifices of many glomeruli showed considerable narrowing (fig. 5.22), sometimes measuring less than 10um. Maximum tubular pole diameters were measured in six transplant nephrectomies (table 5.3), and correlated with the same measurements for normal kidney in six tumour nephrectomies (see table 3.4, page 61).

In the transplant nephrectomies, the mean diameter of 272 tubular poles was 23um ($SD = 8.15\text{um}$, range 8-55um), compared with a mean of 32um ($SD = 8.19\text{um}$, range 12-62um) in normal kidney. The observed difference between the means is therefore 9um; the 99% confidence interval for difference between these means is 7-10um,

Table 5.3: Tubular Pole Diameters in Transplant Nephrectomies.

Kidney No.	n	TPD range	Mean TPD
4	39	17 - 36	25
5	54	9 - 38	20
6	64	8 - 45	23
7	35	10 - 55	30
8	42	8 - 38	22
11	38	8 - 36	20
Totals/Mean	272	8 - 55	23 SD=8.15

n = Number of tubular poles accurately measured.

TPD range = Range of tubular pole diameters (um).

Mean TPD = Mean tubular pole diameter (um).

SD = Standard deviation.

implying a significant difference between the two groups.

b) Proximal tubule: In this study only the most proximal segment of proximal tubules was studied in detail. The luminal brush border showed damage in all cases, though varying in severity, both between and within individual kidneys. The damage consisted of clumped microvilli, partial or complete loss of microvilli (fig. 5.23) and surface blebs. These changes were equally apparent at the proximal segments, irrespective of the presence or absence of tubular pole tuft-to-capsule adhesions, and no specific proximal tubule changes were associated with the tubular pole adhesions.

A brush border was absent at most tubular pole orifices,

since the first 2-3 proximal tubular cells were virtually devoid of microvilli. This gave a similar appearance to the neck segments of normal kidney, but is a reflection of brush border damage, rather than representing true neck segments. The prevalence of neck segments in these kidneys could not be accurately assessed for this reason.

Finally, in some glomeruli, the angle of origin of the proximal tubule was abnormal. In the normal kidney, the direction of the early proximal tubule was invariably in the axis of the glomerular poles (fig. 3.19). In the rejected transplant kidney, the proximal tubule sometimes commenced at an angle (of up to 90 degrees) to this axis (fig. 5.24). These changes appeared related to surrounding interstitial fibrosis.

3. Discussion:

These various lesions at the tubular pole, in particular the tubular pole adhesions, glomerular tuft changes, and proximal tubule changes, are consistent with "glomerular tip changes" (described in detail in chapter 1, see page 17). In these kidneys, these abnormalities are most likely related to chronic transplant glomerulopathy with associated proteinuria.

a) Tubular pole adhesions: Adhesions at the tubular pole have been previously described in renal transplants, particularly in longstanding grafts with chronic transplant glomerulopathy (Lee and Howie 1988). This SEM study has shown that tubular pole adhesions are morphologically distinct from those around the vascular

pole, with parietal podocytes making no contribution to the former. Previous studies have suggested that segmental lesions at the two glomerular poles have a different pathogenesis, with vascular pole damage related to hyperfiltration, and tubular pole damage related to proteinuria (see chapter 1). The different appearances of tubular pole compared with vascular pole adhesions that I have found is consistent with this idea of different pathogenetic mechanisms operating at the two glomerular poles. To establish a relationship between tubular pole adhesions and proteinuria, it would clearly be of interest to correlate their variable numbers in the 12 kidneys with the level of proteinuria immediately prior to nephrectomy. Unfortunately, the amount of proteinuria is not routinely measured in this clinical circumstance, and such a study would have to be performed in a prospective manner.

The importance of tuft-to-capsule adhesions is their possible role in leading to glomerulosclerosis. It was previously considered that adhesions developed secondary to glomerular tuft segmental sclerosis (Elema and Arends 1975). However, recent studies in experimental animal models suggest that adhesions may be the primary abnormality, and act as a nidus for adjacent segmental tuft sclerosis (Nagata and Kriz 1992).

The glomerular tuft, and its individual lobules, are generally considered to be relatively mobile structures within Bowman's capsule. If glomerular mobility is hindered by tuft-to-capsule adhesions, it is likely that the tuft will be subjected locally to tension and

mechanical stresses, maximal at the point of adhesion, which could lead to damage and sclerosis. My finding of established adhesions, stretched-out into elongated bridging connections between the tuft and Bowman's capsule, is consistent with the adhesions being exposed to tension, although it is not certain what effects perfusion fixation may have on these appearances.

In contrast to the vascular pole adhesions, where bridging podocytes may act as precursors, I have identified no obvious precursors of tubular pole adhesions in the normal glomerulus. An occasional podocytic connection between the tuft and Bowman's capsule around the tubular pole was seen in some kidneys (see chapter 3, page 47), but this would seem too infrequent to be relevant to tubular pole adhesions. In the transplant kidneys, the occasional small patch of granulated parietal epithelium (with no associated adhesion) could represent a site where an adhesion develops, since granulated parietal epithelium was also present at some established adhesions.

Tubularization of Bowman's capsule was unrelated to tubular pole adhesions; I found it was uncommon in the transplants compared with normal kidney, in contrast to other studies of renal transplants (Lee and Howie 1988). In previous studies of glomerular tip changes, the only possible suggested "precursor" of tuft-to-capsule adhesion specifically at the tubular pole is expression of the cell membrane protein **epithelial membrane antigen** (EMA) on a thin ring of parietal epithelium around the tubular pole (Howie 1986b). Adhesions occurred next to

the small patch of EMA, and in some cases the antigen extended along the tubular side of the adhesion. However, the mechanism whereby EMA expression could lead to adhesions is not clear, and whilst this EMA expression is a further example of specific properties associated with the tubular pole, it seems likely that cell surface adhesion molecules would be more important in such circumstances.

The major abnormalities related to tubular pole adhesions affected parietal cells rather than podocytes. Previous studies of glomerular tip changes (Howie and Brewer 1984 1985) emphasise podocyte abnormalities (eg. cell swelling, vacuolation and granulation), and tuft changes (eg. prolapse of the tuft into the proximal tubule), as early features in the development of adhesions. Studies of tuft-to-capsule adhesions in animals (Kondo and Akikura 1982, Olson *et al* 1985, Nagata and Kriz 1992) also describe podocyte and capillary loop abnormalities as the initial disorders in the development of adhesions. It is possible that the accentuation of podocyte changes observed in this present study at the tips of some glomeruli (with no associated adhesion) may represent early changes leading to the formation of an adhesion. However, at established tubular pole adhesions, localised podocyte changes were absent.

In contrast, I have found parietal cell abnormalities at sites of established tubular pole adhesions, including parietal epithelial cell granulation. Granulation of glomerular epithelial cells is a common feature of

glomerular damage, particularly in association with proteinuria or intracapillary fibrin deposition as in malignant hypertension (Nakajima et al 1989, Gardiner and Lindop 1992b, Gardiner et al 1992b). The cytoplasmic granules resemble protein reabsorption droplets, and have been shown to contain albumin, immunoglobulins and complement components (Olson et al 1985, Nakajima et al 1989). Similar granules have been previously noted in association with tuft-to-capsule adhesions, but mainly within podocytes rather than parietal cells, (Olson et al 1985, Van Damme et al 1990, Nagata and Kriz 1992).

The parietal epithelial defects observed at adhesions in this present study suggests reflection of the parietal epithelium onto the capillary tuft, with adhesion of the tuft to either the parietal basement membrane of Bowman's capsule or pericapsular interstitial tissue. Such fusion of parietal and glomerular basement membranes has been described in tuft-to-capsule adhesions in glomerular tip changes (Howie and Brewer 1984), and also in membranous glomerulonephritis (Van Damme et al 1990). Such disturbance of visceral and parietal epithelial cells, with focal denudation of capillary loops, could cause leakage of glomerular filtrate into the interstitium specifically at sites of adhesions.

b) Intraglomerular inflammatory cells: This SEM investigation has enabled study of the inflammatory infiltrate within the urinary space of the glomerulus, (not of the inflammatory cells within the glomerular

tuft). This intraglomerular inflammatory infiltrate presumably represents part of the acute cellular rejection processes.

The relatively rare finding of infiltration of inflammatory cells between squamous parietal cells of Bowman's capsule suggests that there are alternative pathways into the urinary space of the glomerulus. Other possible sites of entry include movement through tubular epithelium distal to the glomerulus followed by retrograde passage along the tubule and through the tubular pole, or (more directly) across the capillary loops of the glomerular tuft. Whilst the relative importance of these various pathways cannot be assessed in this type of study, the clustering of cells at the tubular pole orifice would be consistent with their movement through the tubular pole and into the urinary space. Previous light microscopic studies of renal transplants have also suggested that inflammatory cells aggregate and infiltrate into epithelium at the tubular origin (Darmady *et al* 1955, Lee and Howie 1988).

c) Tubular pole narrowing: The narrowing of the tubular orifice probably parallels a similar degree of atrophy in the entire proximal tubules. In these kidneys, this could be a consequence of chronic ischaemia due to transplant-related vascular changes, ie. chronic vascular rejection and cyclosporin effects. Similar tubular pole narrowing has also been described in dog allografts (Darmady *et al* 1955).

d) Proximal tubule: Brush border damage is a non-specific feature of proximal tubular damage.

Similar changes are seen in both acute and chronic tubular damage, eg. acute tubular necrosis (Jones 1979), or in association with chronic proteinuria (Andrews 1979). In acute damage, the changes are reversible, and are followed by regeneration of microvilli. In the transplant kidneys examined in this study, the brush border damage could be related to chronic ischaemia and/or proteinuria and/or cell rejection. Chronic ischaemic damage would also account for severe interstitial fibrosis, which was associated with the altered angle of origin of some proximal tubules. The functional significance of this latter finding is unclear, although it could be related to the development of atubular glomeruli (see chapter 6).

C H A P T E R 6

CHAPTER 6: ATUBULAR GLOMERULI AND GLOMERULAR CYSTS

A. Source of Tissue:

Atubular glomeruli were examined by SEM in histologically normal human kidney from six of the tumour nephrectomies (detailed in chapter 3), and in random areas of chronically-damaged renal parenchyma from six of the transplant nephrectomies (detailed in chapter 5). Perfusion fixation and SEM preparation of consecutive slices of cortex was performed, as described in chapters 2 and 3.

B. Anatomy of Atubular Glomeruli:

Atubular glomeruli were identified by examination of the two hemispheres of bisected glomeruli (see chapter 2). Specimen rotation and tilting confirmed the absence of a tubular pole (fig. 6.01). They were found randomly at all depths of the renal cortex.

1. The Parietal Epithelium:

In atubular glomeruli, Bowman's capsule was lined almost entirely by parietal podocytes. These were similar to the parietal podocytes lining normal glomeruli, but in atubular glomeruli they constituted >90% of the parietal epithelium (fig. 6.01). The parietal podocytes of atubular glomeruli had particularly long major processes (fig. 6.02), which often extended long distances before branching. The major processes of adjacent cells

interdigitated with one another (fig. 6.03) in an analogous fashion to the interdigititation of their terminal foot processes or pedicels (fig. 6.04).

In transplant nephrectomies, the parietal podocytes of the atubular glomeruli showed a number of abnormalities, e.g. a prominent microvillous covering (fig. 6.05), surface blebs (fig. 6.06), fusion of foot processes (fig. 6.07) and focally bossellated (partially granulated) cell bodies (fig. 6.07).

The residual parietal epithelium of atubular glomeruli consisted of squamous parietal cells, identical to those in normal glomeruli. This squamous area was commonly found opposite the residual capillary tuft of the atubular glomerulus. In occasional atubular glomeruli, single squamous parietal cells had a bossellated surface due to numerous cytoplasmic granules.

2. The Glomerular Capillary Tuft:

A glomerular capillary tuft was identified in the majority (over 80%) of atubular glomeruli, but it was never normal. It usually consisted of a contracted capillary tuft which varied in structure; some were round and regular (fig. 6.08), others more irregular and stretched out along the curvature of Bowman's capsule (figs. 6.09, 6.16), as though the glomerular tuft had been splayed apart. In some cases, it appeared that the tuft remnants were divided into separate groups of capillary loops within the Bowman's capsule. In all cases, podocytes bridged between Bowman's capsule and the capillary tuft (figs. 6.02, 6.08). In some of the

larger glomerular cysts, only a few remnant capillary loops remained (fig. 6.10).

Some tuft remnants included processes, consisting of capillary loops covered by podocytes, which connected with the opposite side of Bowman's capsule (fig. 6.11). In some cases, the tuft formed a complex branching structure, with multiple connections to Bowman's capsule (fig. 6.12).

In many atubular glomeruli (30%), the tuft remnant was covered by inspissated proteinaceous material, which filled the urinary space (fig. 6.13). Podocytic processes derived from the capillary tuft passed through this material to connect with the parietal epithelium of atubular glomeruli (fig. 6.14). The material formed a protein cast within atubular glomeruli, with an imprint of the parietal epithelium in its outer surface (fig. 6.15). The cast imprint was sufficiently detailed to see not only the imprint of cell bodies and major processes of parietal podocytes, but also at higher power the imprint of their interdigitating pedicels (fig. 6.15).

3. Intraglomerular Inflammatory Cells:

In transplant nephrectomies, approximately 50% of atubular glomeruli contained small aggregates of inflammatory cells. These were present in the urinary space, lying on the parietal epithelium (fig. 6.16), or over the capillary tuft remnant. The inflammatory cell-types were the same as those within normal glomeruli of the same kidneys (chapter 5). The cells

were sometimes enmeshed within fibrillar material, and those on the parietal epithelium had a tendency to cover the squamous parietal cells, particularly at their junction with parietal podocytes (fig. 6.16). Intraglomerular inflammatory cells were not seen in the atubular glomeruli of normal kidney.

4. Glomerular Cysts:

Many atubular glomeruli were cystically dilated to the extent of forming glomerular cysts. These were defined as dilated Bowman's capsules >200um diameter (figs. 6.09, 6.10, 6.13, 6.15 - 6.17); the largest examples were up to 500um diameter. Glomerular cysts were, like all atubular glomeruli, found throughout the depth of renal cortex, although when numerous they were commonly clustered in the subcapsular cortex.

In all other respects, glomerular cysts were identical to other atubular glomeruli, with extensive parietal podocytes, remnants of the capillary tuft, protein casts and intraglomerular inflammatory cells.

C. Numbers of Atubular Glomeruli and Glomerular Cysts:

The numbers of atubular glomeruli and glomerular cysts in the two groups of kidneys are shown in table 6.1 and 6.2.

Table 6.1: Atubular glomeruli and glomerular cysts in normal kidney. The kidney nos. are those used for the tumour nephrectomies detailed in chapter 3 (see table 3.1, page 33).

Kidney no.	n	AG (%)	GC (%)
3	150	2 (1.3)	1 (0.7)
4	121	2 (1.6)	0 (0)
5	118	0 (0)	0 (0)
6	172	1 (0.6)	1 (0.6)
11	140	0 (0)	0 (0)
12	169	1 (0.6)	1 (0.6)
Totals	870	6 (0.7)	3 (0.3)

n = Number of glomeruli examined.

AG (%) = Number (%) of atubular glomeruli.

GC = Number (%) of glomerular cysts.

In the histologically normal kidney (table 6.1), atubular glomeruli were uncommon; in every kidney <2% of glomeruli were atubular, and overall <1% were affected. Half of the atubular glomeruli were glomerular cysts.

In the transplant kidneys (table 6.2), atubular glomeruli were highly variable in number. In every case, at least 3% of glomeruli were atubular, and in one kidney the majority (61%) were affected. Overall, 17%

Table 6.2: Atubular glomeruli and glomerular cysts in transplant nephrectomies. The kidney nos. are those used for the transplant nephrectomies detailed in chapter 5 (see table 5.1, page 81).

Kidney no.	n	AG (%)	GC (%)
4	204	9 (4)	2 (1)
5	149	4 (3)	3 (2)
6	208	13 (6)	10 (5)
7	108	13 (12)	0 (0)
8	176	107 (61)	63 (36)
11	180	28 (16)	17 (9)
Totals	1025	174 (17)	95 (9)

n = Number of glomeruli examined.

AG (%) = Number (%) of atubular glomeruli.

GC = Number (%) of glomerular cysts.

of glomeruli were atubular, with just over half (9%) forming glomerular cysts.

The observed difference between the overall percentages of atubular glomeruli in the two groups of kidneys is 16.3%; the 99% confidence interval for the difference between these proportions is 13.2% - 19.4%, implying a significant difference between the two groups.

D. Discussion:

In this study, I have used a novel SEM technique to identify atubular glomeruli. Previous workers have used either nephron microdissection (Oliver 1939), or serial sectioning (Heptinstall and Hill 1967, Marcussen 1992) to identify atubular glomeruli. These techniques have inherent disadvantages; my SEM technique is simple, reliable and less time-consuming.

1. Atubular Glomeruli in Normal Kidney:

In otherwise histologically normal adult human kidney, I have found that a small proportion (<1%) of glomeruli are atubular. In serial section studies, Marcussen (1992) found that 2.5% of glomeruli were atubular in control (normal) human kidneys. It is well known that glomeruli undergo obsolescence steadily throughout life (Kaplan *et al* 1975, Kappel and Olsen 1980, Smith *et al* 1989); it is possible that loss of tubular connection (forming atubular glomeruli) is an alternative way in which irreversible glomerular damage can occur. The number of atubular glomeruli I have counted in just 6 kidneys is too small to make meaningful correlation with patient ages, but a larger study would seem worthwhile.

2. Atubular Glomeruli in Renal Transplants:

Rejected transplant kidneys contained more atubular glomeruli, and in one case the majority of glomeruli were affected. Previous studies have shown a high proportion of atubular glomeruli in chronic

tubulointerstitial diseases, eg. renal artery stenosis and chronic pyelonephritis (Marcussen 1992). In human chronic pyelonephritis, atubular glomeruli were maximal in areas with the most severe interstitial fibrosis and tubular loss (Marcussen and Olsen 1990). In renal transplants, chronic tubulointerstitial damage is due to chronic renal ischaemia and continuing cellular rejection. It has been previously noted that in transplanted kidneys with end-stage failure, crowded glomeruli are surrounded by interstitial tissue in which tubules are no longer seen (Bohle *et al* 1989), an observation consistent with atubular glomeruli.

3. Pathogenesis of Atubular Glomeruli and Glomerular Cysts:

Atubular glomeruli must arise due to sealing of the origin of the proximal tubule. The transplant nephrectomies had significant tubular pole abnormalities, including narrowing of the tubular orifice (see chapter 5). It is possible that this narrowing of the tubular pole is involved in the pathogenesis of atubular glomeruli, occurring as part of the process of damage which leads to the glomerulus becoming atubular.

The serial section studies of Marcussen (1992) have demonstrated a high percentages of atrophic tubules associated with atubular glomeruli. The initial site of damage could be at the tubular pole, suggested perhaps by the aggregates of inflammatory cells seen at tubular poles (see chapter 5). Alternatively, tubular damage

could commence at a more distal point, followed by retrograde atrophy back to the glomerulus, causing initially tubular pole narrowing, and ultimately loss of the tubular connection, i.e. forming an atubular glomerulus (Marcussen and Olsen 1990). In cisplatin-induced tubulointerstitial nephropathy in rats, for example, the toxic damage occurs specifically at the S₂-segment of the proximal tubule in the outer stripe of the outer medullary zone, leading to irreversible tubular destruction and atubular glomeruli (Marcussen and Jacobsen 1992).

Once atubular, damage to the capillary tuft may be secondary to high intraglomerular pressure. Obstruction to the flow of glomerular filtrate, resulting from tubular disconnection, may also be responsible for some atubular glomeruli becoming glomerular cysts. These glomerular cysts are clearly acquired, and will contribute to the acquired cystic disease associated with chronic dialysis and end-stage renal failure. This occurs in chronically-rejected renal transplants as well as in native kidneys (Chung et al 1992). Glomerular cysts have also been described in native kidneys from patients on chronic dialysis (Ogata 1990), in human renal artery stenosis (Marcussen 1991), and in experimental chronic pyelonephritis in the rabbit (Shimamura and Heptinstall 1963).

The glomerular cysts described in this study are comparable to those previously described in the renal cortex of one adult macaque monkey (Miyoshi et al 1984). The glomerular cysts in this monkey kidney were also

atubular, with extensive parietal podocytes and damaged capillary tuft remnants. Similar glomerular cysts also follow steroid therapy in neonatal rabbits (Ojeda et al 1979, Ojeda and Garcia-Porrero 1982); they too were lined by extensive parietal podocytes, although they apparently communicated with proximal tubules. In an SEM study of autosomal dominant polycystic kidney disease (Grantham et al 1987), a small minority of the cysts (2.1%) were lined by parietal podocytes. Ultrastructural examination of the glomerular cysts in a case of human renal dysplasia (Pardo-Mindan et al 1978) showed a partial parietal podocyte lining surrounding the tuft remnant. Also, in a case of familial glomerulocystic kidney (Rizzoni et al 1982), electron microscopy showed parietal podocytes lining the glomerular cysts.

It would clearly be of interest to study the glomerular cysts of the various congenital glomerulocystic diseases in human kidney (reviewed by Bernstein and Landing 1989), to investigate if they are also atubular. Review of the literature suggests that this might be the case. Using serial section reconstructions in a case of infantile glomerulocystic kidney, Roos (1941) showed no connections between the cysts and tubules. In microdissection studies of the glomerular cysts found in an infant with multiple associated congenital anomalies (Bialestock 1956), most subcapsular cysts had no connection with tubules. In a study of familial glomerulocystic disease (Melnick et al 1984), an extensive serial section search of renal biopsies showed

no evidence of even the most atrophic tubules arising from the glomerular cysts. Finally, in a light microscopic study of a sporadic case of adult glomerulocystic kidney disease (Dosa *et al* 1984), tubular poles were detected in random sections in a significantly smaller percentage of glomerular cysts (6.2%) than in normal glomeruli (16.5%), ie. suggesting that some of the glomerular cysts were atubular. In addition, this study found that the tubular poles in the glomerulocystic kidney were narrowed, lined by atrophic epithelial cells and surrounded by dense interstitial fibrosis. These observations are similar to the tubular pole changes seen in the renal transplants in this present study, suggesting that tubular pole connections may be lost in association with progressive periglomerular fibrosis.

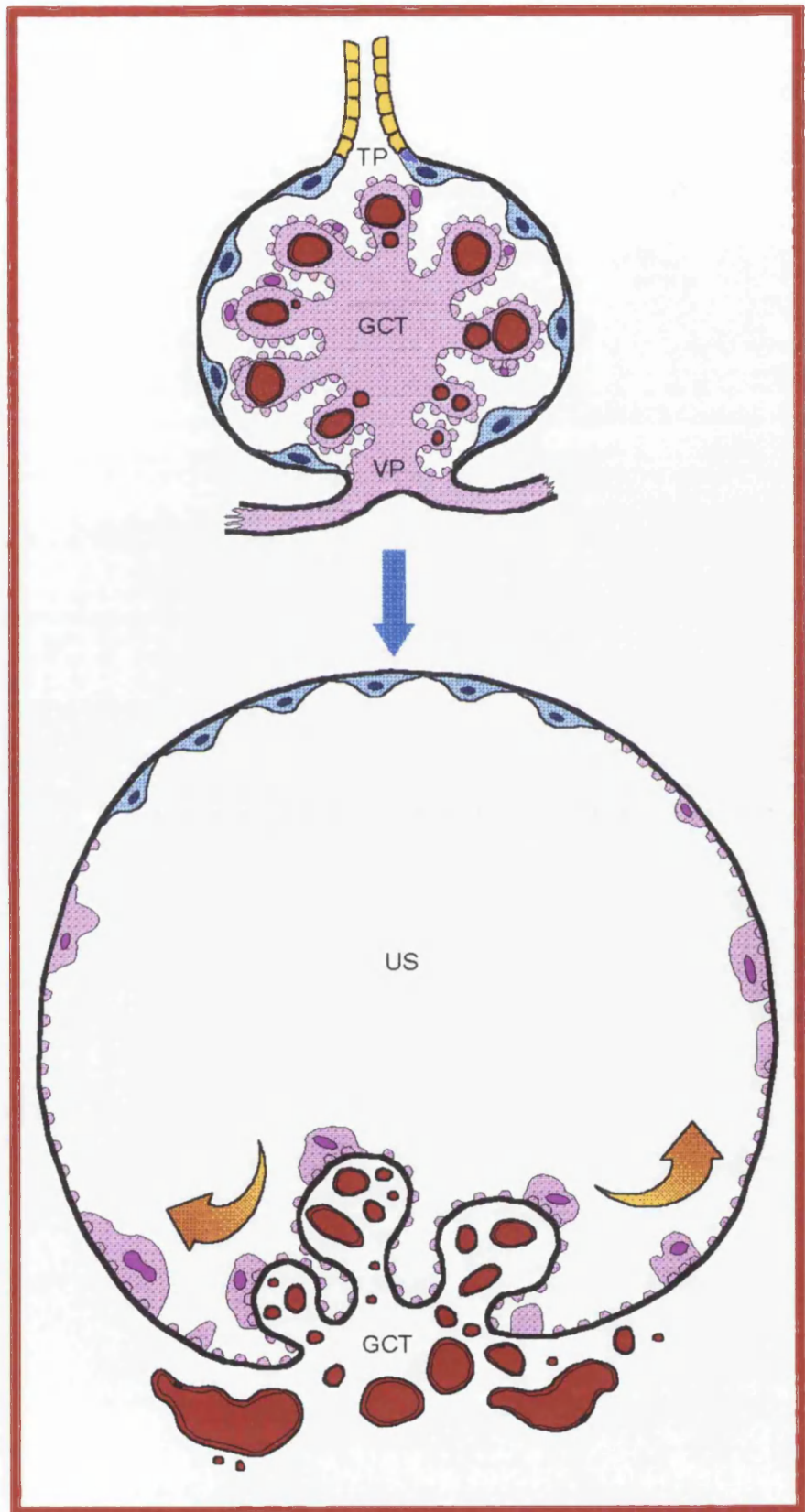
4. Parietal Podocytes in Atubular Glomeruli:

The origin of the parietal podocyte lining of atubular glomeruli and glomerular cysts is unclear. As discussed in chapter 3, metaplasia of the parietal epithelium is one possibility, and was favoured by Ojeda *et al* (1979). An alternative explanation would be evagination or eversion of the capillary tuft (diagram 6.1), subsequent to the presumed high intraglomerular pressures caused by loss of the tubular pole (Pardo-Mindan *et al* 1978, Miyoshi *et al* 1984). As the tuft everts, the visceral podocytes of the tuft will be incorporated into the parietal epithelium as parietal podocytes. The portion of squamous parietal epithelium, invariably found

Diagram 6.1: Proposed pathogenesis of parietal podocytes lining the atubular glomerular cyst. Loss of the tubular pole (TP) is followed by dilatation of Bowman's capsule, and evagination of the glomerular capillary tuft (GCT), as indicated by the arrows. The glomerular capillaries are incorporated into Bowman's capsule, with visceral podocytes becoming parietal podocytes.

VP = Vascular pole

US = Urinary space



opposite the tuft remnant, will derive from the original squamous parietal epithelium of Bowman's capsule. The contracted capillary tufts, particularly those which appeared splayed-out along the wall of Bowman's capsule, with podocytes bridging between the tuft remnant and the parietal lining, would lend support to such an evagination hypothesis. So also does the observation that the largest glomerular cysts often contained only very rudimentary or no obvious tuft remnants. Other studies of glomerular cysts have described a similar inverse relationship between the size of the glomerular tuft and the diameter of the glomerular cyst (Bialestock 1956, Vlachos and Tsakraklidis 1967, Pardo-Mindan et al 1978, Oh et al 1986, Ogata 1990).

This is the first SEM study of atubular glomeruli in human kidney. A previous ultrastructural study of atubular glomeruli (Marcussen et al 1990) showed mesangial increase and glomerular basement membrane thickening, but parietal podocytes were apparently not a feature. It is interesting that this study was of atubular glomeruli in rats with lithium-induced chronic nephropathy; the lithium was administered to neonatal rats with developing renal tissue, and it is possible that this model of atubular glomeruli is not comparable to acquired atubular glomeruli in adult kidney.

5. Filtration in Atubular Glomeruli:

The capillary tufts of atubular glomeruli are structurally intact, with patent capillary loops, but have been assumed not to filter (Marcussen 1992),

because of high intraglomerular pressure in the blind capsular space exceeding the filtration pressure. However, this study is the first to show that atubular glomeruli in human kidney are lined extensively by parietal podocytes which are differentiated for filtration. This parietal podocyte lining could permit some perpetuation of capillary tuft filtration, by allowing secondary filtration across Bowman's capsule (diagram 6.2). This is speculative, but if true would have consequences for the renal interstitium. Filtration across Bowman's capsule into the interstitium could stimulate periglomerular oedema and fibrosis, and interstitial inflammation and fibrosis (as discussed in chapter 3), leading to progressive renal insufficiency. The protein casts within the urinary space of many atubular glomeruli presumably derive from material trapped at this site when the tubular connection is lost. Eosinophilic and PAS-positive casts were described in glomerular cysts in renal biopsies of familial glomerulocystic disease (Melnick *et al* 1984). The imprint of the parietal epithelium on the outer surface of the cast would suggest that in life there is intimate apposition of the material in the urinary space to Bowman's capsule. Filtration of water across the parietal podocytes of atubular glomeruli into the interstitium would produce an increasingly concentrated and inspissated material within the urinary space.

6. Atubular Glomeruli in Renal Disease:

It is evident that atubular glomeruli can themselves

make no contribution to urine formation, and are in this sense equivalent to the totally obsolescent glomeruli. Loss of tubular connection may therefore be an important alternative way in which nephron function can be irreversibly lost in chronic renal impairment. The frequently observed inconsistency between severity of chronic renal failure and degree of glomerular obsolescence might be explained if atubular glomeruli are also taken into account (Marcussen 1992). In experimental studies, the proportion of atubular glomeruli correlates with the impairment of renal function (Marcussen and Jacobsen 1992).

In the assessment of a renal biopsy, it is standard practice to quantify the proportion of totally and partially obsolescent glomeruli. In routine practice, it is common to see glomeruli with shrunken tufts, and cystically dilated urinary spaces filled by inspissated colloid-like cast material (fig. 6.18); these are almost certainly atubular glomeruli / glomerular cysts, and their quantification in a biopsy, in addition to glomerular obsolescence, would seem worthwhile.

C O N C L U S I O N S

CONCLUSIONS

The appreciation of normal biological structure is vital for the determination of function, and for the recognition of disease. Furthermore, in order to advance our understanding of disease, and its functional consequences, the application of new techniques, and the adaptation of established techniques, are critical.

This study illustrates these basic principles in the investigation of the renal glomerulus using scanning electron microscopy (SEM). To facilitate examination of the glomerular vascular and tubular poles, I have developed a new technique of glomerular microdissection, performed after critical point drying of tissue. This adaptation of the normal preparation of renal tissue for SEM has permitted the study of greater numbers of vascular poles than previous techniques. In contrast to previous methods, my technique allows correlation of vascular and tubular pole structure with that of the glomerular capillary tuft from the same glomerulus. In addition, the limitations of the technique, particularly in the study of diseased kidney, have been considered, in order to avoid misinterpretation.

I have used this new technique to study the normal vascular pole of the adult human glomerulus, and shown that many glomeruli have podocytes lining Bowman's capsule around the vascular pole. My study has demonstrated the widespread extent and prevalence of these parietal podocytes in histologically normal

kidney. They are differentiated for filtration with interdigitating pedicels, and they may derive from a process of metaplasia of squamous parietal cells. The prevailing hydrostatic and oncotic pressures dictate filtration across parietal podocytes from the urinary space into the interstitium, particularly in the region of the renin-secreting cells of the juxtaglomerular apparatus (JGA), potentially influencing JGA function. In glomerular disease, the deposition of immune complexes in Bowman's capsule in association with parietal podocytes, makes the vascular pole a potential site of immune complex-mediated damage. Also, filtration of chemotactic factors and cytokines from a damaged glomerulus, across parietal podocytes and into the interstitial compartment, could influence interstitial inflammation and subsequent fibrosis in the glomerulonephritides.

In association with parietal podocytes, I have demonstrated podocytic connections between the normal glomerular tuft and Bowman's capsule, derived from either parietal or visceral podocyte cell bodies. These previously undescribed connections bridge across the urinary space, and may be precursors to the formation of tuft-to-capsule adhesions around the vascular pole in damaged glomeruli.

I have described the anatomical variations at the normal human tubular pole. This region of the glomerulus has previously been extensively studied in animal species, but this is the most detailed SEM examination of the human tubular pole. I have documented the prevalence of

tubularization of Bowman's capsule and of proximal tubule neck segments. The study provides a baseline of normal structure, enabling future critical examination of the tubular pole in renal disease.

I have used glomerular microdissection to perform a species survey of the mammalian peripolar cell, located around the glomerular vascular pole. My findings confirm that the peripolar cell is a morphologically distinct glomerular epithelial cell.

I have defined two distinct morphological types of peripolar cell. The dendritic peripolar cell predominated in rodent species; its structure is best suited to sense the calibre of the arterioles at the vascular pole. The globular peripolar cell predominated in ungulates such as sheep and goat; its abundant cytoplasmic granules produced surface bossellation. The presence of intermediate forms was evidence of a link between the two types of peripolar cells, and suggests that acquisition of numerous granules may produce a morphological change from dendritic to globular cells.

In human kidney, I found that peripolar cells were sparse, and they may have been confused with parietal podocytes in previous light microscopy studies. The presence of parietal podocytes in human glomeruli alters the location of the junction between squamous parietal cells and podocytes; at this site I have described "junctional cells", with similar morphology to dendritic peripolar cells.

I have studied lesions at the vascular and tubular poles in human renal allografts damaged by transplant rejection. Parietal podocytes showed similar morphological changes to visceral podocytes, reflecting non-specific podocyte injury. The renal damage, however, had no effect on peripolar cells in the allografts.

I found structural differences between tuft-to-capsule adhesions at the two glomerular poles. Vascular pole adhesions were formed by podocytes at areas with parietal podocytes; they may develop from pre-existing normal podocyte connections. In contrast, tubular pole adhesions did not involve podocytes, and were associated with variable abnormalities in squamous parietal epithelium. These findings may reflect differences in underlying pathogenesis, with vascular pole adhesions occurring with hyperfiltration/hyperperfusion damage, and tubular pole adhesions occurring in association with proteinuria. At some tubular pole adhesions, defects in the parietal epithelium were found, with adhesion of the tuft to either parietal basement membrane or interstitial tissue. There could be leakage of glomerular filtrate into the interstitium specifically at sites of adhesions.

I have demonstrated intraglomerular inflammatory cells within the urinary space of glomeruli in renal transplants. These cells favoured the tubular pole half of glomeruli, and they may specifically enter into the glomerulus through the tubular pole.

Finally, I have used these adapted SEM techniques to investigate atubular glomeruli in human kidney. They were lined extensively by parietal podocytes, contained contracted capillary tufts, and many formed glomerular cysts. I found that a small number of glomeruli in otherwise normal adult kidney were atubular; the numbers significantly increased with allograft rejection. Associated with atubular glomeruli was narrowing of the tubular pole orifice of glomeruli which retained a tubular connection; this may be important in the pathogenesis of atubular glomeruli.

Based on these observations, there may be an evagination of the capillary tuft, and its incorporation into Bowman's capsule, in atubular glomeruli and glomerular cysts. Parietal podocytes may permit some perpetuation of capillary tuft filtration within atubular glomeruli, by allowing secondary filtration across Bowman's capsule into the renal interstitium.

In conclusion, these adapted SEM techniques have led to important new findings in the renal glomerulus in both health and disease. Future studies in combination with other techniques, such as acellular digestion methods, and with experimental models of glomerular disease, will further elucidate how the glomerulus is damaged in human renal disease.

R E F E R E N C E S

REFERENCES

Ahmadi zadeh M, Echt R, Kus C, Hook JB

Sex and strain differences in mouse kidney: Bowman's capsule morphology and susceptibility to chloroform.
Toxicol. Letters 20: 161-172 1984

Alcorn D, Cheshire GR, Coghlan JP, Ryan GB

Peripolar cell hypertrophy in the renal juxtaglomerular region of newborn sheep.

Cell Tiss. Res. 236: 197-202 1984

Alcorn D, McCausland J, Ryan GB

Immunohistochemical localisation of chromogranin to glomerular peripolar cells of newborn sheep.

Kidney Int. 42: 1049 1992

Andres G, Brentjers JR, Caldwell PR, Camussi G, Matsuo S
Formation of immune deposits and disease.

Lab. Invest. 55: 510-520 1986

Andrews PM

Scanning electron microscopy of human and rhesus monkey kidneys.

Lab. Invest. 32: 610-618 1975

Andrews PM

The urinary system - kidney.

In "Biomedical research applications of scanning electron microscopy", Volume 1

Hodges GM and Hallowes RC (eds)

Academic Press, 1979 pp.273-306

Andrews PM

The presence of proximal tubule-like cells in the kidney parietal epithelium in response to unilateral nephrectomy.

Anat. Rec. 200: 61-65 1981

Andrews PM, Porter KR

A scanning electron microscope study of the nephron.

Am. J. Anat. 140: 81-116 1974

Arakawa M, Edanaga M, Tokunaga J

Scanning electron microscopy of the isolated human glomerulus in normal, nephritic and nephrotic situations.

In "International conference on pathogenesis, pathology and treatment of glomerulonephritis".

Kluthe R, Vogt A, Batsford SR (eds)

J Wiley & Sons, New York 1976 pp.96-108

Arakawa M, Edanaga M, Tokunaga J

The application of scanning electron microscopy to the histological diagnosis of renal biopsy specimens.

S. E. M. Vol.II 171-177 1977

Arakawa M, Tokunaga J

A scanning electron microscope study of the human
Bowman's epithelium.

Contrib. Nephrol. 6: 73-78 1977

Bankir L, Farman N

Heterogeneite des glomerules chez le lapin.

Arch. Anat. Microsc. Morphol. Exp. 62: 281-291 1973

Barajas L

The ultrastructure of the juxtaglomerular apparatus as disclosed by three-dimensional reconstruction from serial sections: the anatomical relationship between the tubular and vascular components.

J. Ultrastruct. Res. 33: 116-147 1970

Barajas L

Anatomy of the juxtaglomerular apparatus.

Am. J. Physiol. 237: F333-F343 1979

Barajas L, Latta H.

A three-dimensional study of the juxtaglomerular apparatus in the rat.

Lab. Invest. 12: 257-269 1963

Barberini F, Familiari G, Vittori I, Carpino F, Melis M
Morphological and statistical investigation of the occurrence of 'tubule-like' cells in the renal corpuscle of the mouse kidney induced by sex hormones.

Renal Physiol. 7: 227-236 1984

Barger AC, Herd JA

The renal circulation.

New Engl. J. Med. 284:482-490 1971

Beaman M, Howie AJ, Hardwicke J, Michael J, Adu D

The glomerular tip lesion: a steroid responsive nephrotic syndrome.

Clin. Nephrol. 27: 217-221 1987

Beeuwkes R

Efferent vascular patterns and early vascular - tubular relations in the dog kidney.

Am. J. Physiol. 221: 1361-1374 1971

Bernstein J, Landing BH

Glomerulocystic kidney diseases.

Prog. Clin. Biol. Res. 305: 27-43 1989

Bialestock D

The morphogenesis of renal cysts in the stillborn studied by microdissection technique.

J. Pathol. Bacteriol. 71: 51-59 1956

Bohle A, Kressel G, Muller CA, Muller GA

The pathogenesis of chronic renal failure.

Pathol. Res. Pract. 185: 421-440 1989

Bohman SO, Olsen S, Petersen VP

Glomerular ultrastructure in extracapillary
glomerulonephritis.

Acta. Pathol. Microbiol. Scand. (A) 82 (suppl. 249)
29-54 1974

Border WA, Baehler RW, Bhathena D, Glasscock RJ

IgA anti-basement membrane nephritis with pulmonary
haemorrhage.

Ann. Intern. Med. 91: 21-25 1979

Boucher A, Droz D, Adafor E, Noel LH

Relationship between the integrity of Bowman's capsule
and the composition of cellular crescents in human
crescentic glomerulonephritis.

Lab. Invest. 56: 526-533 1987

Brenner BM, Meyer TW, Hostetter TH

Dietary protein intake and the progressive nature of
kidney disease: the role of hemodynamically mediated
glomerular injury in the pathogenesis of progressive
glomerular sclerosis in aging, renal ablation, and
intrinsic renal disease.

N. Engl. J. Med. 307: 652-659 1982

Brenner BM, Troy JL, Daugherty TM

The dynamics of glomerular ultrafiltration in the rat.

J. Clin. Invest. 50: 1776-1780 1971

Briere N

Alkaline phosphatase activity at unusual sites of human foetal kidney.

Cell Tiss. Res. 242: 567-573 1986

Briere N, Petitclerc C, Plante G

Presence of alkaline phosphatase and gamma glutamyl transpeptidase on the parietal layer of Bowman's capsule.

Acta Histochem. 73: 237-241 1983

Brown CB, Cameron JS, Turner DR, Chantler C, Ogg CS, Williams DG, Benwick M

Focal segmental glomerulosclerosis with rapid decline in renal function ("malignant FSGS").

Clin. Nephrol. 10: 51-61 1978

Bulger RE

The urinary system.

In "Histology: Cell and Tissue Biology".

Weiss L (ed) Macmillan Press, 1983 pp.869-913

Bulger RE, Siegel FL, Pendergrass R

Scanning and transmission electron microscopy of the rat kidney.

Am. J. Anat. 139: 483-502 1974

Buss H, Kronert W

Zur struktur des nierenglomerulum der ratte.

Rasterelektronenmikroskopische untersuchungen.

Virchows Archiv B Cell. Pathol. 4: 79-92 1969

Carpino F, Barberini F, Familiari G, Melis M

Columnar cells of the parietal layer of Bowman's capsule and their relationship with the sexual cycle in normal female mice.

Experientia 32: 1584-1585 1976

Casellas D

A method for scanning electron microscopic observation of glomerular vascular poles in rat kidneys.

J. Electr. Microsc. Techn. 4: 63-64 1986

Castelletto L, Goya RG

Sex-related incidence of tubular metaplasia in Bowman's capsule of aging rats.

Virchows Archiv B Cell. Pathol. 59: 79-82 1990

Chung WY, Nast CC, Ettenger RB, Danovitch GM, Ward HJ, Cohen AH

Acquired cystic disease in chronically rejected renal transplants.

J. Am. Soc. Nephrol. 2: 1298-1301 1992

Clay RD, Darmady EM, Hawkins M

The nature of the renal lesion in the Fanconi syndrome.

J. Pathol. Bacteriol. 65: 551-558 1953

Crabtree C

Sex differences in the structure of Bowman's capsule in the mouse.

Science 91: 299 1940

Crabtree C

The structure of Bowman's capsule as an index of age and sex variations in normal mice.

Anat. Rec. 79: 395-413 1941

Damadian RV, Shwayri E, Bricker NS

On the existence of non-urine forming nephrons in the diseased kidney of the dog.

J. Lab. Clin. Med. 65: 26-39 1965

Darmady EM, Dempster WJ, Stranack F

The evolution of interstitial and tubular changes in homotransplanted kidneys.

J. Pathol. Bacteriol. 70: 225-231 1955

Darmady EM, Stranack F

Microdissection of the nephron in disease.

Brit. Med. Bull. 13: 21-25 1957

Dietert SE

The columnar cells occurring in the parietal layer of Bowman's capsule. Cellular fine structure and protein transport.

J. Cell Biol. 35: 435-444 1967

Dosa S, Thompson AM, Abraham A

Glomerulocystic kidney disease. Report of an adult case.

Am. J. Clin. Pathol. 82: 619-621 1984

Downie I, Gardiner DS, Downie TT, Gibson IW, Kenyon C, More IAR, Lindop GBM

Non-granulated peripolar cells exist in the rat glomerulus.

Cell Tiss. Res. 268: 567-570 1992

Dunn TB

Some observations on the normal and pathologic anatomy of the kidney of the mouse.

J. Nat. Cancer Inst. 9: 285-301 1948

Dworkin LD, Brenner BM

Biophysical basis of glomerular filtration.

In "The Kidney: Physiology and Pathophysiology".

Seldin DW, Geibisch G (eds)

Raven Press, New York, 1988 pp.397-426

Edwards JG

Efferent arterioles of glomeruli in the juxtamedullary zone of the human kidney.

Anat. Rec. 125: 521-529 1956

Edwards JG, Schnitter C

The renal unit in the kidney of vertebrates.

Am. J. Anat. 53: 55-87 1933

Eldridge C, Merrit S, Goyal M, Kulaga H, Kindt TJ,
Wiggins R

Analysis of T cells and major histocompatibility complex
class I and class II mRNA and protein content and
distribution in anti-glomerular basement membrane
disease in the rabbit.

Am. J. Pathol. 139: 1021-1035 1991

Elema JD, Arends A

Focal and segmental glomerular hyalinosis and sclerosis
in the rat.

Lab. Invest. 33: 554-561 1975

Evan AP, Dail WG

Applications of SEM to problems of kidney development.

S. E. M. Vol.II: 373-380 1977

Evan AP, Gardner KD

Comparison of human polycystic and medullary cystic
kidney disease with diphenylamine-induced cystic
disease.

Lab. Invest. 35: 93-101 1976

Finckh ES, Joske RA

The occurrence of columnar epithelium in Bowman's
capsule.

J. Pathol. Bacteriol. 68: 646-648 1954

Foley WA, Jones DCL, Osborn GK, Kimeldorf DJ

A renal lesion associated with diuresis in the aging Sprague Dawley rat.

Lab. Invest. 13: 439-450 1964

Frank M, Kriz W

Scanning electron microscopy studies of the vascular pole of the rat glomerulus.

Anat. Rec. 204: 149-152 1982

Fujita T, Tokunaga J, Miyoshi M

Scanning electron microscopy of the podocytes of the renal glomerulus.

Arch. Histol. Jpn. 32: 99-113 1970

Gaffney EF

Prominent parietal epithelium: a common sign of renal glomerular injury.

Hum. Pathol. 13: 651-660 1982

Gall JAM, Alcorn D, Butkus A, Coghlan JP, Ryan GB

Distribution of glomerular peripolar cells in different mammalian species.

Cell Tiss. Res. 244: 203-208 1986

Gall JAM, Alcorn D, Coghlan JP, Johnston CI, Ryan GB
Immunohistochemical detection of urinary kallikrein-like material in renal juxtaglomerular peripolar cells in sheep.

Proceedings of the IXth International Congress of Nephrology.

Los Angeles, June 1984

Gardiner DS

The glomerular peripolar cell.

MD Thesis

University of Glasgow, 1991

Gardiner DS, Jackson R, Lindop GMB

The renin-secreting cell and the glomerular peripolar cell in renal artery stenosis and Addison's disease.

Virchows Archiv A Pathol. Anat. 420: 533-537 1992a

Gardiner DS, Lindop GMB

The granular peripolar cell of the human glomerulus: a new component of the juxtaglomerular apparatus?.

Histopathol. 9: 675-685 1985

Gardiner DS, Lindop GMB

The glomerular peripolar cell - an immunohistochemical study.

A. P. M. I. S. 100: 107-115 1992a

Gardiner DS, Lindop GMB

Peripolar cells, granulated glomerular epithelial cells and their relationship to the juxtaglomerular apparatus in malignant hypertension.

J. Pathol. 167: 59-64 1992b

Gardiner DS, More IAR, Lindop GMB

The granular peripolar cell of the human glomerulus : an ultrastructural study.

J. Anat. 146: 31-43 1986

Gardiner DS, More IAR, Lindop GMB

Peripolar cells and other granulated epithelial cells in renal biopsies.

A. P. M. I. S. 100: 701-708 1992b

Gattone VH, Luft FC, Evan AP

Renal afferent and efferent arterioles of the rabbit.

Am. J. Physiol. 247: F219-F228 1984

Gibson IW, Downie I, Downie TT, Han SW, More IAR, Lindop GBM

The parietal podocyte: a study of the vascular pole of the human glomerulus.

Kidney Int. 41: 211-214 1992

Gibson IW, Downie TT, More IAR, Lindop GBM

Immune complex deposition in Bowman's capsule is associated with parietal podocytes.

J. Pathol. 173: 53-59 1994

Gibson IW, Gardiner DS, Downie I, Downie TT, More IAR,
Lindop GBM

A comparative study of the glomerular peripolar cell and
the renin-secreting cell in twelve species of mammal.

Cell Tiss. Res. 277: 385-390 1994

Gomez RA, Lynch KR, Sturgill BC, Elwood JP, Chevalier
RL, Carey RM, Peach MJ

Distribution of renin mRNA and its protein in the
developing kidney.

Am. J. Physiol. 257: F850-F858 1989

Grantham JJ, Geiser JL, Evan AP

Cyst formation and growth in autosomal dominant
polycystic kidney disease.

Kidney Int. 31: 1145-1152 1987

Green NJ, Howie AJ, Rayner HC, Wall J

Effect of cholesterol on the position of segmental
lesions in unilaterally nephrectomized rats.

J. Pathol. 168: 331-334 1992

Grond J, Schilthius MS, Koudstaal J, Elema JD

Mesangial function and glomerular sclerosis in rats
after unilateral nephrectomy.

Kidney Int. 22: 338-343 1982

Gruenwald P, Popper H

The histogenesis and physiology of the renal glomerulus
in early postnatal life: histological examination.

J. Urol. 43: 452 1940

Haensly WE

Metaplasia of the parietal layer of Bowman's capsule: a
histopathological survey of the human kidney.

Anat. Histol. Embryol. 16: 81 1987

Haensly WE, Granger HJ, Morris AC, Cioffe C

Proximal-tubule-like epithelium in Bowman's capsule in
spontaneously hypertensive rats.

Am. J. Pathol. 107: 92-97 1982

Haley DP, Bulger RE

The aging male rat: structure and function of the
kidney.

Am. J. Anat. 167: 1-13 1983

Hanner RH, Ryan GB

Ultrastructure of the renal juxtaglomerular complex and
peripolar cells in the axolotl (*Ambystoma mexicanum*) and
toad (*Bufo marinus*).

J. Anat. 130: 445-455 1980

Harvey JM, Howie AJ, Lee SJ, Newbold KM, Adu D, Michael J, Beevers DG

Renal biopsy findings in hypertensive patients with proteinuria.

Lancet 340: 1435-1436 1992

Hay DA, Evan AP

Maturation of the glomerular visceral epithelium and capillary endothelium in the puppy kidney.

Anat. Rec. 193: 1-21 1979

Heaton JM, Turner DR

Persistent renal damage following pre-eclampsia: a renal biopsy study of thirteen patients.

J. Pathol. 147: 121-126 1985

Helmholz H

The presence of tubular epithelium within the glomerular capsule in mammals.

Proc. Staff Meetings Mayo Clinic 10: 110-112 1935

Heptinstall RH, Hill GS

Experimental pyelonephritis and hypertension: a study on the immunity of pyelonephritic glomeruli from hypertensive change.

Lab. Invest. 16: 96-111 1967

Hepinstall RH, Kissane JM, Still WJS

Experimental pyelonephritis: morphology and quantitative histochemistry of glomeruli in pyelonephritic scars in the rat.

Bull. John Hopkins Hosp. 112: 299 1963

Hill GS

Dysproteinemias, amyloidosis and immunotactoid glomerulopathy.

In "Pathology of the Kidney"

Hepinstall RH (ed) 4th edition

Little Brown & Company, Boston 1992 pp.1631-1713

Hill PA, Coghlan JP, Scoggins BA, Ryan GB

Ultrastructural changes in the sheep renal juxtaglomerular apparatus in response to sodium depletion or loading.

Pathology 15: 463-473 1983

Hill PA, Coghlan JP, Scoggins BA, Ryan GB

Structural and functional studies of the adrenal cortex and renal juxtaglomerular apparatus in pregnant sheep subjected to sodium depletion or loading.

Pathology 16: 285-290 1984a

Hill PA, Coghlan JP, Scoggins BA, Ryan GB

Functional and morphological studies of the adrenal cortex and kidney in ovine toxæmia of pregnancy.

J. Pathol. 144: 1-13 1984b

Hill PA, Fairley KF, Kincaid-Smith P, Zimmerman M, Ryan
GB

Morphologic changes in the renal glomerulus and the
juxtaglomerular apparatus in human preeclampsia.

J. Pathol. 156: 291-303 1988

Hitomi K, Murakami T, Kareshige T

Human kidney glomeruli, with special reference to those
in the aged person: scanning electron microscopic study
of microvascular corrosion casts.

Acta Med. Okayama 41: 165-171 1987

Hollywell CA, Jaworowski A, Thumwood C, Alcorn D, Ryan
GB

Immunohistochemical localization of transthyretin in
glomerular peripolar cells of newborn sheep.

Cell Tiss. Res. 267: 193-197 1992

Honey GE, Pryse-Davies J, Roberts DM

A survey of nephropathy in young diabetics.

Quart. J. Med. 31: 473-484 1962

Hostetter TH, Olson JL, Rennke HG, Venkatachalam MA,
Brenner BM

Hyperfiltration in remnant nephrons: a potentially
adverse response to renal ablation.

Am. J. Physiol. 241: F85-F93 1981

Howie AJ

Changes at the glomerular tip: a feature of membranous nephropathy and other disorders associated with proteinuria.

J. Pathol. 150: 13-20 1986a

Howie AJ

Epithelial membrane antigen in normal and proteinuric glomeruli and in damaged proximal tubules.

J. Pathol. 148: 55-60 1986b

Howie AJ

Segmental sclerosing glomerular lesions.

Pediatr. Nephrol. 7: 370-374 1993

Howie AJ, Brewer DB

The glomerular tip lesion: a previously undescribed type of segmental glomerular abnormality.

J. Pathol. 142: 205-220 1984

Howie AJ, Brewer DB

Further studies on the glomerular tip lesion: early and late stages and life table analysis.

J. Pathol. 147: 245-255 1985

Howie AJ, Brewer DB

The glomerular tip lesion: a distinct entity or not.
Letter to the editor.

J. Pathol. 154: 191-192 1988

Howie AJ, Kizaki T, Beaman M, Morland CM, Birtwistle RJ,
Adu D, Michael J, Williams AJ, Walls J, Matsuyama M,
Shimizu F

Different types of segmental sclerosing glomerular
lesions in six experimental models of proteinuria.

J. Pathol. 157: 141-151 1989

Howie AJ, Lee SJ, Green NJ

Different clinico-pathological types of segmental
sclerosing lesions in adults.

Nephrol. Dial. Transpl. 8: 590-599 1993

Huppes W, Hene RJ, Kooiker CJ

The glomerular tip lesion: a distinct entity or not?

J. Pathol. 154: 187-190 1988a

Huppes W, Hene RJ, Kooiker CJ

The glomerular tip lesion: a distinct entity or not?

Author's reply.

J. Pathol. 156: 353 1988b

Hurley BP, Painter DM

Glomerular tip lesion in nephrotic syndrome.

Kidney Int. 33: 145 1988

Hutt MSR, Pinniger JL, De Wardener HE

The relationship between the clinical and the
histological features of acute glomerular nephritis.

Quart. J. Med. 27: 265-292 1958

Ito H, Yoshikawa , Aozai F, Hazikano H, Sakaguchi H,
Akamatsu R, Matsuo T, Matsuyama S

Twenty-seven children with focal segmental
glomerulosclerosis: correlation between the segmental
location of the glomerular lesions and prognosis.

Clin. Nephrol. 22: 9-14 1984

Jenkins DAS, Wojtacha DR, Fleming S, Cumming AD

Detection of renal kallikrein mRNA in normal human
kidney by in-situ hybridisation.

Renal Association Meeting, Birmingham 1991

Jones DB

Correlative scanning and transmission electron
microscopy of glomeruli.

Lab. Invest. 37: 569-578 1977

Jones DB

Scanning electron microscopy of human hypertensive renal
disease.

S. E. M. Vol. II: 937-942 1978

Jones DB

SEM of human and experimental renal disease.

S. E. M. Vol. III: 679-690 1979

Jones DB

Ultrastructure of human acute renal failure.

Lab. Invest. 46: 254-264 1982

Jorgensen F

Electron microscopic studies of normal visceral epithelial cells.

Lab. Invest. 17: 225-242 1967

Kanel GC, Peters RL

Glomerular tubular reflux. A morphological renal lesion associated with the hepatorenal syndrome.

Hepatology 4: 242-246 1984

Kaplan C, Pasternack B, Shah H, Gallo G

Age-related incidence of sclerotic glomeruli in human kidneys.

Am. J. Pathol. 80: 227-234 1975

Kappel B, Olsen S

Cortical interstitial tissue and sclerosed glomeruli in the normal human kidney related to age and sex. A quantitative study.

Virchows Arch. A 387: 271-277 1980

Kelly G, Downie I, Gardiner DS, More IAR, Lindop GBM

The peripolar cell: a distinctive cell type in the mammalian glomerulus. Morphological evidence from a study of sheep.

J. Anat. 168: 217-227 1990

Kerjaschki D, Farquhar MG

Immunocytochemical localization of the Heymann nephritis antigen (GP330) in glomerular epithelial cells of normal Lewis rats.

J. Exp. Med. 157: 667-686 1983

Knowlson GTG, Cameron AH

Hepatoblastoma with adenomatoid renal epithelium.

Histopathol. 3: 201-208 1979

Kondo Y, Akikura B

Chronic Masugi nephritis in the rat: an electron microscopic study on evolution and consequences of glomerular capsular adhesions.

Acta Pathol. Japonica 32:231-242 1982

Koval'chuk LE

Ultrastructure of the juxtaglomerular complex of the kidney and peripolar cells in the sand lizard.

Arkh. Anat. Gistol. Embriol. 93: 93-98 1987

Kramp RA, MacDowell M, Gottschalk CW, Oliver JR

A study by microdissection and micropuncture of the structure and the function of the kidneys and the nephrons of rats with chronic renal damage.

Kidney Int. 5: 147-176 1974

Kriz W, Bachmann S

Pre- and postglomerular arterioles of the kidney.

J. Cardiovasc. Pharmacol. 7 (suppl.3): 24-30 1985

Lacy ER, Castellucci M, Reale E

The elasmobranch renal corpuscle: fine structure of
Bowman's capsule and the glomerular capillary wall.

Anat. Rec. 218: 294-305 1987

Lacy ER, Reale E

Granulated peripolar epithelial cells in the renal
corpuscle of marine elasmobranch fish.

Cell Tiss. Res. 257: 61-67 1989

Lan HY, Nikolic-Paterson DJ, Atkins RC

Involvement of activated periglomerular leukocytes in
the rupture of Bowman's capsule and glomerular crescent
progression in experimental glomerulonephritis.

Lab. Invest. 67: 743-751 1992

Lan HY, Paterson DJ, Atkins RC

Initiation and evolution of interstitial leucocytic
infiltration in experimental glomerulonephritis.

Kidney Int. 40: 425-433 1991

Lawrence GM, Brewer DB

Studies on the relationship between proteinuria and
glomerular ultrastructural change in hyperalbuminaemic
female Wister rats.

J. Pathol. 138: 365-383 1982

Lee SJ, Howie AJ

Changes at the glomerulo-tubular junction in renal transplants.

J. Pathol. 156: 311-318 1988

Lee SJ, Sparke J, Howie AJ

The mammalian glomerulotubular junction studied by scanning and transmission electron microscopy.

J. Anat. 182: 177-185 1993

Lindop GBM, Gardiner DS, Gibson IW, Kenyon C, More IAR
Effect of altered renal perfusion and manipulation of dietary sodium on the glomerular peripolar cell and the juxtaglomerular apparatus.

Nephrol. Dial. Transplant. 8: 888 1993

Ljungqvist A, Lagergren C

Normal intrarenal arterial pattern in adult and aging human kidney. A microangiographical and histological study.

J. Anat. 96: 285-300 1962

Marais J

Cortical microvasculature of the feline kidney.

Acta Anat. 130: 127-131 1987

Marcus PB

Podocytic metaplasia of parietal Bowman's capsular epithelium.

Arch. Pathol. Lab. Med. 101: 664 1977

Marcussen N

Atubular glomeruli in cisplatin-induced chronic interstitial nephropathy: an experimental stereological investigation.

A. P. M. I. S. 98: 1087-1097 1990

Marcussen N

Atubular glomeruli in renal artery stenosis.

Lab. Invest. 65: 558-565 1991

Marcussen N

Atubular glomeruli and the structural basis for chronic renal failure.

Lab. Invest. 66: 265-284 1992

Marcussen N, Jacobsen NO

The progression of cisplatin-induced tubulointerstitial nephropathy in rats.

A. P. M. I. S. 100: 256-268 1992

Marcussen N, Olsen TS

Atubular glomeruli in patients with chronic pyelonephritis.

Lab. Invest. 62: 467-473 1990

Marcussen N, Christensen S, Patersen JS, Shalmi M

Atubular glomeruli, renal function and hypertrophic response in rats with chronic lithium nephropathy.

Virchows Arch. A 419: 281 1991

Marcussen N, Ottosen PD, Christensen S

Ultrastructural quantitation of atubular and hypertrophic glomeruli in rats with lithium-induced chronic nephropathy.

Virchow Arch. A Pathol. Anat. 417: 513-522 1990

Marcussen N, Ottosen PD, Christensen S, Olsen TS

Atubular glomeruli in lithium-induced chronic nephropathy in rats.

Lab. Invest. 61: 295-302 1989

Mbassa GK

Peripolar cells form the majority of granulated cells in the kidneys of antelopes and goats.

Acta Anat. 135: 158-163 1989

Mbassa G, Elger M, Kriz W

The ultrastructural organization of the basement membrane of Bowman's capsule in the rat renal corpuscle.

Cell Tiss. Res. 253: 151-163 1988

Melis M, Carpino F, Palermo D, Motta P

Scanning and transmission electron microscopic observations on the columnar cells of the parietal layer of Bowman's capsule in normal mice.

J. Microsc. 19: 247-252 1974

Melnick SC, Brewer DB, Oldham JS

Cortical microcystic disease of the kidney with dominant inheritance: a previously undescribed syndrome.

J. Clin. Pathol. 37: 494-499 1984

Miller K, Michael AF

Immunopathology of renal extracellular membranes in diabetes mellitus: specificity of tubular basement membrane immunofluorescence.

Diabetes 25: 701-708 1976

Mitchell GM, Stratford BF, Ryan GB

Morphogenesis of the renal juxtaglomerular apparatus and peripolar cells in the sheep.

Cell Tiss. Res. 222: 101-111 1982

Miyoshi M

Scanning electron microscopy of the renal corpuscle of the mesonephros in the lamprey, Entosphenus japonicus mortens.

Cell Tiss. Res. 187: 105-113 1978

Miyoshi M, Ogawa K, Shingu K, Omayari N

Scanning and transmission electron microscopy of cysts in the renal cortex of the macaque monkey.

Arch. Histol. Jpn. 47: 259-269 1984

Morild I, Christensen JA, Mikeler E, Bohle A
Peripolar cells in the avian kidney.
Virchows Archiv. A Pathol. Anat. Histopathol. 412:
471-477 1988

Morita M, White RHR, Coad NAG, Raafat F
The clinical significance of the glomerular location of
segmental lesions in focal segmental glomerulosclerosis.
Clin. Nephrol. 33: 211-219 1990a

Morita M, Yoshiara S, White RHR, Raafat F
The glomerular changes in children with reflux
nephropathy.
J. Pathol. 162: 245-253 1990b

Morley AR
Peri-hilar rupture of Bowman's capsule in crescentic
glomerulonephritis.
A. P. M. I. S. Suppl. 4: 74-81 1988

Murakami T
Glomerular vessels of the rat kidney: a scanning
electron microscope study of corrosion casts.
Arch. Histol. Jpn. 34: 87 1972

Murakami T, Kikuta A, Akita S, Sano T
Multiple efferent arterioles of the human kidney
glomerulus as observed by scanning electron microscopy
of vascular casts.
Arch. Histol. Jpn. 48: 443-447 1985

Murakami T, Miyoshi M, Fujita T

Glomerular vessels of the rat kidney with special reference to double efferent arterioles. A scanning electron microscopy study of corrosion casts.

Arch. Histol. Jpn. 33: 179-189 1971

Nagata M, Kriz W

Glomerular damage after uninephrectomy in young rats. II Mechanical stress on podocytes as a pathway to sclerosis.

Kidney Int. 42: 148-160 1992

Nakajima M, Mathews DC, Hewitson T, Kincaid-Smith P

Modified immunogold labelling applied to the study of protein droplets in glomerular disease.

Virchows Archiv. A Pathol. Anat. 415: 489-499 1989

Newbold KM, Howie AJ

Analysis of the position of segmental lesions in glomeruli in vasculitic-type glomerulonephritis and other disorders.

J. Pathol. 162: 149-155 1990

Newman WJ, Tisher CC, McCoy RC, Gunnells JC, Kreuger RP, Clapp JR, Robinson RR

Focal glomerular sclerosis: contrasting clinical patterns in children and adults.

Medicine (Balt) 55: 67-87 1976

Ng WL, Chan KW, Ma L

A scanning electron microscope study of isolated glomeruli in glomerulonephritis.

Pathology 15: 138-148 1983

Ng WL, So KF, So PC, Ngai HK

The preparation of glomeruli from renal biopsy specimens for scanning electron microscopy.

Pathology 14: 299-302 1982

Niall JF

Prolonged survival in the nephrotic syndrome.

Med. J. Aust. 1: 843-845 1965

Nopanitaya W

SEM of glomerular microcirculation with special attention on afferent and efferent arterioles.

S. E. M. Vol. III: 395-397 1980

Nyengaard JR, Bendtsen TF

The practical use of the fractionator in glomerular counting.

Acta Stereol. 8: 275-279 1989

Ogata K

Clinicopathological study of kidneys from patients on chronic dialysis.

Kidney Int. 37: 1333 1990

Oh Y, Onoyama K, Kobayashi K, Nanishi F, Mitsuoka W,
Ohchi N, Tsuruda H, Fujishima M
Glomerulocystic kidneys. Report of an adult case.
Nephron 43: 299-302 1986

Ojeda JL, Garcia-Porrero JA
Structure and development of parietal podocytes in renal
glomerular cysts induced in rabbits with
methylprednisolone acetate.

Lab. Invest. 47: 167-176 1982

Ojeda JL, Garcia-Porrero JA, Hurle JM
Experimental formation of podocytes in the parietal
layer of the Bowman's capsule.
Experientia 35: 1658-1660 1979

Ojeda JL, Icardo JM
A scanning electron microscope study of the neck segment
of the rabbit nephron.
Anat. Embryol. 184: 605-610 1991

Oliver J
Architecture of the kidney in chronic Bright's disease.
New York, Paul B Hoeber (ed.) 1939

Olsen P
Extracapillary glomerulonephritis; a semiquantitative
light microscopy study of 59 patients.
Acta Pathol. Microbiol. Scand. A 82 Suppl. 249: 7-19
1974

Olsen P, Peterson VP, Hansen ES

Immunofluorescence studies of extracapillary
glomerulonephritis.

Acta Pathol. Microbiol. Scand. A 82 Suppl. 249: 20-28
1974

Olson JL, de Urdaneta AG, Heptinstall RH

Glomerular hyalnosis and its relation to
hyperfiltration.

Lab. Invest. 52: 387-398 1985

Or SB, Ngai HK, Yau WL

Correlative study of the same isolated glomerulus by
electron and light microscopy.

Med. Lab. Sci. 40: 359-366 1983

Pardo-Mindan FJ, Pablo CL, Vazquez JJ

Morphogenesis of glomerular cysts in renal dysplasia.

Nephron 21: 155-160 1978

Pease DC

Fine structures of the kidney seen by electron
microscopy.

J. Histochem. Cytochem. 3: 295-308 1955

Peter S

Ultrastructural studies on the secretory process in the
epithelioid cells of the juxtaglomerular apparatus.

Cell Tiss. Res. 168: 45-53 1976

Porter KA, Rendall JM, Stolinski C, Terasaki PI,
Marchioro TL, Starzl TE

Light and electron microscopic study of biopsies from 33
human renal allografts and an isograft $1\frac{3}{4}$ to $2\frac{1}{2}$
years after transplantation.

Ann. N. Y. Acad. Sci. 129: 615 1966

Poucell S, Baumal R, Farine M, Arbus GS

Location of glomerular lesions in focal segmental
glomerulosclerosis.

Arch. Pathol. Lab. Med. 109: 482-483 1985

Prescott RJ, McWilliam L, Coyne JD

Are defects in Bowman's capsule specific to crescentic
glomerulonephritis? A study of patterns of
glomerulosclerosis.

J. Pathol. 169 Suppl: 145 1993

Ras NR, Heptinstall RH

Experimental hydronephrosis: a study of the response of
glomeruli and arteries to hypertension.

Nephron 6: 598 1969

Rash JE, Shay JW, Bieseile JJ

Cilia in cardiac differentiation.

J. Ultrastruct. Res. 29: 470-484 1969

Reeves W, Caulfield JP, Farquhar MG

Differentiation of epithelial foot processes and filtration slits: sequential appearance of occluding junctions, epithelial polyanion and slit membranes in developing glomeruli.

Lab. Invest. 39: 90-100 1978

Risak E

Über fehltbildungen der Bowmanschen kapsel.

Virchows Archiv Pathol. Anat. Physiol. 267: 222-232 1928

Rizzoni G, Lourat C, Levy M, Milanesi C, Zachello G,
Matthieu H

Familial hypoplastic glomerulocystic kidney: a new entity?

Clin. Nephrol. 18: 263-268 1982

Ronco P, Neale TJ, Wilson CB, Galceran M, Verroust P
An immunopathologic study of a 330kD protein defined by monoclonal antibodies and reactive with anti-RTEalpha5 antibodies and kidney eluates from active Heymann nephritis.

J. Immunol. 136: 125-130 1986

Roos A

Polycystic kidney: report of a case studied by reconstruction.

Am. J. Dis. Child. 61: 116-127 1941

Rosivall L

Morphology and function of the distal part of the afferent arteriole.

Kidney Int. 38 Suppl. 30: S10-S15 1990

Rosivall L, Taugner R

The morphological basis of fluid balance in the interstitium of the juxtaglomerular apparatus.

Cell Tiss. Res. 242: 525-533 1986

Rosivall L, Taugner R

Fluid balance in the interstitium of the Goormaghtigh cell field.

In "The juxtaglomerular apparatus"

Persson AEG, Boberg U (eds)

Elsevier, Amsterdam 1988 pp.39-49

Ryan GB, Alcorn D, Coghlan JP, Hill PA, Jacobs R

Ultrastructural morphology of granule release from juxtaglomerular myoepithelioid and peripolar cells.

Kidney Int. 22 Suppl.12: S3-S8 1982

Ryan GB, Coghlan JP, Scoggins BA

The granulated peripolar epithelial cell: a potential secretory component of the renal juxtaglomerular complex.

Nature 277: 655-656 1979

Sakai T, Billo R, Nobiling R, Gorgas K, Kriz W
Ultrastructure of the kidney of a South American
caecilian *Typhlonectes compressicaudus* (Amphibia,
gymnophiona). I. Renal corpuscle, neck segment,
proximal tubule and intermediate segment.

Cell Tiss. Res. 252: 589-600 1988

Sakai T, Kawahara K

The structure of the kidney of Japanese newts *Triturus*
(*Cynops*) *pyrrhogaster*.

Anat. Embryol. 166: 31-52 1983

Schainuck LI, Striker GE, Cutler RE, Benditt EP
Structural-functional correlations in renal disease.
Part II. The correlations.

Hum. Pathol. 1: 631 1970

Schonheyder HC, Maunsbach AB

Ultrastructure of a specialised neck region in the
rabbit nephron.

Kidney Int. 7:145-153 1975

Schutz W

Die epithelveranderungen am parietalen blatt der
glomeruluskapsel beim diabetes mellitus.

Virchow Archiv Path. Anat. 251: 669-684 1924

Selye H

The effect of testosterone on the kidney.

J. Urol. 42: 637-641 1939

Shimamura T, Heptinstall RH

Experimental pyelonephritis: nephron dissection of the kidney of experimental chronic pyelonephritis in the rabbit.

J. Pathol. Bacteriol. 85: 421-423 1963

Silva FG

Membranoproliferative glomerulonephritis.

In "Pathology of the kidney" 4th Edition

Heptinstall RH (ed)

Little Brown & Company, Boston, USA 1992

Silva F, Verani R

Crescentic glomerulonephritis: relationship of the stage of crescent formation to gaps in Bowman's capsule.

Kidney Int. 25: 226 1984

Smith JP

Anatomical features of the human renal glomerular efferent vessel.

J. Anat. 90: 290-292 1956

Smith SM, Hoy WE, Cobb L

Low incidence of glomerulosclerosis in normal kidneys.

Arch. Pathol. Lab. Med. 113: 1253-1255 1989

Solez K, Morel-Maroger L, Sraer JD

The morphology of "acute tubular necrosis" in man:
analysis of 57 renal biopsies and a comparison with the
glycerol model.

Medicine 58: 362-376 1979

Spinelli F

Structure and development of the renal glomerulus as
revealed by scanning electron microscopy.

Int. Rev. Cytol. 39: 345-378 1974

Spitzer A

The developing kidney and the process of growth.

In "The kidney: physiology and pathophysiology"

Seldin DW, Gebisch G (eds)

Raven Press, New York 1985

Taugner R, Boll U, Zahn P, Forssmann WG

Cell junctions in the epithelium of Bowman's capsule.

Cell Tiss. Res. 172: 431-446 1976

Taugner R, Hackenthal E

The juxtaglomerular apparatus: structure and function.

Berlin Heidelberg, Springer-Verlag 1989

Taugner R, Rosivall L, Buhrlie CP, Groschel-Stewart U

Myosin content and vasoconstrictive ability of the
proximal and distal (renin-positive) segments of the
preglomerular arteriole.

Cell Tiss. Res. 248: 579-588 1987

Taugner R, Whalley A, Angermuller S, Buhole CP,
Hackenthal E

Are the renin-containing granules of juxtaglomerular
epithelioid cells modified lysosomes?

Cell Tiss. Res. 239: 575-587 1985

Teague CA, Doak PB, Simpson IJ, Rainer SP, Herdson PB
Goodpasture's syndrome: an analysis of 29 cases.

Kidney Int. 13: 492-504 1978

Thumwood CM, Alcorn D, Ryan GB

A scanning electron microscope study of the vascular
pole and associated peripolar cells in newborn lamb
kidney.

J. Anat. 165: 310 1989

Thumwood CM, McCausland J, Alcorn D, Ryan GB

Scanning and transmission electron-microscopic study of
peripolar cells in the newborn lamb kidney.

Cell Tiss. Res. 274: 597-604 1993

Tokunaga J, Edanaga M, Masu Y, Fujita T

Isolated renal glomeruli for scanning electron
microscopy.

J. Electr. Microsc. (Tokyo) 24: 109-114 1975

Trahair JF, Gall JAM, Alcorn D, Coghlan JP, Fernley R,
Penschow J, Grattage LP, Johnston CI, Ryan GB
Immunohistochemical study of peripolar cells of the
sheep.

J. Anat. 162: 125-132 1989

Trahair JF, Ryan GB

Immunohistochemical identification of plasma proteins in
cytoplasmic granules of peripolar cells of the sheep.

J. Anat. 160: 109-115 1988

Trahair JF, Ryan GB

Co-localisation of neuron-specific enolase-like and
kallikrein-like immunoreactivity in ductal and tubular
epithelium in sheep salivary gland and kidney.

J. Histochem. Cytochem. 37: 309-314 1989

Tribe CR, Heptinstall RH

The juxtaglomerular apparatus in scarred kidneys. An
experimental study into the nature of the stimulus
causing hyperplasia of the juxtaglomerular apparatus in
rats.

Br. J. Exp. Pathol. 46: 339-347 1965

Turner DR

Commentary: granular peripolar cells, renin and the
juxtaglomerular apparatus.

Histopathol. 9: 783-785 1985

Valdes AJ, Zhang J

Intraglomerular tubular epithelial cells. A marker of glomerular haematuria.

Arch. Pathol. Lab. Med. 111: 189-191 1987

Van Damme B, Tardanico R, Vanrenterghem Y, Desmet V
Adhesions, focal sclerosis, protein crescents, and capsular lesions in membranous nephropathy.

J. Pathol. 161: 47-56 1990

Velosa JH, Donadio JV, Holley KE

Focal sclerosing glomerulopathy. A clinicopathological study.

Mayo Clin. Proc. 50: 121-133 1975

Verroust PJ

Kinetics of immune deposits in membranous nephropathy.

Kidney Int. 35: 1418-1428 1989

Vlachos J, Tsakraklidis V

Glomerular cysts. An unusual variety of "polycystic kidneys": report of two cases.

Amer. J. Dis. Child. 114: 379-384 1967

Walsh TS, Thomson D, McDonald MK, Cumming AD

Histological and immunological studies on glomerular peripolar cells in sheep and human kidneys.

Proc. Xth Int. Congr. Nephrol. London 1987

Ward AM

Tubular metaplasia in Bowman's capsule.

J. Clin. Pathol. 23: 472-474 1970

Watson ML, Cumming AD, Lambie AJ, Oates JA

Urinary kallikrein and systemic prostacyclin synthesis
during sodium chloride infusion in normal man.

Clin. Sci. 68: 537-543 1985

Waugh D, Schlieter W, James AW

Infraglomerular epithelial reflux. An early lesion of
acute renal failure.

Arch. Pathol. 77: 93-96 1964

Webber WA, Blackbourn J

The permeability of the parietal layer of Bowman's
capsule.

Lab. Invest. 25: 367-373 1971

Webber WA, Lee J

The ciliary pattern of the parietal layer of Bowman's
capsule.

Anat. Rec. 180: 449-455 1974

Weinstein SW, Szyjewicz J

Superficial nephron tubular-vascular relationships in
the rat kidney.

Am. J. Physiol. 234: F207-F214 1978

Whitworth JA, Turner DR, Leibowitz, JS Cameron

Focal segmental sclerosis or scarred focal proliferative glomerulonephritis.

Clin. Nephrol. 9: 229-235 1978

Wilcox CS, Sterzel RB, Dunckel P, Mohrmann M, Perfetto M

Renal interstitial pressure and sodium excretion during hilar lymphatic ligation.

Am. J. Physiol. 247: F344-F351 1984

Wilson RB

Variations in the epithelial lining of Bowman's capsule.

S. E. M. Vol.II: 541-546 1977

Xiong W, Chao L, Chao J

Renal kallikrein mRNA localisation by in-situ hybridisation.

Kidney Int. 35: 1324-1329 1989

Yoshikawa N, Ito H, Akamatsu R, Matsujama S, Hasegawa O,

Nakahara C, Matsuo T

Focal segmental glomerulosclerosis with and without nephrotic syndrome in children.

J. Pediatr. 109: 65-70 1986

Youson JH, McMillan DB

The opisthonephric kidney of the sea lamprey of the Great Lakes, Petromyzon marinus L. I. The renal corpuscle.

Am. J. Anat. 127: 207-232 1970a

Youson JH, McMillan DB

The opisthonephric kidney of the sea lamprey of the Great Lakes, *Petromyzon marinus* L. II. Neck and proximal segments of the tubular nephron.

Am. J. Anat. 127: 233-258 1970b

Zamboni L, DeMartino C

Embryogenesis of the human renal glomerulus. I. A histological study.

Arch. Pathol. 86: 279-291 1968

Zucchelli P, Cagnoli L, Casanova S, Donini U, Pasquali S
Focal glomerulosclerosis in patients with unilateral nephrectomy.

Kidney Int. 24: 649-655 1983





IMMUNE COMPLEX DEPOSITION IN BOWMAN'S CAPSULE IS ASSOCIATED WITH PARIEL PODOCYTES

IAN W. GIBSON, THOMAS T. DOWNIE, IAN A. R. MORE AND GEORGE B. M. LINDOP

University Department of Pathology, Western Infirmary, Glasgow G11 6NT, Scotland, U.K.

Received 7 January 1994

Accepted 24 February 1994

SUMMARY

We have recently documented the presence of podocytes lining part of Bowman's capsule at the vascular pole, in adult human kidney. In this study, we describe the deposition of immune complexes in Bowman's capsule in association with these parietal podocytes. We examined 1 year's consecutive human renal biopsies ($n=170$). Transmission electron microscopy (TEM) revealed 18 cases in which parietal podocytes were present. Of these 18, there were 11 cases of glomerulonephritis, in which immune complexes were demonstrated in the capillary tuft by both TEM and direct immunofluorescence microscopy. In seven of these 11 cases, TEM showed immune complex-type deposits in Bowman's capsule, always associated with parietal podocytes. These deposits were similar in size, appearance, and distribution to the deposits in the capillary tuft. By contrast, non-specific electron densities within Bowman's capsule were found beneath both squamous parietal cells and parietal podocytes. In four cases, Bowman's capsule also showed focal positive immunostaining for complement components and/or fibrinogen. Both parietal and visceral podocytes showed similar fusion of pedicels. We suggest that filtration through parietal podocytes may be responsible for immune complex deposition and subsequent damage to the vascular pole of the glomerulus in human renal disease.

KEY WORDS—Kidney, glomerulus, Bowman's capsule, parietal podocytes, immune complexes.

INTRODUCTION

Bowman's capsule is thought to conduct the glomerular ultrafiltrate passively into the proximal tubule. In most mammals, the parietal epithelial lining of Bowman's capsule is a simple flat epithelial monolayer, continuous with podocytes at the root of the glomerulus.¹⁻⁴ However, in histologically normal human kidney, we have shown that podocytes often line a portion of Bowman's capsule, centred on the vascular pole of the glomerulus.⁵ Since they are morphologically fully differentiated for filtration,⁵ it is likely that these parietal podocytes represent a permeable area in Bowman's capsule where glomerular filtrate could exit the glomerulus.

Immune complexes are deposited in the capillary tuft of the glomerulus in many types of glomerulonephritis. In this study, we have used standard methods to examine 1 year's consecutive renal biopsies to assess whether parietal podocytes are involved in immune complex deposition in Bowman's capsule.

MATERIALS AND METHODS

In our laboratory, light microscopy, transmission electron microscopy (TEM), and direct immunofluorescence staining (IF) are carried out routinely on renal biopsies, when sufficient tissue is available. Tissue from one open renal biopsy in this study was also available for scanning electron microscopy (SEM).

Transmission electron microscopy

During one calendar year, a total of 170 renal biopsies were examined by TEM. Blocks of tissue

Addressee for correspondence: Dr G. B. M. Lindop, Department of Pathology, Western Infirmary, Glasgow G11 6NT, U.K.

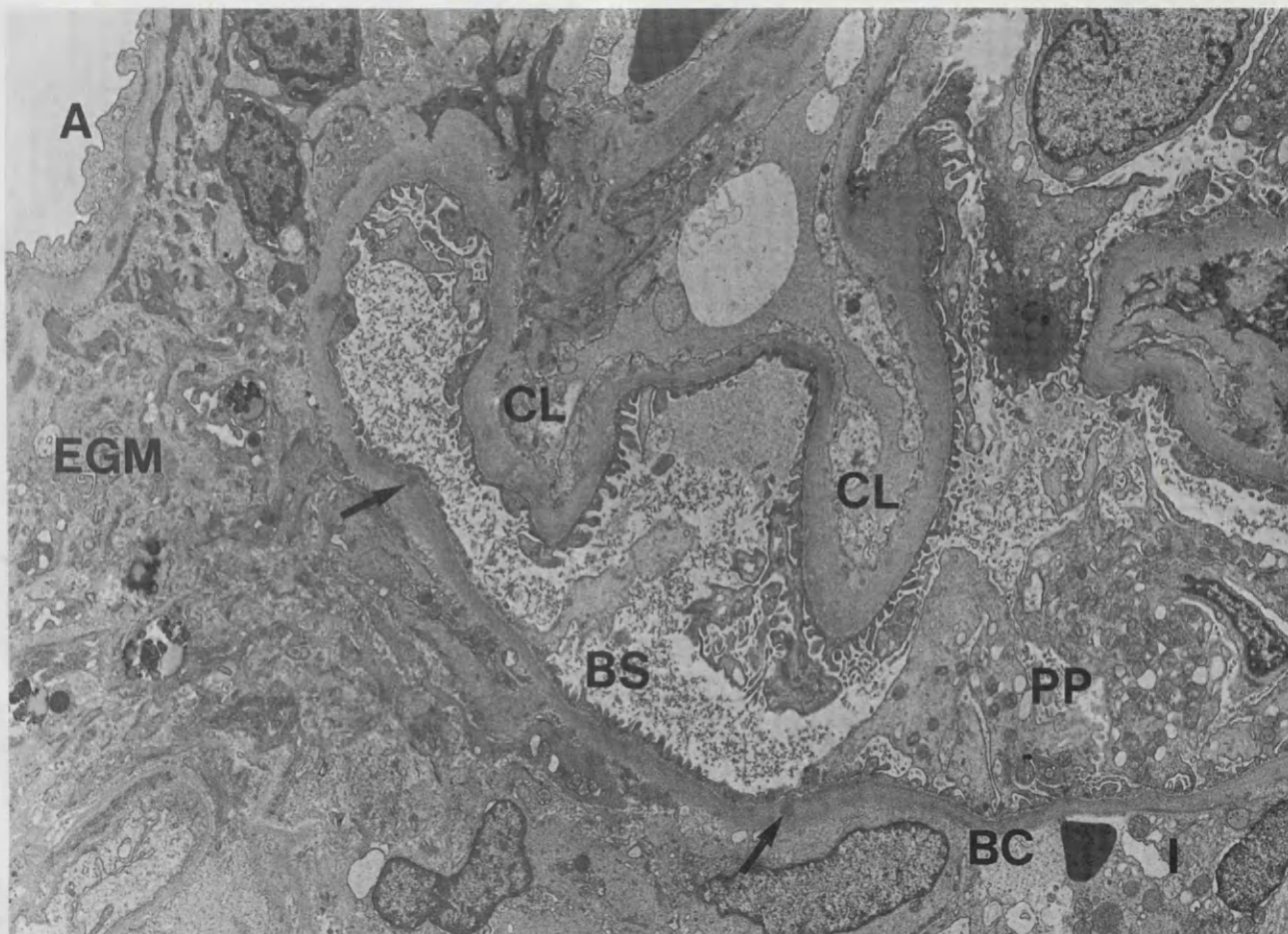


Fig. 1.—Diabetic glomerulosclerosis (case 13). The vascular pole of the glomerulus, with parietal podocytes (PP) lining Bowman's capsule (BC), overlying extraglomerular mesangium (EGM) and the interstitial compartment (I), and continuous with visceral podocytes at the root of the glomerulus. The parietal basement membrane contains occasional non-specific electron densities (arrows). A=arteriole; CL=capillary loop; BS=Bowman's space

(1 mm^3) were fixed in 2 per cent buffered glutaraldehyde, osmicated, dehydrated, and embedded in araldite resin. Sections ($1 \mu\text{m}$ thick) were stained with toluidine blue and examined by light microscopy to locate a glomerulus and, if possible, its vascular pole, but blocks were not sectioned at deeper levels if a vascular pole was not identified on the initial semi-thin sections. Ultrathin sections were mounted on grids, stained with uranyl acetate and lead citrate, and examined with a Philips CM10 TEM. The micrographs were examined for the presence of parietal podocytes and immune complexes in Bowman's capsule.

Scanning electron microscopy

Glutaraldehyde-fixed tissue was cut into 300–500 μm slices using a vibratome and treated with 1 per cent osmium tetroxide for 30 min. The slices

were dehydrated in alcohol and critical point dried in liquid CO_2 . Glomerular tufts were removed from their Bowman's capsules by microdissection using the point of a scalpel.⁶ The specimens were coated with gold and examined with a Jeol scanning electron microscope (JSM 6400).

Immunofluorescence

Cryostat sections were stained with commercial fluorescein-labelled antisera recognizing human IgG, IgA and IgM (Incstar Ltd.) and C3, C1q and fibrinogen (Behring Diagnostics).

RESULTS

Parietal podocytes

Parietal podocytes were most often seen when the vascular pole had been sectioned (Fig. 1). In

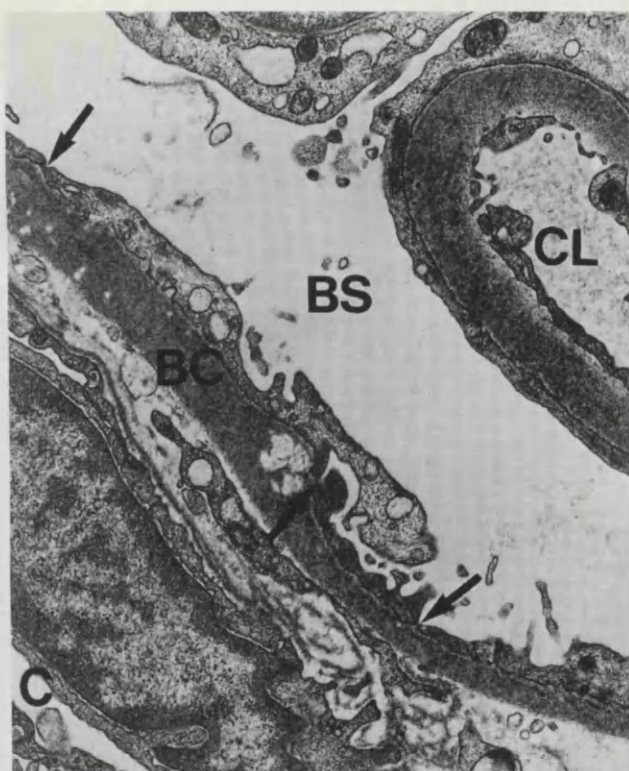


Fig. 2.—Focal glomerulosclerosis (case 12). There is extensive fusion of pedicels both on the capillary loop (CL) and on Bowman's capsule (BC), with occasional persisting slit diaphragms (arrows). BS=Bowman's space; C=periglomerular capillary

some cases, podocytes and their processes bridged across Bowman's space. These 'bridging' podocytes had processes and pedicels on both the glomerular and the parietal basement membranes.

Of the 170 cases, a glomerular vascular pole was identified in 30 (18 per cent); parietal podocytes and/or pedicels were identified in 18. Table I details the pathological diagnoses in these 18 cases.

Parietal podocytes and pedicels overlay components of the juxtaglomerular apparatus (JGA), including both renin-secreting myoepithelioid cells and extraglomerular mesangium (Fig. 1). In addition, parietal podocytes extended beyond the JGA, overlying the interstitial compartment (Figs 1, 3 and 4) and sometimes periglomerular capillaries (Fig. 2).

Interdigitating pedicels on the parietal basement membrane were linked by single and double slit diaphragms. The pedicels of parietal podocytes on Bowman's capsule were fused to a similar extent to the pedicels on the glomerular basement membrane. This was most apparent in cases of focal glomerulosclerosis (case 12; Fig. 2) and membranous glomerulonephritis (cases 1, 2, 5, and 9; Fig. 3). A few persisting slit diaphragms and intact pedicels were identified, confirming their podocytic nature (Figs 2, 3, and 4).

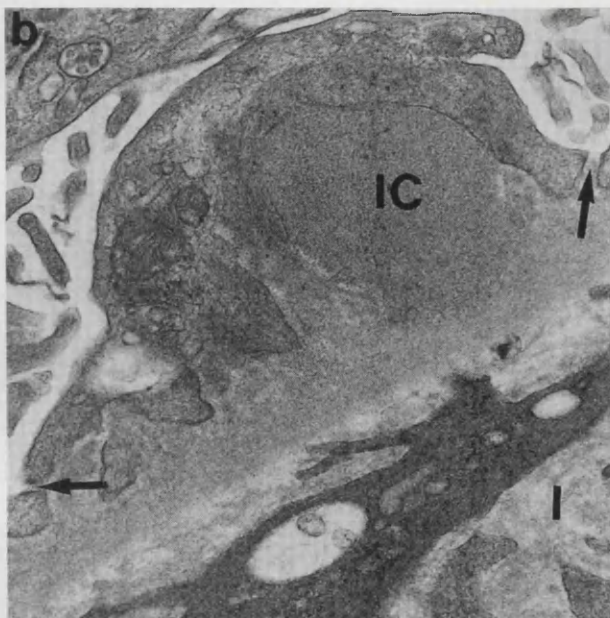
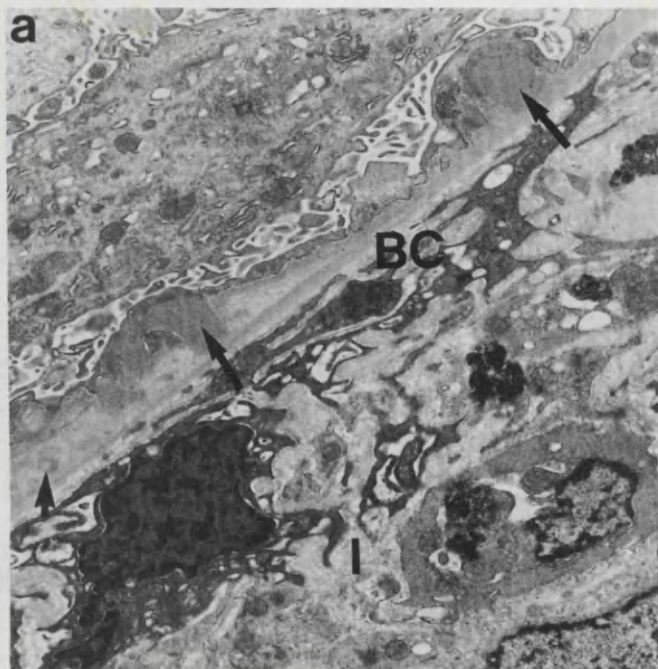


Fig. 3.—Membranous glomerulonephritis (case 1). (a) Area of Bowman's capsule (BC) with two immune complex-type subepithelial deposits (arrows). The parietal basement membrane also contains non-specific electron densities (small arrow). I=interstitium. (b) High-power view of (a) showing one immune complex-type deposit (IC); the overlying parietal podocytes show partial fusion of pedicels, with occasional persisting slit diaphragms (arrows)

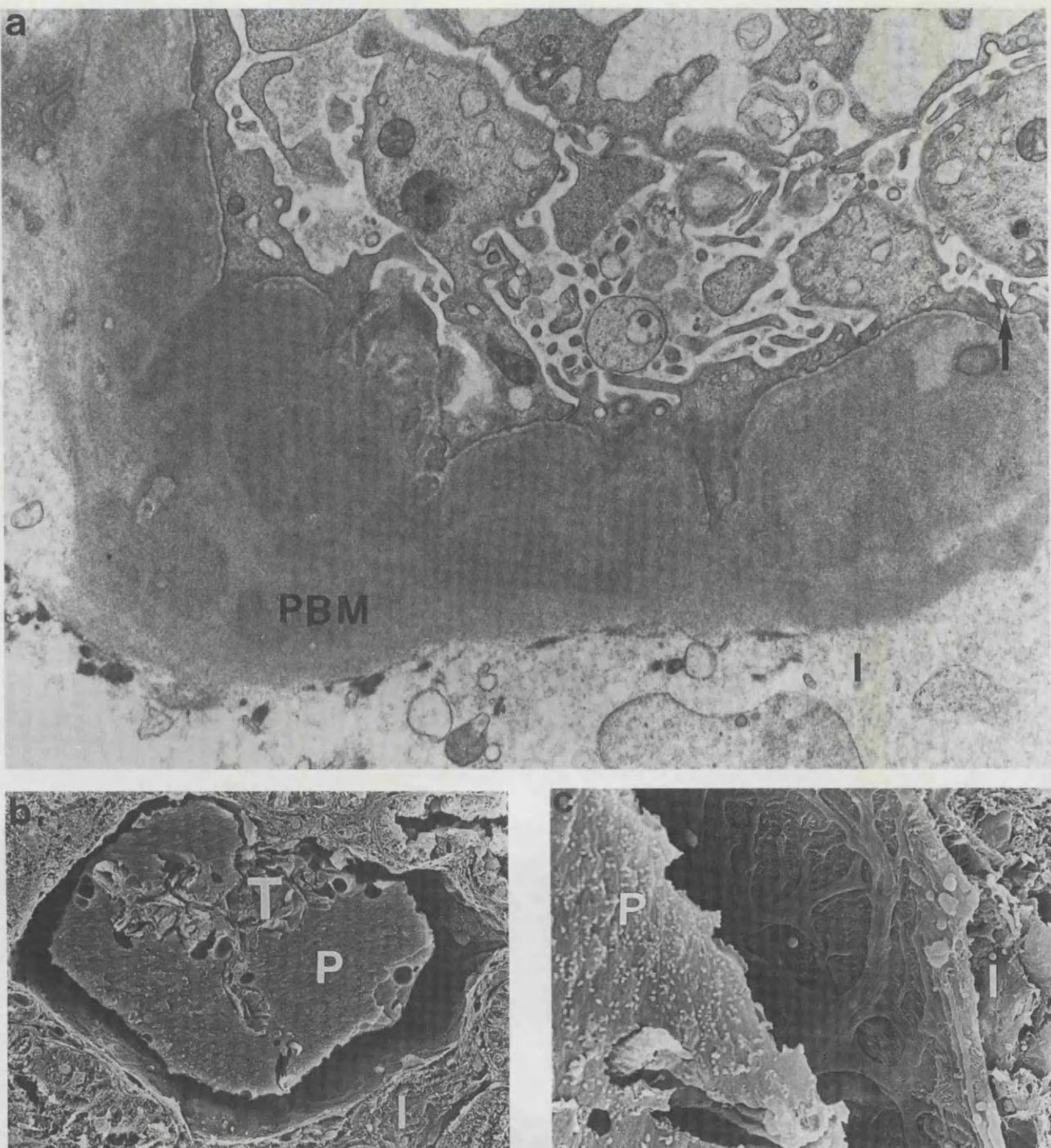


Fig. 4.—IgA nephropathy (case 4). (a) Bowman's capsule with parietal basement membrane (PBM) containing abundant intramembranous immune complex-type deposits. The parietal pedicels are extensively fused, but occasional intact pedicels and slit diaphragms are seen (arrow). I=Interstitium. (b) Low-power view of a Bowman's capsule containing a capillary tuft (T) and surrounding proteinaceous material (P) which has shrunk away from Bowman's capsule. (c) Higher-power view of a portion of Bowman's capsule lined by parietal podocytes with interdigitating processes and pedicels

SEM of case 4 (IgA nephropathy) confirmed the presence of parietal podocytes with extensively fused pedicels. The parietal epithelium was more easily recognized as podocytic with SEM (Fig. 4c)

than with TEM (Fig. 4a). One glomerulus contained an irregular collapsed glomerular tuft, surrounded by proteinaceous material within Bowman's space (Fig. 4b). Removal of this

Table I—Diagnoses in the 18 biopsies in which parietal podocytes were identified

Case No.	Age (years)	Sex	Final diagnosis	ICs in BC	ICs in tuft
1	70	M	Membranous GN	+	+
2	47	M	Membranous GN	+	+
3	39	M	IgA nephropathy	+	+
4	44	M	IgA nephropathy	+	+
5	44	F	Membranous lupus nephropathy	+	+
6	65	F	Membranoproliferative GN	-	+
7	25	F	Membranoproliferative GN	+	+
8	74	M	Membranoproliferative GN	-	+
9	27	F	Transplant with membranous GN	+	+
10	45	M	Transplant with IgA nephropathy	-	+
11	70	M	Chronic GN	-	+
12	58	M	Focal glomerulosclerosis	-	-
13	56	M	Diabetic glomerulosclerosis	-	-
14	61	F	Transplant rejection	-	-
15	61	M	Chronic ischaemic damage	-	-
16	72	M	Chronic ischaemic damage	-	-
17	68	F	Chronic ischaemic damage	-	-
18	69	F	Chronic ischaemic damage	-	-

M=male; F=female; IC=immune complex-type deposit; BC=Bowman's capsule; GN=glomerulonephritis.

capillary tuft showed that Bowman's capsule was almost completely lined by parietal podocytes.

Immune complex-type deposits

The 18 biopsies demonstrating parietal podocytes and/or pedicels included 11 cases of immune complex-mediated glomerulonephritis (Table I). All had immune complex-type deposits in the capillary tuft, demonstrated by both TEM and IF. In seven of these, TEM showed immune complex-type deposits in Bowman's capsule, underlying parietal podocytes (Figs 3 and 4), but not squamous parietal cells. Consequently, such deposits were usually found close to the vascular pole. They were similar in size and appearance to those in the glomerular capillaries. The distribution of immune complex-type deposits in Bowman's capsule was also similar to those in the glomerular tuft; in membranous glomerulonephritis, the deposits were subepithelial both in the tuft and in Bowman's capsule (Fig. 3). However, in cases with subendothelial and mesangial deposits in the tuft, the capsular immune complex-type deposits were found predominantly within the basement membrane of Bowman's capsule (Fig. 4).

Non-specific electron-dense material was also commonly seen in the parietal basement membrane. This was easily distinguished from immune complex-type deposits by its heterogeneous and particulate appearance and, by contrast, was associated both with parietal podocytes (Figs 1 and 3a) and with squamous parietal cells.

In four of the 11 cases of immune complex-mediated glomerulonephritis, Bowman's capsule showed positive immunostaining for fibrinogen (No. 4), C1q (Nos 4 and 11), or C3 (Nos 4, 5, 6 and 11). None showed capsular staining for immunoglobulins. In one other case (No. 15), there was focal C3 staining in Bowman's capsule.

DISCUSSION

In this study, we found parietal podocytes in a range of common renal diseases, from patients with a wide age range. The clinical presentations were all compatible with the final pathological diagnoses and there were no unusual or specific features in those whose biopsies contained parietal podocytes. Parietal podocytes have previously

REFERENCES

- Webber WA, Lee J. The ciliary pattern of the parietal layer of Bowman's capsule. *Anat Rec* 1974; **180**: 449-455.
- Arakawa M, Tokunaga J. A scanning electron microscope study of the human Bowman's epithelium. *Contr Nephrol* 1977; **5**: 73-78.
- Andrews PM. Scanning electron microscopy of human and rhesus monkey kidneys. *Lab Invest* 1975; **32**: 610-618.
- Gibson IW, Gardiner DS, Downie TT, More IAR, Lindop GBM. A comparative study of the glomerular peripolar cell and the renin-secreting cell in mammals. *Cell Tissue Res* (in press).
- Gibson IW, Downie I, Downie TT, Han SW, More IAR, Lindop GBM. The parietal podocyte: a study of the vascular pole of the human glomerulus. *Kidney Int* 1992; **41**: 211-214.
- Gibson IW, More IAR, Lindop GBM. A scanning electron microscopic study of the peripolar cell of the rat renal glomerulus. *Cell Tissue Res* 1989; **57**: 201-206.
- Wilson RB. Variations in the epithelial lining of Bowman's capsule. *Scanning Electron Microsc* 1977; **II**: 541-546.
- Jones DB. Scanning electron microscopy of human hypertensive renal disease. *Scanning Electron Microsc* 1978; **II**: 937-942.
- Evan AP, Gardner KD. Comparison of human polycystic and medullary cystic kidney disease with diphenylamine-induced cystic diseases. *Lab Invest* 1976; **35**: 93-101.
- Marcus PB. Podocytic metaplasia of parietal Bowman's capsular epithelium. *Arch Pathol Lab Med* 1977; **101**: 664.
- Rosivall L, Taugner R. Fluid balance in the interstitium of the Goormaghtigh cell field. In: Persson AEG, Boberg U, eds. The Juxtaglomerular Apparatus. Heidelberg: Elsevier Science Publications (Biomedical Division), 1988; 39-49.
- Kerjaschki D, Farquhar MG. Immunocytochemical localization of the Heymann nephritis antigen (GP330) in glomerular epithelial cells of normal Lewis rats. *J Exp Med* 1983; **157**: 667-686.
- Ronco P, Neale TJ, Wilson CB, Galceran M, Verroust P. An immunopathological study of a 330-kD protein defined by monoclonal antibodies and reactive with anti-RTE^{a5} antibodies and kidney eluates from active Heymann nephritis. *J Immunol* 1986; **136**: 125-130.
- Andres G, Brentgens JR, Caldwell PRB, Camussi G, Matsuo S. Formation of immune deposits and disease. *Lab Invest* 1986; **55**: 510-520.
- Verroust PJ. Kinetics of immune deposits in membranous nephropathy. *Kidney Int* 1989; **35**: 1418-1428.
- Olsen P, Peterson VP, Hansen ES. Immunofluorescence studies of extracapillary glomerulonephritis. *Acta Pathol Microbiol Scand A* 1974; **82** (Suppl 249): 7-19.
- Teague CA, Doak PB, Simpson IJ, Rainer SP, Herdson PB. Goodpasture's syndrome: an analysis of 29 cases. *Kidney Int* 1978; **13**: 492-504.
- Border WA, Baehler RW, Bhathena D, Glasscock RJ. IgA anti-basement membrane nephritis with pulmonary haemorrhage. *Ann Intern Med* 1979; **91**: 21-25.
- Morley AR. Peri-hilar rupture of Bowman's capsule in crescentic glomerulonephritis. *Acta Pathol Microbiol Immunol Scand* 1988; (Suppl 4): 74-81.
- Cohen AH, Glasscock RJ. Anti-glomerular basement membrane glomerulonephritis including Goodpasture's syndrome. In: Tisher CC, Brenner BM, eds. Renal Pathology with Clinical and Functional Correlations. Philadelphia: J B Lipincott, 1989; 494.
- Miller K, Michael AF. Immunopathology of renal extracellular membranes in diabetes mellitus: specificity of tubular basement membrane immunofluorescence. *Diabetes* 1976; **25**: 701-708.
- Silva FG. Membranoproliferative glomerulonephritis. In: Heptinstall RH, ed. Pathology of the Kidney. Boston: Little Brown, 1992; 477.
- Hill GS. Dysproteinemias, amyloidosis and immunotactoid glomerulopathy. In: Heptinstall RH, ed. Pathology of the Kidney. Boston: Little Brown, 1992; 1631.
- Burkholder PM. Ultrastructural demonstration of injury and perforation of glomerular basement membrane in acute proliferative glomerulonephritis. *Am J Pathol* 1969; **56**: 251-266.
- Kondo Y, Shigematsu H, Kobayashi Y. Cellular aspects of rabbit Masugi nephritis. II. Progressive glomerular injuries with crescent formation. *Lab Invest* 1972; **27**: 620-631.
- Bohman SO, Olsen S, Peterson VP. Glomerular ultrastructure in extracapillary glomerulonephritis. *Acta Pathol Microbiol Scand A* 1974; **82** (Suppl 249): 29-54.
- Bonsib SM. Glomerular basement membrane discontinuities: scanning electron microscopic study of acellular glomeruli. *Am J Pathol* 1985; **119**: 357-360.
- Silva F, Varani R. Crescentic glomerulonephritis: relationship of the stage of crescent formation to gaps in Bowman's capsule (Abstract). *Kidney Int* 1984; **4**: 226A.
- Boucher A, Droz D, Asdafor E, Noel LH. Relationship between the integrity of Bowman's capsule and the composition of cellular crescents in human crescentic glomerulonephritis. *Lab Invest* 1987; **56**: 526-533.
- Lan HY, Peterson DJ, Atkins RC. Initiation and evolution of interstitial leucocytic infiltration in experimental glomerulonephritis. *Kidney Int* 1991; **40**: 425-433.
- Lan HY, Nikolic-Peterson DJ, Atkins RC. Involvement of activated periglomerular leucocytes in the rupture of Bowman's capsule and glomerular crescent progression in experimental glomerulonephritis. *Lab Invest* 1992; **67**: 743-751.
- Eldridge C, Merritt S, Goyal M, Kulaga H, Kindt TJ, Wiggins R. Analysis of T cells and major histocompatibility complex class I and class II mRNA and protein content and distribution in anti-glomerular basement membrane disease in the rabbit. *Am J Pathol* 1991; **139**: 1021-1035.

A scanning electron-microscopic study of the peripolar cell of the rat renal glomerulus

Ian W. Gibson, Ian A.R. More, and George B.M. Lindop

University of Glasgow, Department of Pathology, Western Infirmary, Glasgow, United Kingdom

Summary. The interior of Bowman's capsules of rat kidneys has been examined by scanning electron microscopy, and a distinctive population of cells around the exposed vascular poles of glomerular tufts were identified. The cells were situated in the annular groove at the root of the glomerulus, between the parietal epithelial cells and the podocytes. These peripolar cells were dendritic cells with long processes embracing the glomerular arterioles. Up to three peripolar cells were present at each vascular pole and they were mainly distributed in the glomeruli of the outer third of the renal cortex. This first detailed study of the surface morphology of the glomerular peripolar cell supports the suggestion that changes in the diameter of the polar region of the glomerular tuft may cause variations in stretching of the cuff of peripolar cells, and hence modulation of their secretory activity.

Key words: Peripolar cell – Efferent arteriole – Afferent arteriole – Kidney – Scanning electron microscopy – Rat (Wistar)

Traditionally, the juxtaglomerular apparatus (JGA) consists of the macula densa of the distal tubule, the related afferent and efferent glomerular arterioles and the intervening extraglomerular mesangium (Barajas 1979). In 1979, Ryan, Coghlan and Scoggins observed a new epithelial cell at the vascular pole of the glomerulus in sheep and a number of other mammalian species, and called it the granulated peripolar cell. Granulated peripolar cells have since been studied in the rat (Ryan et al. 1982), in Amphibia (Hanner and Ryan 1980) and man (Gardiner and Lindop 1985). Ryan et al. (1979) suggested that these cells may be an additional secretory component of the JGA, but we have shown that their granules probably do not contain renin (Gardiner and Lindop 1985). Since their discovery, many aspects of their detailed anatomy have not been elucidated and their function remains unclear. Alcorn et al. (1984) made a brief investigation, by scanning electron microscopy (SEM), of newborn sheep peripolar cells. We have made a detailed investigation of the peripolar cell in the rat and studied its surface morphology by use of SEM.

Send offprint requests to: Dr. G.B.M. Lindop, Pathology Department, University of Glasgow, Western Infirmary, Glasgow G11 6NT, UK

Materials and methods

Tissue preparation

The kidneys of 10 adult male Wistar rats were fixed by perfusion. Each rat was anaesthetised with intraperitoneal sodium pentobarbital (50 mg/kg) and a cannula was inserted into the distal abdominal aorta. The inferior vena cava was cut and isotonic saline (containing 5000 units/ml heparin and 0.1% lignocaine chloride) was perfused retrogradely, at 120 mmHg, until the kidneys blanched. The aorta was clamped above the renal vessels and the kidneys were perfused with 2% glutaraldehyde in Millonig's buffer for ten minutes. The kidneys were then removed, sectioned at right angles to their long axis, fixed by immersion overnight, washed in buffer, osmicated in 1% osmium tetroxide and dehydrated in graded concentrations of ethanol. Specimens were then critical point dried, from amyl acetate, by use of liquid carbon dioxide. A fine-pointed ophthalmic scalpel was used to remove glomeruli from their Bowman's capsules by microdissection, to reveal the vascular poles within Bowman's capsules. The tissue was mounted on metal stubs and the sectioned surfaces were coated with palladium in a sputter-coater (Polaron E5000) and viewed with a Jeol 100 scanning electron microscope.

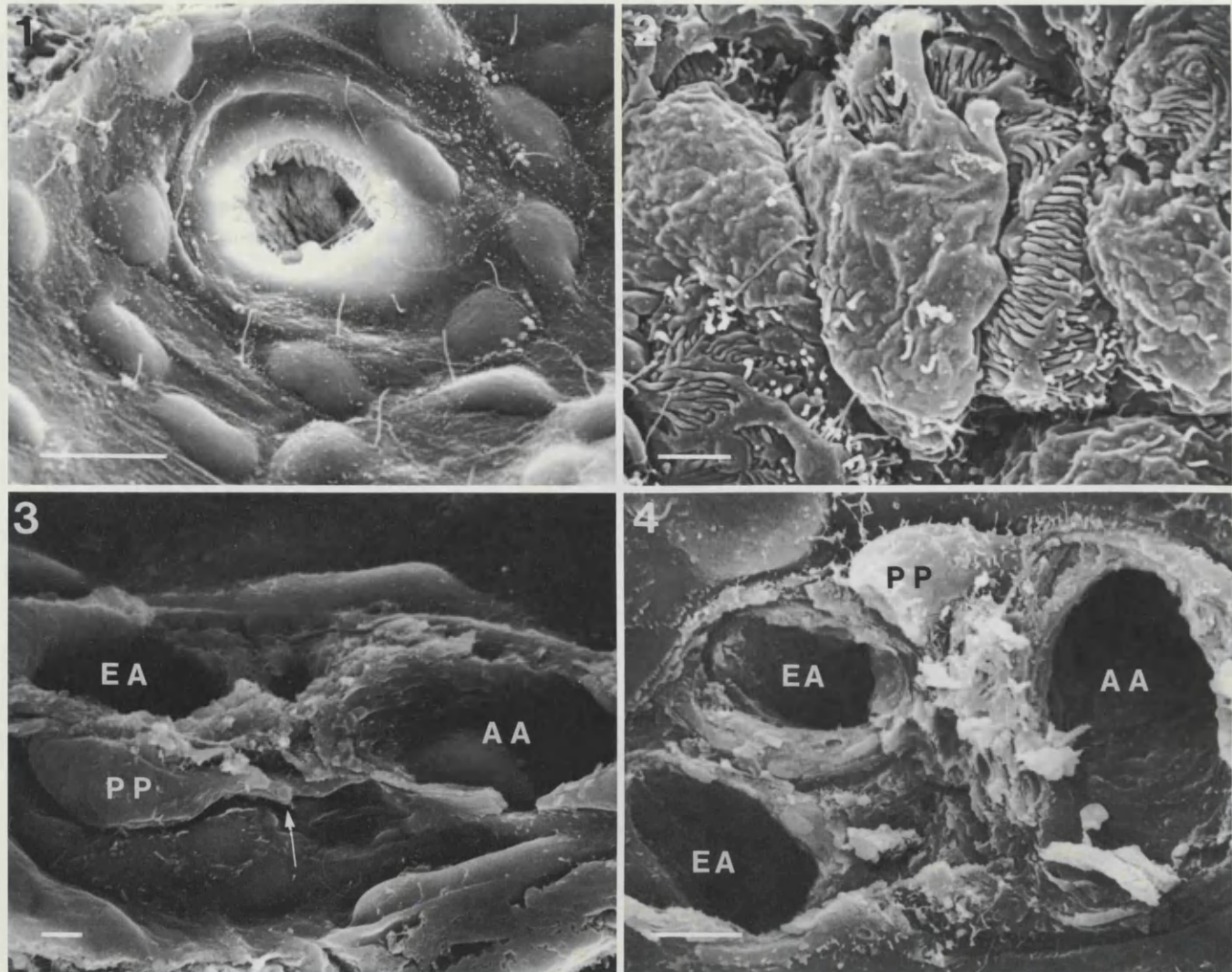
The excised glomerular tufts from four kidneys were collected. The tufts from the outer half of the cortex were separated from those from the inner half and mounted on pieces of adhesive tape. They were coated with palladium as above and examined with SEM at various angles to identify the vascular poles.

Quantification

In each case we examined with SEM every empty Bowman's capsule exposed on the surfaces of at least four pieces of kidney, sectioned at right angles to its long axis. A peripolar cell index (PPI) was derived by expressing the number of vascular poles with one or more peripolar cell as a percentage of the total number of vascular poles observed in each kidney.

Distribution of peripolar cells

Where the full thickness of the renal cortex was visible, we recorded the position of each glomerulus which contained a peripolar cell. On low-power scanning electron micrographs, we measured the distances from the cortico-



medullary junction (the deepest-placed glomerulus) to the glomerulus containing the peripolar cell and from the corticomедullary junction to the cortical surface in the same straight line. These measurements were expressed as ratios and, as before (Gardiner and Lindop 1985), the ratios were used to plot the relative depth within the renal cortex of each peripolar cell.

Results

Bowman's capsule

The parietal epithelial cells of Bowman's capsules were polygonal and, apart from nuclear bulges and single cilia (about 3–5 µm in length), they were flat. A few rudimentary microvilli were present and these were distributed mainly at the cell periphery (Fig. 1). The outer surface of the thin parietal layer, i.e. the basement membrane of Bowman's capsule, was without surface detail. A network of collagenous fibrils extended from the interstitium and was inserted into it.

The visceral epithelial cells of Bowman's capsule, or podocytes, covered the glomerular tufts which had not been removed from their Bowman's capsule. High-power examination (Fig. 2) showed that the podocyte cell bodies and major processes had very sparse microvilli and the surface of the cell body was consistently uneven and ruffled, unlike the smooth surface of the parietal epithelial cells.

Fig. 1. The urinary pole of Bowman's capsule showing the abrupt transition from the parietal epithelium, with nuclear bulges, single cilia and short microvilli, to the microvillous brush border of the proximal tubule. Bar: 10 µm; $\times 1800$

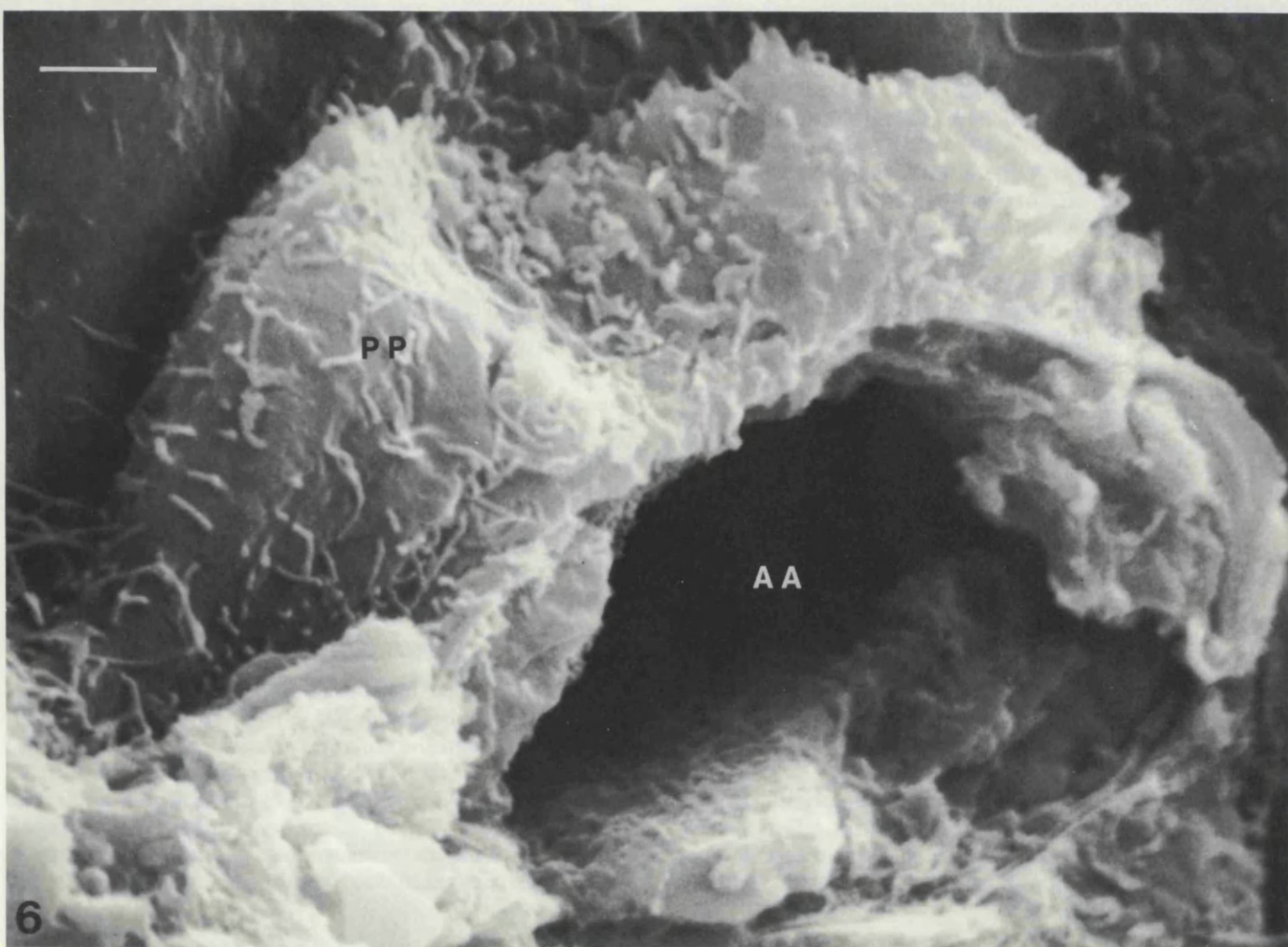
Fig. 2. The glomerular podocyte cell bodies, major processes and interdigitating pedicels have few microvilli and a ruffled surface. Bar: 2.0 µm; $\times 5000$

Fig. 3. Looking into Bowman's capsule, the vascular pole can be seen with the adjacent afferent and efferent arterioles (AA and EA). There is a peripolar cell (PP) lying in the groove between the efferent arteriole and the parietal cells. This peripolar cell possesses an abruptly ending, shortened process (arrow). Bar: 3.0 µm; $\times 2000$

Fig. 4. A vascular pole with three vessel openings, one afferent arteriole (AA) and two efferent vessels (EA). A microvillus-covered peripolar cell (PP) lies between the afferent and efferent arterioles. Bar: 5.0 µm; $\times 2400$

Fig. 5. A vascular pole with three surrounding peripolar cells (PP1, PP2 and PP3), all covered by microvilli. PP1 and PP3 have broken processes (arrows). Bar: 4.0 µm; $\times 3000$

Fig. 6. The microvillus-covered cell body of this peripolar cell (PP) curves around the afferent arteriole (AA). Bar: 1.0 µm; $\times 16000$



Urinary pole

In most cases, the transition from the squamous parietal epithelium to the proximal tubule cells, with their brush border, was abrupt (Fig. 1), but sometimes the parietal cells surrounding the tubular orifice exhibited larger numbers of short microvilli and occasionally the epithelial cells surrounding the urinary pole were covered by a true microvillous brush border similar to proximal tubular cells.

Vascular pole

The site at which the glomerulus was broken off by microdissection was usually the point of reflection of Bowman's capsular epithelium onto the capillary tuft. Usually two arterioles were identified within the capsular crater, with a visible fracture line (Fig. 3).

The vessel lumina varied in size, but in most cases there was a large afferent vessel ($\sim 20 \mu\text{m}$ in diameter) and a smaller efferent vessel ($\sim 10 \mu\text{m}$ in diameter), (Fig. 3). The afferent and efferent arterioles were separated from one another by a $5-20 \mu\text{m}$ mesangial region. When three separate lumina were seen at one vascular pole (Fig. 4), two small efferent openings were present side-by-side, and clearly separated from the larger afferent vessel.

Peripolar cell

At some vascular poles, in a "peripolar" position, a third type of cell was identified. These cells occupied a position between the podocytes and the parietal epithelial cells and were therefore seen to surround the arterioles of the vascular pole (Figs. 3-5). They could be easily distinguished from both types of epithelial cell. Unlike podocytes, the surface of some peripolar cells was covered with many microvilli projecting from a smooth cell body (Figs. 5 and 6). Other peripolar cells had a smoother surface with fewer microvilli (Fig. 3). The peripolar cells were also easily distinguished from the flat, polygonal parietal epithelial cells; they were larger than parietal cell nuclear bulges, possessed no cilia and their microvilli were both larger and present in greater numbers.

Usually one, sometimes two and rarely three peripolar cells (Fig. 5) were identified at a single vascular pole. Peripolar cells were found encircling both the afferent arterioles (Fig. 6), and the efferent vessels (Fig. 3) and sometimes they were situated in the niche between them, sending two processes in opposite directions (Figs. 4 and 5). However, the majority (about 60%) were related to afferent arterioles.

Peripolar cells had a bipolar dendritic structure, with a cell body approximately $10 \mu\text{m}$ long (Figs. 3, 4, 5 and 6) and long tapering processes, which extended round the circumference of an arteriole (Fig. 4). Most commonly long, thin processes extended out from a pyramidal or ovoid cell body and encircled an arteriole (Figs. 4 and 5), but occasional cells were long and fusiform; in this instance, the whole cell curved around an arteriole (Fig. 6). Sometimes a long, tapering process appeared to have been broken off, probably during the extraction of the glomerular tuft, leaving an abruptly-ending, blunted, shortened process with a fracture site (Figs. 3, and 5).

When there was more than one peripolar cell around the same vascular pole, the processes from different cells sometimes overlapped. We could not prove direct contact between these cells although in some instances the appear-

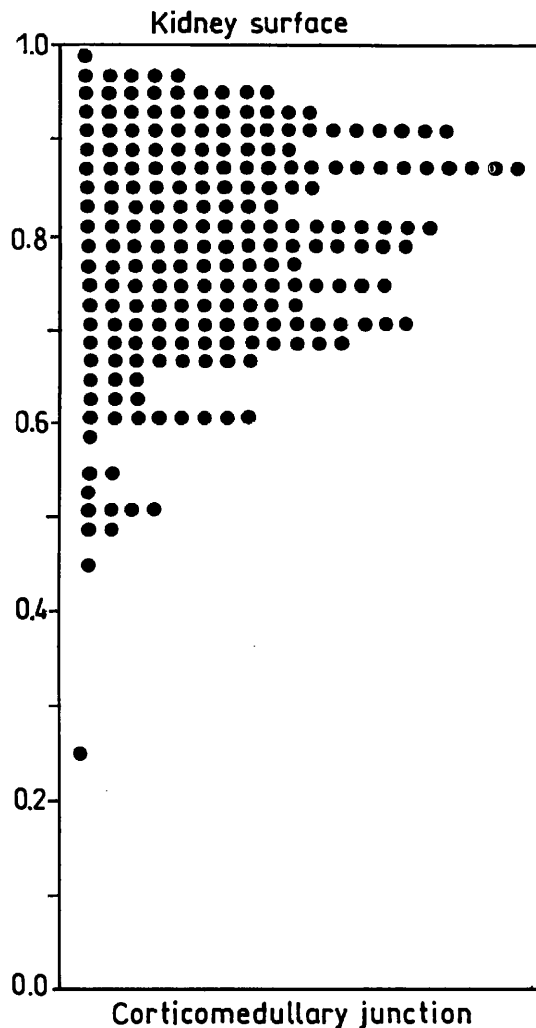


Fig. 7. A scatter diagram showing the distribution of peripolar cells within the renal cortex. The scale is the ratio of the distance from the peripolar cell to the corticomedullary junction and the total thickness of cortex measured in the same straight line. Each circle represents a single peripolar cell

ances were highly suggestive of this because cell bodies and the processes of two adjacent cells were closely apposed.

Quantification

We examined a mean of 315 Bowman's capsules in each kidney (range 174-514). In total, 579 vascular poles and 310 peripolar cells were identified. Peripolar cell indices ranged from 31% to 58%, with a mean of 48%. This means that at least one peripolar cell was found in 48% of the capsular vascular poles examined.

Distribution of peripolar cells

For most peripolar cells, it was possible to determine the distances from the peripolar cell to the corticomedullary junction and from the cortical surface to the corticomedullary junction and then calculate the ratio of these distances. The position of all peripolar cells in ten kidneys was plotted on a scattergram (Fig. 7). It can be seen that most peripolar cells were found in vascular poles in the superficial one third of the cortex.

To confirm that this was a true distribution, we also examined a total of 200 glomerular tufts extracted from both deep and superficial cortex. In no instance could peripolar cells be identified at the vascular poles of any detached glomeruli.

Discussion

Bowman's capsule

The findings of this study are in agreement with previous SEM studies of the parietal layer of the rat Bowman's capsule (Bulger et al. 1974; Webber and Lee 1974). The variable pattern of microvilli on parietal cells led Webber and Lee (1974) to suggest that they may be transitory structures, whose appearance may alter in response to local conditions. The resulting changes in surface area could be related to transfer of substances across the parietal layer.

Single cilia are too sparse to exert any propulsive effects on the glomerular filtrate, but they may have a specific function, e.g. a sensory capacity (Webber and Lee 1974). Transmission EM of these structures in human and monkey kidneys has shown that they possess an irregular intracellular microtubule skeleton (Andrews 1975). They are probably primary cilia, which occur in many tissues and organs during development, e.g. chondrocytes (Scherft and Daems 1967), adrenal cortex (Wheatley 1967), lung (Sorokin 1968) and uterine epithelium (Tachi et al. 1974 and Denholm and More 1980). Most studies correlate the development of a single cilium with the cessation of mitotic activity of the cell (Rash et al. 1969).

It has been suggested that the fine collagenous fibrils of the interstitium which are inserted into Bowman's membrane have an anchoring function, holding the corpuscle in place relative to the surrounding tubules (Andrews 1979).

Vascular pole

In most cases, one vessel opening was significantly larger than the other. By preparing vascular casts, Evan and Dail (1977) found that, except for some juxamedullary glomeruli, the diameter of the proximal end of the efferent arteriole was always smaller than that of the corresponding afferent arteriole. It is reasonable to conclude therefore that the large-sized vessel openings observed in this present study are the afferent arterioles.

When three vessels were present at a vascular pole, it is clear that the large single opening is the afferent arteriole and the two smaller openings situated close to each other are efferent vessels. This is supported by vascular cast studies (Evan and Dail 1977; Weinstein and Szyjewicz 1978) which show that the efferent arterioles of outer and middle cortical glomeruli run a very short course before dividing to form the peritubular capillary plexus, close to or surrounding the parent glomerulus.

Peripolar cell

This SEM study has shown the presence of a morphologically distinct peripolar cell population in nearly half of the vascular poles of rat glomeruli. The surface morphology of the rat peripolar cell is clearly different from both podocytes and parietal epithelial cells.

This study has also shown that a greater proportion of glomeruli contain peripolar cells, identifiable by SEM,

than granular peripolar cells as seen by light microscopy of serial sections in rat and in man (Gardiner and Lindop 1985). To account for the apparent scarcity of granulated peripolar cells in human kidneys, we have previously suggested that non-granular peripolar cells may exist and have a secretory function and only under appropriate conditions become granulated by storing their secretory product (Gardiner and Lindop 1985). If non-granular peripolar cells were present, they could be identified by SEM, but would not be seen by light microscopy.

The glomeruli which contained peripolar cells were mainly in the outer third of the renal cortex, similar to our findings in human kidney (Gardiner and Lindop 1985). Alcorn et al. (1984) suggested that peripolar cells were larger in the outer cortex of newborn lamb kidney. We confirmed that our observation was not artefactual by examining the bases of a sample of the glomeruli which had been removed by microdissection. SEM of the remains of the vascular pole in the glomerular tuft showed no instance of peripolar cells being removed with the glomerulus, whether it was derived from the deep or the superficial cortex. This distribution of peripolar cells is similar to that of JGAs which contain renin-secreting cells, and we have previously pointed out the anatomical proximity of the two cell types (Gardiner and Lindop 1985) which may be functionally related. Whether or not the peripolar cell is a part of the JGA remains unclear.

Ryan et al. (1979) suggested that peripolar cells could release a factor into the glomerular ultrafiltrate to modulate tubular function, but their function remains unknown. The shape and situation of the peripolar cells observed in this present study would favour a sensory function. Their microvillous surfaces could detect alterations in the electrolyte content of the glomerular filtrate bathing the cells, or alterations in the concentration of hormonal factors entering the urinary space from the capillary tuft. In sheep, peripolar cells completely surround the glomerular root (Ryan et al. 1979). This could not be confirmed in the present study on the rat. However, when two peripolar cells were present around the same arteriole their cell bodies and processes did extend to "meet" and overlap each other. Such peripolar cell processes would be more suited to sensing the calibre of a vessel, rather than being able to alter a vessel diameter, since peripolar cells are in a mechanically disadvantageous position to alter vessel sizes. The possibility of peripolar cell contractility has been considered; microfilaments and microtubules have been demonstrated in sheep (Ryan et al. 1982) but not in human peripolar cells (Gardiner et al. 1986). Thus, the results of this present study favour the suggestion of Ryan et al. (1982) that changes in the diameter of the polar region of the glomerular tuft, resulting from variations in arteriolar calibre, could cause stretching of the cuff of peripolar cells and stimulate their secretion.

References

- Alcorn D, Cheshire GR, Coglan JP, Ryan GB (1984) Peripolar cell hypertrophy in the renal juxtaglomerular region of newborn sheep. *Cell Tissue Res* 236:197-202
- Andrews PM (1975) Scanning electron microscopy of human and rhesus monkey kidneys. *Lab Invest* 32:610-618
- Andrews PM (1979) The urinary system - kidney. In: Hodges GM, Hallows RC (eds) *Biomedical research applications of scanning electron microscopy Volume 1*. Academic Press, London New York and San Francisco, pp 273-306

- Barajas L (1979) Anatomy of the juxtaglomerular apparatus. Am J Physiol 237:F333–F343
- Bulger RE, Siegel FL, Pendergrass R (1974) Scanning and transmission electron microscopy of the rat kidney. Am J Anat 139:483–502
- Denholm R, More IAR (1980) Atypical cilia of the human endometrial epithelium. J Anat 131:309–315
- Evan AP, Dail WG (1977) Efferent arterioles in the cortex of the rat kidney. Anat Rec 187:135–146
- Gardiner DS, Lindop GBM (1985) The granular peripolar cell of the human glomerulus: a new component of the juxtaglomerular apparatus? Histopathology 9:675–685
- Gardiner DS, More IAR, Lindop GBM (1986) The granular peripolar cell of the human glomerulus: an ultrastructural study. J Anat 146:31–43
- Hanner RH, Ryan GB (1980) Ultrastructure of the renal juxtaglomerular complex and peripolar cells in the axolotl (*Ambystoma mexicanum*) and toad (*Bufo marinus*). J Anat 130:445–455
- Rash JE, Shay JW, Bieseile JJ (1969) Cilia in cardiac differentiation. J Ultrastruct Res 29:470–484
- Ryan GB, Alcorn D, Coghlan JP, Hill PA, Jacobs R (1982) Ultrastructural morphology of granule release from juxtaglomerular myoepithelioid and peripolar cells. Kidney Int 22:S3–S8
- Ryan GB, Coghlan JP, Scoggins BA (1979) The granulated peripolar cell: a potential secretory component of the renal juxtaglomerular complex. Nature 277:655–656
- Scherft JP, Daems WT (1967) Single cilia in chondrocytes. J Ultrastruct Res 19:546–555
- Sorokin SP (1968) Reconstruction of centriole formation and ciliogenesis in mammalian lungs. J Cell Sci 3:207–230
- Tachi S, Tachi C, Lindner HR (1974) Influence of ovarian hormones on the formation of solitary cilia and behaviour of the centrioles in uterine epithelial cells. Biol Reprod 10:391–403
- Webber WA, Lee J (1974) The ciliary pattern of the parietal layer of Bowman's capsule. Anat Rec 180:449–455
- Weinstein SW, Szyjewicz J (1978) Superficial nephron tubular-vascular relationships in the rat kidney. Am J Physiol 234:F207–F214
- Wheatley DN (1967) Cilia and centrioles of the rat adrenal cortex. J Anat 101:223–237

Accepted September 9, 1988

A comparative study of the glomerular peripolar cell and the renin-secreting cell in twelve mammalian species

I.W. Gibson, D.S. Gardiner, I. Downie, T.T. Downie, I.A.R. More, G.B.M. Lindop

University Department of Pathology, Western Infirmary, Glasgow G11 6NT, UK

Received: 15 December 1992 / Accepted: 20 December 1993

Abstract. The peripolar cell is a glomerular epithelial cell situated within Bowman's capsule at its vascular pole. It is believed to be a secretory cell which forms part of the juxtaglomerular apparatus. Scanning electron microscopy was used to perform a comparative study of the morphology and number of peripolar cells in twelve mammalian species. The number of renin-secreting cells in kidney sections stained by renin antibodies and immunocytochemistry was counted. There was a marked inter-species variation in the number, size and appearance of peripolar cells. They were largest and most abundant in sheep and goat and fewest in dog, cow and human. There was no correlation between the numbers of peripolar cells and renin-secreting cells. This does not support the view that the peripolar cell is part of the juxtaglomerular apparatus.

Key words: Kidney – Glomerulus – Peripolar cell – Renin – Juxtaglomerular apparatus – Scanning electron microscopy – Mammalia, 12 species

peripolar cells in a range of mammalian species, including man.

It has been suggested that the peripolar cell is part of the juxtaglomerular apparatus (JGA) (Ryan et al. 1979) and that the numbers of granulated peripolar cells in each species vary inversely with the number of renin-secreting cells in the JGA (Gall et al. 1986). We therefore compared the numbers of peripolar cells and renin-secreting cells in each species to assess whether there may be a quantitative relationship between these two cell types.

Materials and methods

Tissues and fixation (table 1)

Five laboratory species; rat (4), guinea pig (2), hamster (2), mouse (2) and rabbit (2), were killed by intraperitoneal injection of sodium pentobarbital, 50 mg/kg. A slice from the pole of one kidney was fixed in formalin, then the kidneys were fixed by perfusion with 2% buffered glutaraldehyde (Gibson et al. 1989). Fresh ovine (3), porcine (3) and bovine (3) kidneys were obtained from a commercial abattoir. The kidneys from dog (1), goat (1) and baboon (1) were obtained immediately after sacrifice, either by terminal anaesthesia (dog and baboon) or by captive bolt (goat). Finally, fresh histologically normal human renal cortex was obtained from kidneys surgically removed for either renal cell carcinoma (8) or transitional cell carcinoma (4). The renal arteries were cannulated and the kidneys were fixed by perfusion with buffered glutaraldehyde (Gibson et al. 1992).

Preparation for SEM

Vibratome slices (1 mm thick) of full width renal cortex were post-fixed in 1% osmium tetroxide for 1 h, washed in buffer, then dehydrated in graded concentrations of ethanol and critical point dried from liquid CO₂. In order to visualise the vascular pole, glomerular tufts were removed from Bowman's capsules by microdissection using a fine-pointed scalpel blade (Gibson et al. 1989). All tissue was coated with gold (Polaron SEM sputter-coater) and examined by use of a Jeol scanning microscope (JSM 6400).

Introduction

The glomerular peripolar cell was first recognised by light microscopy as a granulated epithelial cell at the vascular pole of the ovine renal glomerulus (Ryan et al. 1979). In sheep, peripolar cells are large, numerous and present in most glomeruli (Ryan et al. 1979; Kelly et al. 1990). However, in most other species, granulated peripolar cells are sparse and are found in only a minority of glomeruli (Gall et al. 1986); some peripolar cells have no granules (Downie et al. 1992) and are therefore unrecognisable in tissue sections. We have used scanning electron microscopy (SEM) to distinguish peripolar cells from other glomerular epithelial cells (Gibson et al. 1989; Kelly et al. 1990; Downie et al. 1992). In the present study, we used SEM to compare the number and morphology of

Table 1. Quantification of vascular poles and peripolar cells in mammalian kidney. n, Number of animals; VP, number of vascular poles; VPPP, number of vascular poles with peripolar cells; PP, total number of peripolar cells; PPI, peripolar cell index; DPPC%, percentage of dendritic peripolar cells; GPPC%, percentage of globular peripolar cells; PPCm, mean number of peripolar cells per vascular pole; PPCmax, maximum number of peripolar cells at one vascular pole

Species	n	VP	VPPP	PP	PPI	DPPC %	GPPC %	PPCm	PPC max
Guinea pig	2	50	23	32	46	100	0	1.4	3
Hamster	2	33	13	14	39	100	0	1.1	2
Mouse	2	20	9	12	45	100	0	1.3	2
Rat	4	171	92	141	53	100	0	1.5	4
Rabbit	2	39	9	10	23	100	0	1.1	2
Dog	1	22	3	3	14	100	0	1.0	1
Baboon	1	24	11	12	46	100	0	1.1	2
Human	12	322	21	21	6.5	86	14	1.0	1
Cow	3	37	4	5	11	60	40	1.3	2
Pig	3	55	12	14	22	57	43	1.2	3
Sheep	3	52	43	67	84	0	100	1.6	10
Goat	1	35	35	100	100	0	100	2.9	11

Table 2. Quantification of renin-secreting cells. n, Number of animals; JGA+, number of JGAs with renin-secreting cells divided by number of glomeruli; A+, number of arterial sections with renin-secreting cells divided by number of glomeruli; RCI, total number of renin-secreting cells divided by number of glomeruli

Species	n	JGA+ (range)	A+ (range)	RCI (range)
Sheep	3	7.9 (5.4–9.9)	4.7 (2.7–8.5)	32.5 (16.3–50.1)
Dog	1	6.2	0.7	6.9
Pig	1	12.4	1.2	28.6
Hamster	1	5.9	1.5	5.9
Mouse	3	11.5 (3.5–15.6)	2.9 (0.9–4.6)	25.4 (3.5–43.1)
Baboon	1	20.0	1.8	37.4
Rat ^a	6	16.7 (8.2–40.0)	6.0 (2.0–14.5)	65.1 (19.2–167.3)
Man ^b	11	9.4 (3.2–21.4)	2.1 (0–7.1)	35.1 (5.6–76.5)
Man ^c	10	11.6 (6.3–13.8)	1.6 (0–4.0)	32.9 (13.6–70.1)

^a Downie I., MSc thesis, University of Glasgow, 1992

^b Normal autopsy kidney from cases of sudden death

^c Normal parts of surgically removed kidneys

See Gardiner DS, Jackson R, Lindop GBM (1992) The renin-secreting cell and the glomerular peripolar cell in renal artery stenosis and Addison's disease. *Virchows Archiv [A]* 420:533–537

Peripolar cells

In each kidney a minimum of 70 Bowman's capsules were chosen at random from all zones of renal cortex and studied for the presence of peripolar cells. A peripolar cell index (PPI) was derived by expressing the number of vascular poles with at least one peripolar cell as a percentage of the total number of vascular poles. For vascular poles which contained peripolar cells, the mean number of peripolar cells per vascular pole (PPC_m) was also determined.

Renin-secreting cells

A standard immunoperoxidase technique with monospecific antibodies to mouse (Malling and Poulsen 1977) and human (McIntyre et al. 1983) renin was used to demonstrate renin-secreting cells (Lindop et al. 1987; Graham and Lindop 1988). Two 3 µm-thick paraffin sections from each species were stained with antisera and those which stained positively were used to count the renin-secreting cells. At least 100 glomeruli were examined in each kidney by

scanning the full thickness of the renal cortex in a 'battlement' fashion and, as previously (Gardiner et al. 1992), 3 semiquantitative indices were derived (Table 2). Spearman's rank correlation was used to compare variables between groups.

Results

Peripolar cells

In all species, peripolar cells were applied to the vascular pole at the junction between podocytes and parietal epithelial cells (Fig. 1). Their appearance varied but most could be categorised into two main types: dendritic peripolar cells were elongated with cell processes; globular peripolar cells were rounder and had no processes. Intermediate forms were also identified.

Fig. 1. Vascular pole of guinea pig glomerulus consisting of two arterioles (A) and three peripolar cells (arrows) with prominent single cilia. $\times 1800$. Bar: 5 µm

Fig. 2. Rabbit dendritic peripolar cell (P) with a process (arrow) extending around the arteriole (A), which is lined by partially fenestrated endothelium. $\times 4600$. Bar: 2 µm

Fig. 3. Human vascular pole with arteriole (A) and dendritic peripolar cell (P) with process (arrow); the cell body has a ruffled surface. $\times 4900$. Bar: 2.0 µm

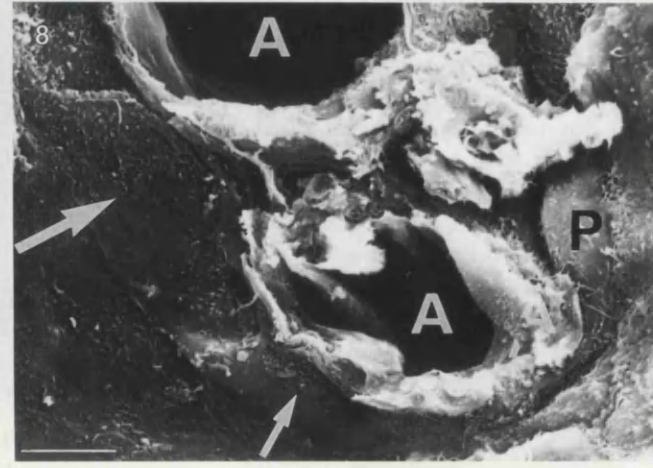
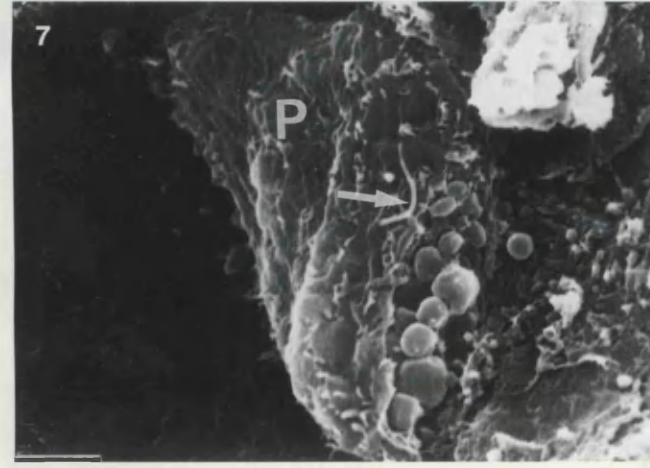
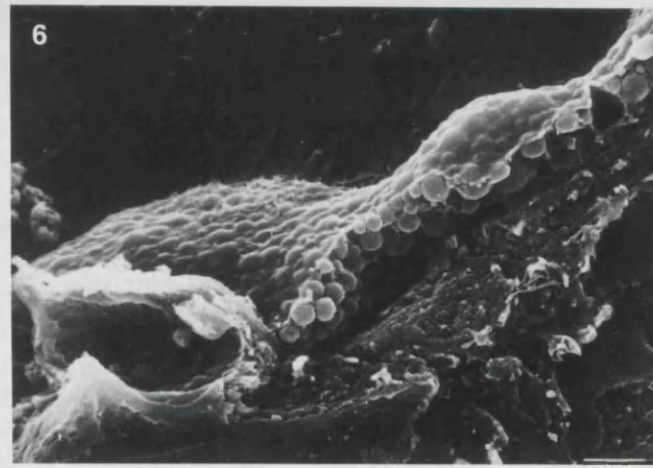
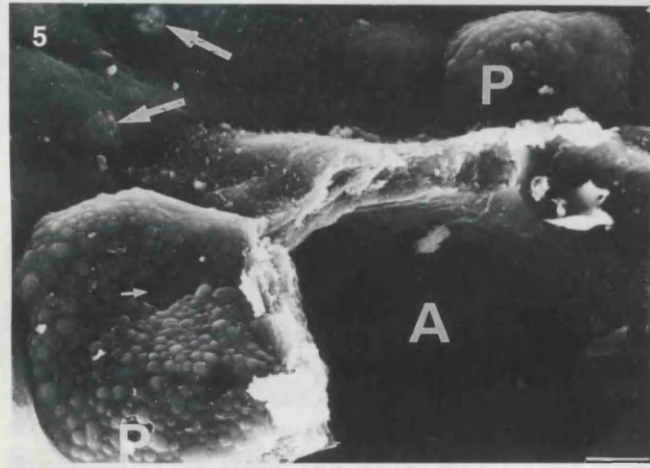
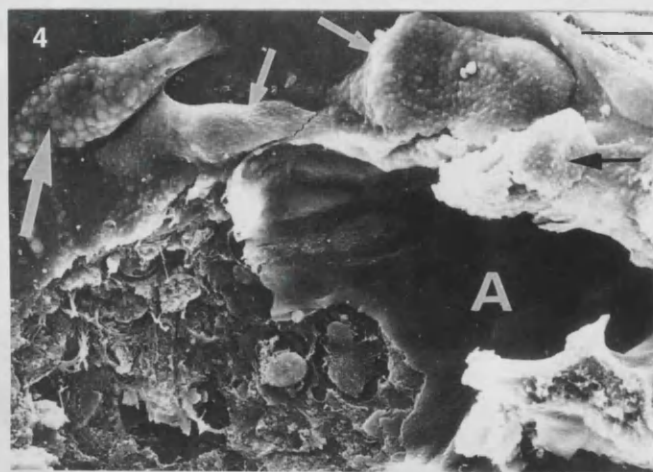
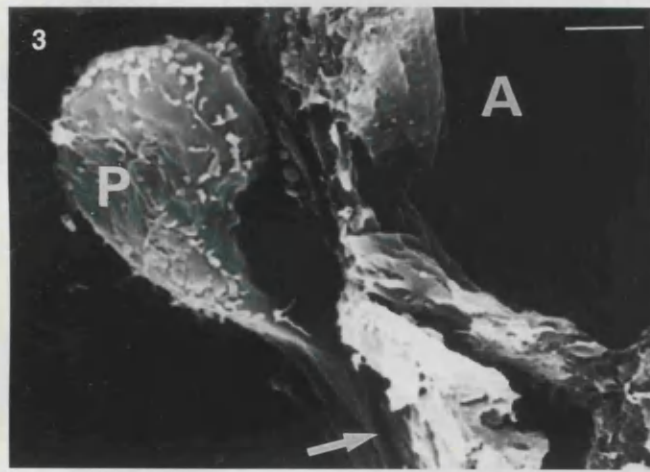
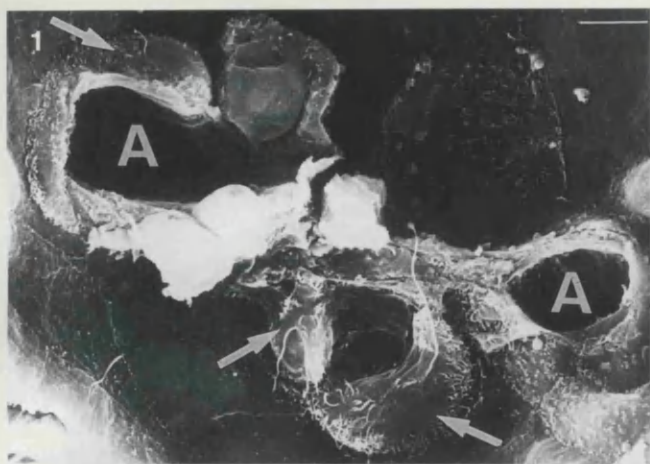
Fig. 4. Goat vascular pole with fractured arteriole (A) surrounded by several globular peripolar cells (arrows), including a fusiform bossellated cell (large arrow). $\times 1000$. Bar: 10 µm

Fig. 5. Goat vascular pole with arteriole (A) and two globular peripolar cells (P). The larger cell has a smooth area on its surface (arrow). Note the focal bossellation of squamous parietal cells (larger arrows). $\times 1700$. Bar: 5 µm

Fig. 6. A flattened, polygonal goat peripolar cell; the fractured surface shows closely-packed cytoplasmic granules. $\times 4100$. Bar: 2 µm

Fig. 7. Guinea pig peripolar cell (P), cracked open by tissue processing, contains intracellular faceted granules. Note the single cilium (arrow). $\times 5500$. Bar: 2 µm

Fig. 8. Hamster vascular pole with arterioles (A) and dendritic peripolar cell (P). One cell resembles a peripolar cell at one end (small arrow) and a squamous parietal cell at the other (large arrow). $\times 2500$. Bar: 5 µm



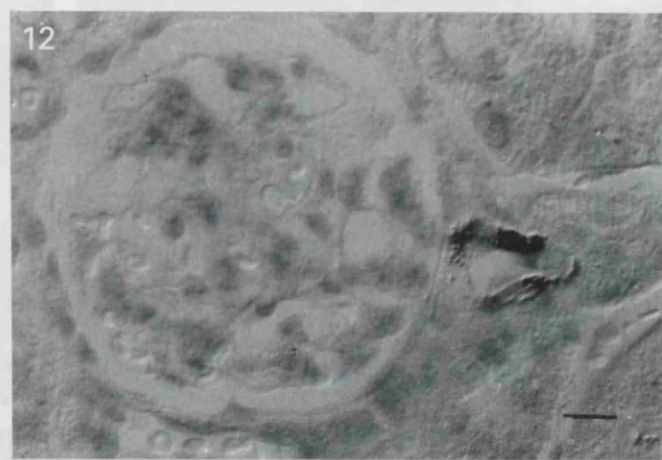
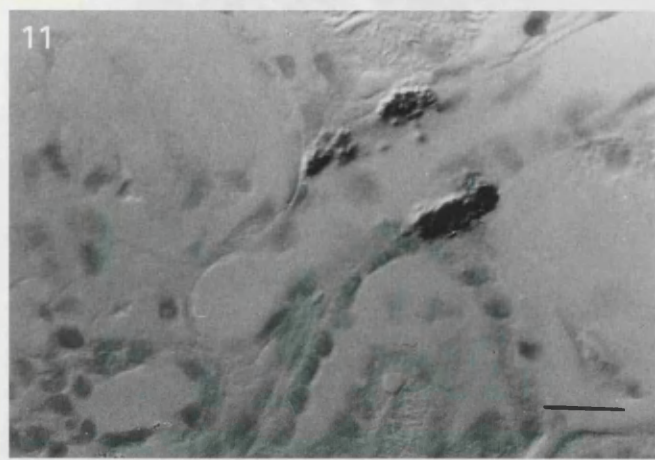
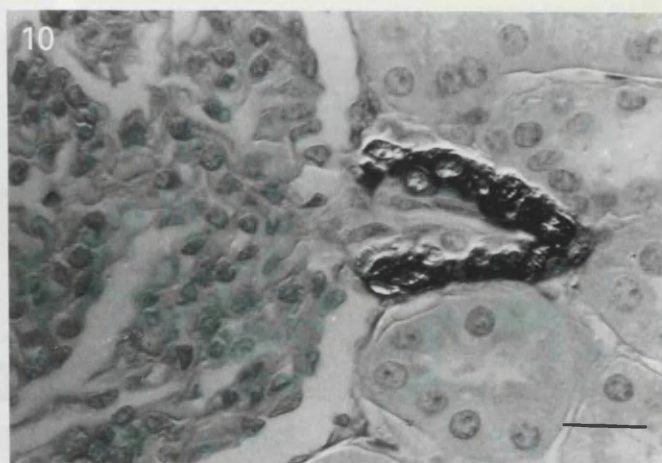
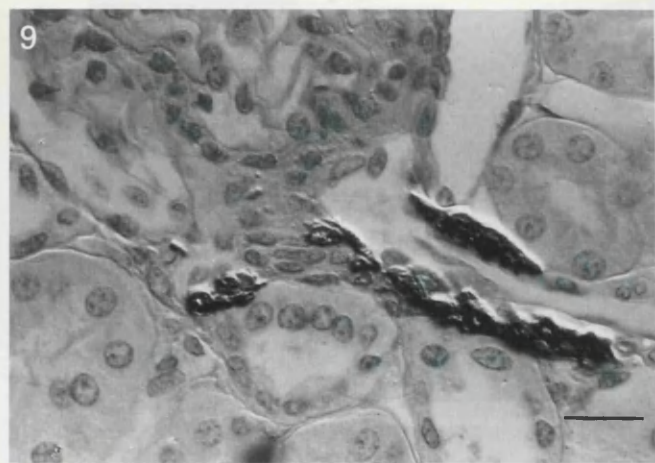


Fig. 9. Baboon JGA showing plump renin-secreting cells extending down the afferent arteriole. A few are also present in the efferent vessel. Renin PAP counter-stained with haematoxylin. $\times 450$. Bar: 10 μm

Fig. 10. Sheep JGA showing many large myoepithelioid cells staining positively with the renin PAP technique. $\times 450$. Bar: 10 μm

Figs. 11, 12. Dog (11) and hamster (12) showing fewer and smaller renin-positive cells in the JGA. 11 $\times 450$; 12 $\times 300$. Bar: 10 μm

A. Dendritic peripolar cells

These cells (Figs. 1–3) were the only type present in rodent, dog and baboon and formed the majority in porcine, bovine, canine and human kidney; they were never seen in sheep or goat (Table 1). Dendritic peripolar cells were largest in the guinea pig (Fig. 1). They had fusiform, ovoid or pyramidal cell bodies (3–10 μm in diameter) and their surface was mainly smooth (Figs. 2, 3). They had microvilli, which were often longer and more numerous than those on parietal epithelial cells. Peripolar cells had a single cilium in the pig and guinea pig (Fig. 1), but not in other species. Most cells had one or a maximum of two non-branching processes which curved around the vascular pole (Fig. 2). Interdigitating pedicels, characteristic of podocytes, were not a feature of dendritic peripolar cells. Some peripolar cells lay in the niche between the afferent and efferent vessels with processes extending in opposite directions. Occasional fusiform cells did not form processes; instead, the entire cell encircled most of the circumference of an arteriole (Fig. 1).

B. Globular peripolar cells

These cells were the only type found in sheep and goat kidney and formed a minority in porcine, bovine and human kidney. None were found in rodents, dog or baboon (Table 1). Several globular peripolar cells often formed an incomplete cuff around the vascular pole (Fig. 4). They were spherical or ovoid (Fig. 5), without cell processes, and were larger (10–30 μm in diameter) than dendritic peripolar cells. Their surface was bossellated due to numerous large (up to 1 μm diameter) cytoplasmic granules. When visualised in cells which had been cracked open by the tissue processing, the granules were faceted, possibly due to close packing (Fig. 6). Some peripolar cells in the sheep and goat had a well delineated smooth area, possibly due to displacement of granules by the underlying nucleus (Fig. 5). Occasional cells had scanty short microvilli, but most had no surface projections or cilia.

C. Intermediate forms

1. *Dendritic/globular peripolar cells.* In rodents (particularly guinea pig), some peripolar cells were plumper and

ovoid-shaped, without cell processes (Fig. 1). Their surface was essentially smooth like other dendritic peripolar cells, although some contained granules identical to those in globular peripolar cells (Fig. 7).

In the sheep and goat, occasional peripolar cells were fusiform like dendritic peripolar cells, but lacked cell processes and had a bossellated surface like globular peripolar cells (Fig. 4).

2. Peripolar cell/parietal cell. In sheep and goat, some large polygonal cells at the vascular pole were flat, and resembled squamous parietal cells, but unlike parietal cells lacked nuclear bulges and cilia and had a bossellated surface (Fig. 6). Also, otherwise typical parietal cells sometimes had a focally bossellated surface, presumably due to small numbers of granules (Fig. 5).

In rodents, some cells resembled a dendritic peripolar cell at one end, while the other end resembled a squamous parietal cell (Fig. 8).

3. Peripolar cell/podocyte. In rodents, occasional dendritic peripolar cells (without branching processes or pedicels) had ruffled cell bodies like podocytes. The cell bodies were also similar in size to those of podocytes on the glomerular tuft (5–10 µm). In some cases, we had difficulty distinguishing between these two cell types, especially when examining cells at the vascular poles of isolated glomerular tufts.

Quantification

Table 1 shows that peripolar cells were more numerous in those species in which they were all of the globular type. In the goat there were almost three per glomerulus. Species with exclusively dendritic peripolar cells had fewer; rabbit kidney contained notably fewer peripolar cells than other rodents. Canine, bovine and human peripolar cells were very sparse.

Renin-secreting cells

The number and size of renin-secreting cells in the JGA varied between species; for example in mice, baboon (Fig. 9) and sheep (Fig. 10) JGAs appeared large and cellular. In addition, in some species such as mice and sheep, renin-secreting cells were commonly found in proximal afferent arterioles, whereas this was unusual in dog, pig and hamster. In these species the renin-secreting cells were both smaller in size and fewer in number (Figs. 11, 12). The semiquantitative indices are given in Table 2. Baboon, sheep, pig, mouse and rat kidneys had relatively high values, whilst the dog and hamster had low values. There was no consistent correlation between the PPI and the renin indices.

Discussion

The nature of peripolar cells

Granules occur in podocytes and in parietal epithelial cells in some glomerular diseases (Morild et al. 1988; Hill et al. 1988; Nakajima et al. 1989). This has led some workers to doubt that the peripolar cell is a specific cell type. In this study of a range of mammalian species we have confirmed that peripolar cells vary in appearance, but are distinguishable from both podocytes and parietal epithelial cells by their surface morphology, and are therefore a specific cell type.

For descriptive purposes, we separated peripolar cells into dendritic and globular types. We have previously used SEM and subsequent sectioning to show that globular peripolar cells of sheep are all granulated (Kelly et al. 1990), whereas in the rat, most dendritic peripolar cells contain no granules (Downie et al. 1992). The granularity of the peripolar cell appears to govern its surface appearance. The presence of intermediates suggests that acquisition of granules accompanies a change from dendritic to globular cells.

Dendritic peripolar cells resembled podocytes more than parietal epithelial cells. By comparison, globular peripolar cells were morphologically closer to parietal epithelial cells and we found cells intermediate between peripolar cells and both parietal cells and podocytes. Thus, although the peripolar cell is a distinctive cell type, it is situated at a junction between two other types of epithelial cell. As at other junctions in epithelia, there may be a gradual change of differentiation from one cell type to another with intermediate forms.

In man, peripolar cells were a mixture of dendritic and globular cells and they were scanty (PPI = 6.5%). The PPI for human kidney obtained by light microscopy of serial sections is approximately 14% (Gardiner and Lindop 1985). In the human glomerulus, parietal podocytes often surround the vascular pole; their significance has been discussed elsewhere (Gibson et al. 1992). Some parietal podocytes could become granulated and be interpreted as peripolar cells by light microscopy. The relationship between the peripolar cell and the parietal podocyte requires clarification.

The function of the peripolar cell

Peripolar cell granules undergo exocytosis into the glomerular filtrate and a secretory function was proposed (Ryan et al. 1979; Hill et al. 1983, 1984, 1988). The peripolar cell could also sense the calibre of the arterioles at the vascular pole or the composition of the glomerular filtrate (Ryan et al. 1979; Gibson et al. 1989). It was originally suggested that the peripolar cell could be part of the JGA (Ryan et al. 1979). This group suggested that there may be an inverse relationship between the numbers of peripolar cells and renin-secreting cells in different species (Ryan et al. 1979; Gall et al. 1986); however, not all studies support this idea (Gardiner et al. 1992) which remains controversial. The evidence has been reviewed

(Gardiner et al. 1991). Immunostaining using renin antisera is the most specific way to detect renin-secreting cells (Lindop 1992). Comparisons between species are difficult, since antibodies may differ in affinity for renins from other species. However, our results are comparable with another species survey of renin-secreting cells (Matsuhashi et al. 1979). Our results contradict the previous impression of Gall et al. 1986, probably because of the superiority of immunostaining with highly specific antisera over conventional stains in assessing the activity of the JGA.

In conclusion, we have used scanning electron microscopy to demonstrate that peripolar cells vary in number, in shape, and in size in a range of mammalian species. While intermediate forms occur, peripolar cells are distinguishable from podocytes and parietal cells, and are therefore a morphologically specialised cell type in the mammalian glomerulus. Their numbers do not correlate with the numbers of renin-secreting cells, hence this study shows no evidence that the two cell types are functionally related. Although the peripolar cell appears to be a morphologically distinctive cell type, its function remains unknown.

Acknowledgements. We are grateful to Professor K. Poulsen for the generous gift of affinity purified Fab fragments prepared from his mouse renin antiserum. I.D. was supported by an MRC Research Project Grant.

References

- Downie I, Gardiner DS, Downie TT, Gibson IW, Kenyon C, More IAR, Lindop GBM (1992) Non-granulated peripolar cells exist in the rat glomerulus. *Cell Tissue Res* 268:567–570
- Gall JAM, Alcorn D, Batkus A, Coghlan JP, Ryan GB (1986) Distribution of peripolar cells in different mammalian species. *Cell Tissue Res* 24:203–208
- Gardiner DS, Lindop GBM (1985) The granular peripolar cell of the human glomerulus: a new component of the juxtaglomerular apparatus? *Histopathology* 9:675–685
- Gardiner DS, Lindop GBM (1992) Peripolar cells, granulated epithelial cells and their relationship to the juxtaglomerular apparatus in malignant hypertension. *J Pathol* 167:59–64
- Gardiner DS, Downie I, Gibson IW, More IAR, Lindop GBM (1991) The glomerular peripolar cell: a review. *Histology Histopathology* 6:567–573
- Gardiner DS, Jackson R, Lindop GBM (1992) The renin-secreting cell and the glomerular peripolar cell in renal artery stenosis and Addison's disease. *Virchows Arch [A]* 420:533–537
- Gibson IW, More IAR, Lindop GBM (1989) A scanning electron microscopic study of the peripolar cell of the rat renal glomerulus. *Cell Tissue Res* 257:201–206
- Gibson IW, Downie I, Downie TT, Han SW, More IAR, Lindop GBM (1992) The parietal podocyte: a study of the vascular pole of the human glomerulus. *Kidney Int* 41:211–214
- Graham PC, Lindop GBM (1988) The anatomy of the renin-secreting cell in adult polycystic kidney disease. *Kidney Int* 33:1084–1090
- Hill PA, Coghlan JP, Scoggins BA, Ryan GB (1983) Ultrastructural changes in the sheep renal juxta-glomerular apparatus in response to sodium depletion or loading. *Pathology* 15:463–473
- Hill PA, Coghlan JP, Scoggins BA, Ryan GB (1984) Structural and functional studies of the adrenal cortex and renal juxtaglomerular apparatus in pregnant sheep subjected to sodium depletion or loading. *Pathology* 16:285–290
- Hill PA, Fairley KF, Kincaid-Smith P, Zimmerman M, Ryan GB (1990) The peripolar cell: a distinctive cell type in the mammalian glomerulus. Morphological evidence from a study of sheep. *J Anat* 168:217–227
- Lindop GBM (1992) The human renin-secreting cell in health and disease. In: Nicholls G, Robertson JIS (eds) *The renin angiotensin system*. Gower, London, pp 19.1–19.15
- Lindop GBM, Millan DWM, Murray D, Gibson AAM, McIntyre GD, Leckie BJ (1987) Immunocytochemistry of renin in renal tumours. *Clin Exper Hyperten A* 9:1305–1323
- Malling C, Poulsen K (1977) A direct radioimmunoassay for plasma renin in mice and its evaluation. *Biochem Biophys Acta* 491:532–541
- Matsuhashi H, Nishida T, Mochizuki K (1977) Comparative studies on granulation of juxtaglomerular cells of some mammalian kidneys and limitation of the specificity of Bowie staining. *Jpn J Vet Sci* 39:379–388
- McIntyre GD, Leckie B, Hahet A, Szelke M (1983) Purification of human renin by affinity chromatography using a new peptide inhibitor of renin, H. 77 (D-His-Pro-Phe-His-Leu-Leu-Val-Tyr). *Biochem J* 211:519–522
- Morild I, Christensen JA, Mikeler E, Bohle A (1988) Peripolar cells in the avian kidney. *Virchows Arch [A]* 412:471–477
- Nakajima M, Matthews DC, Hewitson T, Kincaid-Smith P (1989) Modified immunogold labelling applied to the study of protein droplets in glomerular disease. *Virchows Arch [A]* 415:489–499
- Ryan GB, Coghlan JP, Scoggins BA (1979) The granulated peripolar epithelial cell: a potential secretory component of the renal juxtaglomerular complex. *Nature* 277:655–656

The parietal podocyte: A study of the vascular pole of the human glomerulus

IAN W. GIBSON, IAN DOWIE, THOMAS T. DOWIE, SEON W. HAN, IAN A.R. MORE,
and GEORGE B.M. LINDOP

University Department of Pathology, Western Infirmary, Glasgow G11 6NT, Scotland, United Kingdom

The vascular pole of the glomerulus is an important area of the nephron. The function of the juxtaglomerular apparatus (JGA) and the anatomical relationships of its tubular, glomerular and vascular components have been extensively studied. By comparison, the glomerular epithelium at the vascular pole has been neglected.

In most species, simple squamous parietal cells are often separated from the podocytes on the capillary tuft by peripolar cells [1, 2]. In the human kidney, we found that, at the vascular pole, many Bowman's capsules were lined by cells which resembled podocytes. Since podocytes are highly differentiated for filtration, this finding would have important implications for the function of the glomerulus and its relationship with the underlying JGA and the surrounding interstitium. The aim of this study was to assess the extent of the parietal podocytic lining.

We obtained human kidney tissue from the macroscopically and histologically normal parts of twelve kidneys surgically removed for renal cell carcinoma (8 cases) or transitional cell carcinoma of the renal pelvis (4 cases). The patients' ages ranged from 49 to 80 years. As before [1], the kidneys were perfusion-fixed and prepared for scanning electron microscopy (SEM). After critical point drying, the glomerular tufts were removed by microdissection and mounted on stubs. Tissue slices and glomerular tufts were gold-coated in a Polaron SEM sputter coater and viewed with a Jeol scanning electron microscope (JSM 6400).

In each kidney, we examined a minimum of 20 vascular poles, at least 10 from superficial glomeruli and at least 10 from deep glomeruli. In six kidneys, we mapped the position in the renal cortex of each vascular pole, as before [1]. From these six kidneys, we also took 1 mm cube blocks from the superficial and juxtamedullary cortex of each kidney and processed them for transmission electron microscopy. Semithin sections, 2 μm thick, were examined by light microscopy to identify vascular poles, which were then ultrasectioned, stained with uranyl acetate and Reynold's lead citrate, and examined using a Philip's CM10 transmission electron microscope.

Received for publication February 26, 1991
and in revised form August 27, 1991

Accepted for publication August 30, 1991

© 1992 by the International Society of Nephrology

The glomerular vascular pole (Fig. 1) was identified in 31% of Bowman's capsules. In all twelve kidneys, podocytes formed the parietal layer of many Bowman's capsules at their vascular poles (Figs. 1 and 2). These parietal podocytes were in continuity with visceral podocytes and extended radially from vascular poles for variable distances, up to 100 μm (Fig. 2); they covered some 25% of Bowman's capsule. Podocytes were found around both the afferent (Fig. 1) and the efferent arteriole and sometimes completely encircled the whole vascular pole.

Parietal podocytes were similar in size and shape to visceral podocytes, with long curving major processes extending out in all directions, branching and terminating in pedicels (1 to 2 μm long), which interdigitated with those from an adjacent podocyte (Fig. 3). They formed distinct boundaries with squamous parietal cells (Figs. 1 and 3).

Podocytic processes bridged across the urinary space between glomerular capillaries and Bowman's capsule (Figs. 4 and 7). Their cell of origin was sited either on the capillary tuft or on Bowman's capsule. In some cases, we could identify the broken ends of processes fractured at the time of tuft removal (Figs. 2 and 3). Occasionally, podocyte cell bodies also formed a "bridge" between the capillary tuft and Bowman's capsule (Figs. 4 and 8) sending processes and pedicels to both.

Compared to visceral podocytes, parietal podocytes (Figs. 5 and 8) had more elongated cell bodies, with flatter nuclei and fewer organelles. Their cell bodies rested on the parietal basement membrane. Parietal pedicels were similar to those on the glomerular capillary basement membrane, and were linked by single or multiple (2 to 4) slit diaphragms (Fig. 6).

We found parietal podocytes in all twelve kidneys by SEM. In total, 63% of the 148 vascular poles from six kidneys by SEM had parietal podocytes; 67% of the superficial vascular poles and 59% of the deep vascular poles.

On TEM, parietal podocytes were found in five of the six kidneys; they were in: 60% of all glomeruli, 47% of superficial glomeruli and 77% of juxtamedullary glomeruli.

Large bridging processes (120 in total) were identified with SEM in 55% (51 of 93) of the glomeruli with parietal podocytes; 46% (55 of 120) originated from cell bodies on Bowman's capsule and 54% (65 of 120) arose from cells on the glomerular capillary tuft.

Parietal podocytes have been described previously only in isolated case reports of human renal diseases: malignant hypertension [3], hemolytic-uremic syndrome [4], medullary cystic

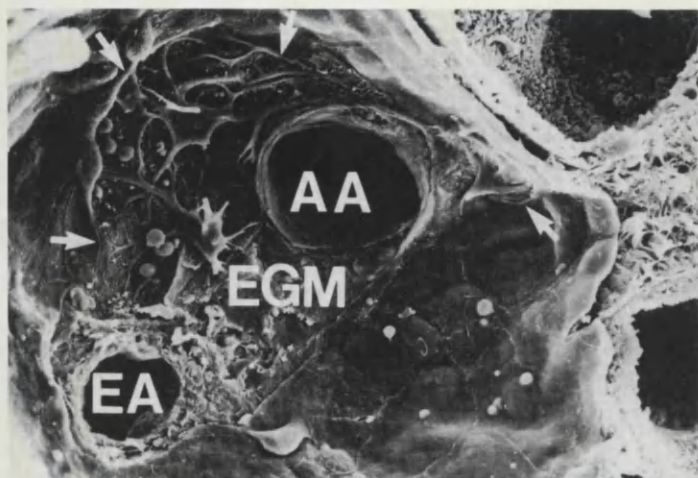


Fig. 1. A vascular pole consisting of the afferent arteriole (AA) approximately 25 μm diameter, the efferent arteriole (EA) approximately 15 μm diameter and intervening extraglomerular mesangium (EGM). Parietal podocytes (outlined by arrows), with scattered overlying material, partially surround the vascular pole, $\times 830$.



Fig. 3. Parietal podocytes with major processes forming enclosed circles (large arrows) and crossing over each other to produce interdigititation of processes from adjacent cells. The boundary with squamous parietal cells consists of long sweeping major processes or scalloped overlapping squamous cells (small arrows). A broken process (P) projects from one parietal podocyte towards the vascular pole, $\times 2100$.

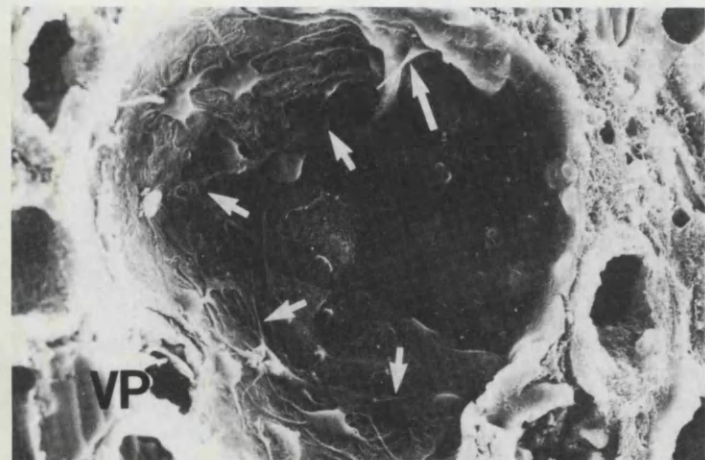


Fig. 2. A Bowman's capsule with its vascular pole (VP). A large area of the parietal epithelium consists of parietal podocytes (outlined by arrows), extending approximately 100 μm from the vascular pole. There is a prominent broken process (large arrow), $\times 490$.

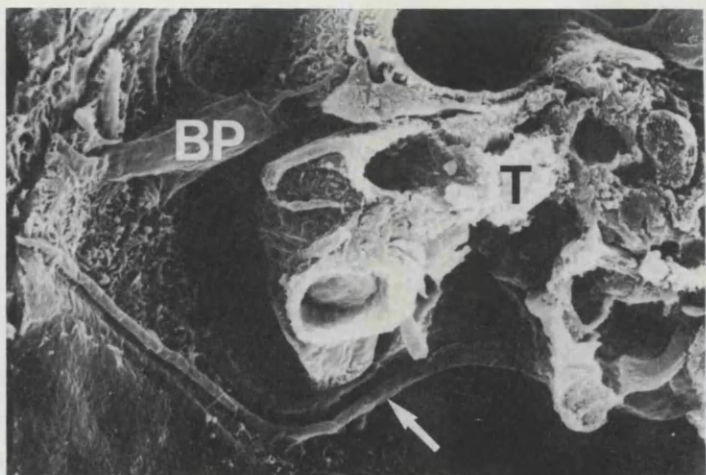


Fig. 4. A Bowman's capsule with part of the glomerular capillary tuft (T) in situ. A bridging parietal podocyte (BP) sends processes to both glomerular and parietal basement membranes. Two bridging processes from visceral podocytes are also present (arrow), $\times 2150$.

kidney disease [5] and glomerulonephritis [4, 6]. Parietal podocytes are also found in experimental cystic disease in rabbits [7, 8].

This study is the first detailed description of parietal podocytes in human kidney and has shown that they are centered on the vascular pole. By SEM, we have found parietal podocytes in a majority of glomeruli, whereas Wilson [4] found them in only 16% of glomeruli. Our SEM technique gives a more comprehensive view of Bowman's capsule and also overcomes the sampling problems inherent in TEM. Parietal podocytes resemble podocytes on the glomerular capillary tufts. The podocytic connections between the capillary tuft and Bowman's capsule mean that the same cell covers portions of both glomerular and parietal basement membrane.

Although the renal cortex was within the limits of histological normality, the nephrectomies were all carried out for renal or

transitional cell carcinomas in an elderly population. This raises the possibility that parietal podocytes could be due to ageing or to an adaptation to a disease process. However, we have also found parietal podocytes in kidneys removed from younger adults for persistent hematuria, transplant rejection, renal artery stenosis, hydronephrosis and chronic pyelonephritis (Gibson et al, unpublished observations). The inability to correlate parietal podocytes with any specific pathology led Wilson [4] to speculate that they may be a feature of normal human kidney. Entirely normal human nephrectomies are not available for study.

Parietal podocytes have normal slit diaphragms which suggests that they are capable of filtering. Pedicels cover the glomerular stalk and form an integral part of the parietal

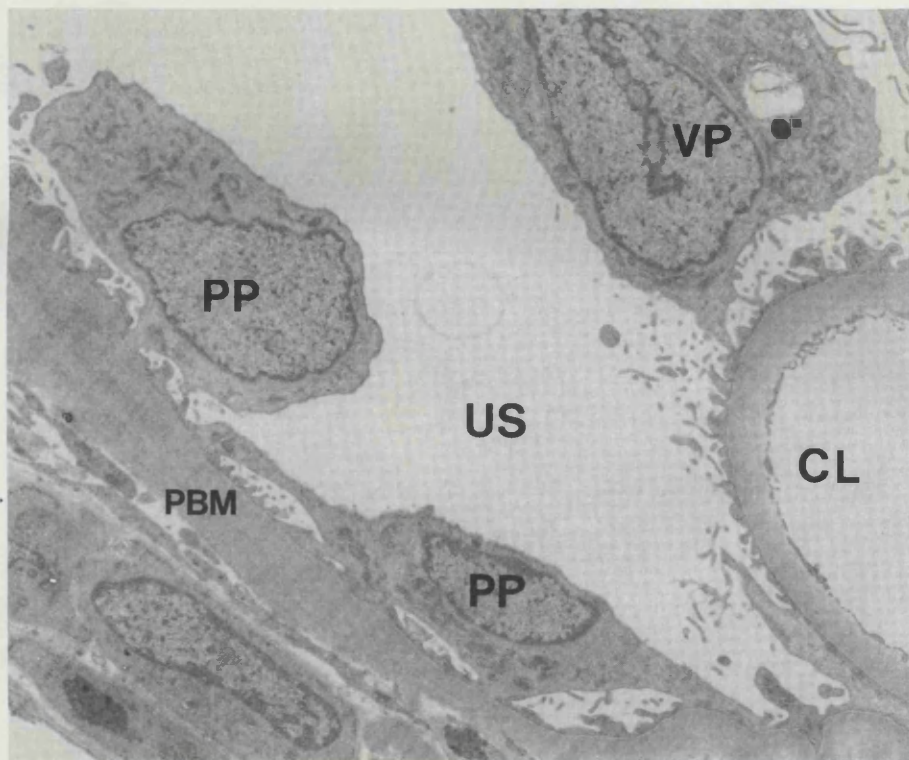


Fig. 5. An area of the parietal epithelium of Bowman's capsule close to the vascular pole showing parietal podocyte cell bodies (PP), processes and pedicels. PBM = parietal basement membrane; US = urinary space; VP = visceral podocyte; CL = glomerular capillary loop, $\times 5,168$.

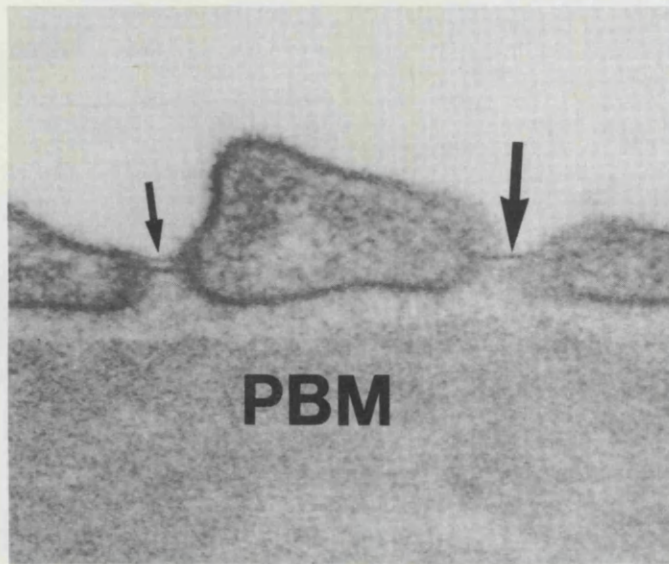


Fig. 6. The pedicels of parietal podocytes and the intervening filtration pores consisting of single (large arrow) and double (small arrow) slit diaphragms. PBM = parietal basement membrane, $\times 104000$.

epithelium of Bowman's capsule in rodents [9]. These pedicels are closely associated with renin-secreting myoepithelioid cells of the afferent arteriole, and this may form the morphological basis of fluid flow from the urinary space into the interstitium of the juxtaglomerular apparatus [10]. The extraglomerular mesangium and arterioles are tightly bound together by basement membrane material and by abundant cell junctions [11], which would prevent a high flow rate. Our findings imply that in

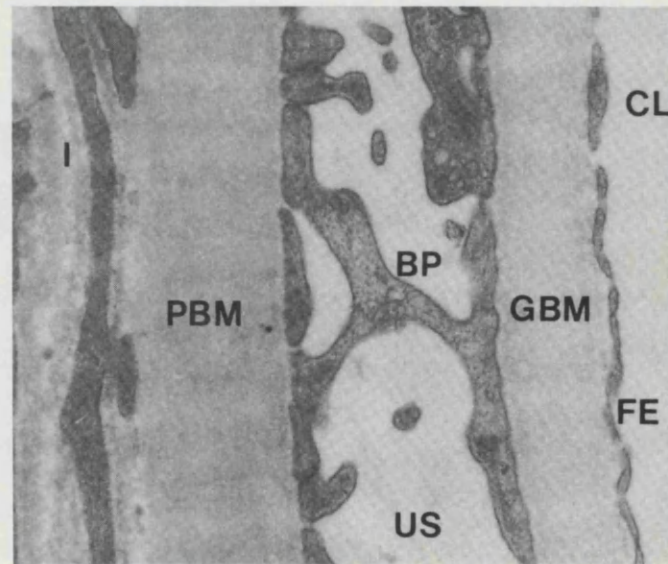


Fig. 7. A bridging process (BP) crosses the urinary space (US) and forms processes and pedicels on both glomerular basement membrane (GBM) and parietal basement membrane (PBM). CL = glomerular capillary loop; FE = fenestrated endothelium; I = interstitial compartment, $\times 23000$.

humans there is filtration and flow from the urinary space, not only into the interstitium of the JGA, but also into the peritubular interstitium, where there is greater potential for bulk fluid flow. This could affect not only the juxtaglomerular apparatus, but also the pressures and the composition of the renal interstitium, with consequent important implications for renal function in health and disease.

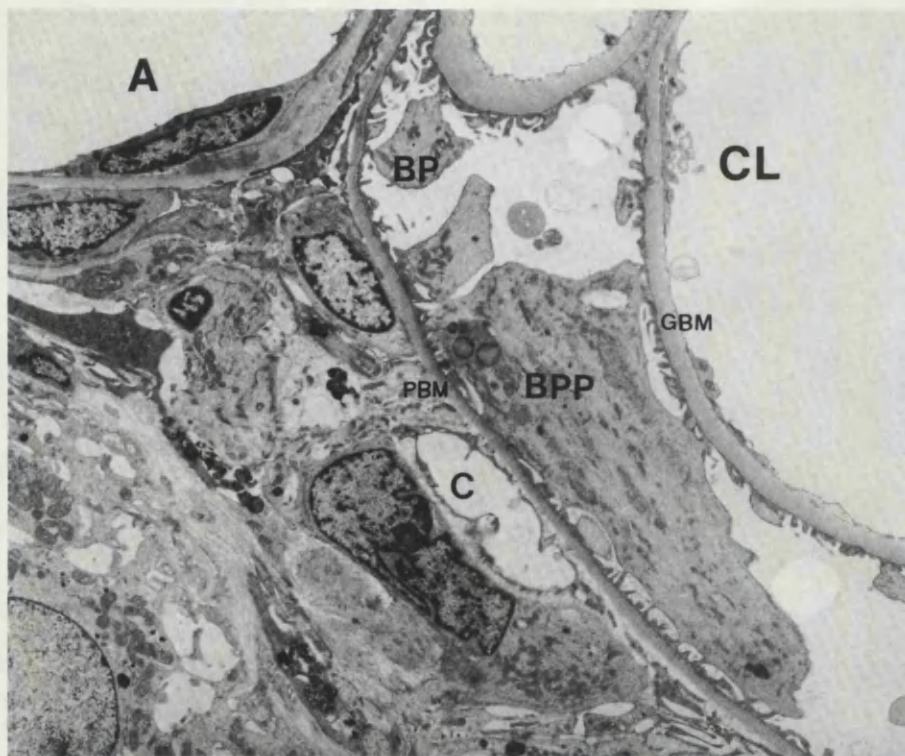


Fig. 8. A bridging parietal podocyte (BPP) and a bridging process (BP) with pedicels on both the glomerular basement membrane (GBM) and the parietal basement membrane (PBM). A = arteriole of vascular pole; C = pericapsular capillary; CL = glomerular capillary loop, $\times 3,218$.

Reprint requests to Dr. G.B.M. Lindop, Department of Pathology, Western Infirmary, Glasgow G11 6NT, Scotland, United Kingdom.

References

1. GIBSON IW, MORE IAR, LINDOP GBM: A scanning electron microscopic study of the peripolar cell of the rat renal glomerulus. *Cell Tissue Res* 257:201–206, 1989
2. KELLY G, DOWNIE I, GARDINER DS, MORE IAR, LINDOP GBM: The peripolar cell: a distinctive cell type in the mammalian glomerulus; morphological evidence from a study of sheep. *J Anat* 168:217–227, 1990
3. JONES DB: Scanning electron microscopy of human hypertensive renal disease. *Scanning Electron Microscopy* II:937–942, 1978
4. WILSON RB: Variations in the epithelial lining of Bowman's capsule. *Scanning Electron Microscopy* II:541–546, 1977
5. EVAN AP, GARDNER KD: Comparison of human polycystic and medullary cystic kidney disease with diphenylamine-induced cystic disease. *Lab Invest* 35:93–101, 1976
6. MARCUS PB: Podocytic metaplasia of parietal Bowman's capsular epithelium. *Arch Pathol Lab Med* 101:664, 1977
7. OJEDA JL, GARCIA-PORRERO JA, HURLE JM: Experimental formation of podocytes in the parietal layer of the Bowman's capsule. *Experientia* 35:1658–1660, 1979
8. OJEDA JL, GARCIA-PORRERO JA: Structure and development of parietal podocytes in renal glomerular cysts induced in rabbits with methylprednisolone acetate. *Lab Invest* 47:167–176, 1982
9. ROSIVALL L, TAUGNER R: The morphological basis of fluid balance in the interstitium of the juxtaglomerular apparatus. *Cell Tissue Res* 243:525–533, 1986
10. ROSIVALL L: Morphology and function of the distal part of the afferent arteriole. *Kidney Int* 38 (Suppl 30):S10–S15, 1990
11. TAUGNER R, HACKENTHAL E: *The Juxtaglomerular Apparatus: Structure and Function*. Berlin, Springer-Verlag, 1989, p. 22

**SCANNING ELECTRON MICROSCOPY OF THE MAMMALIAN RENAL
GLOMERULUS IN HEALTH AND DISEASE**

VOLUME TWO - FIGURES

IAN W. GIBSON BSc (Hons) MB ChB

**University Department of Pathology,
Western Infirmary, Glasgow**

**Thesis submitted for the degree of Doctor of Medicine,
in the Faculty of Medicine, University of Glasgow,**

December 1994

Theril
10239
Copy 1
Vol 2



Figure 2.01: Stereomicrograph of glomerular microdissection on critical point dried human renal cortex. The glomerular tufts lie within Bowman's capsules (small arrows). One tuft (large arrow) has been "broken off" at the vascular pole, and levered out of its Bowman's capsule, exposing the fractured arterioles on both the tuft and capsule.
BV = Blood vessel.

Figure 2.02: A randomly-sectioned human Bowman's capsule, containing both the vascular pole (with two fractured arterioles, small arrows), and the tubular pole (large arrow).

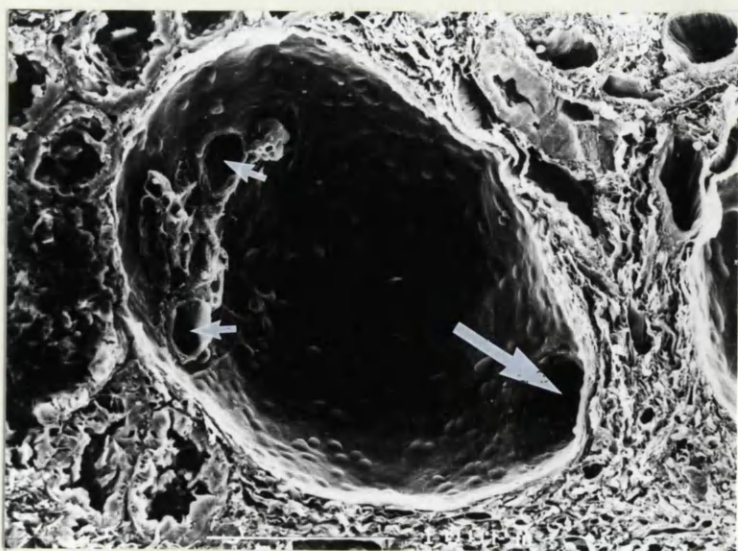
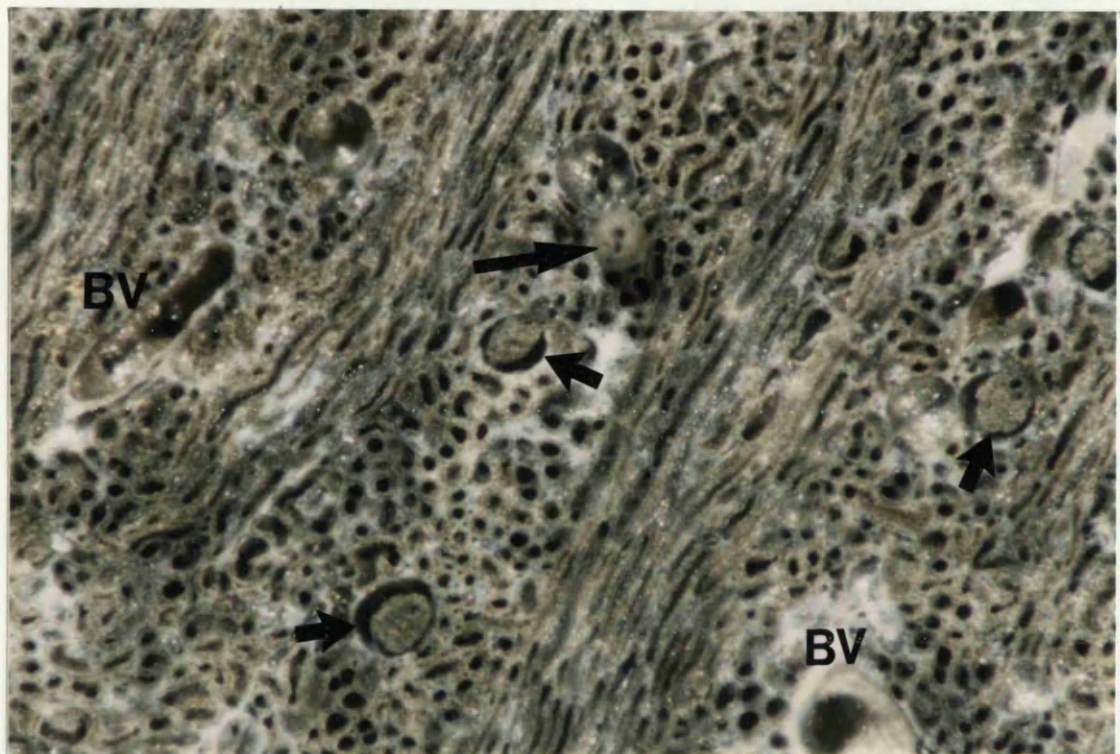


Figure 2.03: Figs. a and b are the complementary faces of sliced human renal cortex after microdissection of capillary tufts. The two hemispheres of each of a total of 97 Bowman's capsules can be examined for their glomerular poles. The pattern of sectioned vessels (arrows) helps localise the respective halves of each Bowman's capsule. C = Renal capsule.

Fig. c shows the isolated capillary tufts aligned in rows. The Bowman's capsule from which each tuft originated can be noted.

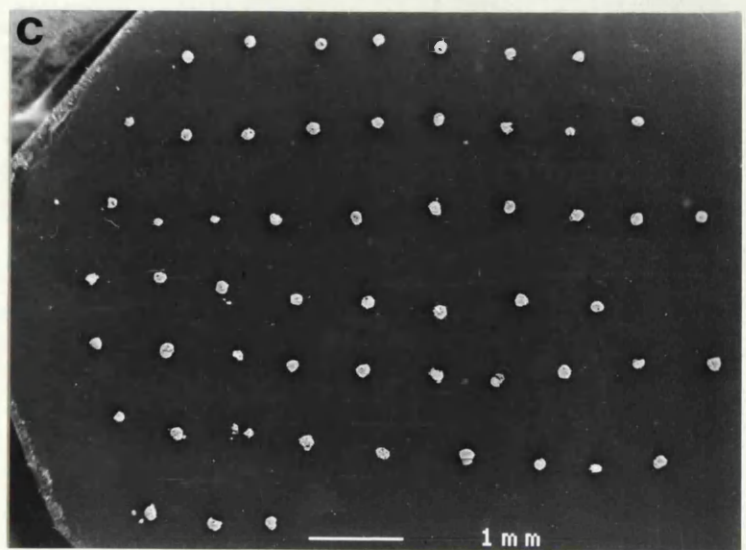
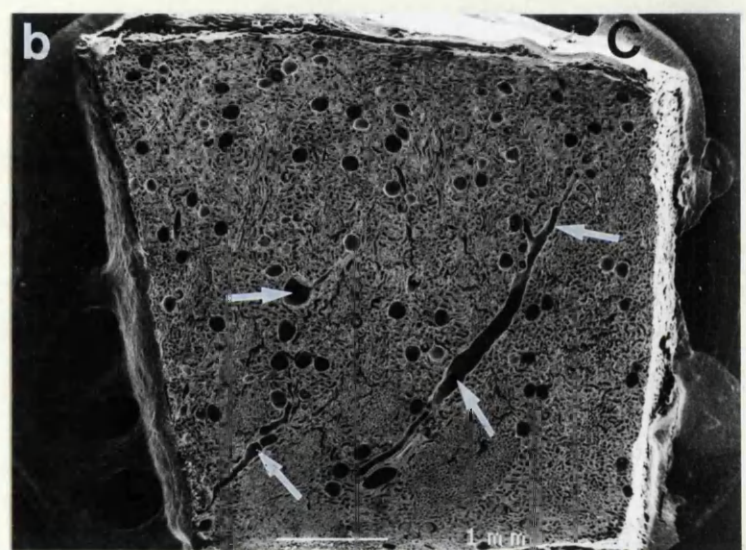
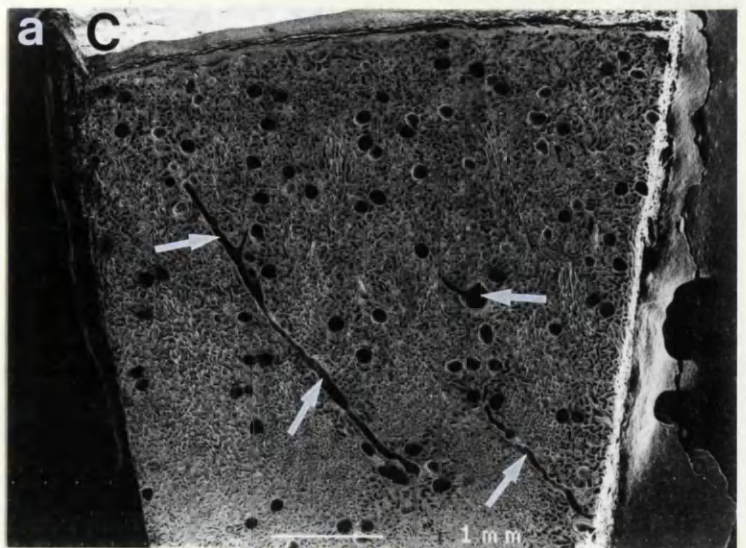


Figure 2.04: A Bowman's capsule (BC) from hamster kidney, with exposed vascular pole. The epithelial fracture line encircles the afferent (large arrow) and narrower efferent (small arrow) arterioles. The extraglomerular mesangium (curved arrow) lies between the arterioles.

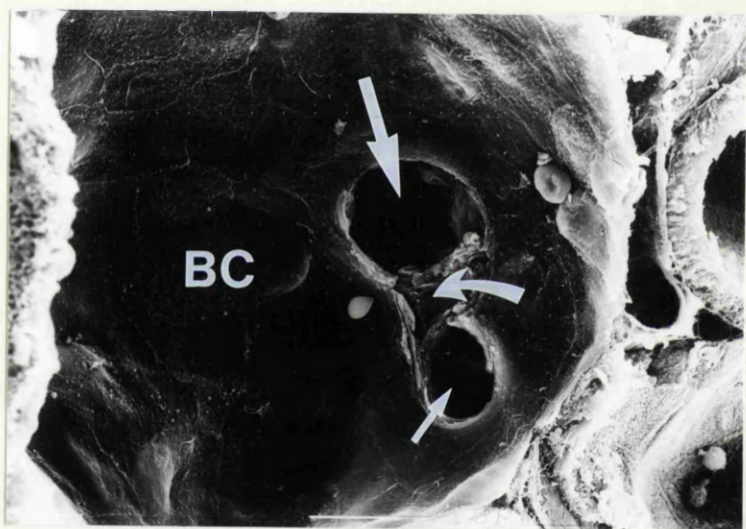


Figure 2.05:

Fig. a: An isolated human capillary tuft, which is largely undamaged allowing examination of the visceral epithelium (ie. podocytes, arrows).

Fig. b: Podocytes have cell bodies, and branching processes which extend over capillary loops and terminate as interdigitating foot processes (ie. pedicels).

Fig. c: An isolated human capillary tuft, rotated to expose the vascular pole, with its two arterioles (arrows).

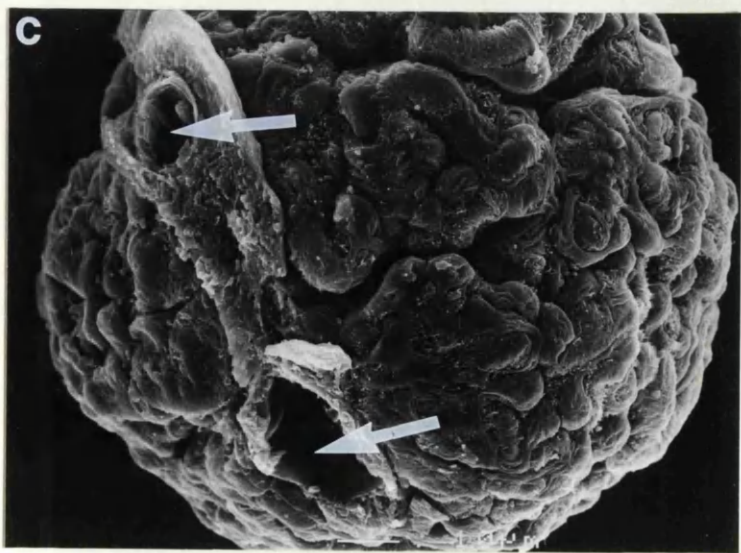
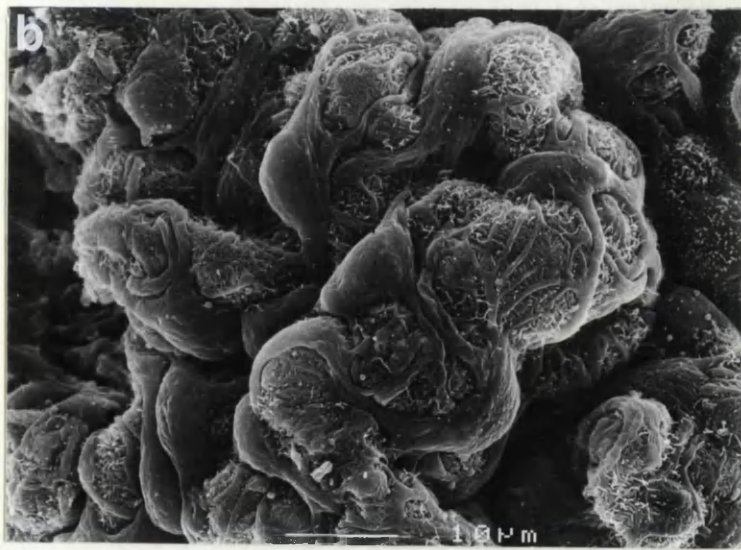


Figure 2.06: Human renal cortex from a damaged transplant nephrectomy before (fig. a) and after (fig. b) glomerular microdissection. Only in the relatively preserved areas of parenchyma were tufts successfully removed (large arrows). In the severely damaged scarred areas, glomerular microdissection was not possible (small arrows).

M = Medulla.

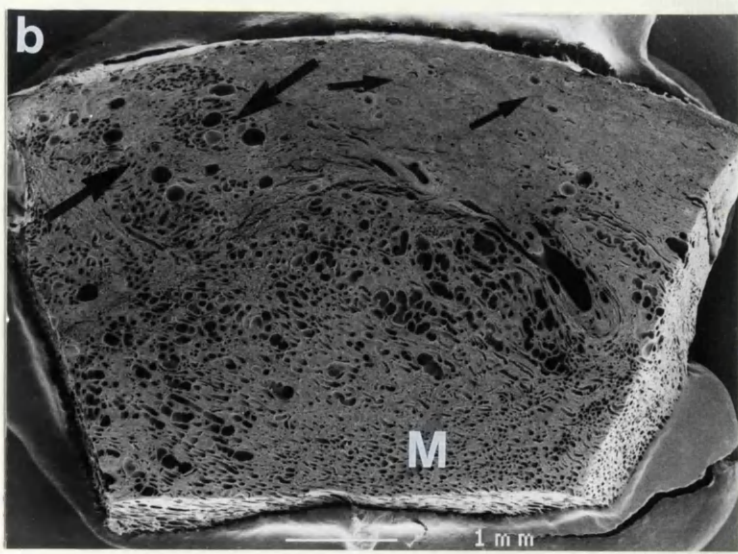
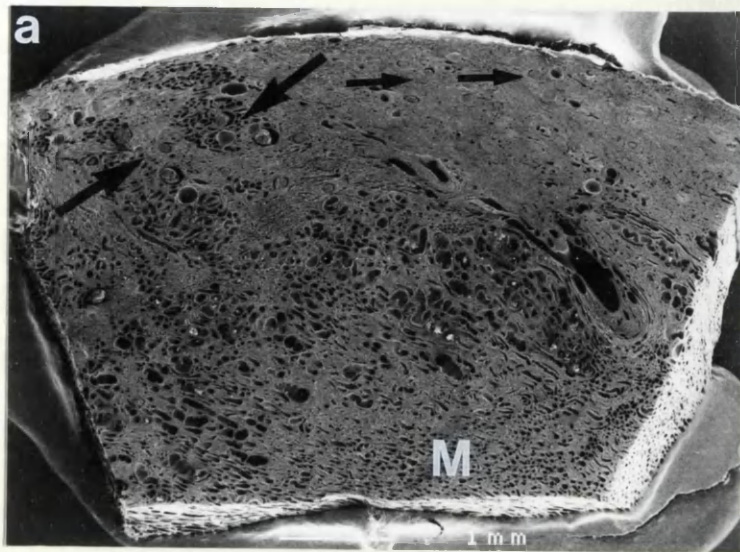


Figure 3.01: A vascular pole consisting of the afferent arteriole (large arrow) approximately 25um diameter, the efferent arteriole (small arrow) approximately 15um diameter, and the intervening extraglomerular mesangium. Parietal podocytes (outlined by small curved arrows) partially surround the vascular pole.

Figure 3.02: Three parietal podocytes on Bowman's capsule with a typical branching dendritic structure. There is a smooth curved overlapping border with squamous parietal epithelium in one area (arrow).

Figure 3.03: Two dendritic parietal podocytes with branching processes terminating in interdigitating pedicels. In both cells, the cell bodies have bossellated protrusions (arrows) due to the presence of cytoplasmic granules.

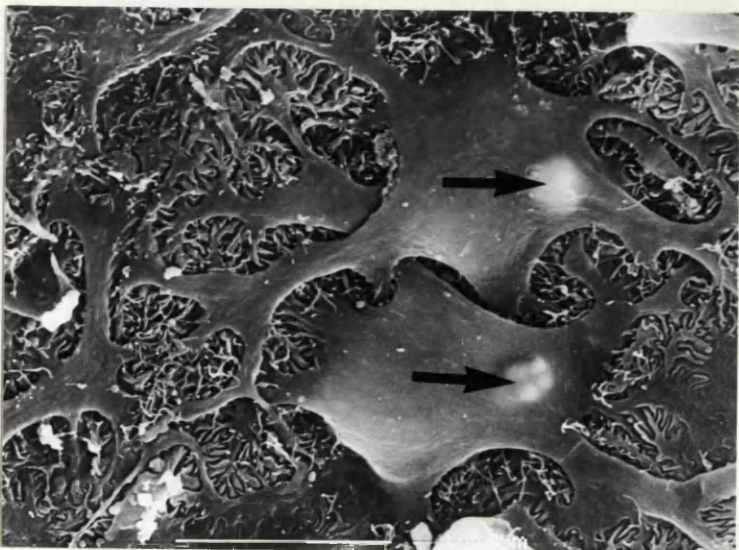
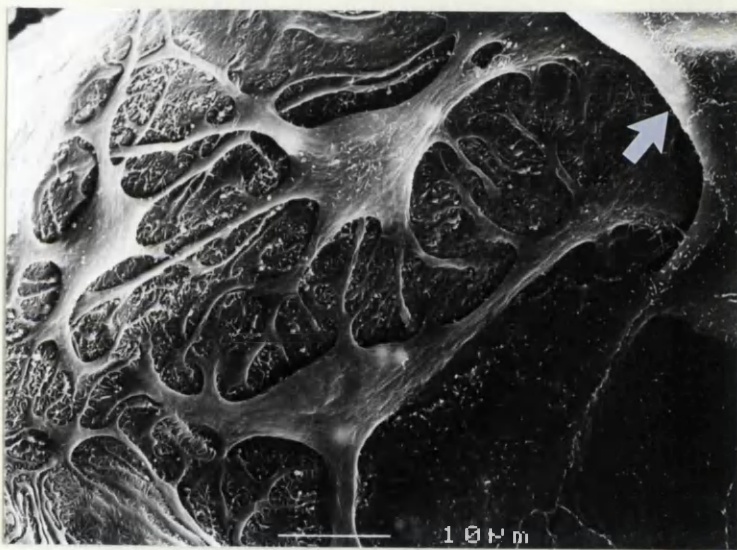
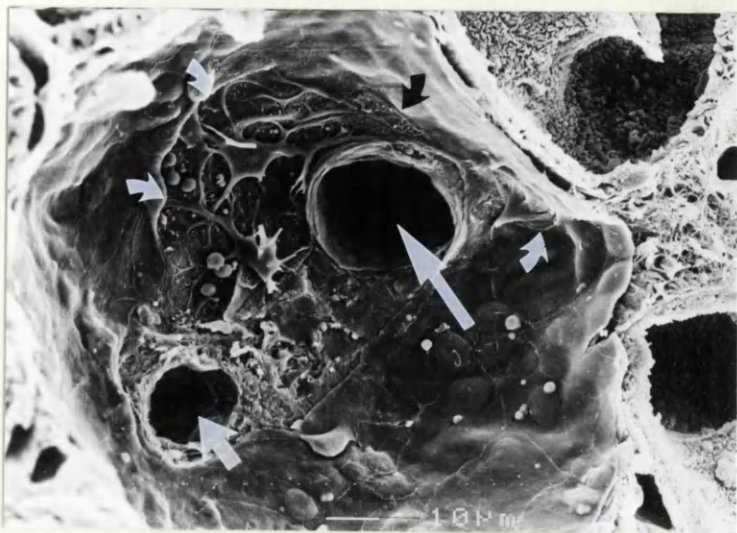


Figure 3.04: Two parietal podocytes with major processes forming enclosed circles (curved arrows). The junction with squamous parietal cells consists of long sweeping major processes (large arrow) or scalloped overlapping squamous cells (small arrows). A broken process (P) projects from one parietal podocyte towards the vascular pole.

Figure 3.05: The branching processes and interdigitating pedicels of parietal podocytes have small numbers of surface microblebs (arrows).

Figure 3.06: Interdigitating processes and pedicels of parietal podocytes covered by sparse microvilli.

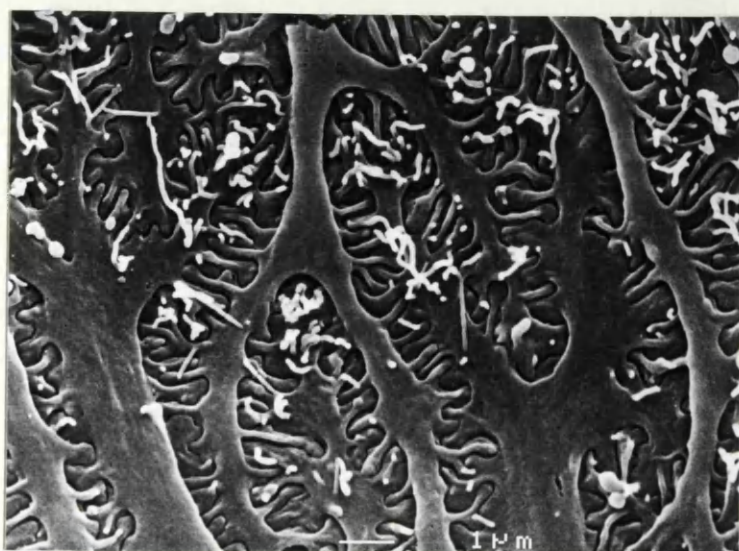


Figure 3.07: Parietal podocytes lining Bowman's capsule with branching processes, but incomplete pedicel formation. One cell body has a bossellated protrusion of cytoplasmic granules (arrow).

Figure 3.08: The lower power view of this Bowman's capsule (fig. a) shows the vascular pole (VP) and a large area of parietal podocytes (outlined by arrows), which extend upto 100um from the vascular pole. The higher power view (fig. b) shows some of the parietal podocytes, and a prominent broken process (larger arrow), apparently derived from a visceral podocyte cell body on the capillary tuft. The process connects to Bowman's capsule at the junction between parietal podocytes and squamous parietal epithelium (smaller arrow).

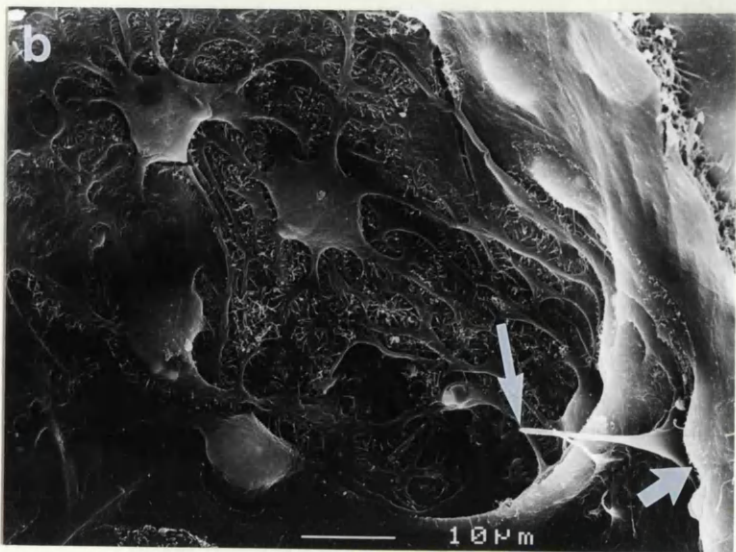
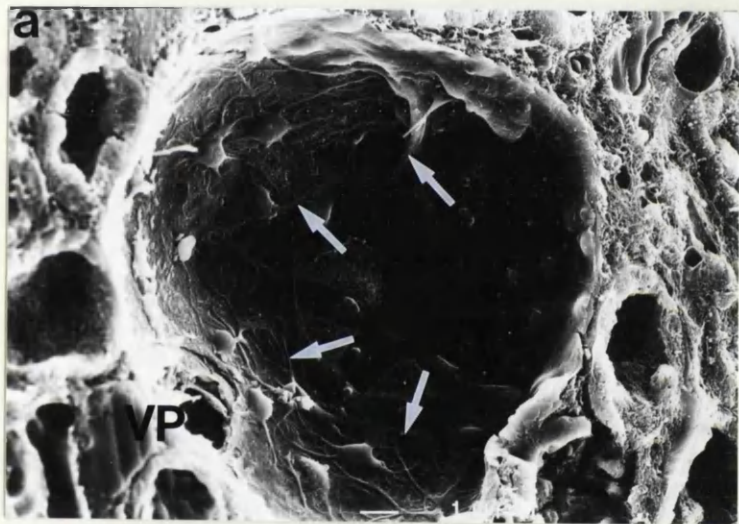
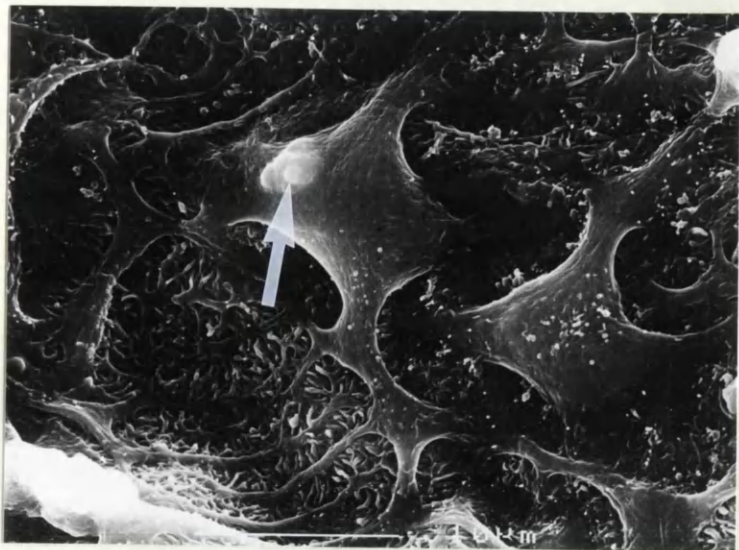


Figure 3.09: In this Bowman's capsule, parietal podocytes (outlined by arrows) extend close to the tubular pole (large arrow).

Figure 3.10: In this case, parietal podocytes extend out from the vascular pole (VP) extensively and irregularly, enclosing two discrete islands of squamous parietal epithelium (arrows).

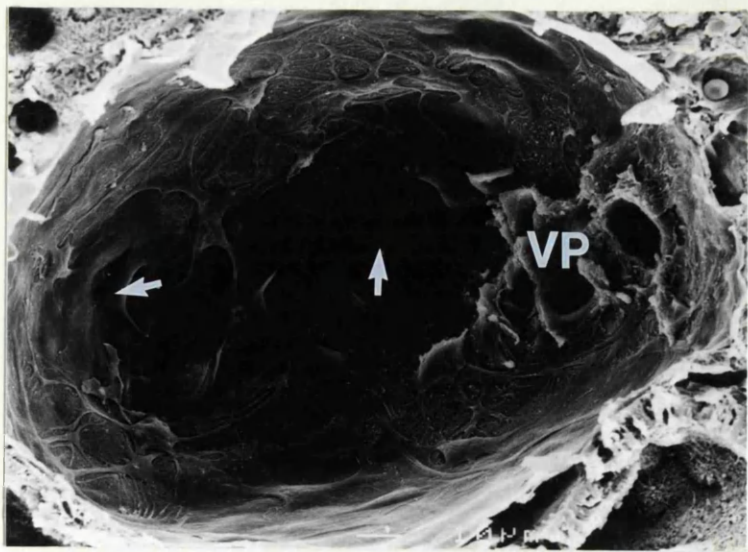
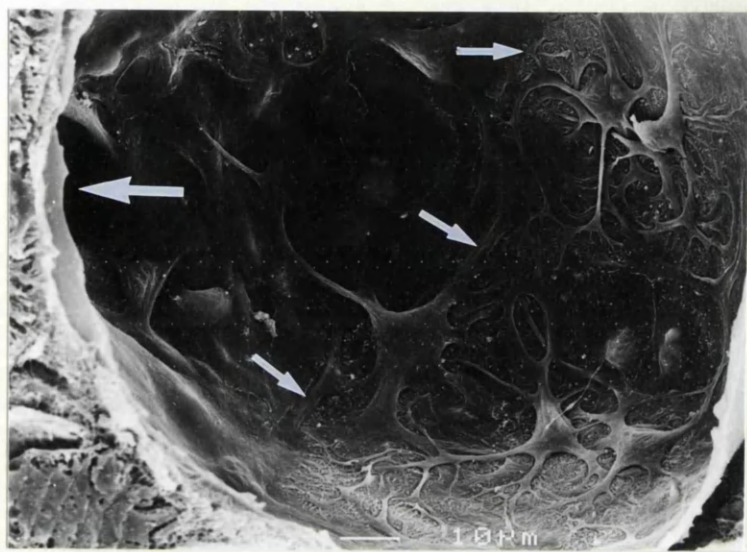


Figure 3.11: A Bowman's capsule with part of the glomerular capillary tuft (T) in-situ. A bridging podocyte (BP) sends processes to both a glomerular capillary and Bowman's capsule. Two bridging processes from visceral podocytes (larger arrow) connect with Bowman's capsule, and one continues as a long process forming the junction between parietal pedicels and squamous parietal epithelium (smaller arrow).

Figure 3.12: In fig. a, two closely-apposed thin-walled efferent vessels (arrows) are surrounded by parietal podocytes. The higher power view of an area of these parietal podocytes (fig. b) shows two broken podocyte processes, the smaller (smaller arrow) branching from a parietal podocyte cell body, the larger (larger arrow) apparently derived from a visceral podocyte, and branching to produce parietal pedicels.

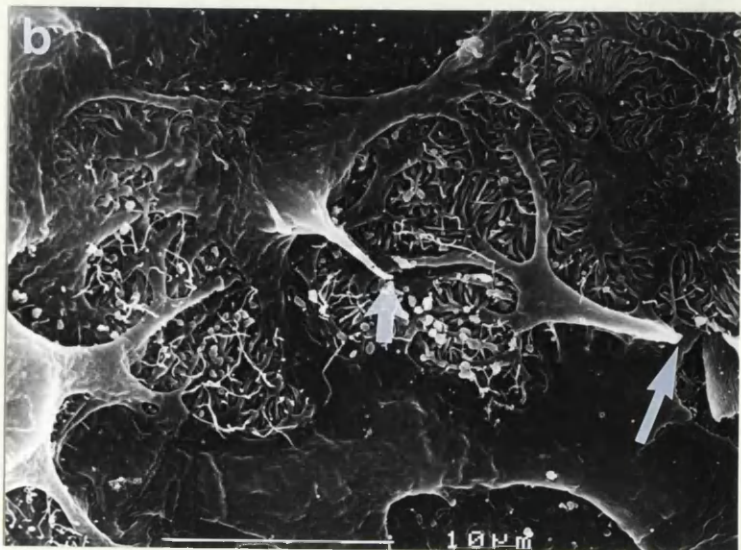
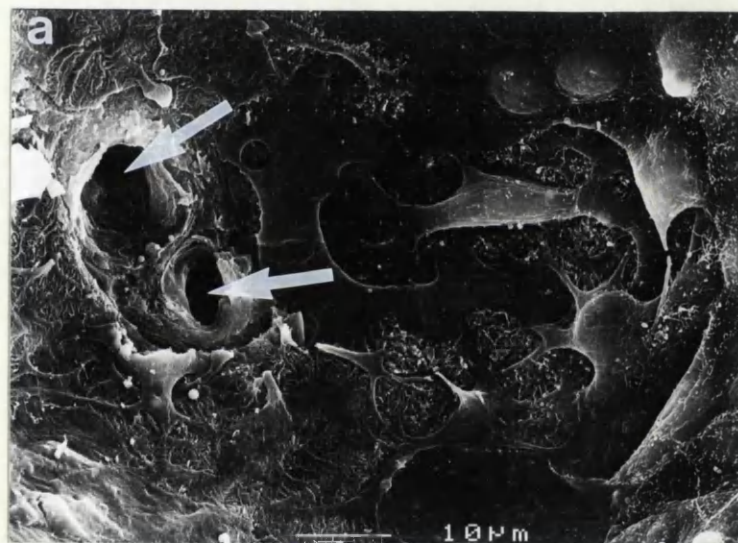
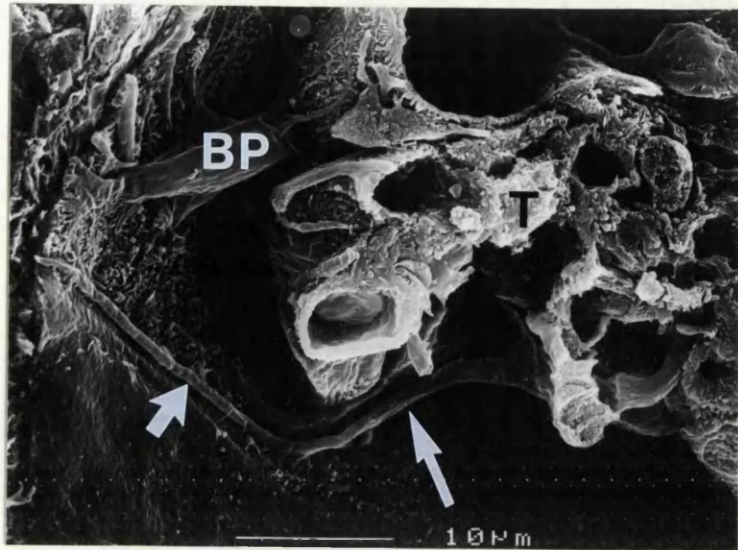


Figure 3.13: A discrete island of podocytic cells with branching processes, but minimal pedicel formation, surrounded by smooth curved overlapping squamous parietal epithelium (arrows).

Figure 3.14: A discrete area of podocytic cells, similar to fig. 3.13, with one broken process (arrow) presumably connecting with the capillary tuft.

Figure 3.15: This Bowman's capsule has a tubular pole (TP), approximately 40um diameter, with a neck segment (hence no tubular brush border is seen). There are two broken podocytic processes (small arrows) apparently derived from visceral podocytes of the tuft, but not related to parietal podocytes. There is a cluster of squamous parietal cell nuclear bulges (large arrow) close to the tubular pole.

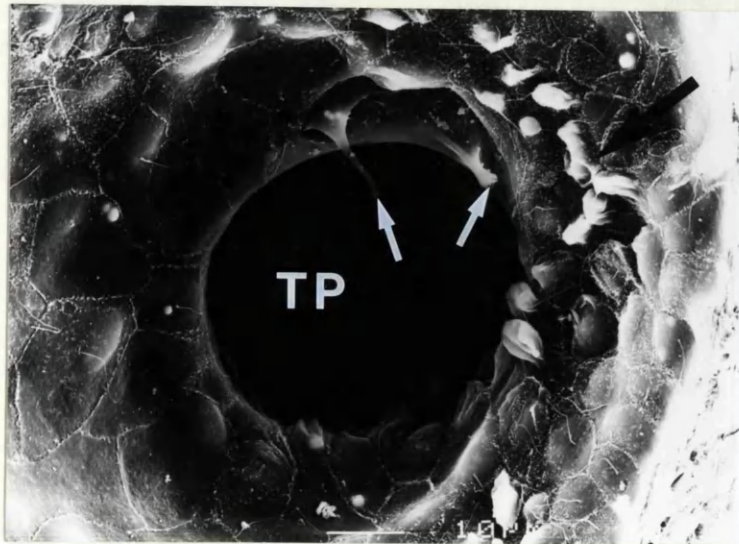
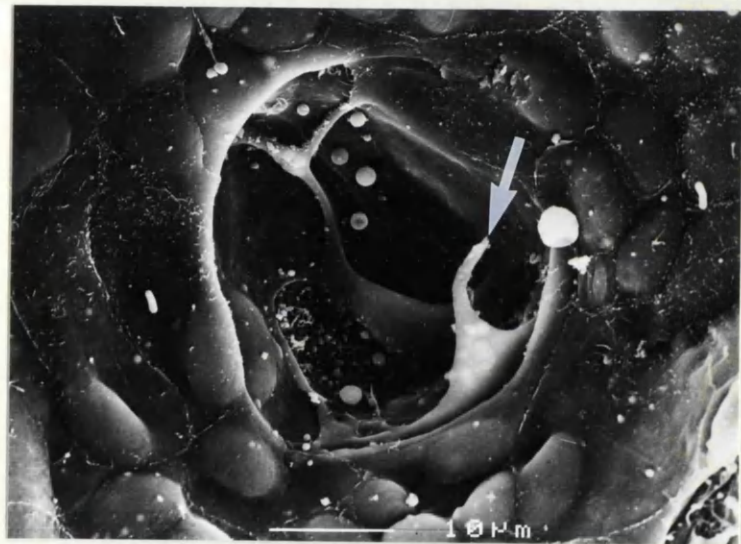
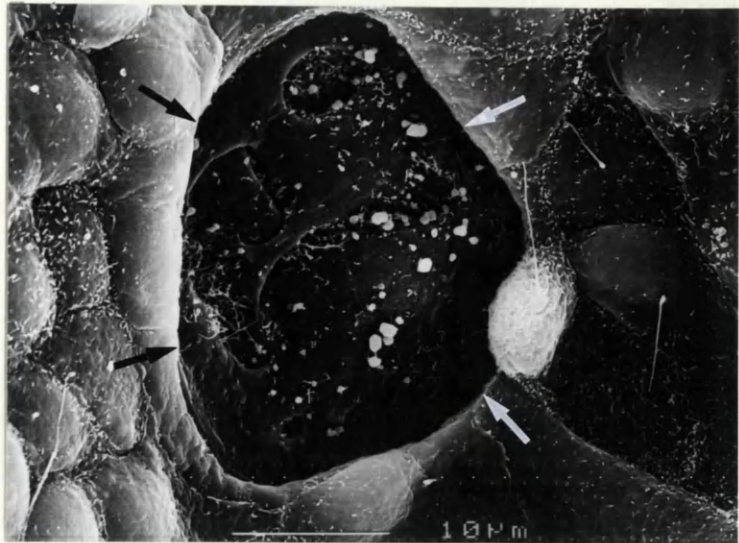


Figure 3.16: This Bowman's capsule has a 30um diameter tubular pole (TP), with the proximal tubule brush border of microvilli beginning abruptly at the tubular orifice. There is a separate patch of parietal cells with a brush border (arrow), indicating tubularization of Bowman's capsule, close to the tubular pole.

Figure 3.17: Tubularization of Bowman's capsule. The larger patch of parietal epithelium with a brush border is continuous with the brush border of the proximal tubule; the smaller brush border patch (arrow) appears to cover a single parietal cell.

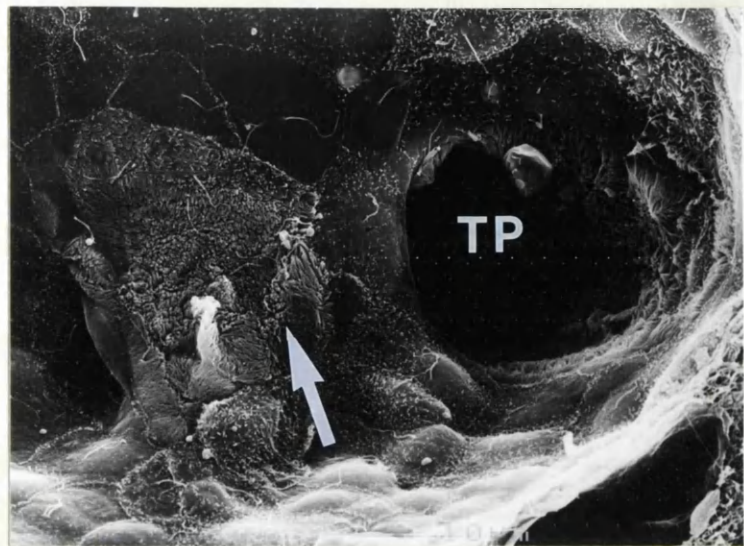


Figure 3.18: A Bowman's capsule with a 30um diameter tubular pole (TP). The absence of proximal tubule brush border implies the presence of a neck segment.

Figure 3.19: A Bowman's capsule (BC) with the tubular pole (larger arrow) in longitudinal section (fig. a). There is a neck segment (approximately 60um long) composed mostly of squamous cells, but also containing a patch of brush border epithelium (seen at higher power in fig. b), prior to the commencement of the proximal tubule brush border (smaller arrow).

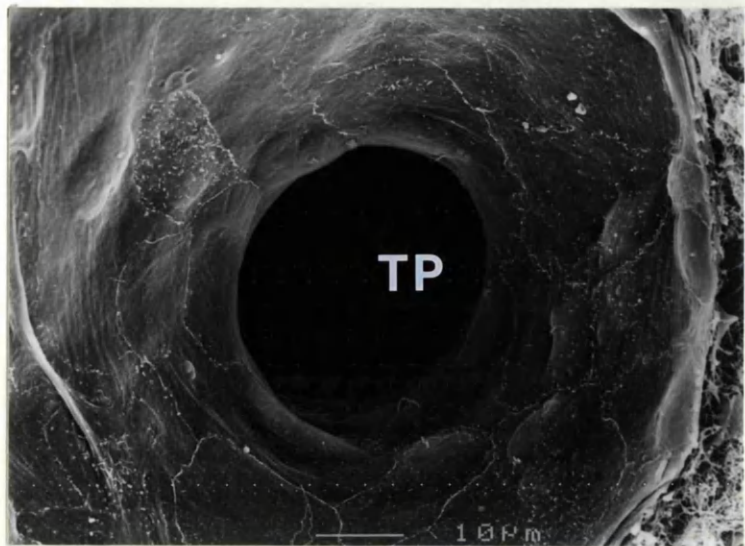


Figure 3.20: A small patch of tubularization of Bowman's capsule, consisting of parietal cells with a brush border identical to proximal tubule cells. One cell (arrow) has an incomplete covering of brush border microvilli.

Figure 3.21: A Bowman's capsule with a tubular pole composed of two separate orifices (arrows). Proximal tubule brush border is present at both orifices.

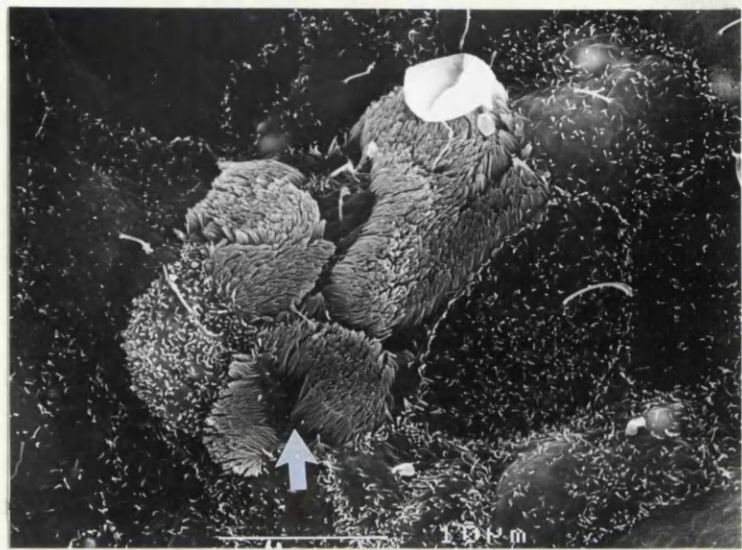


Figure 3.22: Squamous parietal epithelium of Bowman's capsule, with nuclear bulges (N), single cilia (small arrows) and variable short microvilli which help demarcate cell boundaries. Several cells also possess bulging cytoplasmic granules (large arrows).

Figure 3.23: High power view of squamous parietal cells, with several aggregates of bulging granules (arrows). The largest aggregate (large arrow) has formed a "pore-like" opening in the centre of the protrusion.

Figure 3.24: Squamous parietal epithelium of Bowman's capsule, with variable microvilli, and an isolated inflammatory cell (arrow) next to a cluster of parietal cell nuclear bulges.

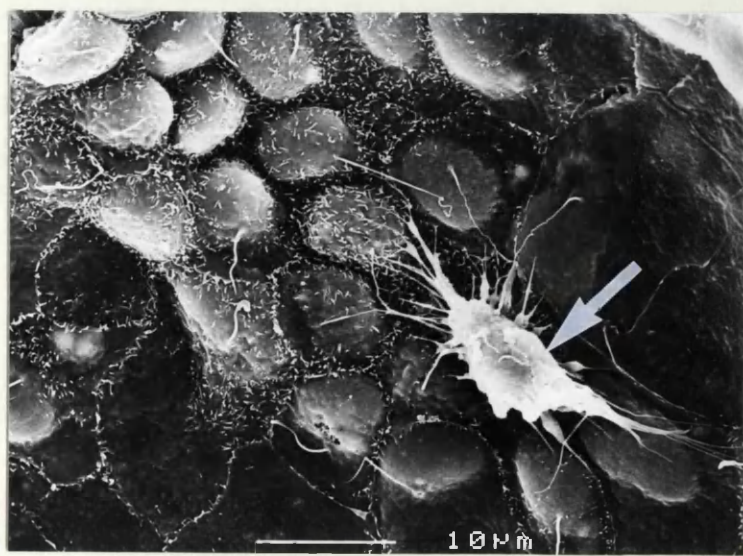
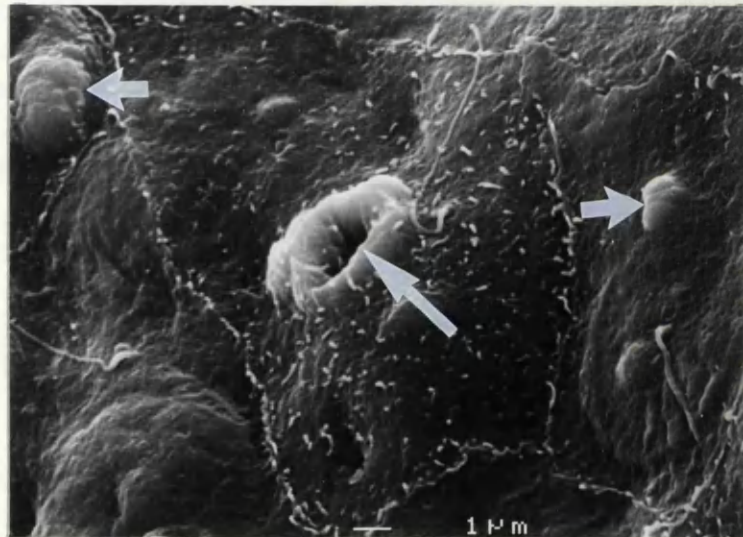
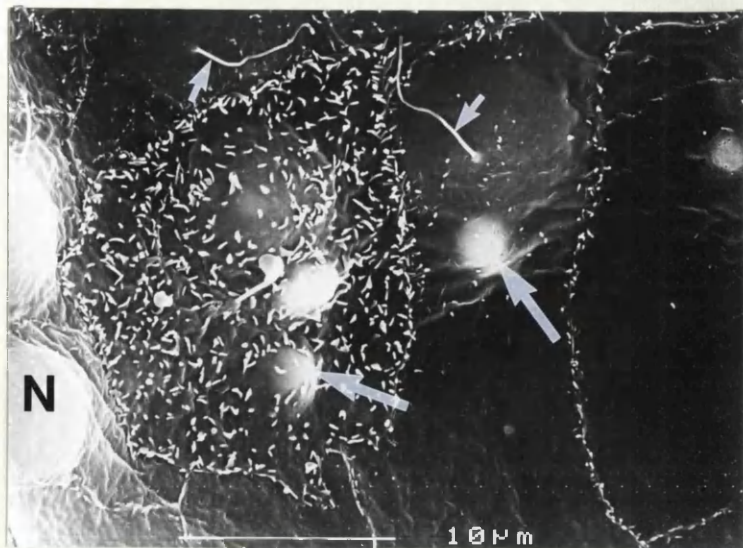


Figure 4.01: A rat vascular pole with two arterioles (A) surrounded by 3 dendritic peripolar cells (numbered 1, 2 and 3). Peripolar cell no.1 has an ovoid-shaped cell body; nos. 2 and 3 have pyramidal cell bodies. There are blunt-ending (presumed broken) cell processes from nos. 1 and 3 (arrows).

Figure 4.02: The afferent arteriole (A) of a rat vascular pole, with a microvillous-covered peripolar cell (arrow) curving round the arteriole.

Figure 4.03: A rabbit dendritic peripolar cell (P) with a process (large arrow) extending around the arteriole (A), which is lined by a partially fenestrated endothelium (small arrows).

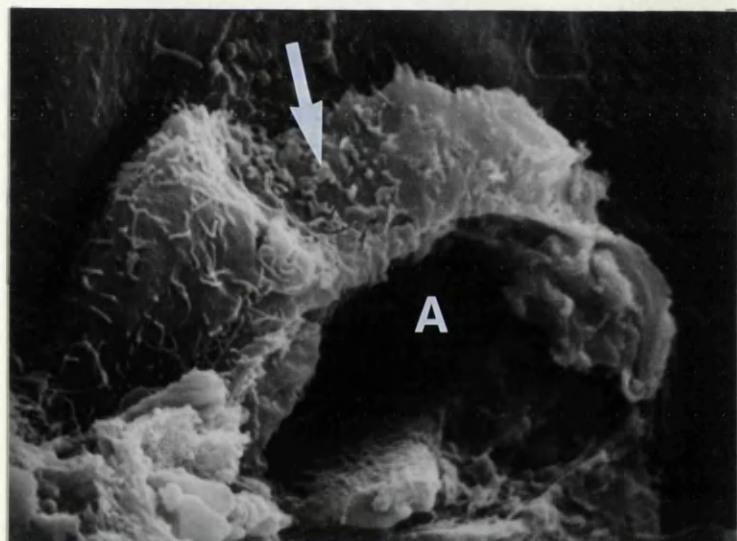


Figure 4.04: Guinea pig kidney; this Bowman's capsule (fig. a) has a vascular pole with two arterioles (A) and 3 peripolar cells (arrows). The peripolar cells (figs. b and c) have single cilia (arrows) and increased microvilli compared with squamous parietal cells. One peripolar cell (fig. b) curves around the arteriole (A); the largest peripolar cell (fig. c) has a plump ovoid shape with no obvious cell processes.

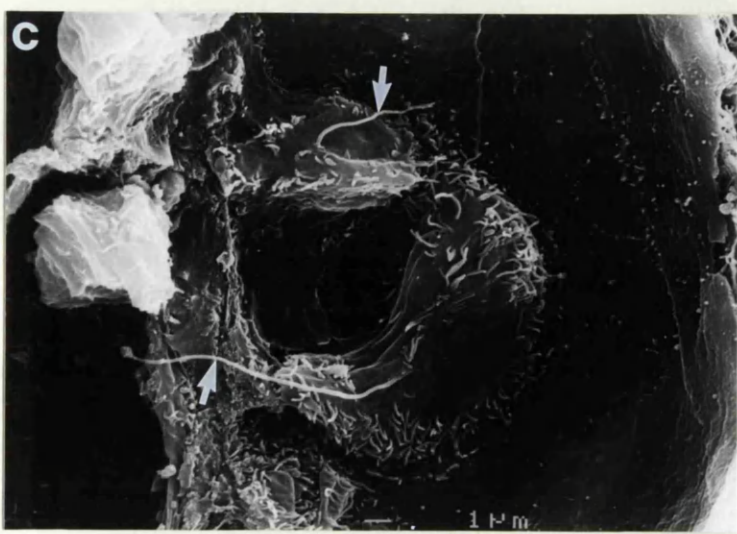
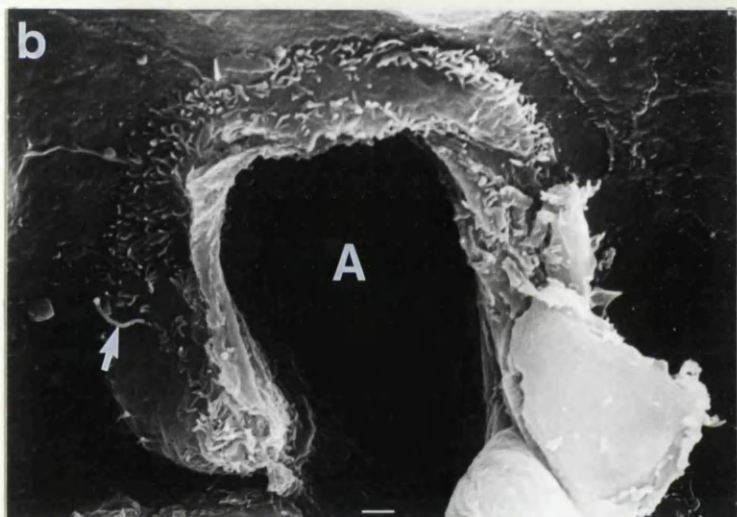
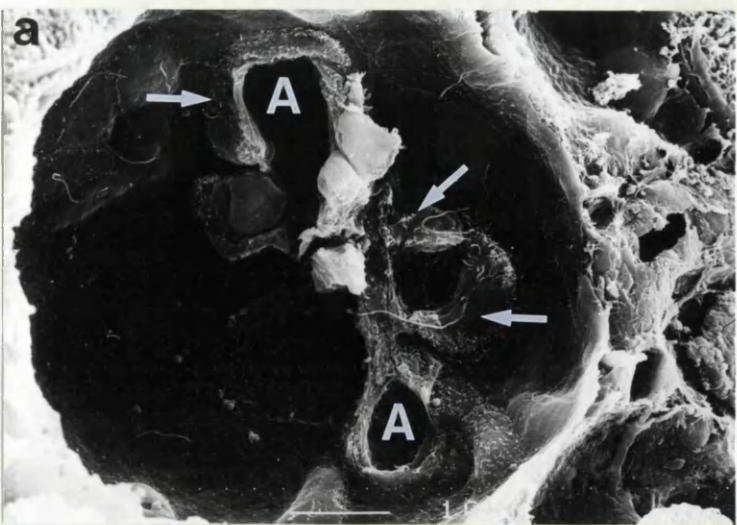


Figure 4.05: Goat kidney; globular peripolar cell (P) with bossellated surface, situated at the vascular pole between the parietal layer of Bowman's capsule (arrows) and remnants of the glomerular capillary tuft (T).

Figure 4.06: Goat kidney; a vascular pole with arteriole (A) and two globular peripolar cells (P). The larger cell has a smooth (ie. non-bossellated) area (small arrow). Note also the focal bossellation of adjacent squamous parietal cells (large arrows).

Figure 4.07: Sheep kidney; the fractured arteriole of this vascular pole is surrounded by 3 bossellated peripolar cells (arrows). One of the cells (large arrow) is elongated and encircles the arteriole; the others are more typically globular in shape.

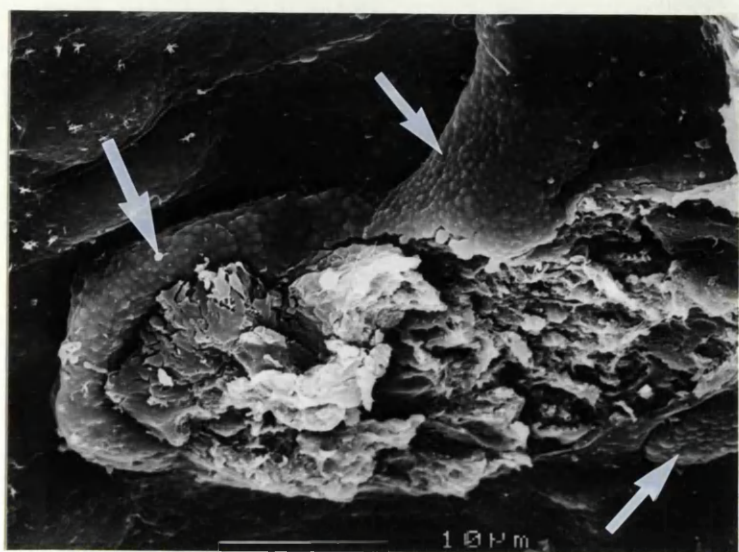
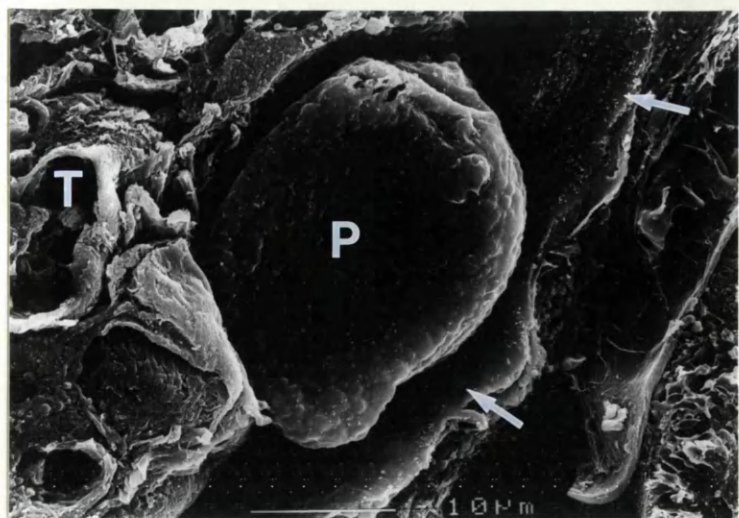


Figure 4.08: A flattened polygonal goat peripolar cell; the fractured cytoplasm (arrow) shows that the bossellated surface is due to closely-packed cytoplasmic granules.

Figure 4.09: Hamster kidney; vascular pole with arterioles (A) and one typical dendritic peripolar cell (P). Another cell resembles a peripolar cell at one end (smaller arrow) and a squamous parietal cell at the other (larger arrow).

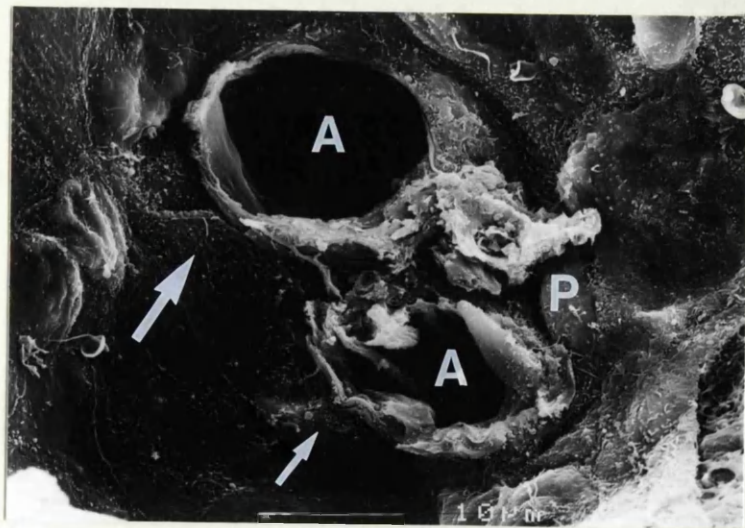
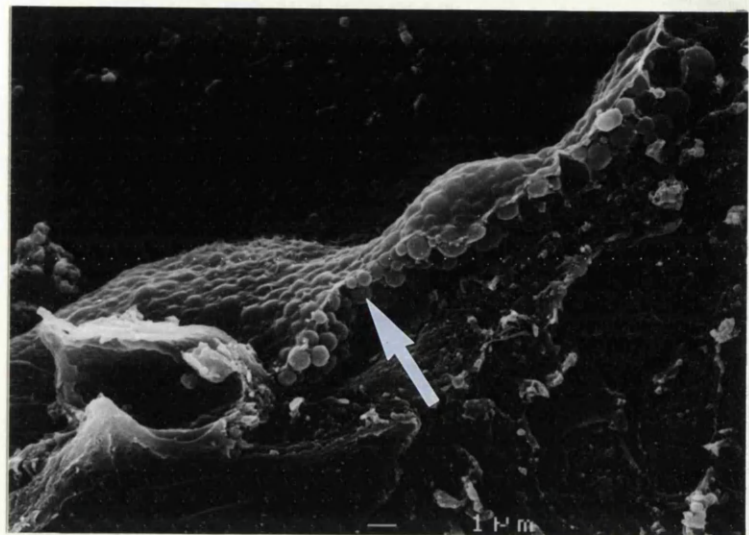


Figure 4.10: Guinea pig vascular pole; in fig. a the arteriole (A) is encircled by a typical microvillous-covered dendritic peripolar cell (smaller arrow). A second peripolar cell (larger arrow) has had its cell body sectioned by the vibratome blade. At higher power (fig. b), this peripolar cell contains closely-packed faceted cytoplasmic granules (larger arrow). The surface of this cell is uneven, but not bossellated like typical globular peripolar cells; there is a single cilium (smaller arrow), short microvilli and small surface pits. The typical dendritic peripolar cell around the arteriole (A) has (fig. c) an identical surface, with microvilli and surface pits (smaller arrow). Notice also the sudden change from arteriolar endothelium to fenestrated capillary endothelium (larger arrow).

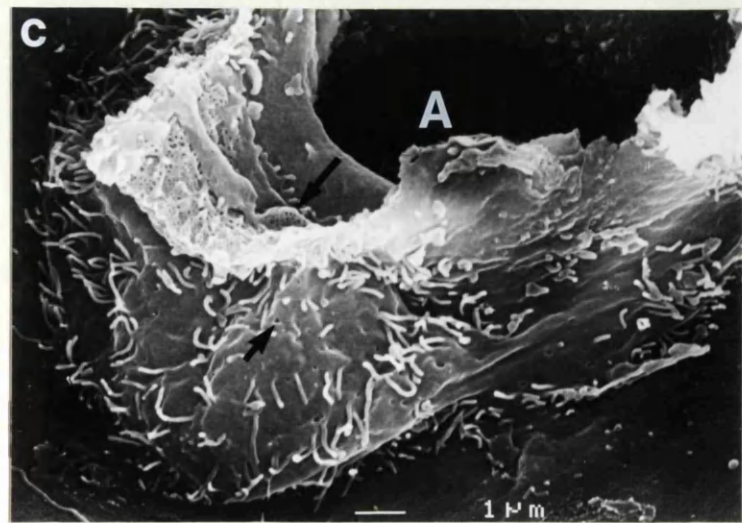
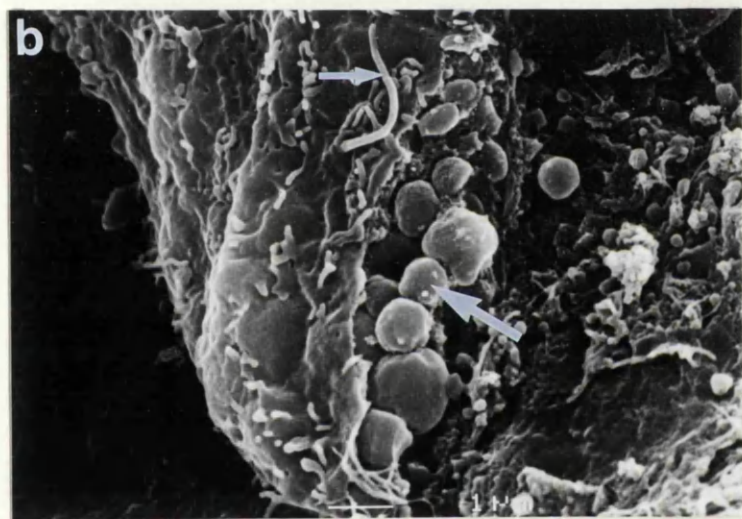
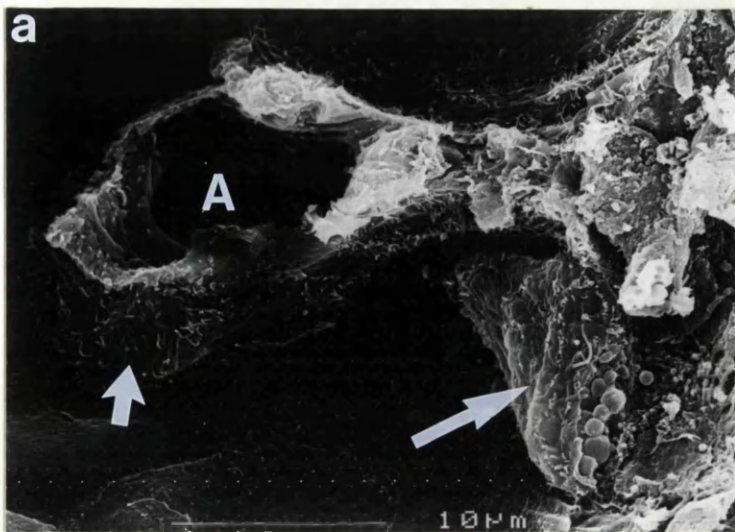


Figure 4.11: Human vascular pole, with arteriole (A) and dendritic peripolar cell (P) with process (arrow). The cell body has a ruffled surface with microvilli.

Figure 4.12: Human vascular pole, with arterioles (A), and a globular peripolar cell (arrow) with bossellated surface due to numerous closely-packed cytoplasmic granules.

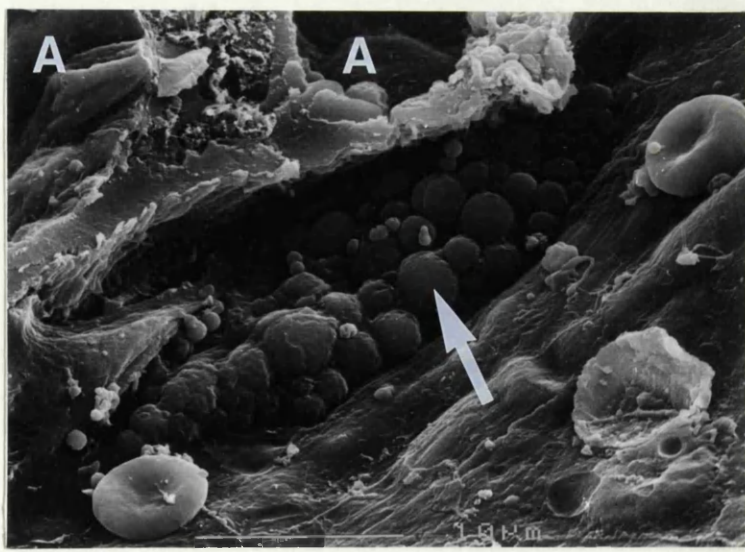
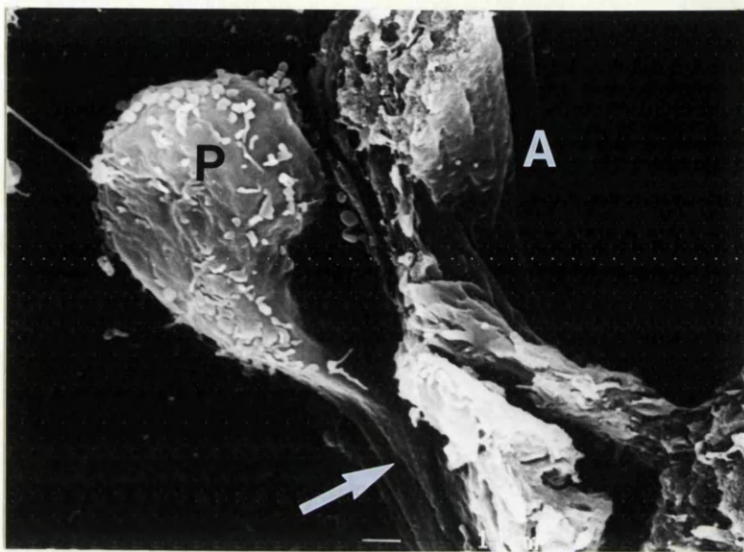


Figure 4.13: Human vascular pole, with arteriole (A), parietal podocytes (P), and a spindle-shaped junctional cell (arrow) at the boundary between parietal podocytes and squamous parietal epithelium.

Figure 4.14: Rabbit vascular pole, with arteriole (A), parietal podocytes (P), and junctional cell (arrow). Notice the similarity with fig. 4.13.

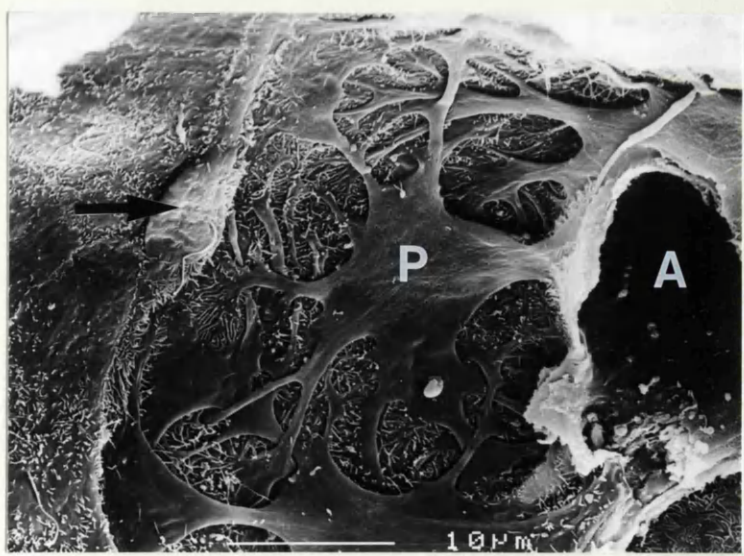
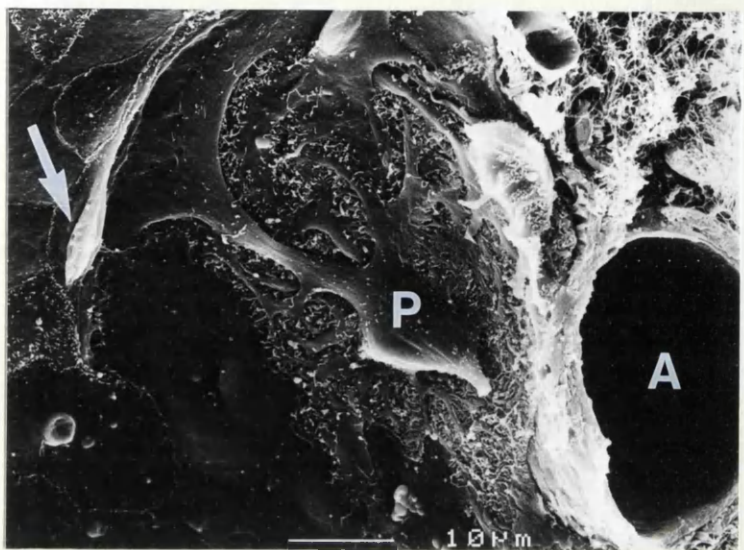


Figure 5.01: Human transplant nephrectomy; globular peripolar cell (arrow) next to the fractured arteriole (A) at the vascular pole. The cell has a typical bossellated surface due to its cytoplasmic granules.

Figure 5.02: Parietal podocytes from transplant nephrectomies, showing surface abnormalities. In fig. a, there is a complete absence of pedicels, and short microvilli cover the area where pedicels would be expected. In fig. b, there are small surface blebs and microvilli covering both cell bodies and pedicel areas. Two cell bodies have bossellated protrusions due to bulging cytoplasmic granules (larger arrows). Several junctional cells (smaller arrows) separate the parietal podocytes from the squamous parietal cells.

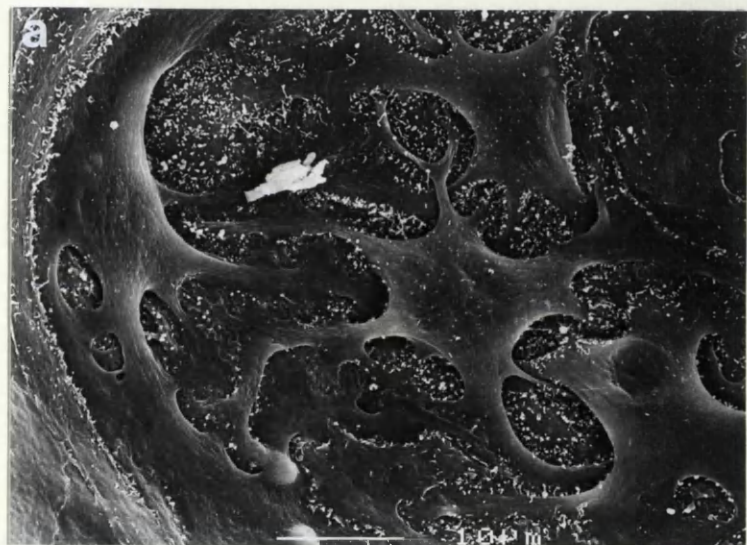
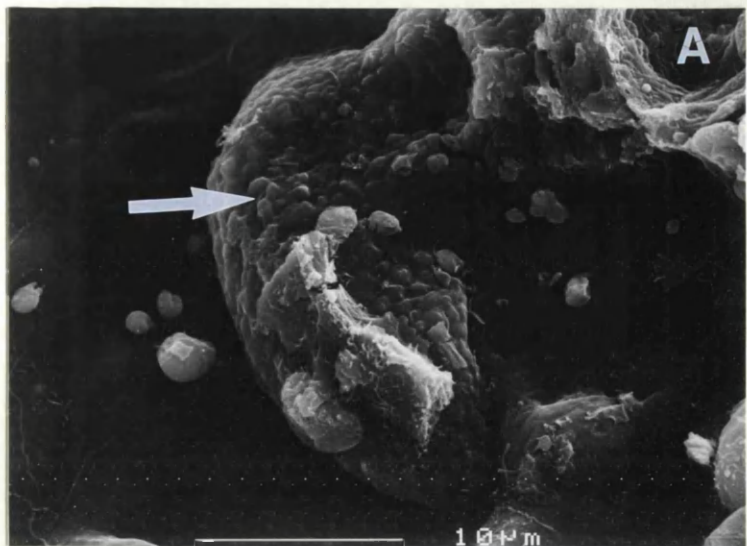


Figure 5.03: A vascular pole-associated tuft-to-capsule adhesion, composed of bridging and parietal podocytes (arrows), some covered by microvilli. T = Capillary tuft, I = Interstitial collagen fibres.

Figure 5.04: The Bowman's capsule in fig. a has a tubular pole (TP), two adjacent tubular pole-associated fractured adhesions (small arrows), and two additional fractured adhesions (large arrows) further from the tubular pole. The latter show the features associated with vascular pole adhesions. Fig. b shows that one of these adhesions is formed by podocyte cell processes (arrows) extending to form the junction between parietal podocytes and squamous parietal epithelium.

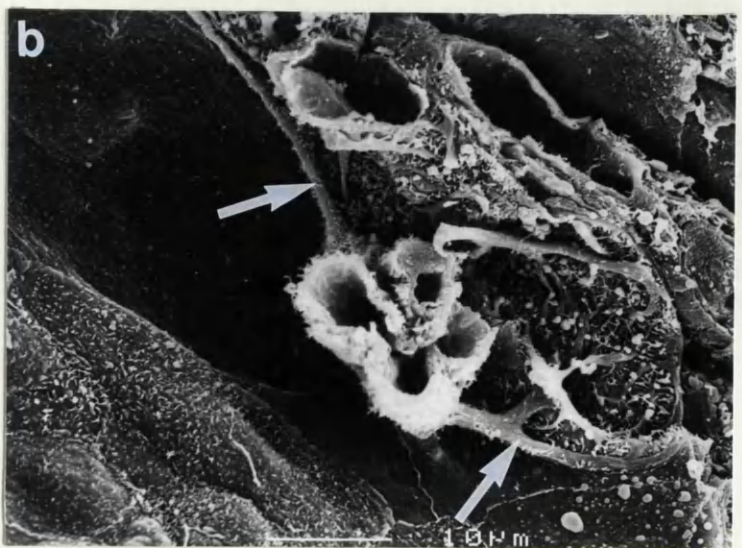
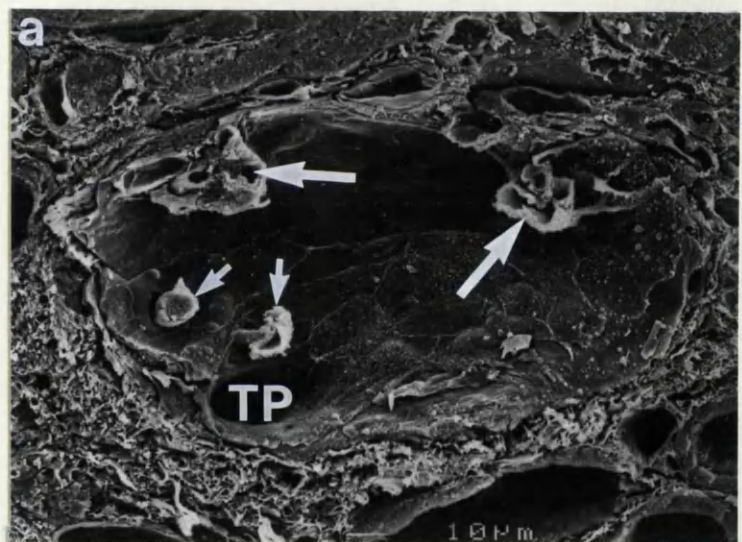
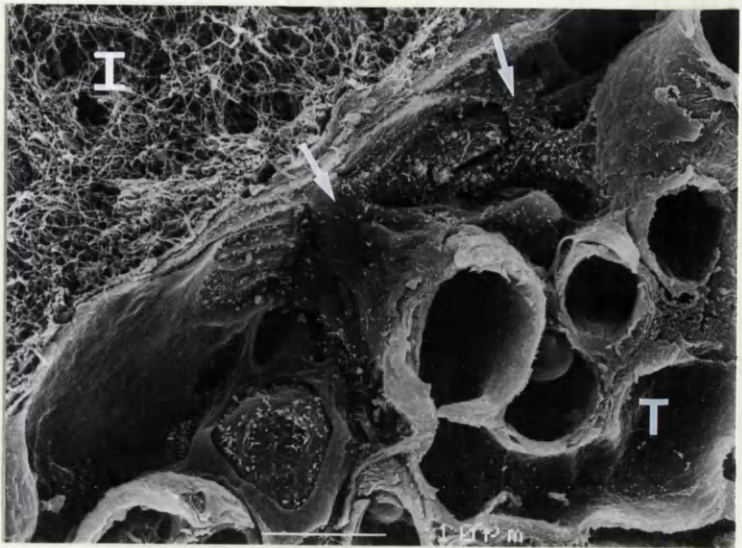


Figure 5.05: There are five fractured tuft-to-capsule adhesions (arrows) associated with the tubular pole (TP) of this Bowman's capsule (fig. a). Two of these adhesions (large arrows, fig. b) are at a discrete defect in the parietal epithelium, containing cells with prominent microvilli (small arrows).

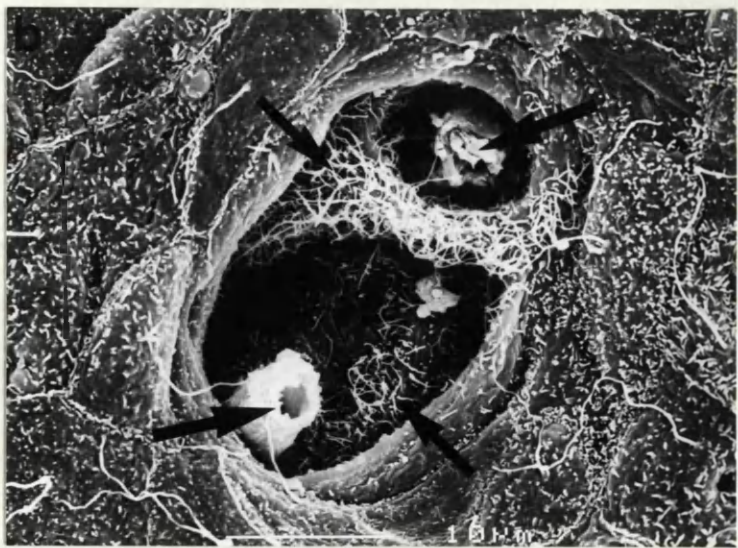
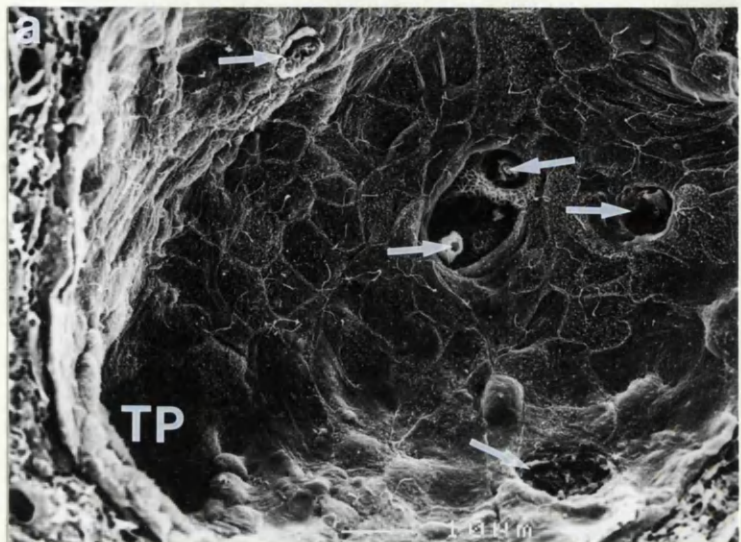


Figure 5.06: The site of a tubular pole-associated tuft-to-capsule adhesion which has fractured at the level of Bowman's capsule. The adhesion (arrow) is related to a circular defect in the squamous parietal epithelium.

Figure 5.07: A similar type of tubular pole-associated adhesion as in fig. 5.06, which has fractured at a distance from Bowman's capsule. The adhesion consists of an elongated "arm-like" process (larger arrow), covered by microvilli, which passes through the defect in the parietal epithelium (smaller arrow).

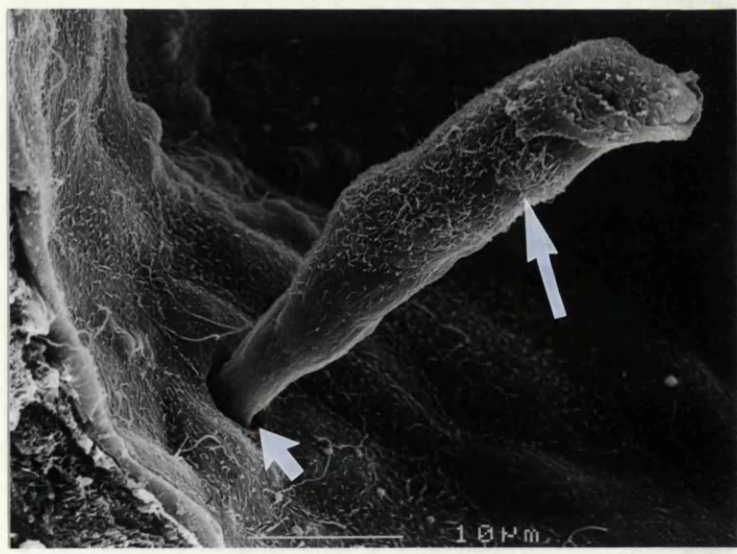


Figure 5.08: A broad-based tubular pole adhesion between glomerular tuft (T) and Bowman's capsule. The adhesion is cracked (large arrow) but remains intact. The adjacent squamous parietal epithelium includes cells with a bossellated surface (small arrows) due to cytoplasmic granules which are visible where Bowman's capsule is sectioned.

Figure 5.09: At this tuft-to-capsule adhesion, adjacent to the tubular pole (large arrow), the fractured capillary loops have markedly thickened walls (small arrows).

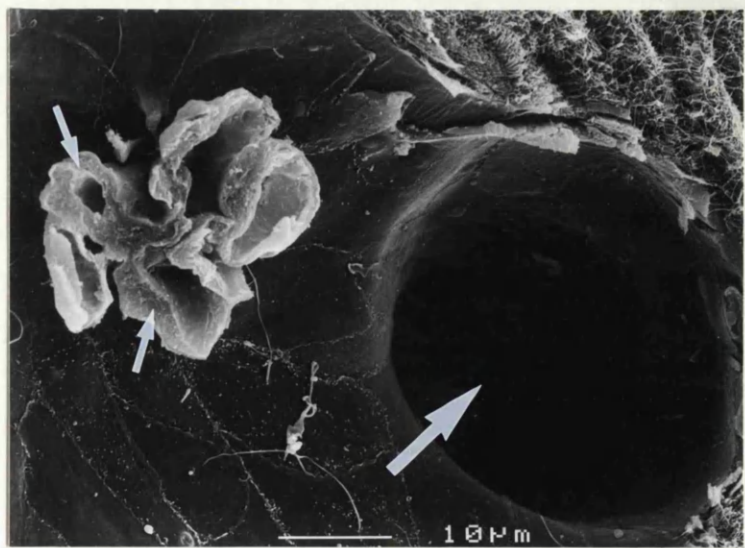


Figure 5.10: In fig. a, there is a Bowman's capsule with tubular pole (TP), and two adjacent tuft-to-capsule adhesions (arrows). In both cases, the adhesion has fractured through the attached capillary loops.

Higher power examination of both adhesions (figs. b and c) shows bossellated (ie. granulated) parietal cells (large arrows), and also occasional inflammatory cells (small arrows).

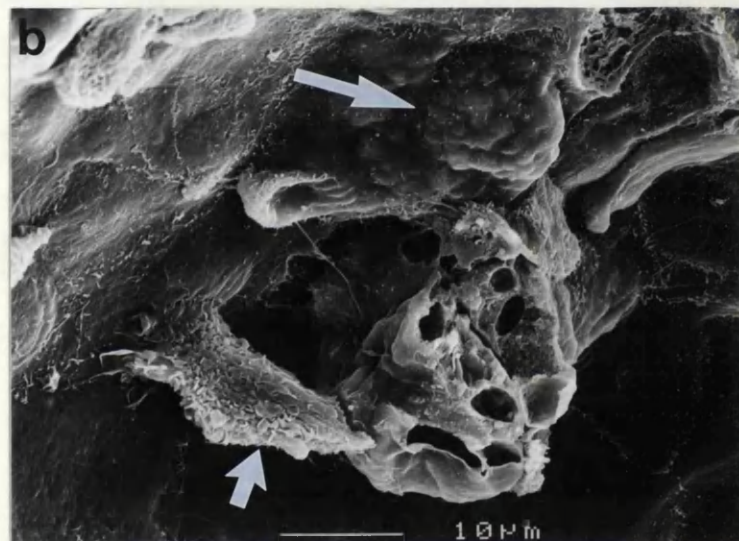
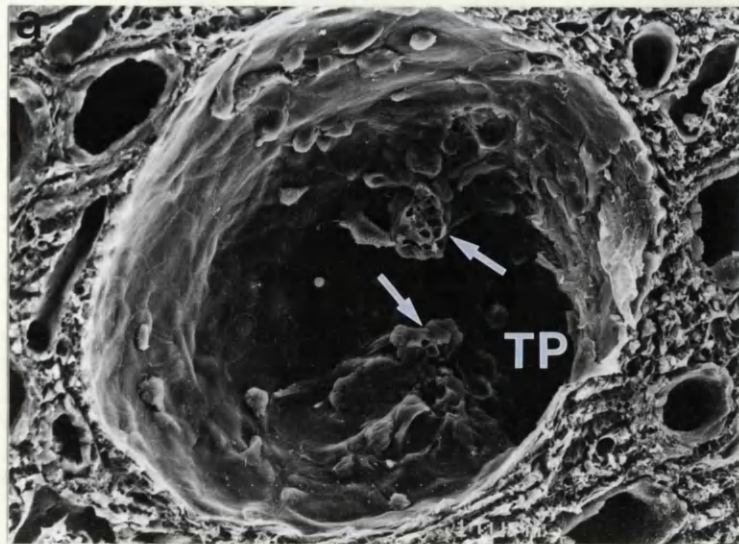


Figure 5.11: Visceral podocyte epithelium from a transplant nephrectomy, with numerous surface blebs and microvilli over both cell processes and pedicel areas.

Figure 5.12: In fig. a, the glomerular capillary tuft (T) lies within Bowman's capsule. The tubular pole (arrow) is sectioned longitudinally. The glomerular tip of the capillary tuft (seen at higher power in fig. b) shows podocyte swelling, irregular protrusions and surface blebs, which are not present over the rest of the tuft.

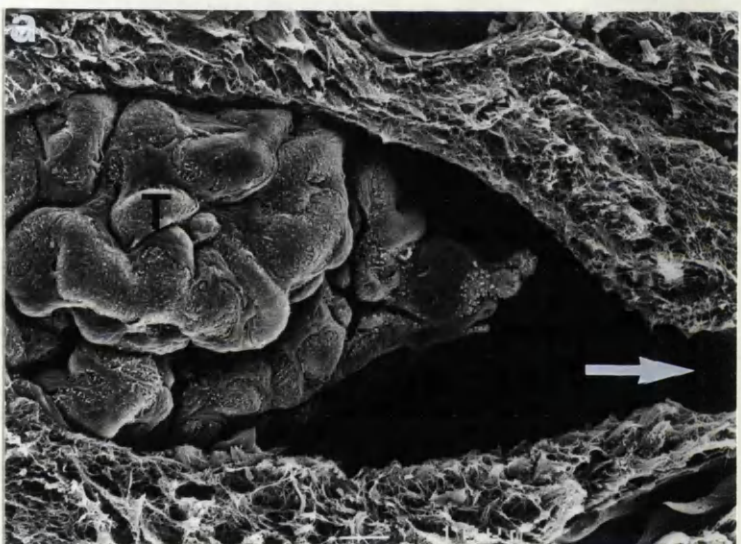


Figure 5.13: In this Bowman's capsule, the capillary tuft has herniated into the tubular pole, with associated adhesion of the tuft at the site of herniation. After glomerular microdissection, fractured capillary loops (arrows) are left "plugging" the tubular pole orifice.

Figure 5.14: A patch of squamous parietal epithelium with bossellated surface due to cytoplasmic granules.

Figure 5.15: A Bowman's capsule with tubular pole (large arrow), and two parietal cells with multiple cilia (small arrows). Most of the typical squamous parietal cells have a single cilium, with variable short microvilli.

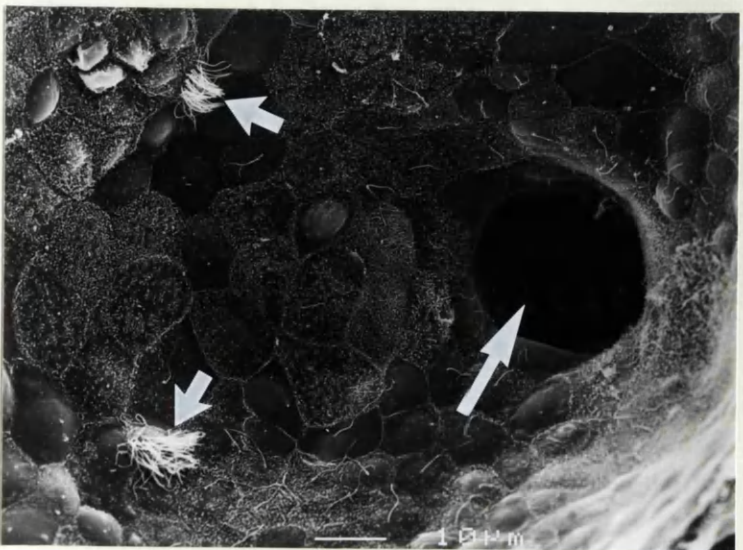
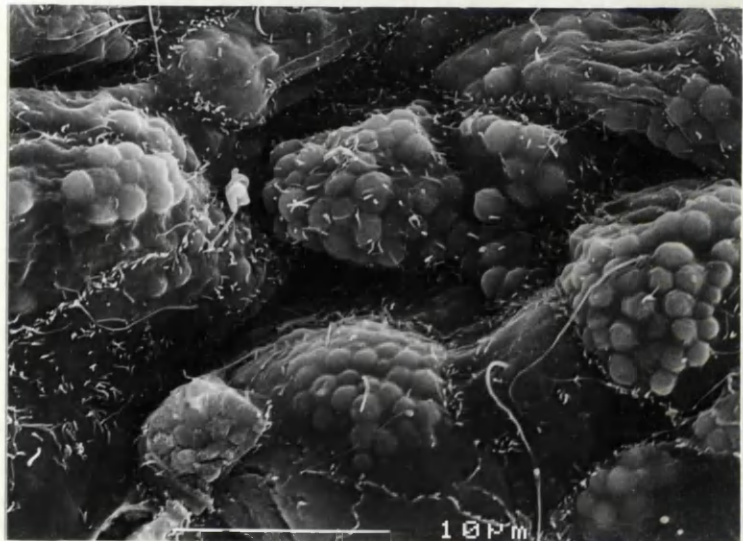
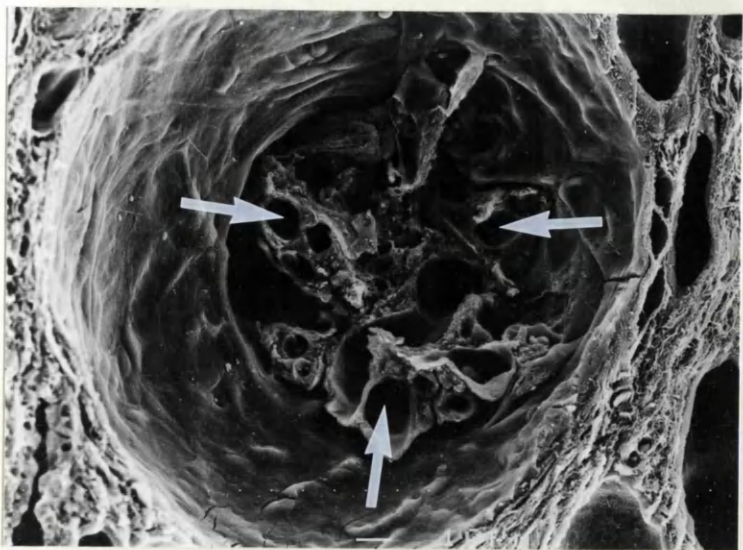


Figure 5.16: Inflammatory cell types; the larger branching cell with surface blebs and fine strands (large arrow) is consistent with a macrophage or lymphoblast. The smaller spherical cells with ruffled surface (small arrows) are small lymphocytes. Some red blood cells are also present.

Figure 5.17: An isolated glomerular capillary tuft, with small lymphocytes on the visceral podocytes.

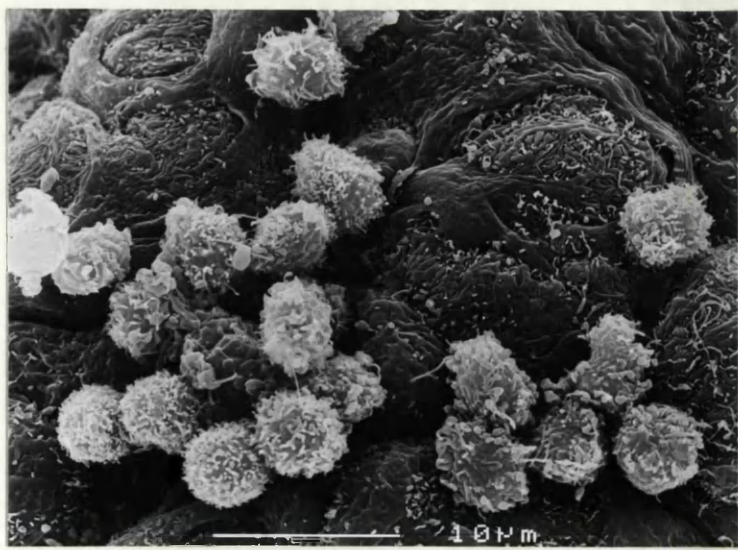
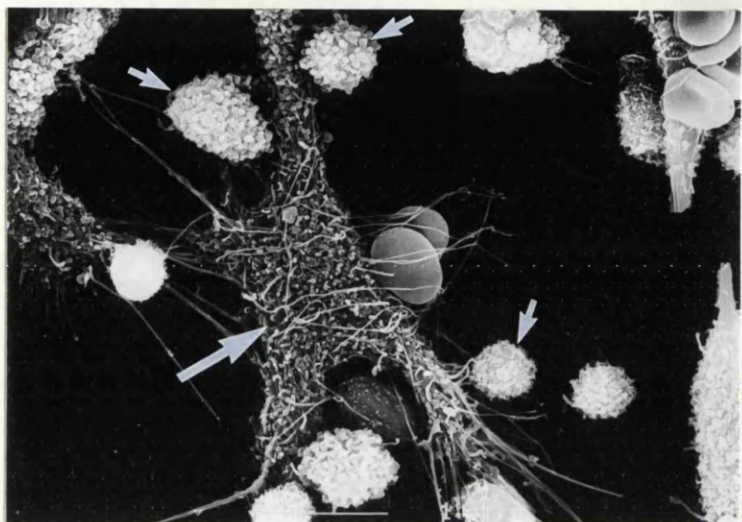


Figure 5.18: In this Bowman's capsule, aggregates of inflammatory cells (small arrows) are present around the tubular pole (large arrow), and on the squamous parietal epithelium of the tubular pole half (figs. a and b). In contrast, a single small lymphocyte (curved arrow) is present on the parietal podocytes which line the vascular pole (VP) half of the glomerulus (figs. a and c).

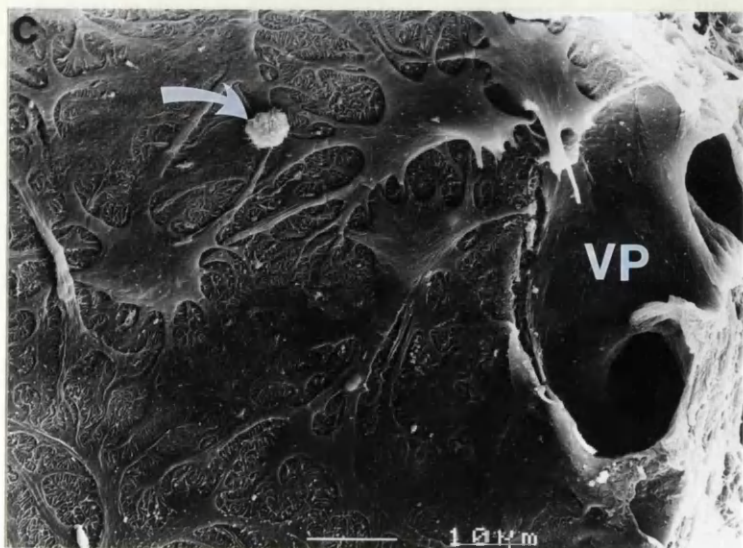
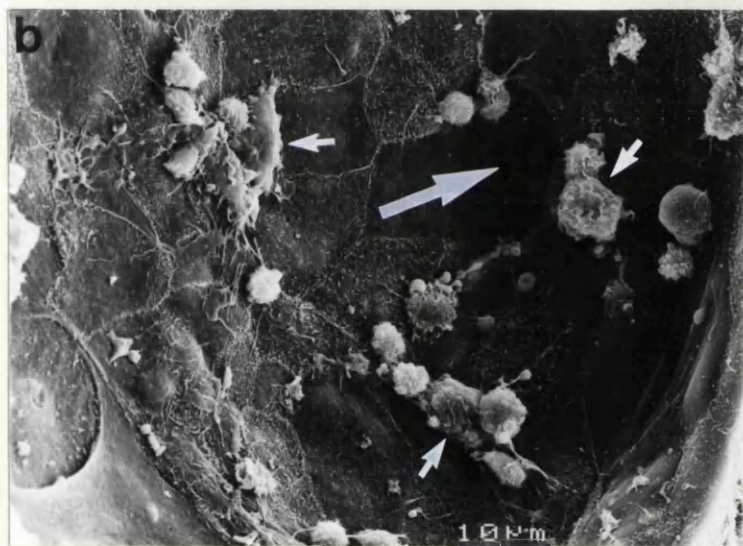
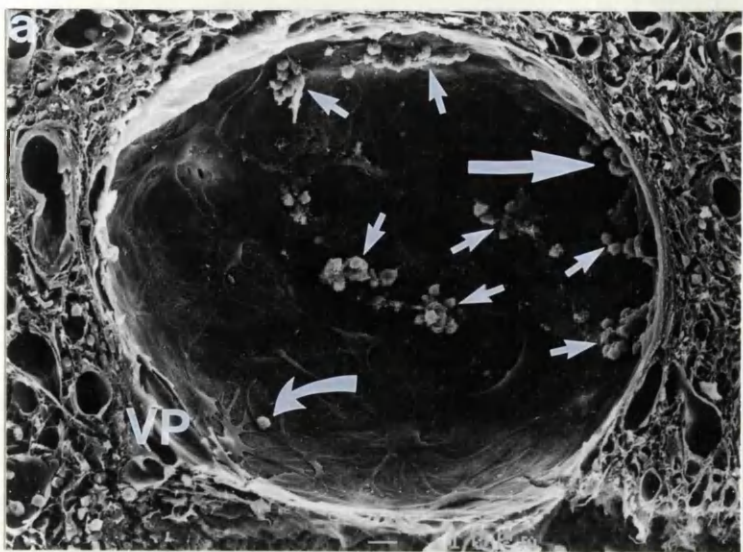


Figure 5.19: An aggregate of small lymphocytes around the tubular pole orifice (arrow) of a glomerulus.

Figure 5.20: A meshwork of fibrillar material, including at least one inflammatory cell (larger arrow), lies on the parietal epithelium. The imprint of visceral podocyte cell bodies (smaller arrow) and processes into the surface indicates contact with the glomerular capillary tuft.

Figure 5.21: This appearance of squamous parietal epithelial cytoplasm partially covering the small lymphocyte (arrow) suggests infiltration of the lymphocyte through the parietal epithelium.

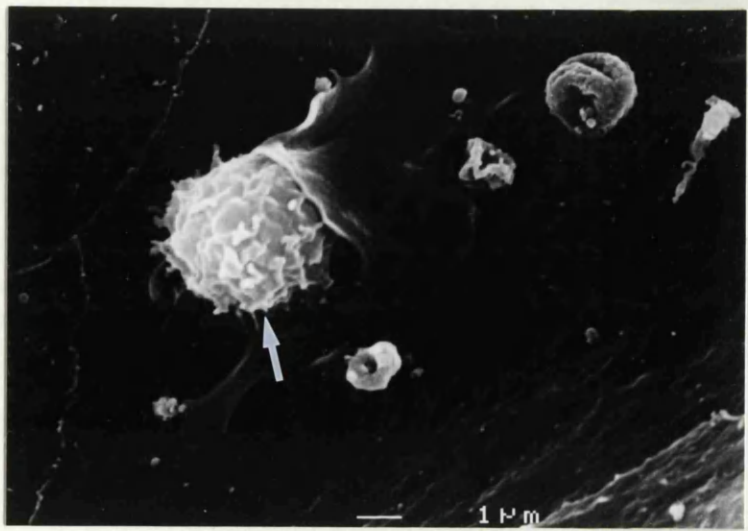
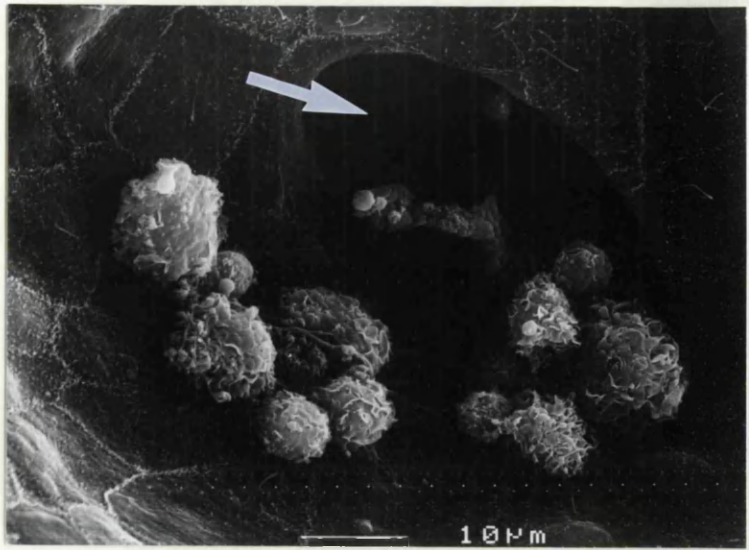


Figure 5.22: A narrowed tubular pole, with a maximum diameter of approximately 15um. Two inflammatory cells (arrows) lie within the tubular pole orifice.

Figure 5.23: A proximal tubule showing variable brush border damage. On most cells, the microvilli are reduced in number and length, producing relative prominence of the single cilia. Over one cell (larger arrow), there is a uniform clumping of microvilli; on another cell (smaller arrow), are irregular areas devoid of microvilli.

Figure 5.24: A Bowman's capsule, showing the vascular pole (VP) and the longitudinally-sectioned tubular pole (arrow). The proximal tubule (PT) commences at a right angle to the axis through the glomerular poles; there is surrounding interstitial fibrosis (I).

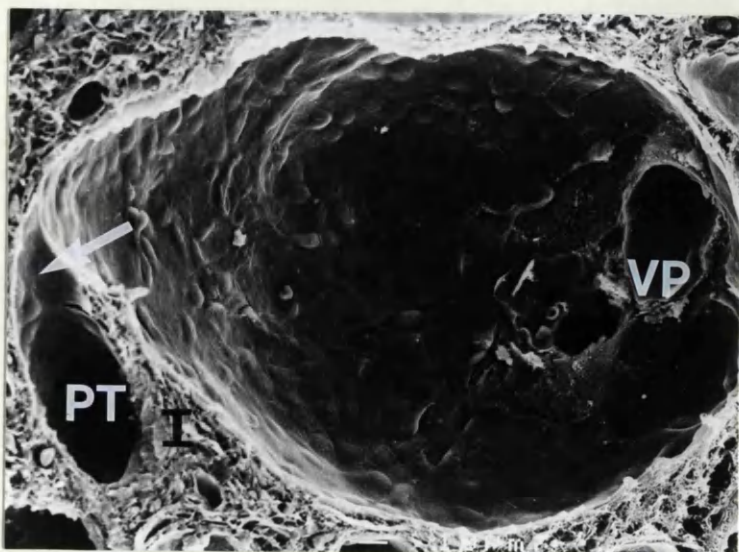


Figure 6.01: These are the complementary hemispheres of an atubular glomerulus, with several surrounding vessels (V). The parietal epithelium consists entirely of podocytes in fig. a, and mostly of parietal podocytes in fig. b. In fig. a is the contracted residual capillary tuft (arrow); in fig. b, a single small lymphocyte (arrow) overlies an area of squamous parietal epithelium.

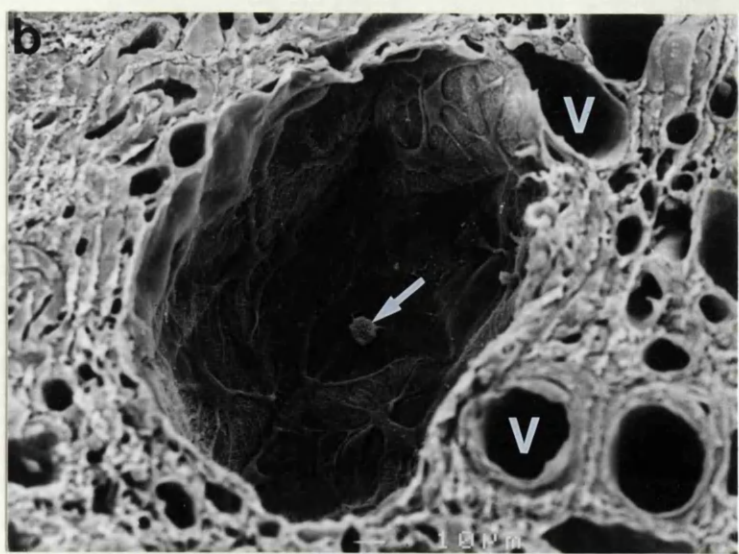
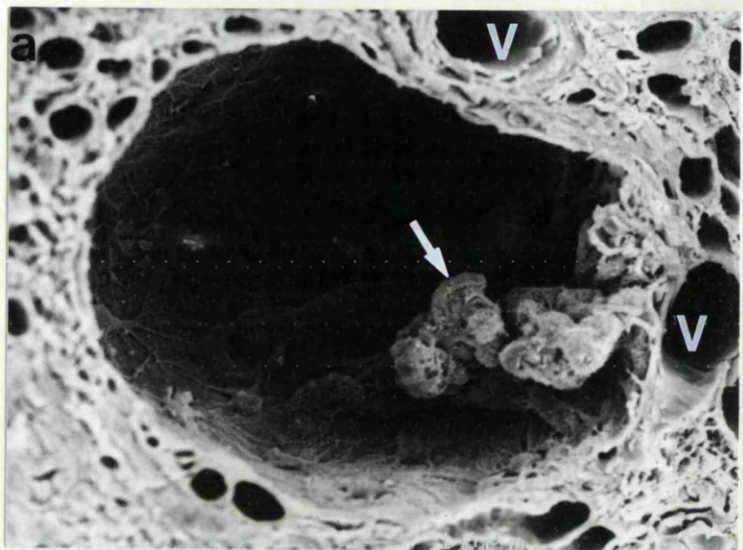


Figure 6.02: The parietal podocytes lining atubular glomeruli have long major processes, giving a "spider-like" appearance to the cells. Some such cells (small arrows) send processes onto the capillary tuft remnants (large arrows).

Figure 6.03: Interdigitation of major processes of parietal podocytes lining an atubular glomerulus.

Figure 6.04: Interdigitation of pedicels of parietal podocytes lining an atubular glomerulus.

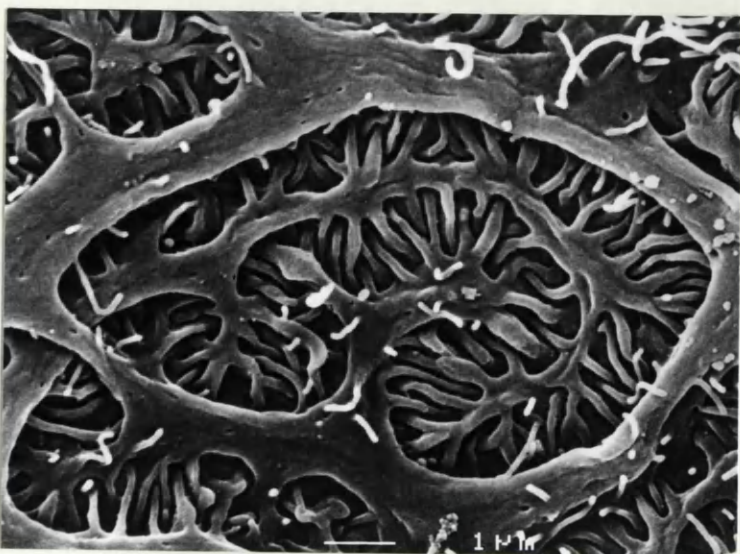
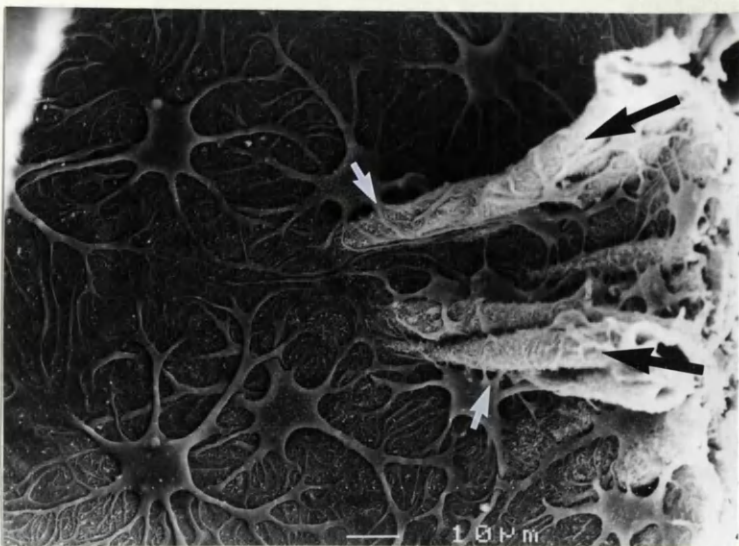


Figure 6.05: Parietal podocyte processes lining an atubular glomerulus in a transplant nephrectomy, with increase in microvilli.

Figure 6.06: Parietal podocytes lining an atubular glomerulus in a transplant nephrectomy, with surface blebs maximal over a cell body (arrow).

Figure 6.07: Parietal podocytes lining an atubular glomerulus in a transplant nephrectomy, with almost complete absence of pedicels. Both cell bodies have bossellated protrusions (arrows) due to cytoplasmic granules.

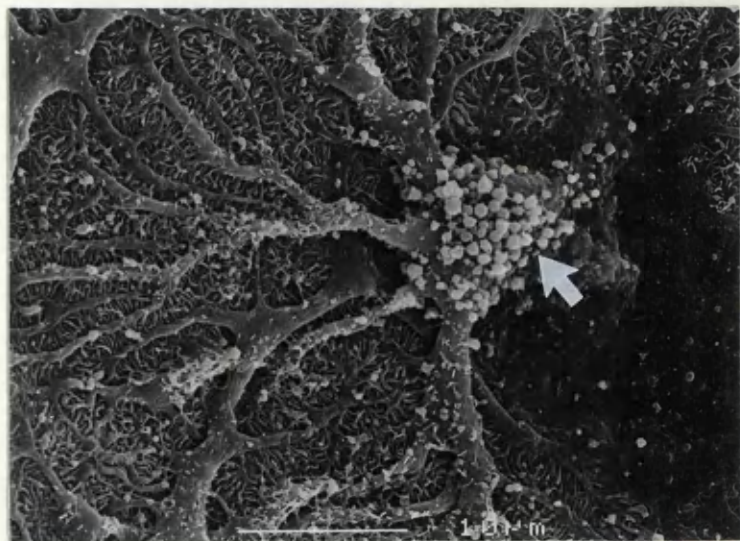
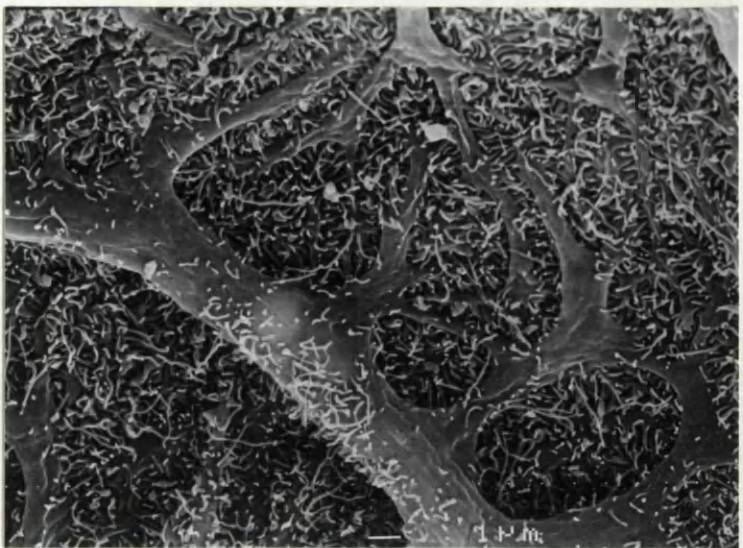


Figure 6.08: An atubular glomerulus, with a small spherical tuft remnant (T). Some lining parietal podocytes have processes (arrows) bridging onto the tuft remnant.

Figure 6.09: A glomerular cyst, with the tuft remnant (T) splayed along the cyst wall.

Figure 6.10: A large glomerular cyst, with two residual capillary loops (large "arrows"). It is lined mostly by parietal podocytes, with one area of squamous parietal epithelium (small arrow).

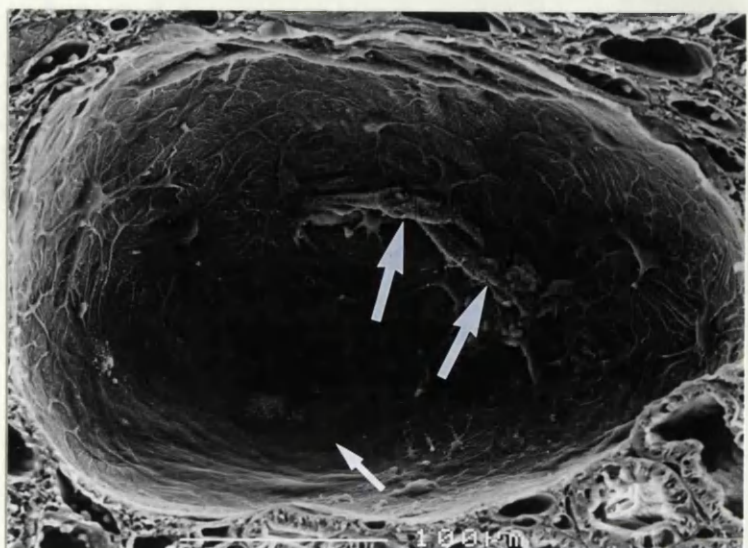
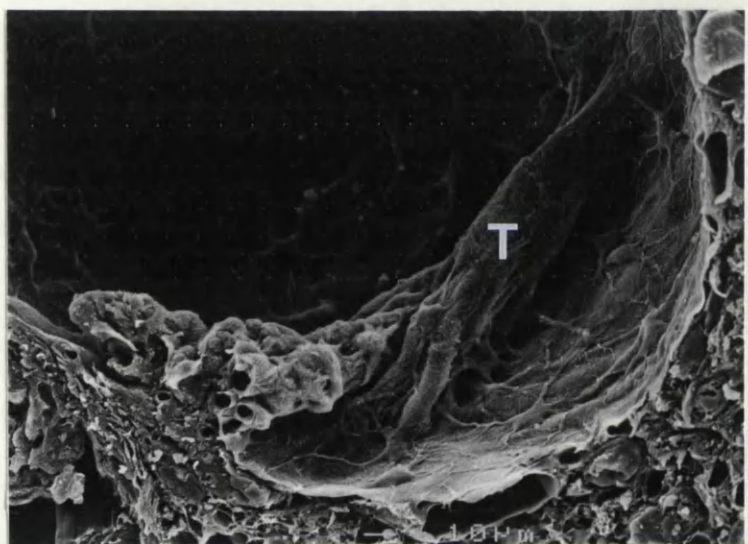


Figure 6.11: An atubular glomerulus, with a tuft remnant (T) which has an elongated process covered by podocytes (arrow) (fig. a). The process connects with the opposite wall of Bowman's capsule (fig. b), at a junction between parietal podocytes and squamous parietal epithelium.

Figure 6.12: This atubular glomerulus has a complex branching tuft remnant (T), with multiple connections to Bowman's capsule (arrows).

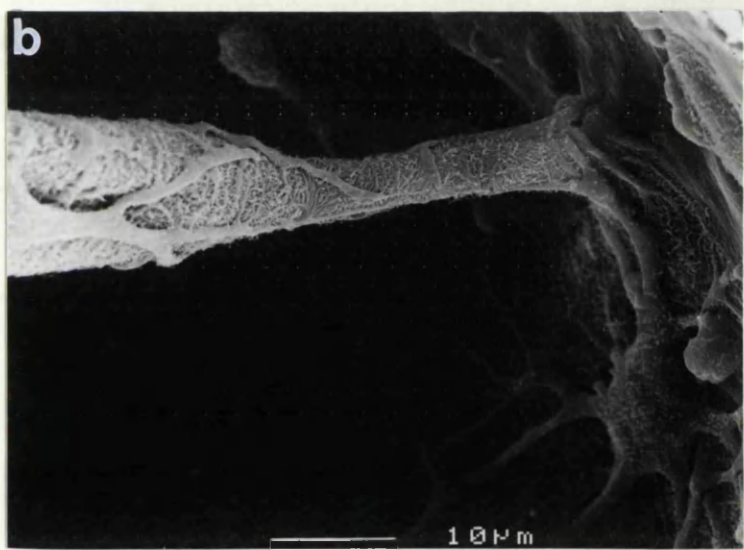
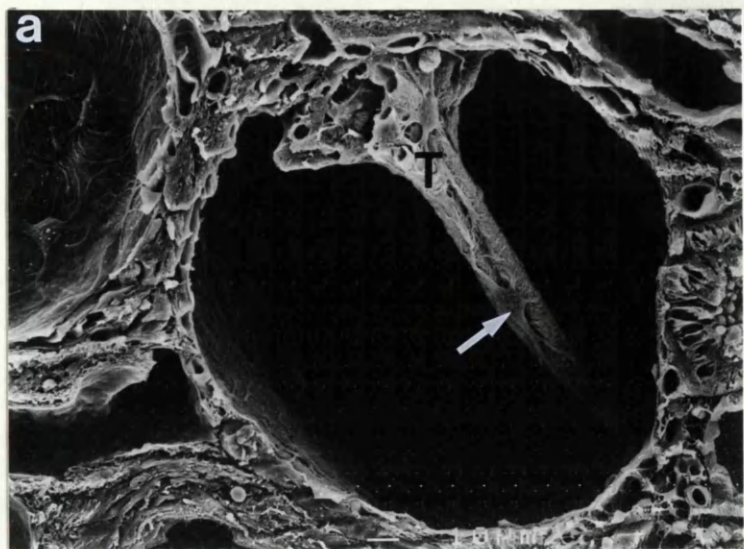


Figure 6.13: A glomerular cyst, with tuft remnants (T) and overlying proteinaceous material (P) within the urinary space.

Figure 6.14: Several podocyte processes (arrows) extend through the proteinaceous material within the urinary space, to contact with the parietal podocyte epithelium of this atubular glomerulus.

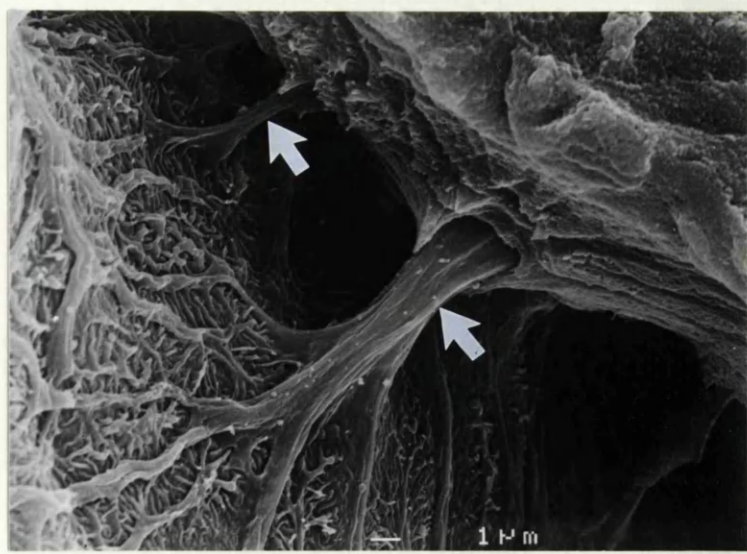
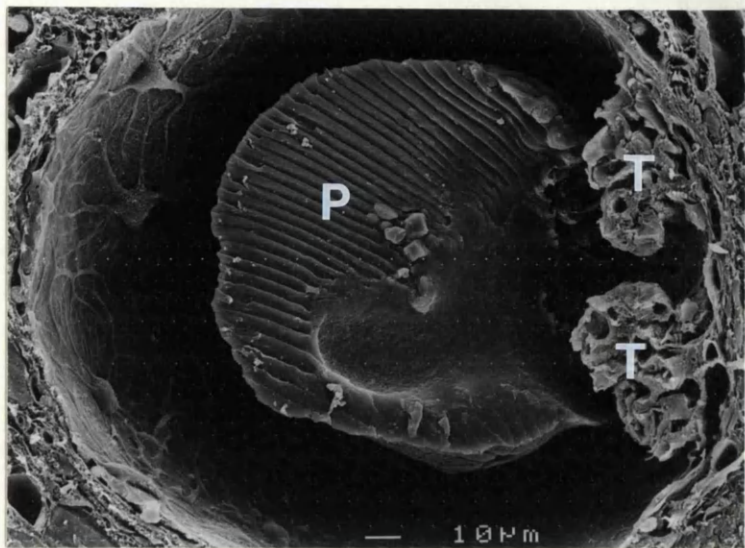


Figure 6.15: The outer surface (arrows) of the proteinaceous material within the urinary space of this glomerular cyst shows a cast of the parietal podocyte epithelium (fig. a). Higher power examination of this cast (fig. b) shows the imprint of parietal podocyte cell bodies (large arrow), major processes (small arrows) and pedicels.

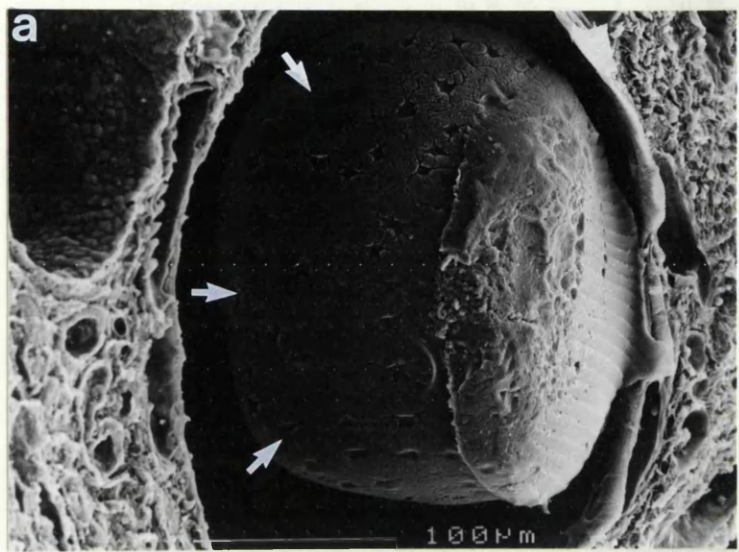


Figure 6.16: This glomerular cyst has a splayed tuft remnant (T), and two groups of inflammatory cells (arrows, fig. a). One inflammatory aggregate (fig. b) consists of small lymphocytes enmeshed by fibrillar material. The other aggregate (fig. c) consists of six separate small lymphocytes lying on squamous parietal epithelium, at its junction with parietal podocytes which line most of the Bowman's capsule.

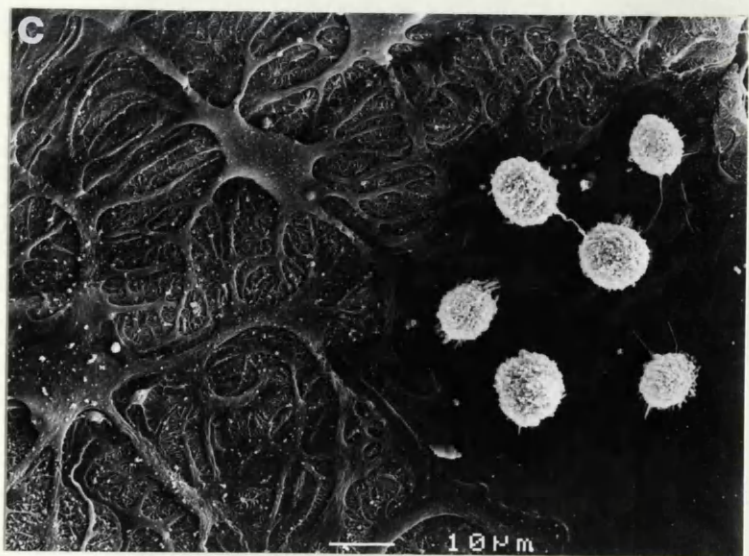
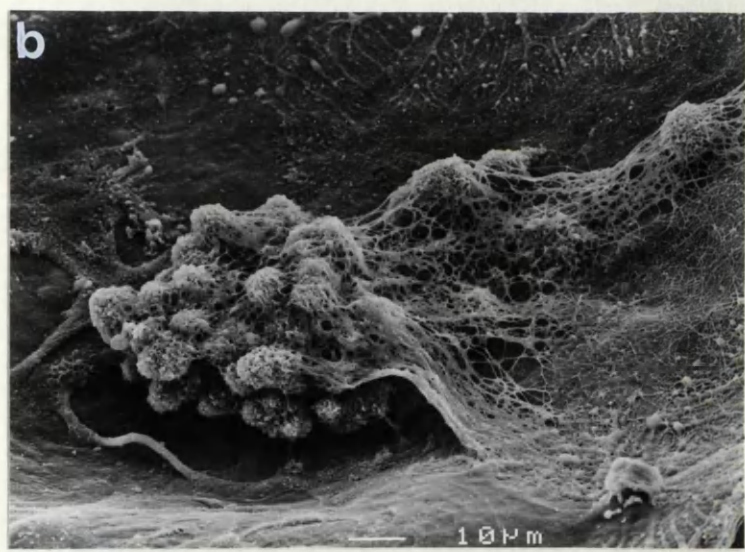
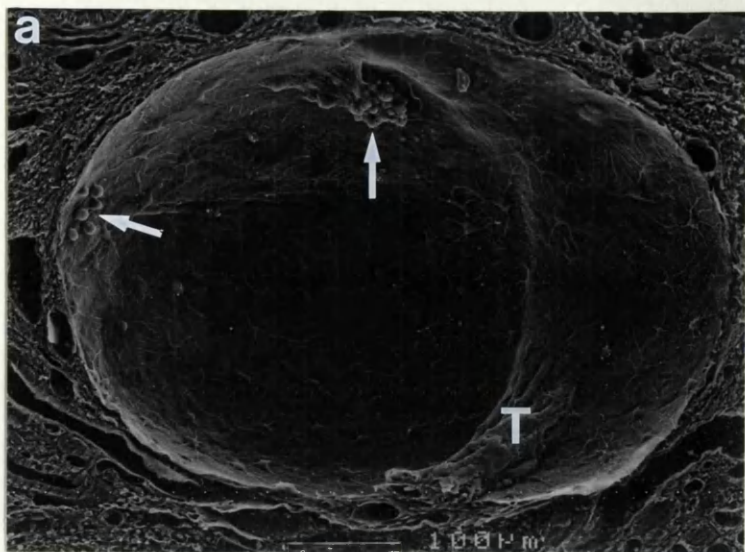


Figure 6.17: Figs. a and b are complementary faces from a transplant nephrectomy showing four glomerular cysts (numbered 6-9) and one normal glomerulus with sectioned capillary tuft (arrow), surrounding two thick-walled arteries (A). Examination of the glomerular cysts shows they are atubular; in contrast, microdissection of the capillary tuft in fig. b revealed a tubular pole.

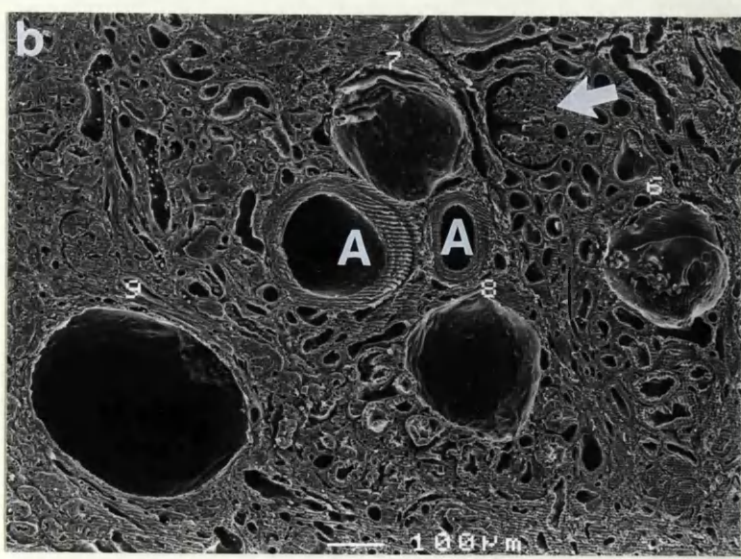
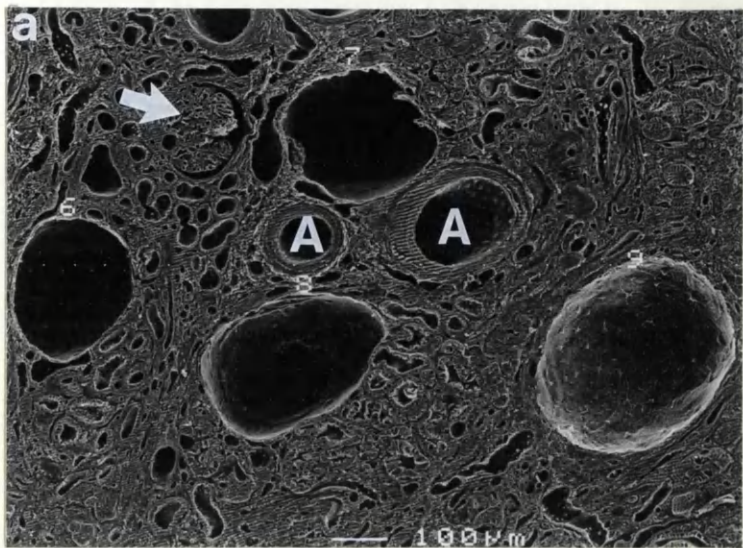


Figure 6.18: The two glomeruli in this photomicrograph (human renal biopsy, PAS stain) consist of one obsolescent tuft (small arrow), and one with a contracted tuft and a proteinaceous cast within the accentuated urinary space (consistent with an atubular glomerulus, large arrow). The latter glomerulus has surrounding interstitial fibrosis, and atrophic tubules with PAS-positive casts (curved arrows).

